August 2020

Analysis of Allocation Rules for Heart Transplantation

Farhad Hasankhani Kohneh Shahri
Clemson University, farhad.hasankhani@gmail.com

Analysis of Allocation Rules for Heart Transplantation

A Dissertation
Presented to
the Graduate School of
Clemson University

In Partial Fulfillment
of the Requirements for the Degree
Doctor of Philosophy
Industrial Engineering

---

by
Farhad Hasankhani
August 2020

Accepted by:
Dr. Amin Khademi, Committee Chair
Dr. Cole Smith
Dr. Burak Eksioglu
Dr. Kevin Taaffe

Preface

Heart failure is a chronic and progressive condition in which the heart is unable to pump enough blood to meet the body's needs. It affects over 5.8 million people in the United States, with increasing diagnosed cases each year. Heart transplantation is the only viable therapy for the patients who suffer from end-stage heart failure to improve their quality of life and survival. The only source of hearts for transplantation is from cadaveric donors, which is very limited compared to the heart transplantation waiting-list patient population. Thus, efficient and fair allocation of this limited source to the patients is of top priority. In this dissertation, we develop mathematical models to study the problem of heart allocation and analyze it by using simulation and optimization techniques.

Because of the challenges in heart allocation, policy makers in the United Network for Organ Sharing (UNOS) have periodically revised the heart allocation policies over time. In order to assess the performance of different allocation policies, researchers have developed simulation models. The Thoracic Simulated Allocation Model (TSAM) is a model of heart allocation system developed by UNOS to evaluate the performance of the proposed changes in policy. However, TSAM makes certain restricting assumptions in the simulation model.

In Chapter 1, we developed a simulation model of the complex heart transplant system in the United States, that relaxes those assumptions and can be used to evaluate the potential impacts of allocation policy modifications on several outcomes such as patients' pre- and post-transplant survivals. Furthermore, we proposed three common-sense policies by slightly modifying the current UNOS allocation policy and compared their performance in terms of efficiency and fairness.

Due to the shortage of donor organs compared to the patients demanding for transplant, donated hearts should be allocated in an efficient way. Furthermore, the allocation must be fair with respect to different patient groups. It is not clear for the transplant community that the

current allocation policy is optimal and there are debates regarding the efficiency and fairness of the policy. In Chapter 2 of this dissertation, we developed a constrained finite horizon Markov Decision Process model to find the optimal allocation policy. Since the state space of the original model is unbounded and the model is intractable, we study its fluid approximation in the presence of several fairness constraints. The performance of our proposed optimal policy is evaluated and compared with several benchmark policies by using the simulation model developed in Chapter 1. We conducted an extensive numerical analysis and provided insights about the structure of the proposed optimal policy. In addition, we conducted fairness analysis of the proposed policy by comparing its outcomes in the presence of several fairness constraints. The proposed optimal policy tends to emphasize on the post-transplant outcomes of the transplantation system by shifting allocation priority from sicker and older patients to healthier and younger ones. Our results show that such a policy will significantly improve the efficiency of the allocation even in the presence of fairness constraints.

In Chapter 3, we introduced a new fairness measure in organ allocation and study its potential benefits. In particular, while existing measures of fairness in the literature of organ allocation are inefficient and have high prices, policies based on proportional fairness yield a lower price of fairness and decrease performance loss. We formulate organ allocation with the goal of imposing proportional fairness as a queuing model and analyze its fluid approximation. By studying necessary and sufficient optimality condition of a transformation of this problem, we analytically show that the optimal allocation policy under proportional fairness measure is an assortative partition policy, if certain assumptions hold. Such allocation policies are easy to implement in practice and have interesting insights. Our numerical results show that in terms of total utility, policies based on proportional fairness perform in the midway point between the policy based on max-min fairness measure and the one based on utilitarian approach. Thus, they significantly reduce price of fairness in organ allocation systems.

Acknowledgments

Firstly, I would like to thank my advisor, Dr. Amin Khademi, for his continues and invaluable support, for his patience and mentorship, for the knowledge he helped me gain, and for all the great opportunities he created for me. His guidance helped me in all the time of research and writing of this thesis. Without his helps and guidance, this dissertation would never have been accomplished. I am grateful to him not only for being an amazing advisor, but also a true friend.

I would also like to thank my wonderful committee members, Dr. Burak Eksioglu, Dr. Cole Smith, and Dr. Kevin Taaffe for their kind support and their constructive feedback during my graduate studies. Their great comments helped me improve the quality of this dissertation. I am also thankful to the faculty, staff and my fellow graduate students in the department of Industrial Engineering at Clemson University.

My sincere thanks also goes to Dr. Brian Fralix who provided me an opportunity to collaborate with him and Dr. Amin Khademi on a very interesting research study during my graduate studies.

Last but not the least, I would like to thank my parents, Bakhshali Hasankhani and Mahzar Alerostam, my sister, and all my friends for their unconditional love and friendship and for supporting me throughout this journey.

Table of Contents

Title Page . . . . . **i**

Preface . . . . . **ii**

Dedication . . . . . **iv**

Acknowledgments . . . . . **iv**

List of Tables . . . . . **vi**

List of Figures . . . . . **ix**

1 A Simulation Model of Heart Transplant Queueing System **1**
1.1 Introduction 2
1.2 Methods 4
1.3 Results 14
1.4 Conclusion and Discussion 18

2 Optimal Allocation Rules for Heart Transplantation **21**
2.1 Introduction 22
2.2 Related Work 25
2.3 Problem Formulation 27
2.4 Fluid Approximation 33
2.5 Alternative Objective Functions 38
2.6 U.S. Heart Transplantation System 39
2.7 Conclusions and Managerial Insights 49

3 Proportionally Fair Organ Allocation Rules for Transplantation **51**
3.1 Introduction 51
3.2 Problem Formulation 58
3.3 Analysis of the Optimal Policy 61
3.4 Numerical Results 70
3.5 Conclusion 74

Appendices **77**
A Appendix of Chapter 1 78
B Appendix of Chapter 2 117

Bibliography **173**

List of Tables

1.1 Validation of Model Results . . . 15
1.2 p-values of t-test for Comparing Real Data and Simulation Outputs . . . 16
1.3 Survival Rates of Patients Transplanted During 2006-2008 . . . 16
1.4 Results of Fairness Comparison of Policies . . . 18

2.1 Percentage Improvement of OPL over UNOS . . . 41
2.2 Benchmark Policies Comparison . . . 43
2.3 Color-Coded Graph of Age and Health Prioritization for OPL Policy . . . 45
2.4 LYs/Death Trade-off for Patient Health Groups (OPL minus UNOS) . . . 46
2.5 LYs/Death Trade-off for Patient Age Groups (OPL minus UNOS) . . . 46
2.6 Improvement of the OPL over UNOS in the presence of age fairness constraints (%) 47
2.7 Improvement of the OPL over UNOS in the presence of health fairness constraints (%) 47
2.8 Improvement of the OPL over UNOS in the presence of age-health fairness constraints (%) . . . 47
2.9 Percentage Improvement of OPL over UNOS for Different Cases of Parameters (%) . 48

3.1 Policy Comparison . . . 72
2 Patient Characteristics . . . 78
3 Heart Characteristics . . . 79
4 Waiting List Disease Group Categorization in Feb 2016 (Adults) . . . 80
5 Disease Categorization in Model . . . 81
6 UNOS Table of Reasons for Heart Transplantation . . . 82
7 Adult Status 1A Requirements for Candidates Currently Admitted to the Transplant Hospital . . . 84
8 Adult Status 1A Requirements for Candidates Current Hospitalization Not Required 85
9 Number of OPO and Transplant Centers in Each Region . . . 88
10 Regression p-values for Testing the Time Dependency of Attributes . . . 90
11 P-values for Chi-squared Independency Test for Gender . . . 92
12 P-values for Chi-squared Independency Test for PTX Status . . . 92
13 P-values for Chi-squared Independency Test for Disease . . . 92
14 Second Level Dependency of Patient Attributes . . . 93
15 Regression p-values for Testing the Time Dependency of Attributes . . . 95
16 P-values for Chi-squared Independency Test for Age Group . . . 96
17 P-values for Chi-squared Independency Test for Blood Type . . . 96
18 P-values for Chi-squared Independency Test for Ethnicity . . . 96
19 Second Level Dependency of Heart Attributes . . . 96
20 P-values for the Kolmogorov-Smirnov Test . . . 98
21 Number of Yearly and Daily Delisting for UNOS Waiting List During 2006-2014 . . 99
22 Heart Waitlist Mortality Rates (07/01/2012-06/30/2013) . . . 100
23 Abridged Life Table for the U.S. Total Population, 2013 . . . 102
24 1-Year Patient Post-Transplant Survival . . . 104

25 Primary Blood Type Matching Requirements . . . 105
26 Secondary Blood Type Matching Requirements . . . 105
27 Zone Definition for the UNOS Policy . . . 106
28 Allocation of Hearts from Deceased Donors At Least 18 Years Old in the UNOS Policy 106
29 Zone Definition for Policy I . . . 108
30 Allocation of Hearts from Deceased Donors At Least 18 Years Old in Policy I . . . 108
31 Allocation of Hearts from Deceased Donors At Least 18 Years Old in Policy II . . . 109
32 Notations Used in Stochastic Formulation in Section 2.3 . . . 118
33 Notations Used in Fluid Approximation (P_1) in Section 2.4 . . . 119
34 Notations Used in Stochastic Formulation in Section B.3 . . . 120
35 Notations Used in Alternative Objective Function Formulation in Section B.5 . . . 120
36 Abbreviations Used Throughout the Text . . . 121
37 Each Objective Function Component for OPLS Policy . . . 138
38 Mean and Standard Deviation of Waiting Time for OPLS Policy . . . 138
39 Optimality Gap in a Markovian Setting . . . 139
40 Practical Aspects of Allocation in Simulation and Mathematical Modeling . . . 142
41 Primary Blood Type Matching Requirements . . . 144
42 Secondary Blood Type Matching Requirements . . . 144
43 Priority Zone Definition . . . 144
44 Allocation of Hearts from Adult Deceased Donors in the UNOS Policy . . . 145
45 Mapping from 3-tiered to 7-tiered Health Status Classification . . . 146
46 Allocation of Hearts from Adult Deceased Donors in the UNOS 7-Tiered Policy . . . 147
47 P-values for the Chi-Squared Goodness of Fit Test . . . 148
48 P-values for the Kolmogorov-Smirnov Test . . . 148
49 Each Objective Function Component for HAS-F Policy . . . 152
50 Mean and Standard Deviation of Waiting Time for HAS-F Policy . . . 152
51 Details for Fairness Constraints . . . 160
52 Mapping between Heart Types and Age and Blood type of Donor Hearts . . . 163
53 Color-Coded Graph for OPL Policy without Fairness Constraints (Heart type 1) . . . 163
54 Color-Coded Graph for OPL Policy without Fairness Constraints (Heart type 2) . . . 163
55 Color-Coded Graph for OPL Policy without Fairness Constraints (Heart type 3) . . . 163
56 Color-Coded Graph for OPL Policy without Fairness Constraints (Heart type 4) . . . 163
57 Color-Coded Graph for OPL Policy without Fairness Constraints (Heart type 5) . . . 163
58 Color-Coded Graph for OPL Policy without Fairness Constraints (Heart type 6) . . . 164
59 Color-Coded Graph for OPL Policy without Fairness Constraints (Heart type 7) . . . 164
60 Color-Coded Graph for OPL Policy without Fairness Constraints (Heart type 8) . . . 164
61 Color-Coded Graph for OPL Policy without Fairness Constraints (Heart type 9) . . . 164
62 Color-Coded Graph for OPL Policy without Fairness Constraints (Heart type 10) . . . 164
63 Color-Coded Graph for OPL Policy without Fairness Constraints (Heart type 11) . . . 164
64 Color-Coded Graph for OPL Policy without Fairness Constraints (Heart type 12) . . . 164
65 Color-Coded Graph for OPL Policy without Fairness Constraints (Heart type 13) . . . 164
66 Color-Coded Graph for OPL Policy without Fairness Constraints (Heart type 14) . . . 165
67 Color-Coded Graph for OPL Policy without Fairness Constraints (Heart type 15) . . . 165
68 Color-Coded Graph for OPL Policy with Age Fairness Constraints ([35+]) . . . 165
69 Color-Coded Graph for OPL Policy with Age Fairness Constraints ([50+]) . . . 166
70 Color-Coded Graph for OPL Policy with Age Fairness Constraints ([65+]) . . . 166
71 Color-Coded Graph for OPL Policy with Age Fairness Constraints ([50-65] and [65+]) 166
72 Color-Coded Graph for OPL Policy with Age Fairness Constraints ([35-50] and [50-65] and [65+]) . . . 167
73 Color-Coded Graph for OPL Policy with Health Fairness Constraints ([1A]) . . . 167
74 Color-Coded Graph for OPL Policy with Health Fairness Constraints ([1B]) . . . 167

75 Color-Coded Graph for OPL Policy with Health Fairness Constraints ([2]) 167
76 Color-Coded Graph for OPL Policy with Health Fairness Constraints ([1A] and [1B]) 167
77 Color-Coded Graph for OPL Policy with Age-Health Combination of Fairness Constraints ([65+] and [1A]) 168
78 Color-Coded Graph for OPL Policy with Age-Health Combination of Fairness Constraints ([50-65] and [65+] and [1A]) 168
79 LYs/Death Trade-off for Patient Health Groups (OPL-F minus UNOS 171
80 LYs/Death Trade-off for Patient Age Groups (OPL-F minus UNOS) 171
81 LYs/Death Trade-off for Patient Health Groups (OPL minus UNOS-7-tiered) 171
82 LYs/Death Trade-off for Patient Age Groups (OPL minus UNOS-7-tiered) 172

List of Figures

1.1 Overview of the Simulation Model of Heart Transplantation Waiting List 6
1.2 Comparison of Pre-transplant, Post-transplant, and total number of deaths for UNOS, Policy I, Policy II, and Policy III (years: 2006-2014) 17

3.1 Percentage of Hearts Allocated to Each Health Group 74
3.2 Percentage of Hearts Allocated to Each Age Group 75
3.3 Percentage of Hearts Allocated to Each VAD Status Group 75
4 Map of UNOS Regional Categorization 87
5 Map of OPO Locations 88
6 Pattern of Dependency in Patient Arrival Data 94
7 Pattern of Dependency in Heart Arrival Data 97
8 Total Number of Deaths for Different Patient and Heart Arrival Rates 111
9 Pre-Transplant Deaths for Different Patient and Heart Arrival Rates 112
10 Post-Transplant Deaths for Different Patient and Heart Arrival Rates 112
11 Pre-Transplant Deaths 114
12 Post-Transplant Deaths 114
13 Total Deaths 114
14 Proportional Fairness Measure 115
15 Max-Min Fairness Measure 115
16 Total Number of Deaths for 10 Percent Increased Patient Arrival Rates for Different Policies 116
17 Heart Allocation Simulation Model 143
18 Health, Age, VAD, and Zone Priorities for UNOS and OPL 170

Chapter 1

A Simulation Model of Heart Transplant Queueing System

Summary: The optimal allocation of limited donated hearts to patients on the waiting list is one of the top priorities in heart transplantation management. We developed a simulation model of the U.S. waiting list for heart transplantation to investigate the potential impacts of allocation policies on several outcomes such as pre- and post-transplant mortality. We used data from the United Network for Organ Sharing (UNOS) and the Scientific Registry of Transplant Recipient (SRTR) to simulate the heart allocation system. The model is validated by comparing the outcomes of the simulation with historical data. We also adapted fairness schemes studied in welfare economics to provide a framework to assess the fairness of allocation policies for transplantation. We considered three allocation policies, each a modification to the current UNOS allocation policy, and analyzed their performance via simulation. The first policy broadens the geographical allocation zones, the second modifies the health status order for receiving hearts, and the third prioritizes patients according to their waiting time. Our results showed that the allocation policy similar to the current UNOS practice except that it aggregates the three immediate geographical allocation zones, improves the health outcomes, and is "closer" to an optimal fair policy compared to all other policies considered in this study. Specifically, this policy could have saved 319 total deaths (out of 3738 deaths) during 2006-2014 time horizon, in average. This policy slightly differs from the current UNOS allocation policy, and allows for easy implementation. We developed a model to compare

the outcomes of heart allocation policies. Combining the three immediate geographical zones in the current allocation algorithm, could potentially reduce mortality rate and is closer to an optimal fair policy.

1.1 Introduction

Heart failure (HF) is a progressive disease that affects 5.8 million people in the U.S., with 550,000 new cases diagnosed annually. Heart transplantation is a life-saving treatment and improves the quality of life and survival of late-stage HF patients (Stevenson, 2015). The source of hearts for transplantation is from cadaveric donors, with patients joining the waiting list to receive a cadaveric donor heart.

Since 2004, the number of new active adults (18+) joining the waiting list has increased by 40%. However, the donation rate remains flat with 3.5 donations per 1,000 deaths in 2012, which increased the size of the waiting list by 25% (Colvin-Adams et al., 2014). According to the UNOS data, since 2006 to 2014 total of 27119 adult patients has joined the waiting list which is significantly larger than 18962 heart donations during the same period. As of December 1, 2016, 3773 adult patients are on the UNOS heart transplantation waiting list. These numbers clearly indicate a major imbalance in supply and demand resulting in a substantial mortality for the patients on the waiting list (Colvin-Adams et al., 2014). This shortage of supply raises the allocation question: which patients should receive priority when a donor heart becomes available? This allocation problem is one of the top priorities in heart transplant management (Colvin-Adams et al., 2014).

To enhance the fairness of organ allocation, the National Organ Transplant Act enacted new rules to ensure the fair and equitable distribution of available organs (Davis and Delmonico, 2005). Moreover, the allocation should be based on a priority rule for patients on the waiting list; i.e., if an organ is procured, patients should be ranked and the organ is offered to the highest priority patient until it is accepted (Organ Procurement and Transplantation Network, 2015). Allocation policies, which substantially affect the quality-adjusted life years (QALYs) of the population, should provide fair access to organs to all patients, independent of their race, age, and other characteristics. Faced with such challenges, policy makers in UNOS have periodically revised their policies over time (Colvin-Adams et al., 2012). The original heart allocation system, approved in 1988, was a two-tiered

policy using medical emergency status applied to both adults and pediatrics (Colvin-Adams et al., 2012). In 1989 UNOS/OPTN (Organ Procurement and Transplantation Network) implemented the heart allocation policy to place the highest priority upon those patients who are most likely to die while waiting (Mancini and Lietz, 2010). In 1998, this allocation method was restructured into a three-tiered system (status 1A, 1B, and 2) in which higher priority was assigned to the sickest patients with a short survival rate (Renlund et al., 1999). Details of the revisions to heart allocation policy from 1988 to 2012 are provided by (Colvin-Adams et al., 2012). Current UNOS allocation policy was issued in July 2006 allowing a broader regional sharing of donor hearts (Singh et al., 2012). However, the optimality of the current UNOS practice in terms of efficiency and fairness is not clear and the OPTN/UNOS Heart Subcommittee recently suggested a reassessment of the current allocation policy (Stevenson, 2015). Meyer et al. (2015) studied the limitations of the current three-tiered medical urgency system and depicted the future direction of heart transplantation in the U.S.

As assessing the performance of allocation policies for the nation is not amenable to clinical trials, researchers have developed simulation models to analyze allocation policies. For example, the Thoracic Simulated Allocation Model (TSAM) is a model of heart allocation system from July 1, 2009 to June 30, 2011, which has been used to evaluate the proposed changes in policy. TSAM makes the following assumptions: (1) Arrivals of candidates/donors are input to the model with a data file, (2) The initial waiting list is input to the model with a data file, (3) An entire history of waiting-list status changes must be input to the model for each patient. As a result, in each simulation, the same actual donors and candidates are used, thus statistical tests of comparisons are not possible (Scientific Registry of Transplant Recipients, 2015b). We relaxed those assumptions by developing models for arrivals of patients and hearts, as well as models for change of health status in the waiting list. van den Hout et al. (2003) built a model for the Eurotransplant waiting list for heart transplantation and showed that international organ exchange reduces waiting list mortality in different countries by 1.9% to 12.4%. Shechter et al. (2005) created a simulation model for the liver allocation system to compare the performance of different allocation policies in liver transplantation. Su and Zenios (2006) built a mechanism design model to examine the effect of post-transplant information asymmetry on the kidney allocation system in terms of efficiency and equity. Bertsimas et al. (2013) developed a framework to derive optimal policies for kidney allocation

while considering fairness constraints.

In this study, we developed a simulation model of the U.S. heart allocation system and validated it to evaluate the potential impacts of allocation policy modifications on several outcomes such as pre- and post-transplant survivals. We used the current UNOS allocation policy as the baseline policy for our simulation model. With a few exceptions, this policy ranks patients in three different levels, i.e., geographical (proximity to the donor hospital), health status, and waiting time level. Specifically, when a donor heart becomes available for transplantation, the policy first categorizes patients on the waiting list based on their distance from the procurement Organ Procurement Organization (OPO) into six zones, where each zone includes all transplant centers within some distance of the donor hospital. Note that these zones are not geographical districts but are defined by proximity to the donor hospital. It first offers the procured heart to the patients who are in the Designated Service Area (DSA) of the same OPO as the heart is (Zone DSA); if no one is matched, the heart will be offered to the patients of Zone A; if still no match is found, it will be offered in hierarchy to patients in Zones B, C, D, and E. At each zone it classifies patients by their health status and then primary and secondary blood type match with the donor heart. Within each classification, patients are ranked by the total waiting time accumulated at that health status (see Appendix A.8 for details).

In addition to the current UNOS practice in allocating donor hearts, we considered three additional heart allocation policies based on modifications of the current practice. Specifically, Policy I preserved the current prioritization rule but combined Zones A, B, and C into one zone. Policy II preserved the current prioritization rule but changed the priority of health status from 1A>1B>2 to 1B>1A>2. Policy III preserved the current allocation prioritization but prioritized waiting time over health status. Furthermore, we provided a framework to analyze the fairness of allocating donor hearts by adapting similar concepts in the context of general resource allocation with a single decision maker and multiple self-interested players.

1.2 Methods

Because the heart allocation system is complex with several components such as queues and allocation schemes, we designed a simulation model to represent its behavior. Data from several

sources is used to calibrate and validate the model from 2006, the last year in which changes to the heart allocation policy were made (Kobashigawa et al., 2015), to the end of 2014. Patient records for 30,394 adults who are reported in the UNOS database were used. Among these patients, 2623 died while waiting on waiting list and 17,667 went under transplantation. Also the SRTR annual data reports were used to obtain more detailed information about the patients on the waiting list, as well as the organ donation process (Colvin-Adams et al., 2015). Patient survivals were estimated using risk adjustment models provided in the SRTR database (Scientific Registry of Transplant Recipients, 2015a).

1.2.1 Overview of the Model

In order to design a flexible model to test the performance of a broad class of allocation policies, we developed a simulation model of the heart allocation process on a daily basis. The simulation model consists of six main modules: patient arrival, heart arrival, patient's health status change, pre-transplant survival, heart allocation, and post-transplant survival. Each module consists of several sub-modules interacting together to simulate the allocation system (1.1).

Patient Arrival Module

This module generates patient arrivals to the waiting list and assigns various clinical and demographic attributes according to conditional distributions. We modeled patient arrivals as a nonstationary Poisson process (commonly used for modeling arrivals (Gallager, 2013)) with the arrival rate depending on year. Daily arrival rates for the patient arrival process were estimated by dividing the yearly arrival rates by 365 (see Appendix A.9 for sensitivity analysis on patient arrival rates). We validated the model by comparing the outcomes generated by the model with that observed in historical data. Each patient joining the waiting list has several characteristics and attributes such as age group, gender, disease type, ethnicity, blood type, region, ventricular assist device (VAD) status, pre-transplant (PTX) status, waiting time, and health status. UNOS considers more than 70 disease groups for classifying the patients. Because the sample sizes in each group were not enough to design statistical distributions, we aggregated these 70 groups into 9 broader groups according to the organ data source of UNOS (Appendix A.1). At the time of listing, each patient is assigned with one of four health statuses used by UNOS to represent the health condition of a patient joining the waiting list. For details on medical criteria to assign a patient's health status

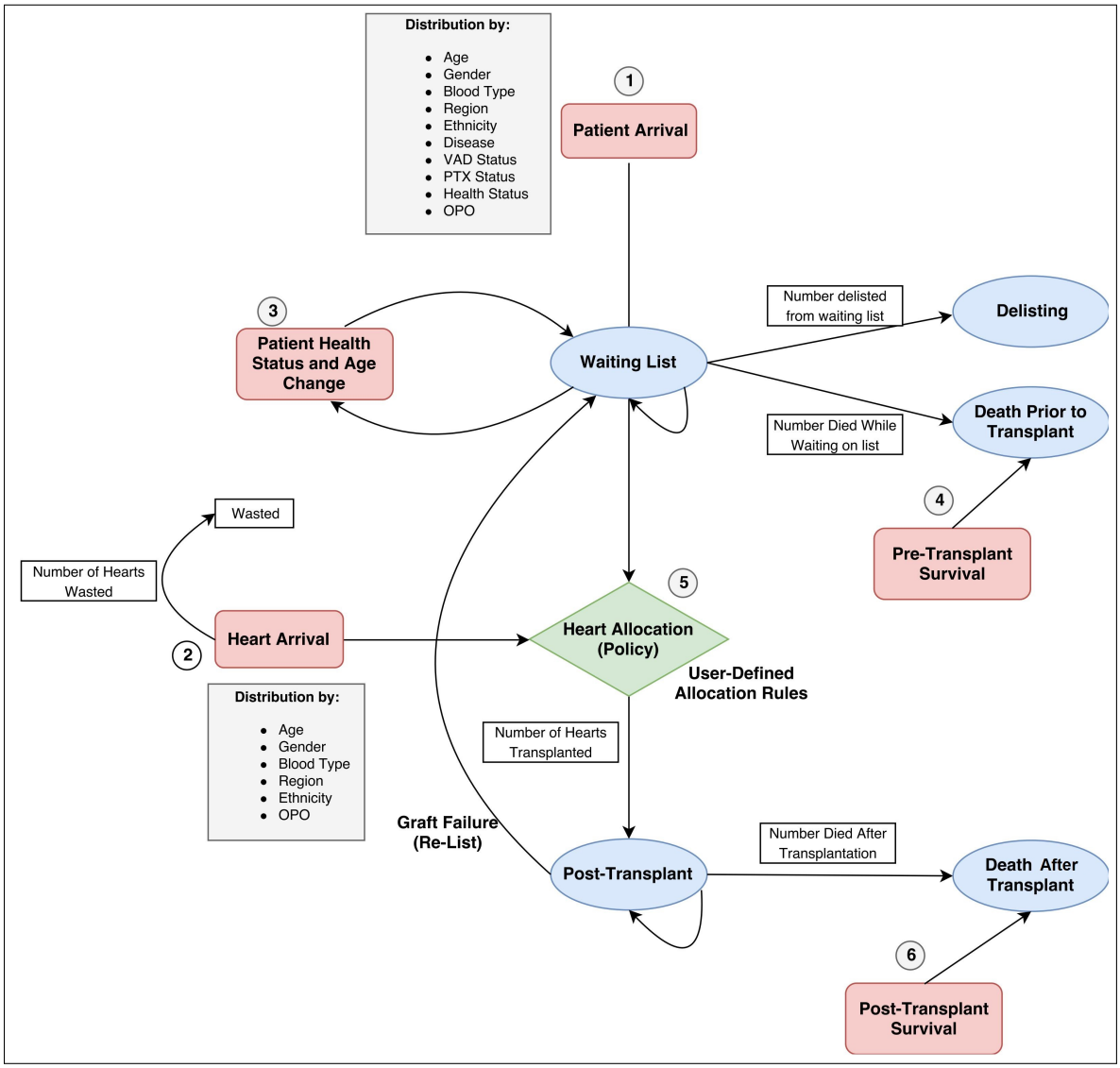

Figure 1.1: Overview of the Simulation Model of Heart Transplantation Waiting List

see Appendix A.1.

The patient arrival module considers some hierarchal and conditional distributions to assign attributes to patients (Figure 6 in Appendix). At the first level, regression was used to test the time-dependency of each attribute and then the Chi-squared independence test was used for each pair of attributes to assess the dependency among attributes. Among all the attributes, disease group, VAD status, PTX status, gender, and arrival rates depended on calendar year. The distribution of each of these attributes for each calendar year was generated based on historical data. Heart status and age distributions were conditioned on disease group and the conditional distributions derived from historical data. After obtaining the distribution of age group conditioned on the disease type, patient age was generated from a continuous uniform distribution for each age group. Ethnicity and blood type are conditioned on gender, and their distributions were derived based on gender distribution. The conditional region distribution was obtained using annual arrival rates. In order to estimate the conditional distributions for each OPO, we aggregated the patient arrivals of all the hospitals in that OPO. Hence, when a patient's region was determined, the patient's OPO was generated according to the conditional distributions (Figure 6 in Appendix). Appendix A.2 elaborates on statistical dependency tests and creation of such hierarchy.

Heart Arrival Module

This module generates a newly donated heart and assigns its attributes that will be used in the allocation process. Similar to the patient arrival module, each donated heart has several attributes such as donor age, gender, blood type, region, ethnicity, and OPO.

Donated hearts arrive according to a nonstationary Poisson process varying by year, and the daily arrival rates are estimated by dividing the yearly rates by 365 (see Appendix A.9 for sensitivity analysis on heart arrival rates). UNOS datasets consider hearts from pediatric and adult donors as the source for donated hearts. As we only considered the hearts from adult donors, we adjusted the yearly arrival rates of hearts to account for this issue, as well as heart wastage. We did not include the decision processes of patients in accepting/rejecting the offered heart, which depends on the patient and heart characteristics, as well as geographical remoteness. However, extending our simulation to incorporate such decisions is straightforward. Conditional arrival distributions for

each heart attribute were estimated from historical data. Similar to the patient arrivals, at the first level, the time-dependency of each attribute was tested using regression. Results showed that blood type, age, and ethnicity depend on calendar year, and each distribution was estimated via historical data. The Chi-squared test was then used to analyze the dependency of each pair of attributes in the heart arrival process to create the second level conditional distributions. At the second level, donor region, and gender depended on blood type and age, respectively (Figure 7 of Appendix). Appendix A.3 elaborates on statistical tests and conditional distributions.

Patient Health Status Change Module

UNOS considers four medical urgency (health) statuses for the patients on the waiting list: 1A, 1B, 2, and Inactive. Health status 1A is for the patients with the most urgent health status. These patients are mostly in hospitals requiring multiple intravenous (IV) medications and have some sort of mechanical assist devices in their heart. Health status 1B is for the patients with less urgent health status, who could be possibly at home using left ventricular assist devices (LVADs) or multiple IV medications. The least urgent patients are assigned with the health status 2. A patient who has already been evaluated and accepted by a transplant center, but cannot receive a heart, is assigned with the Inactive health status. For instance, if a patient has another active illness or infection that can possibly jeopardize the transplant process, she will be assigned with this health status. Requirements for each health status are described in detail in OPTN policies (Organ Procurement and Transplantation Network, 2015) (see Appendix A.1 for more details). However, the health status of a patient may change while waiting for transplant. We modeled the daily health status progression of patients on the waiting list as a Markov chain and used UNOS/SRTR datasets to estimate its transition probability matrix via maximum likelihood estimator (Ross, 2014). In particular, we used the frequency of health status changes between each pair of health statuses over time. Therefore, the module observes the health status of each patient at the start of each day and determines her health status at the next day according to a transition probability matrix. This module was validated by comparing the portion of patients in each health status produced by the model with that observed in historical data (Table 20 in Appendix A.4).

Pre-Transplant Survival and Delisting Module

In the absence of transplantation, removal of a patient from the waiting list may be due to death or delisting. Different allocation policies induce different death and delisting distributions. Therefore, in order to study the impacts of allocation policies on waiting list outcomes, one cannot directly use historical data for death and delisting distributions (van den Hout et al., 2003). We estimated the probability of death via Cox proportional hazard models. In particular, we used the risk adjustment models of SRTR for estimating death probabilities (Scientific Registry of Transplant Recipients, 2015a). We included all covariates of the Cox model regardless of statistical significance because the magnitude of the proportional hazards is more important. The baseline hazard function was estimated from the Centers for Disease Control and Prevention (CDC) datasets (Centers for Disease Control and Prevention, 2015). Appendix A.6 provides details regarding pre-transplant survival.

Delisting from the waiting list may occur as the patient has clinically improved or became too ill to transplant. Annual number of delisted patients was used to estimate yearly delisting distributions. Also, Chi-squared tests revealed a significant correlation between delisting and health status. Therefore, we produced annual delisting distributions for each health status (Appendix A.5). Death and delisting modules were validated by comparing the outcomes produced by the model with those observed in historical data. This module at the start of each day generates the probability of death and delisting for each patient and updates the list accordingly. If none of these events happen, the health status, waiting time, and age of the patient is updated and she moves to the next period (day) (see Appendix A.6 for details).

Heart Allocation Module

Upon procurement of a donor heart to the system, this module ranks the patients on the waiting list and offers it to the highest ranked patient. Because one of the purposes of this study was to analyze the performance of any allocation policy, we used object-oriented programming to create a flexible framework such that any combination of attributes could be used to rank the patients. The current UNOS allocation rule was used as the baseline. With a few exceptions, the allocation process uses the following hierarchy. Once a heart is procured in an OPO, it is offered to a suitable candidate (based on prioritizing health status and considering primary and then secondary blood

type match with the donor) that is registered on the waiting list of the same OPO. If the heart is not matched or accepted at the procurement OPO, it is offered to larger areas with a hierarchy until it is accepted and a match is found (see Appendix A.8 for details).

Post-Transplant Survival Module

In the model, after receiving a donor heart, patients enter the post-transplant phase. This module keeps track of these patients and estimates their survival. To that end, we used the Cox proportional hazard models reported in SRTR database to estimate the death probabilities after transplantation (Scientific Registry of Transplant Recipients, 2015a). Similar to the pre-transplant survival module, all covariates were incorporated regardless of their statistical significance, and the baseline hazards were estimated via CDC database (Centers for Disease Control and Prevention, 2015). Therefore, at the start of each day, this module generates the probability of death for each patient after transplantation and if a patient dies in a period, both the patient and graft are removed from the system as organs are never transplanted more than once. Note that, however, we did not consider graft survival and instead considered the patients who relist (after transplanted with a heart) in the patient arrival module as UNOS datasets provide the arrival of patients demanding a re-transplant (see Appendix A.7 for details).

1.2.2 Allocation Policies

Policy I: The geographical configuration of zones is a critical aspect in the heart allocation system. An ideal zone is a geographically small one with a large population as the likelihood of finding a match is higher and transportation time is short. We propose a three-tiered zone allocation system: If a donor heart is matched with no one in its DSA, it is offered to Zone 1 (union of Zones A, B, and C of UNOS allocation rule). Similarly, if it is not matched with a patient in Zone 1, it is offered in hierarchy to patients in Zone 2 (Zone D of UNOS allocation rule) and Zone 3 (Zone E of UNOS allocation rule). Note that in each zone we considered the same health status, blood type match, and waiting time prioritization rules as UNOS. The rationale behind combining Zones A, B, and C to form Zone 1 is that the 4- to 6-hour cold ischemic time for a heart is equivalent to approximately 1,500 air-line miles (Scientific Registry of Transplant Recipients, 2015b) (Zone C also contains all transplant hospitals within 1,500 miles of the donor hospital). A similar approach is proposed for patients who are multi-listed for kidney transplantation (Ata et al., 2016) (see Appendix A.8 for

details). In Appendix A.9, we conduct sensitivity analysis on priority zones combinations.

Policy II: To prioritize patients according to their health status, UNOS gives the first priority to health status 1A, the second priority to health status 1B, and finally the third priority to health status 2. The patients assigned with health status 7 (Inactive) are not considered in the heart-patient matching algorithm. This allocation rule gives priority to patients with a higher medical urgency status. However, it has led to a significant imbalance in the distribution of donated hearts. In particular, more than 67% of all transplants correspond to status 1A while status 1A patients are only 10% of those on the waiting list. Moreover, less than 30% of all transplants correspond to health status 1B while these patients compromise 40% of the waiting list. This disparity has caused some patients in status 1B relocate together with their families to other regions with shorter waiting time (Stevenson, 2015). Also, prioritizing the sickest patients may not be optimal as they may experience a shorter post-transplant survival compared to status 1B patients. Thus, in Policy we followed the UNOS allocation system except that status 1B was prioritized over 1A in each classification (see Appendix A.8 for details).

Policy III: In the current UNOS allocation policy, waiting time is the last priority. Prioritization based on waiting time is unclear as van den Hout et al. (2003) wrote "waiting time as an allocation factor has been a point of discussion for more than a decade." Policy considered the UNOS allocation rule except that in each zone waiting time is prioritized over health status, i.e., considering primary and secondary blood type match, patients are ranked first by longer waiting time (see Appendix A.8 for details).

1.2.3 Model Validation

In order to compare the outcomes of the proposed allocation policies, we wanted to ensure that the difference between policy outcomes is because of the real performance differences of policies rather than randomness in the model. We used the standard variance reduction techniques to decrease the effects of randomness in outcomes of allocation rules (Shechter et al., 2005). Because patient and donor heart arrivals were assumed to be independent of the allocation policy, one stream of random numbers was used to produce the patient population and another stream of random numbers was used to produce the donor hearts across all policies.

Once we combined all the modules, we validated the simulation model by comparing its outcomes with the historical data for several measures, such as the number of patients on the waiting list at the end of each year, yearly patient arrivals, yearly heart arrivals, number of transplants performed at each year, number of deaths on waiting list at each year, and 1- and 5-year post-transplant survivals. The simulation was run 30 times using the current UNOS allocation policy and the average and standard deviation of the 30 replications were reported (Table 1.1). We also conducted statistical t-tests to check the statistical difference between real data and simulation outputs (Table 1.2).

1.2.4 Fairness Analysis

Fairness is extensively studied in resource allocation problems involving a central decision maker and multiple players where each player receives a utility based on the allocation chosen by the central decision maker. In this context, the utility of a patient could be her post-listing life expectancy or quality-adjusted life expectancy (one might also include perioperative pain and distress). The utilitarian principle implies that an efficient allocation is one that maximizes the sum of the expected utilities of the players, i.e., post-listing life expectancy of the patient population (Rawls, 2009). However, the decision maker may settle on the utility allocation which incorporates fairness considerations. In this work, we considered two axiomatically justified notions of fairness: proportional fairness and max-min fairness (Young, 1995; Sen et al., 1997). The idea of max-min fairness is to prioritize the players that are the least well off, so as to ensure the highest minimum expected utility that each player derives (Rawls, 2009; Kalai and Smorodinsky, 1975). Proportional fairness is the generalization of Nash solution where multiple players are involved (Nash, 1950). In this fairness scheme, a transfer of resources is justified if the gainer utilities increase by a larger percentage than loser utilities decrease. That is, an allocation rule is proportionally fair, if compared to any other allocation rule, the aggregate proportional change is non-negative.

Suppose there are N players and U_j denotes the utility of player j and ω_j is a weight such that $\sum_{j=1}^{N} \omega_j = 1$. Note that since humans are equally precious, in the fairness analysis, we considered

equal weights for all the patients (i.e., $\omega_j = \frac{1}{N}$). Define

$$M_\alpha(U,\omega) = \begin{cases} \prod_{j=1}^{N} U_j^{\omega_j} & \text{if } \alpha = 1, \\ \left(\sum_{j=1}^{N} \omega_j U_j^{\alpha-1}\right)^{\frac{1}{1-\alpha}} & \text{if } \alpha \geq 0, \alpha \neq 1, \end{cases} \tag{1.1}$$

and let π denote an admissible policy. To find the fairest allocation, we considered a decision maker who seeks to find a policy that yields the maximum value for the expected value of fairness measure defined in (1.1), that is, a policy maker seeks a policy that maximizes the following quantity

$$v^\pi(s_0) = \mathbb{E}^\pi \left\{ M_\alpha(U,\omega) \mid s_0 \right\} \tag{1.2}$$

where s_0 is the initial patient population and expectation $\mathbb{E}^\pi \{\cdot\}$ is taken over all randomness in the system. Let π^* be the policy that maximizes formulation (1.2). Computing π^* requires solving Bellman optimality equations and since the state space is extremely huge (may increase exponentially) , the current methods do not apply (Puterman, 2014). Thus, one needs to use approximate solutions by approximate dynamic programming or fluid scaling (Powell, 2007), which is beyond the scope of this study.

However, the fairness analysis studied in this section only provides the fairness ranking among the policies and it reveals nothing about the fairness measure for the optimal fair policy. In order to study the fairness in the heart allocation context, we considered a family of α-fairness that include both max-min and proportional fairness as special cases. In particular, $\alpha = 1$ and $\alpha \to \infty$ correspond to proportional and max-min fairness, respectively. Therefore, for a given allocation policy π and initial patient population s_0, we defined a metric $(v^\pi(s_0))$, which measures the fairness of allocation policies based on the α-fairness concept, i.e., assigns a numerical value to policy π. Then, an optimal α-fair policy can be found by searching over all possible allocation policies.

In our implementation, we considered post-listing life expectancy as the utility for each patient, defined as the expected life years that each patient gains from when he/she joins the waiting list, until he/she dies. In order to estimate $v^\pi(s_0)$ for a given policy π, we created the initial patient population s_0 according to the waiting list distribution in 2006 and simulated the system until 2014. Recall that we generated the same patient population and donor heart for all allocation policies. For

each patient in the system (those who were in the system and arrived through the entire horizon), we calculate the post-listing life expectancy as we know when he/she joined the system and when he/she died. A patient may die while waiting for transplant or after transplant. For patients who went under transplantation, after our simulation ends at 2014, we let the simulation of post-transplant patients continue until all died. For patients who are still alive at the end of simulation horizon, we let the simulation run until all die. This approach assumes that patients on the waiting list at the end of the simulation horizon do not go under transplantation. However, this assumption is not restrictive as this procedure (i) can easily incorporate the heart arrivals in the future, and (ii) holds for all policies, therefore, their rankings remain intact. We removed the patients delisted from the analysis as we could not locate historical data on their survival distribution. We estimated the expected values in formulation (1.2) by the Monte Carlo simulation, i.e., we simulated the system and in each simulation record the total utility of the entire patient population and take an average over all runs. For each of the four considered policies, after simulating the policy, we calculated (1.2) for both cases $\alpha = 1$ and $\alpha \to \infty$. These values are reported in Table 1.4. Note that our simulation uses pre- and post-transplant Cox survival models to estimate the probability of death at each time period for patients on the waiting list and those on the post-transplant phase. We validated these models, which are the base for estimating post-listing life expectancies, by comparing our simulation results with those in real data (Tables 1.1, 1.2, and 1.3).

1.3 Results

This section provides the numerical results of our analysis, including validation of the model and comparison of proposed allocation policies in terms of efficiency and fairness. Table 1.1 shows the result of the simulation model outcomes along with UNOS reports from the start of 2006 to the end of 2014. In particular, we reported the average and standard deviation of each output, as well as the percentage of relative difference between historical data and model outputs. The results of the simulation such as new patients listed, donor hearts, transplants performed, and delisted patients closely match those observed in historical data for almost all years. Specifically, we conducted statistical t-tests (Table 1.2) and our results show that simulation outputs are not statistically different than real data. Our model slightly overestimated the pre-transplant deaths and consequently underestimated the number of patients on the waiting list. All in all, the model

mimics all the trends in different outcomes appropriately.

Table 1.1: Validation of Model Results

Outcome Measure	**2006**	**2007**	**2008**	**2009**	**2010**	**2011**	**2012**	**2013**	**2014**
New Patients Arrival									
UNOS	2554	2633	2825	2966	3029	2894	3115	3373	3730
Model Mean ($\bar{x}$)	2586.3	2733.73	2953.7	3035.83	3129.5	2907.36	3293.83	3544.36	3816.1
Model Standard Deviation (s)	50.53	61.03	57.88	59.24	63.23	61.89	52.84	49.35	67.28
Difference (%)	1.24	3.68	4.35	2.3	3.21	0.45	5.42	4.83	2.25
Diseased Donors Arrival									
UNOS	1893	1938	2100	1958	2080	2084	2165	2307	2437
Model Mean ($\bar{x}$)	1897	1944.5	2107.6	1968.03	2072.1	2080.1	2158.53	2295.76	2429.43
Model Standard Deviation (s)	36.81	42.3	42.61	49.22	52.61	48.17	43.62	45.58	55.49
Difference (%)	0.21	0.33	0.36	0.5	-0.38	-0.18	-0.29	-0.48	-0.31
Deaths While on Waiting List									
UNOS	331	279	299	301	263	287	269	285	309
Model Mean ($\bar{x}$)	323.66	311	315.2	322.26	295	309.66	303.13	279.15	295.84
Model Standard Deviation (s)	23.23	22.35	26.54	28.37	22.37	30.59	26.6	25.36	26.84
Difference (%)	-3.51	5.45	5.32	-3.87	16.25	8.54	-5.4	-5.88	-3.16
Number of Patients on the Waiting List									
UNOS	2551	2417	2466	2712	2904	2847	3063	3332	3400
Model Mean ($\bar{x}$)	2504.23	2389.1	2224.4	2433.1	2565.8	2431.36	2606.36	2847.73	3044.06
Model Standard Deviation (s)	98.25	120.34	126.11	130.96	149.69	174.65	155.08	133.34	165.92
Difference (%)	-1.86	-1.16	-10.86	-11.46	-13.18	-17.09	-17.51	-17	-11.69
Transplants Performed									
UNOS	1870	1877	1796	1851	1967	1944	1998	2123	2241
Model Mean ($\bar{x}$)	1897	1944.5	2107.6	1968.03	2072.1	2080.1	2158.53	2295.76	2429.43
Model Standard Deviation (s)	36.81	42.3	42.61	49.22	52.61	48.17	43.62	45.58	55.49
Difference (%)	1.42	3.47	14.78	5.94	5.07	6.54	7.43	7.52	7.75
Delisted Patients									
UNOS	524	604	690	570	607	736	641	711	893
Model Mean ($\bar{x}$)	520.43	609.26	694.96	569.33	598.26	740.23	640.66	710.16	890.8
Model Standard Deviation (s)	22.89	23.46	28.17	25.43	21.51	28.79	22.94	23.88	29.83
Difference (%)	-0.68	0.86	0.71	-0.11	-1.45	1.24	1.5	0.44	0.87

Note. UNOS= United Network for Organ Sharing. Mean ($\bar{x}$) and standard deviation (s) are the results of 30 replications.

Table 1.2: p-values of t-test for Comparing Real Data and Simulation Outputs

Measure	New Patients Arrival	Diseased Donors Arrival	Deaths While on Waiting List	Number of Patients on the Waiting List	Transplants Performed	Delisted Patients
p-value	0.58	0.99	0.1	0.14	0.07	0.99

Table 1.3 shows 1- to 5-year post-transplant survival rates produced by simulation and UNOS data for patients transplanted between 2006 and 2014. The model predicts the post-transplant survival rates accurately, especially 3- to 5- year post-transplant survival rates.

Table 1.3: Survival Rates of Patients Transplanted During 2006-2008

Survival	1-Year Survival Rate	2-Year Survival Rate	3-Year Survival Rate	4-Year Survival Rate	5-Year Survival Rate
UNOS Reports	0.89	0.85	0.82	0.79	0.75
Model Mean ($\bar{x}$)	0.93	0.88	0.84	0.8	0.75
Difference (%)	4.3	3.4	2.38	1.25	0

We compared the three policies described in the "Allocation Policies" section along with the UNOS practice in terms of efficiency and fairness. We considered a policy to be the most efficient if it achieves the least number of total deaths (pre- and post-transplant deaths), and closest to a fair (proportional or max-min) policy if yields the highest value for the fairness measure defined in formulation (1.2). Figure 1.2 shows pre-transplant, post-transplant, and total patient deaths for each proposed policy from 2006 to 2014. The total number of deaths in the study period for the current UNOS policy is 3788. However, this number is 3419, 3514, and 4148 for the Policies I, II, and III, respectively. Policy I which combines Zones A, B, and C outperforms other policies. In fact, Policy I reduced the expected number of deaths by 319. Also, policy II outperformed the UNOS policy. Moreover, the performance of Policy III was worse than the UNOS practice. The results indicate that prioritizing health status 1B over 1A and prioritizing waiting time are suboptimal.

Table 1.4 shows the results for $v^{\pi}(s_0)$ to analyze the fairness of proposed policies. Intuitively speaking, a higher value of $v^{\pi}(s_0)$ for proportional (max-min) fairness indicates that the allocation policy π is closer to an optimal proportional (max-min) fair policy for the initial population s_0. In particular, in an optimal proportionally fair policy, the aggregate proportional change in post-listing life expectancy of patients compared to any other allocation rule is non-negative. Also, an optimal

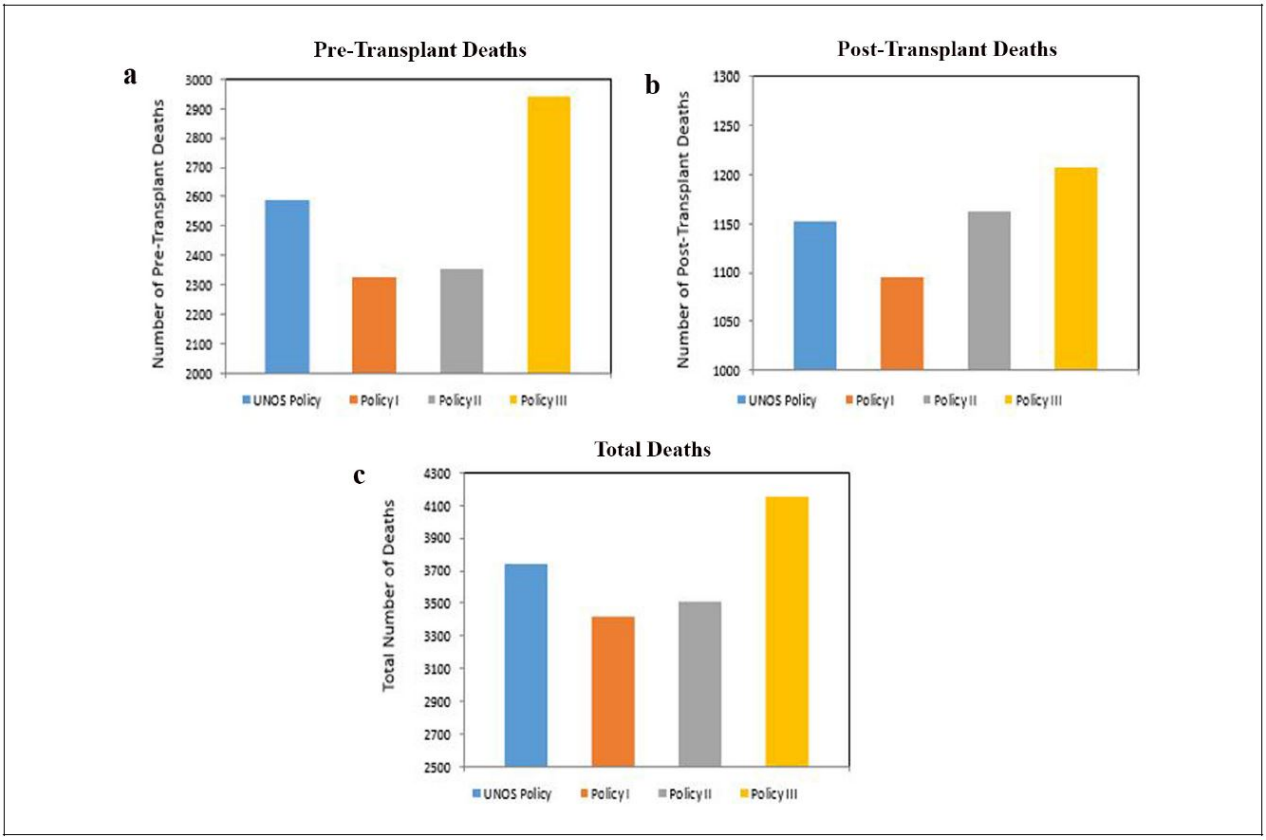

Figure 1.2: Comparison of Pre-transplant, Post-transplant, and total number of deaths for UNOS, Policy I, Policy II, and Policy III (years: 2006-2014)

Table 1.4: Results of Fairness Comparison of Policies

Policy	Proportional Fairness Measure	Max-Min Fairness Measure
UNOS	2209.28	108.76
Policy I	2356.5	109.45
Policy II	2294.4	109.77
Policy III	1921.92	108.86

Note. The proportional and max-min fairness measure columns indicate the values of $v^{\pi}(s_0)$ defined in formulation (1.2) for $\alpha = 1$ and $\alpha \to \infty$, respectively. Note that a higher number implies a smaller gap from the optimal policy. We used life days as a metric for each individual's utility.

max-min fair policy obtains the largest post-listing life expectancy for the patients who have the least life expectancy estimates, compared to any other allocation rule. Results show that Policy I is closer to an ideal proportional fair policy among others as it has the highest fairness measure. Also, our results show that in terms of proportional fairness, UNOS policy outperforms Policy III, which prioritizes based on waiting time. Moreover, our results show that all the proposed policies perform similarly in terms of max-min fairness.

1.4 Conclusion and Discussion

The problem of optimally allocating limited donor hearts to the patients on the waiting list is one of the top priorities in heart transplant management as the imbalance between supply and demand has increased over the last decade. Simulation models can help policy makers and medical professionals to analyze allocation rules without actually implementing them. We developed a stochastic simulation model of heart allocation system and validated it in several dimensions by comparing the model outcomes with historical data from 2006 to 2014. We also adapted two well-accepted fairness notions to develop a framework to analyze the fairness of allocation policies in the context of organ allocation. In addition to the UNOS allocation rule, we considered three additional policies: (1) one that combines Zones A, B, and C, (2) one that prioritizes status 1B over 1A, and (3) one that prioritizes candidates based on waiting time. Our results showed that the policy that combines Zones A, B, and C could avert 319 total deaths (pre- and post-transplant deaths) and was closer to an ideal proportionally fair allocation policy. Hence, it seems that combining these priority zones and broadening the organ sharing area may result in more efficient and fair policies. Moreover, combining zones is easy to understand and straightforward to implement. Our

results have a similar message with those observed for the Eurotransplant heart allocation simulation model, where international organ exchange is estimated to reduce waiting list mortality in different countries by 1.9% to 12.4% (van den Hout et al., 2003). Studies on other organs also found that broadening the organ sharing area by multiple listing can significantly reduce the mortality rate (Ata et al., 2016). Our results for the fairness analyses revealed that proportional fairness may be of more interest to measure the fairness of organ allocation policies as the max-min fairness measure for different policies was not significantly different. Our results show that this is due to the fact that the post-listing expected life of the very sick patients does not significantly change by different policies.

Our results indicated that the simulation model produced outcomes close to historical data, which increases the confidence that the model can reasonably approximate the quantities of interest to transplant community. In particular, one can use this model to analyze the performance of other allocation policies and derive insights on how allocation policies change the waiting list population dynamics. However, this study has several limitations, and by addressing them, we can develop a more accurate decision-making tool to evaluate allocation rules.

First, although detailed data on patient and donor heart arrivals were available in the UNOS/SRTR datasets for each region, these data were not available for each transplant center or OPO. Therefore, we generated appropriate distributions for each region and assigned the OPO of a new patient or donor heart based on a uniform distribution. The validation results show that patient and heart arrivals closely match historical data. Second, since UNOS/SRTR datasets reported the frequency of health status change independent of other patient attributes, we constructed a Markov chain in the patient health status change module based only on health status and ignored other dependencies such as age, gender, and waiting time. The validation of this module indicated that the distributions produced by the model are statistically the same as observed data. Third, because detailed data for heart wastage was not available in UNOS/SRTR datasets, we adjusted the heart arrivals to compensate heart wastage. Fourth, we did not model the patient choice in accepting/rejecting the offered heart. However, adding such a feature to the model is straightforward upon availability of data. Fifth, we considered post-listing life expectancy in analyzing the fairness of policies and did not consider quality-adjusted life expectancy or cost. The cost component, which includes pre- and

post-transplant care, may impact policy recommendations.

Chapter 2

Optimal Allocation Rules for Heart Transplantation

Summary: Identifying an efficient and fair allocation of limited donated hearts to patients on the waiting list is one of the top priorities in heart transplantation management. The recent heart allocation rule by the United Network for Organ Sharing (UNOS) has emphasized medical urgency to address the heart transplant crisis by further dividing the previous sickest patient group into three subgroups. However, there is significant debate on optimality and fairness of such policy. We undertake a rigorous study to address this debate. In particular, we quantify the price that the society pays for following a medical urgency approach, which favors the sickest patients, compared to a utilitarian approach, which seeks to maximize total life years (LYs). Our results, produced by a validated simulation model, reveal that said price is 8% of total LYs and increases to 10% by considering a broader regional sharing aligned with four hour cold-ischemic time for heart. In fact, we provide concrete numbers for pre-transplant death and LYs broken down for each health and age group to further shed light on this debate. We also consider relevant objectives in transplantation and our results show that the "optimized" utilitarian policy outperforms that of the medical urgency one in other measures. Our analysis provides novel insights on optimal patient allocation and sheds light on the debate around this challenging problem. Furthermore, the UNOS Heart Subcommittee plans to develop a scoring system for heart. We develop a heart allocation system which achieves a similar performance to the optimized utilitarian policy in terms of LYs, and pave the way for

designing future heart allocation systems.

2.1 Introduction

Motivation. Heart failure (HF) is a chronic and progressive condition in which the heart is unable to maintain the blood flow. Over 5.8 million people in the U.S. are suffering from HF and each year around 550,000 new cases are diagnosed (Bui et al., 2011). For late-stage HF patients, heart transplantation is a life-saving treatment (Stevenson, 2015). Patients join a waiting list to receive a cadaveric donor heart. Since 2004, the number of new adult candidates on the waiting list has increased by 51%. The number of patients actively awaiting heart transplant has increased by 90% from 2004 to 2015. However, the donation rate remains flat with 2.8 donations per 1,000 deaths in 2015 (Colvin et al., 2017). As a result of the shortage of supply, more than 3,000 patients died on the heart transplant waiting list while waiting for a heart offer during 2006-2014 time horizon. This shortage of supply raises an allocation question: How does one prioritize patients on the waiting list in an efficient and fair manner?

The National Organ Transplant Act enacted new rules to ensure the fair and equitable distribution of donated organs (Davis and Delmonico, 2005). Furthermore, certain priority rules for patients on the waiting list should be used in the allocation process to find the best match for an available donor organ (Organ Procurement and Transplantation Network, 2015). Therefore, designing such allocation policies is extremely challenging and faced with such issues, UNOS has revised the organ allocation policies periodically over time (Colvin-Adams et al., 2012). Over the past two decades, heart allocation policies have evolved due to the evolution of the clinical profile of end-stage HF patients. The initial heart allocation policy, approved in 1988, was a two-tiered rule such that donor hearts were allocated based on medical urgency and waiting time (Colvin-Adams et al., 2012). In 1998, UNOS revised the latest policy and restructured it into a three-tiered urgency-based system (status 1A, 1B, and 2) which prioritized sickest patients with shorter survival rates (Renlund et al., 1999). In July 2006, UNOS allowed a broader regional sharing of donor hearts keeping the three-tiered urgency system intact (Singh et al., 2012). Recently, UNOS extended the three-tiered system to a seven-tiered one, which is mainly medical urgency driven (Meyer et al., 2015). The seven-tiered policy was approved by the OPTN/UNOS in December 2016 and is in effect since January 2018

(Davies et al., 2017).

However, it is not clear that the current allocation policy is optimal for the transplant community, and there are still significant discussions regarding enhancing its efficiency and fairness. In fact, there are still debates among surgeons and policy makers in accepting the benefits of the seven-tiered policy for the patient population (Organ Procurement and Transplantation Network, 2016a; Stevenson et al., 2016). Although the new proposal helps to reduce pre-transplant mortality rates among sicker patients, it may worsen the post-transplant outcomes as it trades off a potential decrease in waiting list mortality for an almost certain increase in post-transplant mortality.

Main Contributions and Results: In order to address the aforementioned debates, we quantify the extent that LYs can be improved by shifting attention from a medical urgency approach, which favors the sickest patients, to a utilitarian approach, which considers total LYs of the population. In particular, we undertake the first study that investigates an optimal and fair dynamic allocation of limited cadaveric hearts to heterogeneous patients on the waiting list for both perspectives rigorously. Previous attempts are ad-hoc, i.e., the proposals from OPTN/UNOS Heart Subcommittee are evaluated via Thoracic Simulation Allocation Model (TSAM), which is a simulation model of the waiting list, and decisions are made based on simulation results, among other factors. Our results reveal that the said extent is around 8% of the total LYs and shed light on the trade-off between life years gained and the number of deaths for each patient group by providing concrete numbers produced by a validated simulation model. In addition, the said extent increases to 10% if a broadening of regional sharing is allowed in line of four-hour cold ischemic time for heart. Our analysis shows that the improvement is mostly due to the post-transplant component of the total life years objective function. In fact, the UNOS policy performs slightly better than optimized utilitarian policy (proposed policy) in terms of pre-transplant LYs, but its post-transplant performance is significantly worse than that of the proposed policy. The analysis of the proposed allocation rule reveals that its advantage emanates mainly from offering donor hearts away from the sickest patients and older ones toward healthier and younger patients. Our results also show that the benefits from change in health prioritization is more than that of age prioritization. Furthermore, our work sheds light on the current debate around prioritization of patients with Ventricular Assistance Device (VAD). In particular, our results show that the proposed policy does not prioritize patients with VAD, similar

to UNOS.

We also consider other relevant objective functions and several methods developed for the total LYs objective. In particular, policies produced by the utilitarian approach outperform UNOS policies in terms of mean and standard deviation of waiting time among patient classes, which are measures of fairness in transplantation. Specifically, the average waiting time can be reduced to half by following the utilitarian approach. Moreover, if the objective is to minimize pre-transplant mortality (a true medical urgency objective), our results show that UNOS or UNOS 7-tiered policy is near-optimal.

The UNOS Heart Subcommittee plans to develop a scoring system for heart allocation similar to other organs such as kidney, liver, and lung (Meyer et al., 2015). We design such a heart allocation scoring system (HAS), which involves two main challenges: (i) identifying relevant score components, and (ii) estimating the coefficient of each component. We consider numerous sets of relevant score components, use a data-driven approach to estimate the coefficients, and choose the best setup. In fact, our proposed HAS policy achieves a similar performance to the optimized utilitarian policy in terms of total LYs.

Finally, our results echo the recent change of heart allocation rules in Eurotransplant and France, where post-transplant survival is included in prioritization (Smits et al., 2017). Moreover, post-transplant survival is included in UNOS allocation rules for other organs. For example, UNOS lung transplantation allocation rules consider post-transplant survival and age (Organ Procurement and Transplantation Network, 2015). Historically, a paradigm shift happened for kidney transplantation: around two decades ago, the allocation rules prioritized the sickest patients but now they do include post-transplant survival (Organ Procurement and Transplantation Network, 2015). In fact, in "The Complete Lives System" which seeks to establish an ethical framework to allocate scarce treatment to a patient population, Persad et al. (2010) do not recommend a sickest-first prioritization as it deprives treatment from other patients who may have benefited more (a utilitarian approach). They also mention that when every patient cannot be saved, saving the sickest one is "flawed," and recommend an explicit preference for the young.

2.2 Related Work

Two streams of work are related to our study: organ allocation and control of network queuing systems.

Organ Allocation. We briefly review optimization/simulation work related to organ allocation from a patient's and policy maker's perspective and then review related work on heart transplantation. One stream of work in organ allocation focuses on finding the optimal time to accept an offered organ based on patient/organ characteristics: see, e.g., Ahn and Hornberger (1996), David and Yechiali (1985), and Alagoz et al. (2004, 2007). Our work is different from these studies because we study the organ allocation problem from a policy maker's perspective to find efficient and fair allocation rules. In fact, optimal time to accept an organ is an optimal stopping problem while the allocation problem is an optimization problem on a queuing network. Several studies considered organ exchange programs such as Zenios (2002), and Ashlagi et al. (2011), which do not apply to heart transplantation as organ exchange is not possible.

Transparency in the waiting list, regional redesign, and geographical equity are also addressed in different contexts. For example, Sandıkçı et al. (2008) estimated the price of privacy in liver transplantation; Kong et al. (2010) considered the redesign of allocation regions; Ata et al. (2016) studied the problem of geographical disparities in access to donor kidneys. However, the objective of our work is to find efficient allocation rules by considering fairness constraints and the methods developed in these studies do not apply.

In a series of papers, Su and Zenios (2004, 2005, 2006) examined the impacts of patient choice on (i) organ wastage and waiting times, (ii) efficiency of kidney allocation system, and (iii) post-transplant information asymmetry on the kidney allocation system. We apply two methodologies developed in these studies to heart allocation problem: one that seeks to improve the efficiency by maximizing the total quality adjusted life years (QALYs) of the population, and one that seeks to improve equity by maximizing the minimum QALYs of the patients. Also, Lee et al. (2008) studied the allocation of dialysis capacity for patients with end stage renal disease considering fairness.

Bertsimas et al. (2013) developed a data-driven approximate dynamic programming model to derive efficient policies for kidney allocation to maximize the total life expectancy while considering

fairness constraints. We use this method to estimate the coefficients of numerous collections of point systems that we design for heart transplantation in order to develop a novel scoring system for heart allocation.

Akan et al. (2012) investigated the trade-off between medical urgency and efficiency in liver allocation. A fluid model is used to minimize the total number of patient deaths while waiting for transplant and to maximize total QALYs through a weighted combination of the two objectives. Our work is different from this study in several dimensions: (1) we study the heart allocation problem, where the source of hearts is only from cadaveric donors; (2) The fluid approximation of our stochastic formulation differs from that in Akan et al. (2012). In particular, we consider fairness constraints in formulating the stochastic system and show that the corresponding fluid approximation, which contains integral constraints, has an optimal solution of the priority index type and provide novel insights about the impact of fairness constraints on priority indices. Considering fairness constraints is one of the major approaches to address fairness in organ transplantation (RFI, 2008).

In order to identify an efficient and fair heart allocation rule, simulation models are developed to test the performance of different policies. For example, the TSAM is a model of heart allocation system by UNOS/SRTR, which has been used to evaluate the proposed changes in policy (Scientific Registry of Transplant Recipients, 2015b). van den Hout et al. (2003) developed a simulation model of the Eurotransplant waiting list for heart transplantation to examine potential allocation policies. Hasankhani and Khademi (2017) created a flexible simulation model of the U.S. heart allocation system to compare the performance of several allocation policies. However, simulation models are not able to find optimal allocation rules, which is the focus of this study.

Optimal Control of Queuing Networks. The fluid approximation is extensively used for analyzing stochastic queuing networks for a variety of applications such as communication networks, manufacturing systems, and service management.

Harrison and Zeevi (2005) studied a large call center with several numbers of input flows and agent pools to minimize the expected total personnel costs and abandonment penalties via fluid approximation. Kiani et al. (2019, 2020); Yousefi et al. (2019) used classical techniques for solving MDPs to find optimal appointment scheduling for healthcare systems. Bassamboo and Randhawa (2010)

considered capacity selection in queuing problems with impatient customers who may abandon the system to minimize the total cost. A fluid approximation of the original queue is applied to find the optimal solution. Savin et al. (2005) formulated the problem of allocating capacity in rental systems as a discrete-time MDP and analyzed the structure of the optimal policy of the original stochastic system via fluid approximation. In a single server fluid network, Bäuerle and Rieder (2000) showed that the optimal policy is a priority index policy. Perry and Whitt (2011) studied two queuing systems each having their own designated service pools, where servers of one queue may serve customers of the other queue in the case of unexpected overload. They analyzed the system by approximating it by a fluid model, and described its transient behavior under heavy traffic averaging principle. Meyn (1997) studied the optimal scheduling problem for multiclass queuing network with deterministic routing. It is shown that there is a close connection between the optimization of queuing networks and the optimal control of their corresponding fluid network model. However, our study is different from the literature of controlling queuing systems in several dimensions. For example, (1) If an analogy is made where patients resemble customers and organs resemble servers, in our system the number of servers is not fixed as servers arrive to the system according to a stochastic process and leave permanently upon transplant; (2) There are two sources of abandonment as patients on the waiting list may die or be delisted; (3) Patients on the waiting list may change their class as the health of a patient on the waiting list may change, among other dynamics; (4) The objective is to maximize total pre-transplant (waiting time) and post-transplant life years, which is different from standard objective functions in queuing theory literature.

2.3 Problem Formulation

This section formulates the heart allocation problem as a finite-horizon continuous-time constrained stochastic dynamic program. In particular, we consider a finite-horizon model because UNOS changes allocation policies after a finite time (e.g., 10 years) and a continuous-time model since arrival processes of patients and hearts are random. Patients arrive to the system according to a random process and join a waiting list to receive a donor heart. We consider all patient characteristics that affect the dynamics of the system, as well as pre- and post-transplant survival, e.g., age group, health status, blood type, etc. Also, donor hearts arrive to the system according to a stochastic process and are assigned to patients on the waiting list. We consider all donor heart characteristics

that affect the evolution of the system such as donor age group and blood type. The donor heart characteristics along with patient characteristics determine the (random) post-transplant survival. Let $\mathcal{I} := \{1, 2, \ldots, I\}$ and $\mathcal{H} := \{1, 2, \ldots, H\}$ be the set of patient and heart types.

Upon arrival of an organ, the decision maker offers it to a patient on the waiting list. If the patient accepts the offer, a transplantation is carried out and the patient moves to the post-transplant phase. If the patient declines the offer, the decision maker offers it to another patient on the waiting list and this procedure continues until the organ is accepted or wasted (after several tries).

State Space. We assume that we keep track of N patients in the waiting list and let $p = (p_1, p_2, \ldots, p_N)$ denote the state of all patients, where p_n contains all information about patient n. This assumption is not restrictive because one may consider a large N. The state of patient n is given by $p_n = (i_n, \tau_n, z_n)$, where $i_n \in \mathcal{I}$ denotes the class of patient n, τ_n denotes the time that patient n arrived to the system, and z_n is a binary variable indicating whether patient n has declined the current available heart. The indicator z_n is set to zero upon patient arrival. If a patient declines an offer, z_n becomes 1 such that we do not re-offer the current available heart to the patient. If the available heart becomes accepted or wasted, z_n is set to zero for all patients on the waiting list. Note that we keep track of patient arrival time to calculate his/her waiting time, among others.

Without loss of generality we assume that the dynamics of the system are driven by events. We consider the following events in the system: "patient n arrives," "heart type h arrives," "patient n dies," "patient n delists," "patient n changes class," "patient n accepts offer of heart type h," "patient n declines offer of heart type h," and "heart type h declined $\mathcal{N}$ times," which triggers the event "heart type h is wasted." Therefore, state transitions take place at discrete points in time when an event happens in the system.

Policy makers may face fairness constraints in offering high quality organs to specific groups of patients. Therefore, let b_i^h denote the total cumulative offers of heart type h to patient type i and $b = (b_i^h : i \in \mathcal{I}, h \in \mathcal{H})$. Hence, the state of the system is represented by $s = (p, e, b, t)$, where p is the list of patients containing state of all patients on the waiting list, e is the event type, b is the offer history at time t, and t is the current time. Let $\mathcal{P}$ denote the set of all possible patient lists, $\mathcal{E}$ the set of all possible events, and $\mathcal{B}$ the set of all possible offer histories. Therefore, the state space

of the system can be expressed by

$$\mathcal{S} := \{s = (p, e, b, t) : p \in \mathcal{P}, e \in \mathcal{E}, b \in \mathcal{B}, t \in \mathbb{R}^+\}.$$

Because the state of the system does not change between events, the state trajectory is completely characterized by $\{s_\kappa : \kappa = 1, 2, \ldots, \mathcal{K}\}$, where s_κ is the system state right after the κ^{th} event, and $\mathcal{K}$ denotes the final decision epoch, which corresponds to the end of the planning horizon. We let $t(s_\kappa)$ be the time that event κ occurs, $e(s_\kappa)$ be the type of κ^{th} event, and $b(s_\kappa)$ be the offer history up to the occurrence of κ^{th} event.

Action Space. When an organ becomes available, the decision maker offers it to the patients on the waiting list. Let the event type be "heart type h becomes available." Let $H(s) = \{h\}$ be the set that points to the available heart type, and let $P(s)$ be the set of eligible patients with heart type h when the state of the system is s, e.g., in terms of blood type compatibility, avoiding offer to inactive patients on the list, and proximity consideration. Define $a_n^h(s) = 1$ if the available heart of type h is offered to patient n, and $a_n^h(s) = 0$, otherwise. Let $a(s) := \left(a_n^h(s) : n \in P(s)\right)$ for $h \in H(s)$, the action space reads

$$\mathcal{A}(s) := \left\{a(s) \in \{0,1\}^{|P(s)|} : \sum_{n \in P(s)} a_n^h(s) = 1; h \in H(s)\right\}. \tag{2.1}$$

If an offer is made, $b(s)$ is updated based on patient and heart types.

An offered organ may be declined by a patient. In this case, the organ will be offered to other patients until it is accepted or wasted. Because the cold ischemic time for heart is around four hours and each patient has about an hour to accept or decline the offer, the heart will be wasted after a few offers, e.g., $\mathcal{N} = 4$ (Organ Procurement and Transplantation Network, 2017). Therefore, if the event is of type "patient n declines heart type h offer," patient n is removed from the list of eligible patients, i.e., $P(s) \leftarrow P(s) \setminus \{n\}$ and an offer is made similar to formulation (2.1). If the organ is declined in the second effort, we continue offering it to the eligible patients until one of these events happen: "patient n accepts heart type h offer," or "heart type h is declined $\mathcal{N}$ time," which triggers the event "heart type h is wasted." In modeling the patient decision in accepting/declining the offer, we assume that the sequence of such events, that starts with heart arrival and ends with heart

acceptance or wastage, happen sequentially but without time delay. That is, the time between organ arrival and organ acceptance/wastage is zero. This assumption is for modeling purposes and is not restrictive because when a heart becomes available, it will be accepted or wasted in less than four hours, which is much less than the expected time for the arrival of the next heart in a Designated Service Area (DSA). If the event is not of type "heart type h arrives," or "patient n declines heart type h offer," the action space is empty, i.e., $\mathcal{A}(s) = \emptyset$.

Transitions. We assume that patients of type i join the waiting list according to a stochastic process with finite mean. Also, hearts of type h arrive to the system according to a stochastic process with finite mean. In particular, our estimates of real data for the U.S. transplant system show that the arrival processes of patients and hearts are non-stationary Poisson processes. Patients on the waiting list may die before transplantation. The probability of death in a period on the waiting list depends on patient characteristics such as age, health status, type of heart disease, etc, and is estimated via a Cox proportional hazard model. Patients on the waiting list may be delisted due to several reasons such as unsuitability for transplantation. Delisting probabilities may also depend on patient characteristics. Dynamic characterization of patients may change over time. The age of patients changes deterministically. The health of a patient may change probabilistically while waiting for transplantation, which may depend on other characteristics and the time that a patient has been in a health status. We assume that a heart is accepted by a patient with a probability that depends on heart quality and patient characteristics.

Recall that κ denotes the index of the κ^{th} event. The complete trajectory of the system is therefore represented by $\{(s_\kappa, a_\kappa) : \kappa = 1, 2, \ldots, \mathcal{K}\}$, where s_κ is the system state and a_κ is the action taken (if any) at the time of the κ^{th} event. The stochastic evolution of the system can be presented by $s_{\kappa+1} = F(s_\kappa, a_\kappa, \omega(s_\kappa, a_\kappa))$, where $F(.,.,.)$ is a transfer mapping and $\omega(s_\kappa, a_\kappa)$ is a random element that contains all the sources of randomness in the system. In fact, $\omega(s_\kappa, a_\kappa)$ produces the time and type of the next event considering all the stochastic processes involved.

Rewards. We consider a policy maker who seeks to maximize the QALYs of the entire patient population in a finite horizon. Let $h(s_\kappa, a_\kappa, s_{\kappa+1})$ be the total QALYs received by transition from state s_κ to $s_{\kappa+1}$ when action a_κ is taken at the time of the κ^{th} event. Let $X_i(t)$ denote the number

of patients of type i on the waiting list at time t. The expected immediate reward is then given by

$$h(s_\kappa, a_\kappa, s_{\kappa+1}) = \begin{cases} (t(s_{\kappa+1}) - t(s_\kappa))(\sum_{i=1}^{I} \beta_i X_i(t(s_\kappa))) & \text{if the event } e(s_\kappa) \text{ is of the form "patient } n \\ & \text{arrives," or "patient } n \text{ dies," or "patient } n \\ & \text{delists,"or "patient } n \text{ changes class"} \\ & \text{or "heart } h \text{ wasted,"} \\ (t(s_{\kappa+1}) - t(s_\kappa))(\sum_{i=1}^{I} \beta_i X_i(t(s_\kappa))) + \alpha_i^h & \text{if the event } e(s_\kappa) \text{ is of the form "patient } n \\ & \text{accepted heart type } h \text{ offer,"} \end{cases}$$

and is zero otherwise, where $t(s_\kappa)$ denotes the occurrence time of event κ, β_i is the quality of life for a patient type i on the waiting list, and α_i^h denotes post-transplant QALYs of a type i patient receiving heart type h.

Recall that $\mathcal{K}$ denotes the last event index in the system which corresponds to the end of the horizon, i.e., $t(s_\mathcal{K}) = \mathcal{T}$. Let the final reward $r(s_\mathcal{K})$ be the total future QALYs of the patients who are on the waiting list at the end of the planning horizon. We then have $r(s_\mathcal{K}) = \sum_i \eta_i X_i(t(s_\mathcal{K}))$, where η_i is the future expected QALYs for patients who are in the system at the end of the planning horizon.

Optimality Equation. Let $\mathit{\Pi}$ denote the set of all non-anticipative policies. Let $J_\pi(s)$ be the expected total reward starting from state $s_0 = s$ under policy $\pi \in \mathit{\Pi}$. By letting $\pi(s_\kappa)$ denote the action selected by an admissible policy π in state s_κ, $J_\pi(s)$ can be written as:

$$J_\pi(s) = \mathbb{E}^\pi \left\{ \sum_{\kappa=1}^{\mathcal{K}-1} h(s_\kappa, \pi(s_\kappa), s_{\kappa+1})) + r(s_\mathcal{K}) \middle| s_0 = s \right\}, \text{ for } s \in \mathcal{S}, \pi \in \mathit{\Pi}.$$

Therefore, the decision maker solves for $V(s) = \sup_{\pi \in \Pi} \{J_\pi(s)\}$, where $V(s)$ is the optimal value function, which satisfies the Bellman optimality equation

$$V(s) = \max_{a \in \mathcal{A}(s)} \Big\{ \mathbb{E}_a \Big(h(s, a, s') + V(s') \Big) \Big\}, \ \forall s \in \mathcal{S}, \tag{2.2}$$

with a boundary condition $V(s_\mathcal{K}) = r(s_\mathcal{K})$, where s' is the next state after taking action a in state s, and the expectation is taken with respect to action a.

In organ transplant, fairness may be seen by considering a lower bound on the percentage of total offers to specific groups of patients (RFI, 2008). For example, if a policy maker seeks to offer at least 10% of good quality hearts h' to the oldest age group i', a constraint of type $\mathbb{E}^\pi \Big\{ b_{i'}^{h'}(s_\mathcal{K}) \Big\} \geq \mathbb{E}^\pi \Big\{ 0.1 \sum_i b_i^{h'}(s_\mathcal{K}) \Big\}$ should be imposed, where $b_{i'}^{h'}(s_\mathcal{K})$ is the total number of heart type h' offers made to type i' patients at the last event $\mathcal{K}$. Consider K fairness constraints and let $\{\mathcal{F}_k\}_{1 \leq k \leq K}$ be a collection of subsets of patient indices, where $\mathcal{F}_k \subseteq \mathcal{I}$ for $1 \leq k \leq K$, $\{\mathcal{G}_k\}_{1 \leq k \leq K}$ be a collection of subsets of heart type indices, where $\mathcal{G}_k \subseteq \mathcal{H}$ for $1 \leq k \leq K$ and $\{a_k\}_{1 \leq k \leq K}$ be a collection of real numbers, where $a_k \in [0, 1]$ for $1 \leq k \leq K$ denotes the lower bound on the percentage of the hearts belong to set $\mathcal{G}_k$, allocated to the patients whose indices belong to the set $\mathcal{F}_k$. Then, the fairness constraints can be written as follows:

$$\mathbb{E}^\pi \Big\{ \sum_{i \in \mathcal{F}_k} \sum_{h \in \mathcal{G}_k} b_i^h(s_\mathcal{K}) \Big\} \geq \mathbb{E}^\pi \Big\{ a_k \sum_{i \in \mathcal{I}} \sum_{h \in \mathcal{G}_k} b_i^h(s_\mathcal{K}) \Big\}; \ \ 1 \leq k \leq K.$$

Therefore, by letting $b(s_\mathcal{K}) = \big(b_i^h(s_\mathcal{K}) \big)_{i \in \mathcal{I}, h \in \mathcal{H}}$ fairness is modeled by imposing constraints of type $\mathbb{E}^\pi \{ Ab(s_\mathcal{K}) \} \geq 0$, where A is a K by IH matrix, with elements $a_{k,ih}$ defined by

$$a_{k,ih} = \begin{cases} 1 - a_k, & \text{if } i \in \mathcal{F}_k, h \in \mathcal{G}_k \\ -a_k, & \text{if } i \in \mathcal{I} \setminus \mathcal{F}_k, h \in \mathcal{G}_k. \end{cases}$$

In this case, the policy maker solves

$$\sup_{\pi \in \Pi} \Big\{ J_\pi(s) : \mathbb{E}^\pi \{ Ab(s_\mathcal{K}) \} \geq 0 \Big\}, \tag{2.3}$$

which is a constrained stochastic dynamic program (Altman, 1999). The standard dynamic programming principles do not apply to (2.3) because of the fairness constraints.

2.4 Fluid Approximation

Solving formulations (2.2) and (2.3) to optimality is intractable due to the curse of dimensionality. Therefore, we employ fluid approximation techniques to produce feasible allocation rules to the constrained stochastic problem, and evaluate them in Section 2.6.

In creating the fluid approximation, we assume that the death, class change, and delisting rates do not depend on the waiting time of patients. Our simulation results, however, show that the solutions produced by this approach have high quality in a setting where these rates do depend on waiting times. Recall that patients on the waiting list are categorized by different characteristics such as age group, blood type, VAD status, and health status, indexed by $i \in \mathcal{I}$. Therefore, there are I number of queues for patients in the system. We let $\lambda_i(t)$ be the arrival rate of class i patients at time t. Similarly, hearts are categorized by different characteristics to reflect quality indexed by $h \in \mathcal{H}$. Hence, there are H classes associated with hearts and let $\mu^h(t)$ denote the arrival rate of heart type h at time t. Let $x_i(t)$ be the number of patients in class i at time t, and $x(t) = (x_1(t), ..., x_I(t))^T$ be the state trajectory, which is an I-dimensional column vector with T denoting the transpose of a matrix. There are $x_i(0)$ patients in class i initially, and $x(0)$ is the initial state of the system. According to the UNOS classification (2006-2018), there are four health statuses: 1A, 1B, 2, and 7 (Inactive), where health status 1A is the worst and 2 is the best health status. Status 7 is for patients who are not considered in the allocation process, e.g., those who are too sick to transplant. The health status of a patient may change over time, which corresponds to a change of queue in our fluid model. Let ρ_{ij} be the rate at which patients of class i become patients of class j and $\rho = [\rho_{ij}]$ be the class change matrix. For transitions that are not possible, set the rate $\rho_{ij} = 0$ and $\rho_{ii} = 0$ for all i. Also, define $\hat{\rho} = [\hat{\rho}_{ij}]$ as an $I \times I$ diagonal matrix with $\hat{\rho}_{ii} = \sum_j \rho_{ij}$. Patients of class i die with rate d_i, which incorporates the delisting rate of class i patients as well. Let d be an $I \times I$ dimensional diagonal matrix with d_is on the diagonal and q^h for $h = 1, \ldots, H$ be the offer acceptance probability matrix, which is an $I \times I$ dimensional diagonal matrix, with q_i^hs on its diagonal, where q_i^h denotes the acceptance probability for patients in class i when offered with a

heart with quality h. In particular, if p_i^h is the probability that a patient type i accepts an offer of heart type h, then $q_i^h = 1 - (1 - p_i^h)^{\mathcal{N}}$. Since UNOS dynamically allocates organs to patients, let the control variables $u_i^h(t)$ be the rate of allocating a heart type h to patients of class i at time t, and $u^h(t) = (u_1^h(t), \ldots, u_I^h(t))^T$ for $h = 1, \ldots, H$. Denote the control variable of the system by $u(t) = (u^h(t) : h = 1, ..., H; t \geq 0)$ which satisfies three sets of constraints: donor heart limitation, non-negativity constraints, and constraints of type $u_i^h(t) = 0$ for $(i, h) \in$ INF, where INF indicates the infeasible set of patient-heart pairs, e.g., the pair (i, h) does not satisfy blood type matching. Hence, a control $u(t)$ is feasible if

$$u(t) \in \Omega(t) := \{u(t) : \ e.u^h(t) \leq \mu^h(t); \ u^h(t) \geq 0, \ \forall h; \ u_i^h(t) = 0, \ \forall (i, h) \in \text{ INF}\}, \tag{2.4}$$

where e is an I-dimensional row vector of ones. Given a feasible control $u(t)$, the system state evolution can be expressed by the following system of equations:

$$\dot{x}(t) \ = \ \lambda(t) - \sum_{h=1}^{H} q^h u^h(t) - (d + \hat{\rho} - \rho^T)x(t), \quad x(0) = x_0 \tag{2.5}$$

$$x(t) \geq 0, \ t \geq 0, \tag{2.6}$$

where $\lambda(t)$ is a column vector whose i^{th} entry at time t is $\lambda_i(t)$. In order to incorporate fairness constraints in an average sense (over time) into the fluid model, we consider the following set of K fairness constraints

$$\int_0^{\mathcal{T}} \Big(\sum_{i \in \mathcal{F}_k} \sum_{h \in \mathcal{G}_k} u_i^h(t) \Big) dt \geq a_k \int_0^{\mathcal{T}} \Big(\sum_{i \in \mathcal{I}} \sum_{h \in \mathcal{G}_k} u_i^h(t) \Big) dt; \quad k = 1, \ldots, K. \tag{2.7}$$

Consider a policy maker who seeks to maximize the total QALYs of the population over a finite horizon, which captures both pre- and post-transplant life expectancy of each patient on the transplantation waiting list. In order to capture the reward accrued by patients on the waiting list, let β_i be the quality-adjusted coefficient of a patient in class i while waiting for transplantation and $\beta = (\beta_1, ..., \beta_I)$. Hence, the total QALYs rate for the entire population at time t can be written as $\beta x(t)$. To capture the post-transplant life expectancy of patients, let α_i^h denote the expected QALYs of a patient in class i transplanted with a heart with quality h, and $\alpha^h = (\alpha_1^h, ..., \alpha_I^h)$. The total

post-transplant QALYs can then be written as $\sum_{h=1}^{H} \int_0^{\mathcal{T}} \alpha^h q^h u^h(t) dt$, where $\mathcal{T}$ denotes the end of the planning horizon. Finally, in order to capture the final rewards, let η_i be the expected future QALYs of a patient in class i who is still waiting for an organ at time $\mathcal{T}$, and $\eta = (\eta_1, ..., \eta_I)$. The expected final reward is then $\eta x(\mathcal{T})$. Hence, the fluid model for the stochastic system in Section 2.3 is as follows:

$$\begin{cases} V_F(x_0) = \max \int_0^{\mathcal{T}} \left(\sum_{h=1}^{H} \alpha^h q^h u^h(t) + \beta x(t) \right) dt + \eta x(\mathcal{T}) \\ \text{subject to } (2.4) - (2.7), \end{cases} \tag{P_1}$$

where $V_F(x_0)$ is the optimal objective function of the fluid model given that the initial state of the system is x_0, which is an optimal control problem with pure state constraints, as well as integral constraints. Because the optimal control problem (P_1) has integral constraints, the standard necessary and sufficient conditions for optimality do not directly apply. Therefore, we transform (P_1) to a pure state optimal control problem with final time state constraints and show that the optimal policy is a priority rule.

Let $k_i(t)$ be the shadow price of the i^{th} state evolution constraint in (2.5), which measures the future benefit of type i patients in terms of QALYs if not transplanted at time t, and $k(t) = (k_1(t), \ldots, k_I(t))$. Let $y_i^h(t)$ be the shadow price of the ih^{th} constraint corresponding to the evolution of auxiliary state variables $z_i^h(t)$ defined to transform (P_1) (see B.2), $y^h(t) = (y_1^h(t), \ldots, y_I^h(t))$, and $y(t) = (y^h(t) : h = 1, ..., H; t \geq 0)$. Let $w_i(t)$ be the shadow price associated to the i^{th} non-negativity constraint in (2.6), and $w(t) = (w_1(t), \ldots, w_I(t))$. Finally, let γ_k be the k^{th} adjoint variable associated to the k^{th} fairness constraint, and $\gamma = (\gamma_1, \ldots, \gamma_K)$. The following theorem characterizes the structure of the optimal policy.

Theorem 2.1. *A feasible triple of state and control variables (x, z, u) is an optimal solution for (P_1) if and only if there exist shadow prices $k(t)$ and $y(t)$ with one sided limits everywhere, a non-*

decreasing vector $w(t)$, and an adjoint vector γ such that

$$\dot{k}(t) \leq (k(t) - w(t))(d + \hat{\rho} - \rho^T) - \beta, \quad \forall\ t \in [0, \mathcal{T}],\ k(\mathcal{T}) = \eta,$$

$$\textit{if } x_i(t) > 0\ ,\ \dot{k}_i(t) = [(k(t) - w(t))(d + \hat{\rho} - \rho^T)]_i - \beta_i,$$

$$\dot{y}(t) = 0, \quad \forall\ t \in [0, \mathcal{T}],\ y(\mathcal{T}) = \gamma A, \tag{2.8}$$

$$\gamma \cdot (Az(\mathcal{T})) = 0, \gamma \geq 0 \tag{2.9}$$

$$u^h(t) \in \underset{v}{argmax}\Big\{\Big(\big(\alpha^h - k(t)\big)q^h + y^h(t)\Big)v : v \in \mathbb{R}_+^{|I|},\ e \cdot v \leq \mu^h(t),\ v_i^h = 0;\ (i,h) \in\ INF\Big\}\ \ \forall h \in \mathcal{H}. \tag{2.10}$$

Equation (2.10) gives the optimal control of the fluid model, which shows that given the shadow prices $k(t)$, and $y(t)$ the optimal control at each time t can be found by solving a Knapsack problem whose solution is given by sorting the patient groups. In fact, at each time t and for each available heart type h, the optimal solution prioritizes the patient groups based on the quantity $\big(\alpha_i^h - k_i(t)\big)q_i^h + y_i^h(t)$, which can be interpreted as the marginal benefit in terms of QALYs that a patient type i may gain from transplanting a heart type h while considering the impact of the fairness constraints. Given shadow prices, the optimal policy is of priority rule type which is easy to understand and implement. A policy maker creates a priority list of patient types and offers the available heart according to the priority list. In each class, the offer is given to the patients with the largest waiting time. If there are less than $\mathcal{N}$ patients in a priority, a rejected heart will be offered to patients in lower priorities. We denote this policy by optimal priority list (OPL) policy.

Theorem 2.1 shows that even in the presence of fairness constraints, the optimal policy is a priority index policy with priority coefficients $\big(\alpha_i^h - k_i(t)\big)q_i^h + y_i^h(t)$. To provide insights on this quantity, note that by (2.8), shadow prices $y_i^h(t)$ are constant in $[0, \mathcal{T}]$ and this constant value is the ih^{th} element of the vector γA, i.e., $y_i^h(t) = \big(\gamma A\big)_{ih} = \sum_{k=1}^K \gamma_k a_{k,ih}$. Therefore, the priority index policy is with respect to the priority coefficient $\big(\alpha_i^h - k_i(t)\big)q_i^h + \sum_{k=1}^K \gamma_k a_{k,ih}$. The shadow price $y_i^h(t)$ can be interpreted as the impact of fairness constraints in the QALYs of the patients in class i receiving a heart type h, where the contribution of the k^{th} fairness constraint is equal to $\gamma_k a_{k,ih}$. By the definition of matrix A (see Section 2.3), for $i \in \mathcal{F}_k$, the entry $a_{k,ih} = 1 - a_k$ is non-negative, meaning that the impact of k^{th} fairness constraint on the priority coefficient is non-negative and imposing fairness constraint k favors patients in $\mathcal{F}_k$. On the other hand, the entry of matrix A for $i \in \mathcal{I} \setminus \mathcal{F}_k$,

$a_{k,ih} = -a_k$ is nonpositive, showing the negative impact of the k^{th} fairness constraint on the patients in $\mathcal{I} \setminus \mathcal{F}_k$. In other words, in the presence of the k^{th} fairness constraint, patients in $\mathcal{F}_k$ have a higher priority coefficient and patients in $\mathcal{I} \setminus \mathcal{F}_k$ have a lower priority coefficient (note that $\gamma_k \geq 0$ for $k = 1, \ldots, K$). In addition, γ_k, the shadow price associated to the fairness constraint k, must be zero when the corresponding constraint is not binding by (2.9), i.e., when the fairness constraint is not active in the optimal solution, its contribution to $y_i^h(t)$ is zero. Hence, when none of the fairness constraints is active in the optimal solution (i.e., all fairness constraints are redundant), $\gamma = 0$ and in such a case, the OPL policy coincides with the policy proposed in Akan et al. (2012).

The implementation of the OPL policy requires an efficient procedure to calculate shadow prices. From the proof of Theorem 2.1 one can see that, when the system is overloaded, i.e., $x(t) > 0$ for all $t \in [0, \mathcal{T}]$, $k(t)$ satisfies the following linear system of differential equations: $\dot{k}(t) = -\beta + k(t)(d + \hat{\rho} - \rho^T)$, with final condition $k(\mathcal{T}) = \eta$, which is solved by using the matrix methods for solving linear systems of differential equations.

Remark 2.1. *The indexibility property of the optimal policy holds when the fairness constraints are applied in an "average" sense, i.e., during the planning horizon $[0, \mathcal{T}]$ at least a_k percent of the total hearts of type $\mathcal{G}_k$ are allocated to the patients of type $\mathcal{F}_k$. However, the indexibility property of the optimal policy is not generelizable to an "almost sure" setting, where at each time $t \in [0, \mathcal{T}]$ the constraints must hold true, i.e., at least a_k percent of the total hearts of type $\mathcal{G}_k$ are allocated to the patients of type $\mathcal{F}_k$, which can be written as $Au(t) \geq 0$. In this case, the optimal solution solves the following LP at time t: maximize $\sum_{h=1}^{H} [\alpha^h - k(t)].q^h u^h(t)$, subject to, $u^h(t) \in \Omega(t) \cap \{Au(t) \geq 0\}$, whose solution is a randomized policy using a proof similar to Theorem 2.1.*

Remark 2.2. *Fluid models may provide an upper bound on the optimal value function of the stochastic system. We show that the fluid model of a bounded Markovian version of our problem also provides an upper bound, which can be used to assess the quality of solutions in that setting. We also test the validity of such assumptions in our problem using real data: see Section B.3.*

Remark 2.3. *In our simulation model, the fluid model (P_1) is solved for each region separately based on data specific to that region for creating the priority lists. However, regional sharing is an important issue in organ transplantation, which may address geographical disparity. In order to address this issue, we reformulate problem (P_1) to include Organ Procurement Organization (OPO)*

as one of the factors defining patient and heart classes, derive the optimal policy in the presence of certain proximity constraints, and simulate it to investigate insights from such regional inclusion: see B.6 for details.

2.5 Alternative Objective Functions

The main objective function considered in this work is the maximization of total QALYs of the entire patient population. However, there are other related objective functions in organ transplantation.We analyze the heart allocation problem with four alternative objective functions. In particular, we formulate two optimal control problems with different objective functions but the same feasible state-action region as (P_1): one to minimize the total number of pre-transplant deaths, and the other to minimize the total wastage of donor hearts, denoted by problems (P_2) and (P_3), respectively. In particular, a policy maker who seeks to minimize the pre-transplant deaths solves for

$$\begin{cases} \min \int_0^{\mathcal{T}} e.dx(t)dt \\ \text{subject to } (2.4) - (2.7). \end{cases} \tag{P_2}$$

Similarly, if the objective of a policy maker is to minimize the total organ wastage, which is equivalent to maximizing the total transplanted organs, the policy maker solves

$$\begin{cases} \max \sum_{h=1}^{H} \int_0^{\mathcal{T}} e \cdot q^h u^h(t)dt \\ \text{subject to } (2.4) - (2.7), \end{cases} \tag{P_3}$$

where e is an I-dimensional vector of all ones. Denote the optimal policies derived from solving problems (P_2) and (P_3) by MPD, and MTW, respectively.

Similar arguments as in proof of Theorem 2.1 show that the optimal solution of both problems are priority type policies. Specifically, at time t, the optimal solution of problem (P_2) prioritizes patients according to ascending order of the coefficients $q_i^h \hat{k}_i(t) - \hat{y}_i^h$, where $\hat{k}_i(t)$ is the i^{th} component of adjoint variables vector associated to state evolution constraints in (2.5) and $\hat{y}_i^h(t)$ is the shadow price associated to the evolution of auxiliary variables introduced for each integral constraint (see B.5.2). In fact, if the acceptance probability is the same among patients, and patients are only

categorized by their health, then in the absence of fairness constraints, the optimal solution of problem (P_2) coincides with the UNOS policy, which prioritizes patients in the order of worst to best health status (1A $>$ 1B $>$ 2), as pre-transplant death rates satisfy $d_{1\mathrm{A}} > d_{1\mathrm{B}} > d_2$ from real data estimation. On the other hand, when the objective is to minimize the total wastage of hearts, the optimal policy prioritizes patients according to coefficient $q_i^h + \tilde{y}_i^h(t)$ where q_i^h is the i^{th} diagonal element of the acceptance matrix q^h and $\tilde{y}_i^h(t)$ is the shadow price associated to the auxiliary variables introduced to transform integral fairness constraints (see B.5.2). In other words, the optimal solution of problem (P_3) is a priority index policy for each available heart type h, which prioritizes patients with higher heart acceptance probability in the absence of fairness constraints.

Furthermore, we study two other objective functions related to the expected waiting time of patient classes on the waiting list, because reducing the waiting list and time to transplantation is a top priority of UNOS. Zenios (1999) studied the organ allocation problem as a queuing model with reneging and derived asymptotic expressions for the expected waiting time of different patient classes. We use these expressions and formulate a problem that minimizes the mean of the expected waiting time across all patient classes (MWT Policy). Furthermore, we study the equity policy (VWT Policy) introduced in Zenios (1999), which equalizes waiting times of patient classes: see B.5 for details.

2.6 U.S. Heart Transplantation System

This section presents the result of applying the methods discussed in Sections 2.3-2.5 to the U.S. heart transplantation waiting list and explains novel insights. In the U.S., the OPTN maintains the national registry for donated organs and manages the organ allocation process under the administration of UNOS. Patients demanding transplant have to register in OPOs waiting lists to receive an offer. Donated hearts also become available in OPOs and are offered to the patients according to a policy which is based on certain priority rules. There are a total of 59 OPOs in the U.S. distributed in 11 geographical regions across the country and each OPO includes one or more transplant centers. According to the UNOS data reports, adult patients are categorized into four age groups ([18-35], [35-50], [50-65], and [65+]), four health status groups (1A, 1B, 2, and Inactive), four blood type groups (O, A, B, and AB), and two VAD status groups (showing whether a patient

has ventricular assist device in their heart) (Colvin-Adams et al., 2015). Hence, we classify the patients on the waiting list into 128 classes. Similarly, donor hearts are classified into 16 heart types based on the age (four age groups) and blood type (four blood type groups) of the donor. We consider the planning horizon 2006-2014 because the three-tiered allocation policy was implemented since 2006 (Kobashigawa et al., 2015). The initial population in each class at the start of the planning horizon is estimated by using the SRTR annual data reports. All the parameters defined in Sections 2.3-2.5 are directly estimated from the UNOS and SRTR data sets or, if not available, by the validated simulation model of Hasankhani and Khademi (2017). The overview of the simulation model is enclosed in B.4. Using this set of parameters, we solve the discretized version of the optimal control problem (P_1), explained in Section B.3, for each region separately to find its optimal solution and calculate the total LYs received by the patients of each region in the absence of the fairness constraints. In the numerical analysis we use LYs instead of QALYs due to unavailability of data.

2.6.1 Benchmark Policies

We consider several benchmark policies along with the policies proposed in Sections 2.4 and B.3 and study their performance via the simulation model. In particular, we consider UNOS, UNOS 7-tiered (new OPTN proposed policy), Su/Zenios efficiency (SZE), and Su/Zenios equity (SZQ) policies, a heart allocation scoring system (HAS) policy, as well as a broadening regional sharing (BRS) policy and policies that reverses the health prioritization of patients in UNOS/UNOS 7-tiered policy (UNOS-HR/UNOS 7-tiered-HR). This is motivated by the fact that prioritizing healthier patients achieves a higher total LYs in our simulations. The UNOS allocation policy which was implemented by UNOS during the 2006-2018 time period, prioritizes patients on the waiting list in three different levels, i.e., geographical (proximity to the donor hospital), health status, and waiting time level. Each policy has its own prioritization criteria. See B.5 for details.

2.6.2 Numerical Results

This section reports the results of applying said policies in the validated simulation model. Table 2.1 compares the total LYs in simulating the OPL policy with those resulted from the UNOS policy for each region. Results indicate that the total LYs under the OPL policy is significantly greater than that of the UNOS policy in each region. The improvement is as large as 8.6% in Region

Table 2.1: Percentage Improvement of OPL over UNOS

Region	**R1**	**R2**	**R3**	**R4**	**R5**	**R6**	**R7**	**R8**	**R9**	**R10**	**R11**	**Total**
OPL vs. UNOS (%)	7.2	8.1	7.8	7.5	8.6	8.5	7.7	7.1	8.0	8.4	8.1	7.9

5 and for the whole country is 7.9%.

Total LYs consists of three parts: (i) pre- and (ii) post-transplant LYs for the patient population during the planning horizon 2006-2014, and (iii) future LYs for the patients who are on the waiting list at the end of the planning horizon (final reward). Table 2.2 compares the results of simulating the OPL, UNOS, and other benchmark policies for these three measures. Our results show that the OPL policy is worse than UNOS in terms of pre-transplant LYs and final reward. However, it is significantly better than UNOS in terms of post-transplant LYs such that in overall it outperforms the UNOS policy by 7.9%. Furthermore, Table 2.2 illustrates that the recently proposed UNOS 7-tiered policy performs similarly to the UNOS policy in terms of all the measures except a slight improvement for the pre-transplant LYs. In addition, a comparison between OPL and SZE reveals that the performance of SZE is similar to that of OPL in terms of pre-transplant and final LYs, while it is outperformed by OPL in terms of post-transplant and total LYs. A similar conclusion holds true between OPL and SZQ as the former yields a significantly higher post-transplant and total LYs. The BRS policy achieves an improvement over UNOS in terms of pre- and post-transplant as well as total LYs by broadening the regional sharing of donor organs. In fact, BRS is the best in terms of pre-transplant mortality.

Furthermore, Table 2.2 reports the results of simulating the MPD, MTW, MWT, and VWT policies introduced in Section 2.5. Recall that MPD seeks to minimize the number of pre-transplant deaths, roughly speaking, an objective that UNOS is seeking in heart transplantation. Our results show that the performance of MPD is marginally better than UNOS or UNOS 7-tiered in terms of pre-transplant LYs, which suggest that if the objective is to focus on pre-transplant LYs, UNOS is already doing a good job. Furthermore, recall that we analytically show that MPD prioritizes patients similar to UNOS in terms of health, if health is the only patient characteristic (note that the improvement of MPD over UNOS in terms of pre-transplant LYs is because MPD considers age and VAD prioritization as well). In addition, results indicate that the MWT and VWT policies

that minimize the mean and variance of waiting times respectively, perform slightly worse than UNOS in terms of pre-transplant LYs while outperform UNOS in post-transplant LYs. Although MWT and VWT have a better pre-transplant performance in simulation compared to the SZE, their post-transplant outcomes are outperformed by the SZE which yields a similar total LYs for these policies. In summary, our results suggest that the policies that consider post-transplant survival such as OPL, SZE, and SZQ perform better than those that consider pre-transplant survival like UNOS and MPD in terms of maximizing the LYs of the patient population. Table 2.2 also reports the results of simulating the OPL-RS policy that is derived from solving the fluid model (P_o) discussed in Section B.6. The OPL-RS policy that considers proximity in allocating organs, performs similar to OPL in terms of pre-transplant LYs but achieves a higher post-transplant and total LYs. The reason is that under OPL-RS organs can be shared within patients of a wider area and as a result the opportunity of finding healthier and younger matches is higher compared to OPL. In addition, we provide an estimate for LYs per patient by dividing total LYs gain under each policy by total number of patients.

Table 2.2 for each policy, next to the last column, indicates the average waiting time among patient groups over several simulation runs and the last column reports the standard deviation of the waiting times across patient classes. Our results show that OPL significantly reduces the expected waiting time and is the closest to the MWT policy (which minimizes the mean of waiting times), e.g., it reduces the waiting time by almost half compared to UNOS. We also observe that the order of the policies in terms of mean waiting time in Table 2.2 is similar to that of pre-transplant LYs, i.e., the mean waiting time of a policy increases if pre-transplant LYs increases. This observation is an application of Little's law: the mean waiting time is proportional to the expected number of patients in the queue, which depends on the allocation policy. In particular, allocation policies that seek to minimize the number of pre-transplant deaths give more priority to sicker patients who have higher pre-transplant mortality rates, causing healthier patients who have lower pre-transplant mortality rates to stay on the waiting list, which consequently results in large waiting list and expected waiting time. In fact, our results show that the size of waiting list is smaller under OPL than UNOS. In summary, in this context because the pre-transplant mortality rate is significantly greater for sicker patients, with similar arrival rates, their prioritization naturally increases the size of waiting list, thus the waiting time.

Table 2.2: Benchmark Policies Comparison

	Objective Function (Life-Days $\times 10^6$)					Waiting Time (Days)	
Policy	**Pre-TX**	**Post-TX**	**Final**	**Total**	**Life Days per Patient**	**Mean**	**STD**
UNOS	9.05 (0.216)	147.25 (0.899)	0.035 (0.0012)	156.33 (0.710)	5073 (23.05)	189	168
UNOS 7-Tiered	9.14 (0.243)	147.28 (1.010)	0.035 (0.0012)	156.45 (0.892)	5077 (28.98)	191	191
OPL	6.89 (0.372)	163.00 (0.0572)	0.021 (0.0009)	169.91 (0.509)	5514 (16.52)	91	63
SZE	7.22 (0.207)	157.91 (0.665)	0.025 (0.0003)	165.16 (0.506)	5359 (16.43)	110	73
SZQ	7.24 (0.138)	155.57 (0.735)	0.025 (0.0001)	162.83 (0.596)	5284 (19.35)	105	72
BRS	10.74 (0.167)	148.58 (0.187)	0.034 (0.0004)	159.36 (0.285)	5171 (9.27)	206	234
HAS	6.77 (0.148)	162.38 (0.883)	0.021 (0.0011)	169.71 (0.997)	5507 (32.37)	97	75
UNOS-HR	7.63 (0.162)	150.02 (0.707)	0.032 (0.0007)	157.68 (0.793)	5117 (25.74)	96	66
UNOS 7-tiered-HR	7.57 (0.076)	149.44 (0.722)	0.031 (0.0011)	157.041 (0.776)	5096 (25.19)	101	65
MPD	9.55 (0.868)	146.6 (1.0759)	0.034 (0.0015)	156.07 (1.113)	5064 (36.15)	157	140
MTW	7.86 (0.429)	151.28 (1.520)	0.032 (0.0019)	159.17 (1.188)	5165 (38.58)	122	56
MWT	7.63 (0.031)	156.41 (1.470)	0.024 (0.0004)	164.08 (1.439)	5324 (46.70)	82	147
VWT	8.81 (0.474)	154.63 (0.352)	0.031 (0.0005)	163.49 (0.335)	5305 (10.88)	136	53
OPL-RS	6.72 (0.126)	165.24 (0.587)	0.023 (0.0009)	171.98 (0.642)	5581 (20.84)	95	82

Note. Numbers in parenthesis show the standard deviation of each measure over the simulation runs; SZE: Su and Zenious efficiency policy; SZQ: Su and Zenious equity policy; BRS: a policy that broadens regional sharing priority; HAS: heart allocation scoring system policy; UNOS-HR: a policy that reverses the UNOS health priority; UNOS 7-Tiered-HR: a policy that reverses the UNOS-7-Tiered health priority; MPD: a policy that minimizes pre-transplant death ; MTW: a policy that minimizes total heart wastage; MWT: a policy that minimizes mean waiting time among patient classes; VWT: a policy that minimizes variance of waiting times among patient classes; OPL-RS: OPL policy with proximity considerations (regional sharing)

Regarding standard deviation of waiting times our results show that the policies that prioritize healthier patients such as OPL and SZE have a lower standard deviation and are closer to the VWT policy (which equalizes the waiting times among patient classes) compared to those that prioritize sicker patients. The reason for this observation is that in heart transplantation, where the arrival rates of sick and healthy patients are not significantly different, prioritizing sicker patients with high mortality rates causes more healthier patients be on the waiting list who have lower mortality rates. Therefore, the difference between the waiting times of sicker and healthier patients is exacerbated, thus a higher variance. Furthermore, SZQ which considers equity in allocation yields a waiting time variance similar to that of SZE and is closer to the OPL and VWT policies in terms of this measure. These results suggest that OPL improves the variance of waiting time among patient groups, which is a measure of equity, compared to UNOS.

2.6.3 Policy Analysis

As shown in Table 2.2, the improvement of the OPL policy over UNOS is due to the post-transplant LYs. This section analyzes the OPL and UNOS policies in detail to shed light on how these policies allocate hearts and provide insights on the proposed policy. Note that the OPL policy prioritizes patients at each time based on shadow prices, which are time dependent. In particular, it ranks patient groups by $\big(\alpha_i^h - k_i(t)\big)q_i^h + y_i^h(t)$, which represents the life expectancy benefit from transplant compared to not having one while reflecting the impact of fairness constraints. Among patient characteristics we focus on health and age as they are important factors in heart transplantation and subjects of debate. Therefore, Table 2.3 shows the value of $\big(\alpha_i^h - k_i(t)\big)q_i^h$ for each pair of (health, age) when the effect of other patient characteristics, time, and heart types is averaged out. Note that red and green indicate higher and lower priority, respectively. Similar tables are provided in B.8 for each heart type $h \in \mathcal{H}$. Results in Table 2.3 provide insights about how the OPL policy prioritizes patients and suggests implementable guidelines for allocating donor hearts. In particular, it indicates that the marginal benefit of younger and healthier patients from transplant is much larger than that of the oldest and sickest ones, emphasizing the fact that the OPL policy gives priority to younger and healthier patient groups, those with higher post-transplant survival. B.8 shows similar tables in the presence of fairness constraints.

Table 2.3: Color-Coded Graph of Age and Health Prioritization for OPL Policy

Health GroupAge Group	[18-35]	[35-50]	[50-65]	[65+]
1A	9358.52	6189.24	3278.25	1148.56
1B	9682.77	6725.66	4199.26	1913.78
2	10288.39	6590.31	3973.45	3282.51

Note: Red denotes higher and green shows lower priority.

Next, in order to investigate how in practice (simulation), the OPL policy prioritizes patients, we record the number of times heart type h is allocated to patient type i for all (i, h) pairs. A similar count is carried over for UNOS policy. In particular, we conduct further analysis on the OPL policy by using the simulation model and comparing the percentage of hearts allocated to different patient classes under OPL and UNOS. In the simulation, for both policies the same stream of random number generators are used for patient and organ arrival to have a fair comparison. Results of this analysis is reported in B.8. Specifically, the percentage of donor hearts assigned to different patient health status (Figure 18a), age groups (Figure 18b), and VAD groups (Figure 18c) are calculated for each policy. Results suggest that the OPL policy, unlike UNOS, prioritizes healthier and younger patients, but similar to UNOS patients with VAD are not prioritized.

Further analysis of the pre- and post-transplant death rates shows that the expected survival of younger and healthier patients after transplantation is higher than older and sicker ones. Moreover, the expected post-transplant survival is much larger than the expected pre-transplant survival. Therefore, if the goal of a policy is to maximize the total life expectancy (pre- and post-transplant) of the patient population, it naturally gives higher priority to younger and healthier patients. This observation is consistent with our results that the OPL policy significantly outperforms the UNOS policy in post-transplant survival while it is dominated by UNOS in pre-transplant LYs. In particular, since the OPL policy prioritizes the younger and healthier patients, the percentage of older and sicker patients, who have larger pre-transplant death rates, increases on the waiting list under the OPL policy, which results in shorter pre-transplant life-years compared to UNOS. The same logic holds true for the final reward.

In order to provide further insights on the trade-off between utilitarian and medical urgency approaches, Tables 2.4 and 2.5 report the number of pre-transplant deaths the OPL policy trades off to obtain an increase in total LYs for each health and age group compared to UNOS. The results

Table 2.4: LYs/Death Trade-off for Patient Health Groups (OPL minus UNOS)

Health Group	1A	1B	2	Inactive	Total
Death	215	22	-171	511	577
Total Life-Days ($\times 10^7$)	-5.48	1.55	5.41	-0.012	1.46

Table 2.5: LYs/Death Trade-off for Patient Age Groups (OPL minus UNOS)

Age Group	[18-35]	[35-50]	[50-65]	[65+]	Total
Death	-39	-262	470	408	577
Total Life-Days ($\times 10^7$)	1.1	0.47	-0.066	-0.043	1.46

indicate that the OPL policy produces 577 more pre-transplant deaths compared to UNOS, but achieves 1.46×10^7 more total life days. See B.8 for similar analysis for UNOS 7-tiered and OPL policy with fairness constraints.

2.6.4 Fairness Analysis

Policy analysis for the UNOS and OPL allocation rules reveals that the improvement of the objective function is related to a shift in allocation rule towards prioritizing younger and healthier patients. However, this efficient policy may disproportionately affect sickest and older patients on the waiting list, which may raise equity issues. Therefore, this section provides a systematic and flexible framework to study fairness by applying lower bounds on the percentage of donor hearts allocated to specific groups of patients. Specifically, we match the percentage of hearts allocated to different age and health groups by UNOS in the following analysis, by which the contribution of age/health on the objective function can be assessed separately. To that end, a fairness analysis on the optimization problem (P_1) is conducted by adding extra constraints to the set of feasible actions. See Section B.7 for details. Recall that by Theorem 2.1 the OPL policy in the presence of fairness constraints is still a priority index policy depending on shadow prices, which are estimated by the optimal dual values of the corresponding constraints in the discretized version of problem (P_1), a linear program. The improvement of our proposed OPL policy over UNOS in the presence of several fairness constraints is reported in Tables 2.6-2.8. Table 2.6 reports the results of imposing age fairness constraints. In particular, our results suggest that imposing age fairness constraints to match UNOS reduces the

Table 2.6: Improvement of the OPL over UNOS in the presence of age fairness constraints (%)

Constraint Applied for	[35+]	[50+]	[65+]	[50-65] and [65+]	[35-50] and [50-65] and [65+]
Improvement	3.0	3.9	5.7	2.2	2.1

Table 2.7: Improvement of the OPL over UNOS in the presence of health fairness constraints (%)

Constraint Applied for	[1A]	[1B]	[2]	[1A] and [1B]
Improvement	1.5	4.9	7.2	0.8

percentage of improvement, but there is still room for improvement because, e.g., by optimizing health priority and other age groups, the OPL policy outperforms UNOS by 5.7% if only the oldest age group is matched. All in all, results in Table 2.6 illustrates the significance of allocation priority shift from older to younger patients in improvement of OPL compared to UNOS. Table 2.7 reports the improvement of the OPL policy over UNOS in the presence of each health fairness constraint. Results show that if we set the percentage of allocated hearts to the patients with health status 1A to be at least as high as UNOS, the improvement over UNOS reduces to 1.5%. This result suggest that the OPL improvement is mainly due to a priority shift from the sickest patient group (status 1A) to the healthier ones (status 1B and 2). However, considering a health fairness constraint of [1B] reduces the 7.9% improvement to 4.9% which shows that in terms of health priority, the most part of improvement is due to a priority shift from 1A toward 1B and 2. The results in Table 2.7 corroborate this insight. Finally, Table 2.8 reports the improvement of the OPL policy over UNOS in the presence of combined age-health constraints and shows that in these cases the improvement becomes marginal. See B.7 for more details regarding the fairness constraints studied in this work.

Table 2.8: Improvement of the OPL over UNOS in the presence of age-health fairness constraints (%)

Constraint Applied for	[65+] and [1A]	[50-65] and [65+] and [1A]
Improvement	0.8	0.4

Table 2.9: Percentage Improvement of OPL over UNOS for Different Cases of Parameters (%)

Case	**Baseline**	**Case (1)**	**Case (2)**	**Case (3)**	**Case (4)**	**Case (5)**	**Case (6)**
Improvement	7.9	11.2	5.6	5.9	10.1	7.8	7.7

2.6.5 Sensitivity Analysis

This section provides the results of conducting sensitivity analysis on the patient and heart arrival rates. In order to test the robustness of the results to the change in model parameters, we conduct several one- and two-way sensitivity analysis. Specifically, we change the arrival rates of patients and hearts by 10% and calculate the percentage improvement of the OPL policy over UNOS in terms of the total LYs for the following cases: (1) patient arrival rates increased by 10%, (2) patient arrival rates decreased by 10%, (3) heart arrival rates increased by 10%, (4) heart arrival rates decreased by 10%, (5) patient and heart arrival rates both increased by 10% simultaneously, and (6) patient and heart arrival rates both decreased by 10% simultaneously. Note that we use a mis-specified policy in conducting the sensitivity analysis, i.e., we keep the policy derived under the base case parameters fixed and run the simulation in different cases using the corresponding parameter values. The results are reported in Table 2.9 and show that as we increase arrival rates of patients (Case (1)), or decrease arrival rates of hearts (Case (4)), the improvement of the OPL over UNOS increases to 11.2% and 10.1%, respectively, compared to the 7.9% improvement of the baseline scenario. The reason is that in cases (1) and (4) the system becomes closer to a fully overloaded one and the fluid model provides a more accurate approximation. Also, the OPL policy has more opportunity to allocate hearts in a near-optimal fashion. However, as we decrease the arrival rates of patients (Case (2)), or increase arrival rates of hearts (Case (3)), the percentage improvement of the OPL over UNOS practice decreases from 7.9% to 5.6% and 5.9%, respectively. Furthermore, the results in Table 2.9 show that in Case (5) and (6) the improvement of OPL over UNOS does not significantly change compared to the baseline case.

2.7 Conclusions and Managerial Insights

We studied the problem of dynamically allocating scarce donor hearts to a heterogeneous patient population on the transplant waiting list from a variety of viewpoints in the efficiency and fairness spectrum. For efficiency we considered (i) maximization of total QALYs of the entire patient population; (ii) minimization of the expected waiting time; and (iii) minimization of pre-transplant mortality. For fairness we considered (i) maximization of the minimum QALYs over patient groups; (ii) minimization of the variance of expected waiting time among patient groups; and (iii) applying fairness constraints. We applied the optimal policies for each measure of efficiency and fairness into a simulation model of the U.S. heart allocation system, developed and validated from UNOS/SRTR data.

Our results provide the following insights into heart transplantation allocation rules: (1) OPL outperforms UNOS by almost 8% in terms of total LYs and reduces the expected waiting time by almost half. Our analyses show that the improvement for total LYs and expected waiting time is due to significant improvement on post-transplant LYs and reducing the size of the waiting list, respectively. (2) Our analytical and numerical analyses show that, unlike UNOS, the OPL policy prioritizes healthier and younger patients who have a higher post-transplant survival. In addition, OPL does not prioritize VAD status. (3) In order to investigate the contribution of health and age in the improvement, we applied certain constraints that matched UNOS allocation percentages for each age and health and our results show that health prioritization is more important than age. (4) The new proposed UNOS 7-tiered policy marginally improves over the previous UNOS practice. In fact, UNOS/UNOS 7-tiered policies perform similarly to the policy that minimizes the pre-transplant mortality. This suggests that if the objective is to focus on pre-transplant mortality, the UNOS policy is near-optimal. (5) The performance of OPL with respect to mean and variance of waiting time is closer to that of MWT (which minimizes expected waiting time) and VWT(which minimizes variance of waiting time) than UNOS. A similar result is observed with respect to the objective of maximization of the minimum LYs. These results suggest that OPL is more robust than UNOS with respect to change in different objective functions especially in terms of fairness measures considered in this study. (6) Incorporating the location of patients and organs in allocation rules and considering a broader regional sharing can significantly improve total LYs, size of the waiting list, and help address geographical disparity.

The OPTN/UNOS Heart Subcommittee plans to develop a point-based heart allocation rules in the near future similar to Kidney Allocation System. We developed a Heart Allocation System by designing relevant score components and estimating the corresponding coefficients by a data-driven approach. Our simulation results show that HAS achieves a similar performance to OPL in terms of LYs and could pave the way for the future UNOS HAS. A natural path forward is to test our proposed policies and HAS by TSAM, the UNOS/SRTR heart simulation model. This is because although we used a simulation model that is validated in several dimensions, it has limitations which may impact the results. For example, (i) detailed data on patients and donors were available for each region and not for every DSA or OPO. Therefore, appropriate distributions were generated for each region and a new patient/heart in a region is assigned to OPOs based on a uniform distribution; (ii) the patient health status change module only considers health and does not consider other attributes such as age, gender, etc.; (iii) because detailed data for heart wastage was not available, the donor heart arrival rates were adjusted for wastage compensation; (iv) the acceptance probabilities for each heart type depends only on patient health; (v) we used health classes and age groups definitions by UNOS and better results may be obtained if there was flexibility in such definitions; (vi) our analysis focused on life years and did not consider quality of life due to unavailability of data. However, considering QALYs will bolster our results because the sicker and older patients have a lower quality of life and as a result the gap between the utilitarian and medical urgency-based approaches is likely to increase. Finally, we did not consider the cost of changing allocation rules, which may impact the recommendation based on the results.

Chapter 3

Proportionally Fair Organ Allocation Rules for Transplantation

3.1 Introduction

Organ transplantation is the only viable life-saving treatment option for patients with late-stage organ disease, who join a waiting list to receive a donated organ and have a transplant. There are more than 113,000 patients on the waiting list as of April 29, 2019, which is caused by a significant imbalance between the rate of patients joining the waiting list (demand) and that of donor organs (supply) (United Network for Organ Sharing, 2019). In fact, on average, 18 patients die every day while waiting for a transplant (United Network for Organ Sharing, 2019).

This public health crisis has received significant attention from governmental entities and research communities. For example, the White House Office of Science and Technology issued a call to action to reduce the size of the waiting list noting that "ending the wait for organ transplant ... [is] some of what America can do" (The White House Office of Science and Technology Policy, 2016). Because of the notable imbalance between supply and demand, organ transplantation rules play a critical role in the performance of the transplant system and have striking impact on patients' life and society.

To that end, the United States (US) Congress passed the National Organ Transplant Act (NOTA) in 1984, which enacted new rules to ensure that organ allocation rules are efficient and fair. However, designing efficient and fair allocation policies is extremely challenging and the United Network for Organ Sharing (UNOS) has periodically changed them because of advancements in research and technology (Colvin-Adams et al., 2012). In fact, there is a fundamental and natural conflict between efficiency and fairness in organ allocation as long as organ shortage persists.

The principles of efficiency is well-established and the consensus is around maximization of the overall utility of patients, which is dominantly measured by total Quality-Adjusted Life Years (QALYs) of the entire patient population (United Network for Organ Sharing, 2019). While the bulk of the literature on organ allocation is driven by the objective of maximizing total QALYs of the patient population, we believe that fairness is a crucial objective in organ transplantation systems. However, because of the subjective nature of fairness, it is difficult to lay out a universally accepted framework for fair organ allocation. In fact, following an axiomatic approach, no fairness scheme can satisfy all five axioms of fairness simultaneously under mild conditions (Bertsimas et al., 2011). Nonetheless, in order to provide some principals for fair allocation, UNOS proposed the following six factors: 1) medical urgency, 2) likelihood of finding a suitable organ in the future, 3) waiting time, 4) first versus re-transplantation, 5) age, and 6) geographical fairness considerations (United Network for Organ Sharing, 2019).

The goal of this study is to propose a new measure of fairness in organ allocation, elaborate its potential benefits, analyze the structure of optimal allocation policies under this measure, and numerically quantify the benefits via a simulation model validated by real data for heart transplantation. Next, we discuss the results of studies that consider efficiency and fairness in organ allocation and close the discussion by providing evidence on inefficiency of current measures of fairness. In particular, because our focus is in proposing a fairness measure in the objective function, we begin with discussing other perspectives of fairness in organ transplantation and then focus on available measures of fairness for the objective function.

As mentioned earlier, geographical disparity is a factor that UNOS highlights for fairness purposes. Ata et al. (2016) addressed this issue by proposing multiple listing and initiating Organ Jet service. Fairness may also be imposed by incorporating lower bounds on percentage of total offers

to specific groups of patients (Bertsimas et al., 2013). Bertsimas et al. (2013) applied a data-driven approach to design allocation rules, where fairness constraints were studied. Now, we describe the fairness measures as the objective and report their inefficiencies compared to a utilitarian policy.

(1) Medical urgency. Medical urgency is perhaps a major criteria that UNOS has followed for organ allocation, which tends to prioritize the sickest patients. For example, the current heart allocation policy is mainly medical urgency driven (Organ Procurement and Transplantation Network, 2015). A natural path to formulate this measure in the objective function is to minimize pre-transplant mortality. However, numerical evidence reveals that allocation policies that are medically urgent driven cause significant performance loss. For example, see Su and Zenios (2006), Akan et al. (2012), and Hasankhani and Khademi (2017).

(2) Waiting (list) time. In many queuing systems involving human beings, the principle of first-come first-served is believed to be the most relevant in terms of fairness. However, in transplant systems it is not a primary factor in prioritization because prioritization based on waiting time will cause severe consequences in terms of total life yeas of the patient population. In fact, Childress (1991) mentioned that "length of time on the waiting list is the least fair, most easily manipulated, and most mindless of all methods of organ transplantation." Therefore, the current practice is to use waiting time as a tie-breaker or a part of the scoring system. Our numerical results shows that prioritizing patients solely based on waiting time will cause around 10% efficiency loss and around 24% more total deaths in heart transplantation.

(3) Equalizing waiting time among patient groups. One measure of fairness in service queuing theory is the minimization of the variance between the expected waiting time of customer (patient) classes. Inspired by observing a notable difference between waiting times of different ethnic groups, Zenios (1999) studied the transplant queuing system with this objective and observed significant inefficiency of such policies. In particular, he wrote "Focusing on equalizing waiting time alone can be misleading because the patient mortality serves as a confounding factor." Our simulation results corroborate with previous studies and show that following such policies results in 5% performance loss.

(4) Max-min utility. The notion of max-min fairness was introduced as a design objective in the literature of communication networks by Bertsekas et al. (1992) and is widely used in the political sciences (Rawls, 2009). In the resource allocation problems, the principle of max-min fairness is to allocate network resources such that the utility of a player cannot be increased without decreasing

the utility of another player having a smaller utility. Under max-min fairness for a multi-player game, the decision maker allocates resources to the players to maximize the lowest utility level among players. Then, tries to maximize the second lowest utility level and so on. The main principle of max-min fairness in organ allocation systems is to design allocation rules that guarantee that the QALYs of the worst patient group is maximized (Rawls, 2009). However, the said measure will result in a significant performance loss. For example, see Su and Zenios (2006) and Hasankhani and Khademi (2017).

Since the common measures of fairness in organ allocation cause a significant performance loss, a natural question arises: can an alternative fairness measure be applied to transplant systems with a less performance loss? This study provides an answer to this question and our results yield an affirmative answer. In particular, we propose an application of proportional fairness, which is a generalization of Nash standard for comparison, in organ transplantation.

Proportional fairness is widely used in queuing networks and resource allocation problems such as bandwidth allocation of network capacities. For example, Bonald et al. (2006) study a communication network whose resources are shared by a random number of data flows under proportional, max-min, and balanced fairness and compare their performance. Li et al. (2008) study a multi-rate wireless LAN network. Their model allocates access points to the users in order to achieve optimal proportional fairness in a network with several access points. Manfredi (2014) propose a healthcare traffic control over the modern heterogeneous wireless network to avoid congestion and guarantee quality of service from the service reliability and responsiveness point of view. They propose policies based on proportional fairness and study the performance of the proposed policies in simulation. Swenson (1992) study the problem of allocating scarce resources (incentive care units) to patients demanding for ICU. They used Rawl's theory of justice to rank patients on the waiting list in a fair fashion.

Under the Nash principle for two players, an allocation is fair if the percentage increase in utility of one player is larger than the percentage decrease in utility of the other player. By the generalization of the Nash solution for multiple players, a fair policy is the one that achieves a non-positive aggregate proportional change, compared to any feasible allocation policy. In particular, for N players, the PF policy is proportionally fair if for every feasible policy $\pi \in \Pi$ and its induced

feasible utility $u^\pi = (u_1^\pi, \ldots, u_N^\pi) \in U$,

$$\sum_{j=1}^{N} \frac{u_j^\pi - u_j^{\mathrm{PF}}}{u_j^{\mathrm{PF}}} \leq 0, \tag{3.1}$$

where Π and U are the set of feasible allocations and utilities, respectively. We interpret this inequality by dividing the N players into two groups, the ones who gain utility due to switching from allocation π to PF, and the ones who lose utility. The inequality (3.1) ensures that the amount of utility that gainers gain is not less than that of the losers lose. For a convex utility set U, the fair allocation under proportional fairness PF is unique and can be obtained by solving the following problem:

$$\max_u \sum_{j=1}^{N} \log(u_j),$$

$$\text{subject to } u \in U.$$

The first order optimality condition for this problem coincides with the Nash standard of comparison principle for N players. The Nash bargaining game is a game between two players that demand a portion of some good, in our context divisible organ. Both players receive their request if the total amount requested by the players is less than that available, and they receive nothing, otherwise (disagreement value is set to zero here). John Nash proposed a solution satisfying the axioms of scale invariance, symmetry, efficiency, and independence of irrelevant alternatives. Various solutions are proposed for this game with slightly different assumptions.

To better understand the application of Nash principle for a two patient problem in transplantation queuing systems and the distinctions between different fairness measures, consider the following example:

Example 3.1. *Suppose we have two patients: Patient 1 is sick and Patient 2 is healthy, and one organ is available. Patient 1 lives 1 year if she does not receive the organ, and lives 2 years if she receives an organ. Patient 2 lives 3 year if she does not receive the organ, and lives 5 years if she receives an organ. Define the utility as the life-years of the patients. That is,* u_1 *and* u_2 *are the utility of Patients 1 and 2, respectively. The allocation question is to whether allocate the organ to the sick or healthy patient. Thus, if we assign the organ to the sick patient, then* $u_1 = 2$ *and* $u_2 = 3$*;*

if we assign the organ to the healthy patient, then $u_1 = 1$ *and* $u_2 = 5$*. However, assume in general that the organ assignment could be randomized. Let the decision variable be* $\pi = (\pi_1, \pi_2)$*, where* π_1 *and* π_2 *are the probability that the organ is assigned to the sick and healthy patient, respectively and belong to the set of admissible decisions* $\mathcal{X} = \{(\pi_1 + \pi_2) : \pi_1 + \pi_2 = 1, \pi_1, \pi_2 \geq 0\}$*. Thus, we can write the utilities of patients as* $u_1 = 2\pi_1 + \pi_2$ *and* $u_2 = 3\pi_1 + 5\pi_2$*. In the following, we find the optimal allocation rule following the (1) utilitarian approach, (2) max-min fairness, and (3) proportional fairness.*

Utilitarian approach*: The objective is to maximize the total utility, i.e., maximize* $u_1 + u_2 = 5\pi_1 + 6\pi_2$ *subject to* $\pi \in \mathcal{X}$*. Then it follows that the solution* $\pi = (0, 1)$ *is the optimal solution. Therefore, the optimal allocation in the utilitarian approach is to allocate to the healthy patient with probability one with utilities* $u_1 = 1, u_2 = 5$*.*

Max-min fairness: *The objective here is to maximize the minimum utility across patients, i.e.,* $\max_{\pi \in \mathcal{X}} \min\{u_1, u_2\} = \max_{\pi \in \mathcal{X}} \min\{2\pi_1 + \pi_2, 3\pi_1 + 5\pi_2\}$*. The optimal solution is* $\pi = (1, 0)$ *in this case. Thus, the optimal allocation is to allocate to the sick patient and the utilities are* $u_1 = 2, u_2 = 3$*.*

Proportional fairness: *The objective is to maximize the multiplication of the utilities, i.e.,* $u_1 \times u_2 = (2\pi_1 + \pi_2)(3\pi_1 + 5\pi_2)$ *subject to* $\pi \in \mathcal{X}$*. It is not difficult to see that the optimal solution is* $\pi = (0.75, 0.25)$*, which is a randomized policy allocating the organ to the sick patient with probability 0.75 and to the healthy one with probability 0.25 and the utilities are* $u_1 = 1.75, u_2 = 3.5$*.*

The optimal solution of the proportional fairness problem satisfies the equilibrium point of the Nash bargaining problem. In particular, we have

$$\sum_{i=1}^{2} \frac{u_i - u_i^{PF}}{u_i^{PF}} = \frac{2\pi_1 + \pi_2 - 1.75}{1.75} + \frac{3\pi_1 + 5\pi_2 - 3.5}{3.5} \leq 0,$$

for all $\pi \in \mathcal{X}$*. Therefore, aggregate proportional change is non-positive and the solution* $\pi = (0.75, 0.25)$ *is the Nash bargaining solution and hence the optimal proportional fair policy. This result is in line with the fact that a policy is proportionally fair if compared to any other allocation policy, the players who gain utility, gain higher than those who lose utility. Note that this observation is true only when the organ is assumed to be divisible and in the case of indivisible organ there is no solution to the Nash bargaining problem.*

As can be seen from this example, the total utility $(u_1 + u_2)$ under the utilitarian approach (UA), max-min fairness (MF), and proportional fairness (PF) are 6, 5, and 5.25, respectively. This observation shows that the total utility under the PF policy is between that of MF and UA policies. The utilitarian approach is maximizing the total utilities of the patient population by prioritizing healthier and younger patients who have better post-transplant survival but it is not fair with respect to older and sicker patients. On the other hand, max-min fairness achieves a lower total utility compared to the utilitarian approach, but improves the minimum expected utility among patients. This observation encouraged us to propose proportional fairness in organ transplantation queuing systems, a fairness measure that sits at the midway point between the two extremes, utilitarian approach and max-min fairness and compensates for the utility loss in max-min fairness. This observation is in line with the results in Bertsimas et al. (2011), where they compare the max-min and proportional fairness and show that the bounds on the price of fairness are higher for the max-min fairness criteria resulting in a lower total utility for this policy compared to the proportional fairness criteria. The price of fairness is defined by the total utility loss under max-min/proportional fairness criteria compared to the utilitarian criteria.

One interpretation for Nash solution is that it is a solution to a bargaining among players, i.e., the solution to the bargaining is the proportional fairness utility for each player. For the construction of Nash bargaining between two individuals and the required assumptions for the Nash solution see Nash (1950). Since we apply proportional fairness as a measure of fairness in transplant systems, the solution that we propose may have similar interpretations. That is, patients seek to maximize their QALYs (utility) and bargain among themselves for the limited organs. Then, UNOS allocation based on the proportionally fair policy in organ allocation implies that UNOS believes a fair policy is the one that corresponds to the patient bargaining in the Nash bargaining sense. Viewing the transplant system as a game among patients and UNOS seeking an objective is not unprecedented in the literature. Ata et al. (2020) modeled the transplant system as a game among rational patients who seek to maximize their total QALYs by accepting/rejecting the offered organ and UNOS seeks to optimize the total QALYs over the Nash equilibrium of the game among patients. Note, however, that the proportional fairness can be used as a measure by itself and not tied to a bargaining problem similar to the literature of bandwidth allocation of network capacity.

The goal of our study in this chapter is to (I) quantify the extent that efficiency loss due to fairness consideration in organ allocation can be improved by introducing proportionally fair organ allocation, and (II) provide insights on the structure of optimal proportionally fair organ allocation policies in different settings. While policy makers in UNOS have significant debates on the efficiency and fairness of the current allocation policy (Organ Procurement and Transplantation Network, 2016a; Stevenson et al., 2016), our results in this study can pave the way to modify the organ allocation policies and shift them towards incorporating fairness measures that are less sensitive to the inequality in utility allocation compared to the policies considering max-min fairness. To that end, we make the following contributions.

We formulate an optimization problem to incorporate proportional fairness as an equity measure in organ allocation. In particular, in Section 3.2 we use a fluid approximation of the transplantation queuing system for deriving the necessary ingredients for utility estimation and feasibility set. In Section 3.3 an achievable region based approach is utilized to transform the said optimization problem to an equivalent one over the space of all performance outcomes. Then, we show that the optimal policy is assortative if certain assumptions are made on the problem parameters (Theorem 3.1). Assortative policies are attractive, easy to understand and implement, and have the following insight: higher quality organs are assigned to higher QALYs-to-gain patients (see Section 3.2 for detailed discussions). Section 3.4 presents the numerical results and contributions and Section 3.5 concludes.

3.2 Problem Formulation

We formulate the organ allocation problem as a queuing model with n queues associated with patient types. Available organs, which their type lies between $[0, 1]$, are partitioned into n subsets where each subset is allocated to one of the patient classes. As a result of this allocation, each patient receives a utility, which depends on the patient type and their expected waiting time, as well as the type of the donor organ. Su and Zenios (2006) studied a similar queuing system for kidney transplantation and provided expressions for the expected waiting times and the utilities by studying a fluid approximation of the queuing model. They formulate a partitioning problem to study the kidney allocation problem. We consider a similar formulation where decision is to find

a way to partition the organ pool (available donor organs with different qualities) into n subsets such that the resulting allocation is optimal in terms of proportional fairness. A policy is optimal in being proportionally fair (PF), if it attains the maximum value for the sum of the logarithm of patient utilities compared to any other allocation (partition).

Let $I = \{1, \ldots, n\}$ be the set of patient classes with λ_i being the arrival rate of patients in class $i \in I$, and $\lambda = \sum_{i=1}^{n} \lambda_i$ be the total arrival rate of patients. Donor organs arrive to the system according to a Poisson process with rate μ with $\mu < \lambda$ (without loss of generality assume $\mu = 1$). Patients on the waiting list may die within an exponentially distributed time with mean d (note that we assume $d_1 = \ldots = d_n = d$, that is the life expectancy while waiting is the same across all patient classes). We make this assumption to derive structural properties for the policy and relax it in our numerical results. Also, arriving organs have different types (categorized based on their qualities) and for each organ there is a random number $X \in \mathcal{X}$ associated to the organs in an i.i.d. fashion. We assume that X is uniformly distributed in the interval $\mathcal{X} = [0, 1]$. Let $L_i(x)$ be the post-transplant life expectancy of a patient in class i that receives an organ of type x. The goal of our formulation is to find the best way to divide the arriving organ pool into n subsets each allocated to one of the patient classes. Thus, we formulate the organ allocation problem as a partitioning problem of organ pool, where the decision maker looks for the best partition $\mathcal{A} = \{A_1, \ldots, A_n\}$ of $[0, 1]$ into disjoint subsets A_i. The resulting allocation policy corresponding to a partition $\mathcal{A}$ under the fluid scaling allocates an organ with type X to a patient in class i if $X \in A_i$, where X is a uniform $[0, 1]$ random variable. The utility of patients in class i under any allocation partition $\mathcal{A}$ is given by (Su and Zenios, 2006):

$$U_i = \beta D_i + \alpha p_i T_i,$$

where the utility function U_i denotes the Quality Adjusted Life Years (QALYs) of the patients in class i, D_i denotes pre-transplant life years (from the time a patient has arrived until death or transplant), T_i denotes post-transplant life years (from the time a patient receives an organ until death), p_i denotes the probability that a patient survives until receiving a transplant, and α and β are the quality of life scores corresponding to pre- and post-transplant life years, respectively. The quantities D_i, p_i, T_i depend on the allocation policy (partition $\mathcal{A}$). Under the fluid scaling these

quantities are estimated in Su and Zenios (2006) and are as follows:

$$D_i = \left[\frac{\lambda_i - \mu_i}{\lambda_i}\right]^+ d_i,$$
$$p_i = \frac{\mu_i}{\lambda_i},$$
$$T_i = \mathbb{E}\big[L_i(X)|X \in A_i\big],$$

where $\mu_i = \mu\mathbb{P}(X \in A_i) = \mathbb{P}(X \in A_i)$ is the allocation rate to the patients in class i. Then, the utility function for patients in class i can be written as follows:

$$U_i = \beta\left[\frac{\lambda_i - \mu_i}{\lambda_i}\right]^+ d_i + \alpha\frac{\mu_i}{\lambda_i}\mathbb{E}\big[L_i(X)|X \in A_i\big].$$

We consider a decision maker seeking for an allocation (partition) $\mathcal{A}$ that maximizes the proportional fairness objective ($\sum_{i=1}^n \lambda_i \log(U_i)$), subject to the fluid condition $\mu_i \leq \lambda_i$ for every i:

$$\max_{\mathcal{A}} \left(\sum_{i=1}^{n} \lambda_i \log\left(\beta d_i(\frac{\lambda_i - \mu_i}{\lambda_i}) + \alpha\frac{\mu_i}{\lambda_i}\mathbb{E}[L_i(X)|X \in A_i]\right)\right) \tag{P_4}$$

$$\text{subject to} \qquad 0 \leq \mu_i \leq \lambda_i \quad i = 1, 2, \ldots, n. \tag{3.2}$$

Next, we simplify the objective function. We assume that $L_i(x) = m + c_i g(x)$, where $m > 0$ denotes the LYs gained by receiving an organ of the lowest quality, $g(x) \geq 0$ is the quality of the type x organ, and $c_i > 0$ denotes the risk of death for patients in class i after transplantation. Without loss of generality, we order patient and organ types such that $c_i > c_{i+1}$ for $i = 1, \ldots, n-1$ (i.e., patients with lower index have a lower post-transplant risk) and $g(\cdot)$ is a decreasing function on organ type x, i.e., organs with smaller x have a higher quality. Our numerical study in Section 3.4 reveals that these assumptions are all satisfied for the heart transplantation dataset considered as the case study. By using these assumptions and setting $a = m\alpha - d\beta,\ b_i = c_i\alpha$, and $\gamma_i = \mathbb{E}[g(x)1\{X \in A_i\}]$ we can rewrite the utility of patients in class i as follows:

$$\begin{aligned} U_i &= \frac{\lambda_i - \mu_i}{\lambda_i} d\beta + \frac{\mu_i}{\lambda_i}\Big(m + c_i\mathbb{E}[g(X)|X \in A_i]\Big)\alpha \\ &= d\beta + \frac{\mu_i}{\lambda_i}a + b_i\frac{\gamma_i}{\lambda_i}. \end{aligned}$$

After omitting the constant term $d\beta$ from the utility function of all the patient classes, we end up with the following formula for the utility, which only depends on μ_i and γ_i as the decision variables:

$$U_i = \frac{a\mu_i + b_i\gamma_i}{\lambda_i}.$$

Thus, we observe that the utility of patients in class i depends on the allocation policy (partition $\mathcal{A}$) through the variables $\mu_i = \mathbb{P}\{X \in A_i\}$ and $\gamma_i = \mathbb{E}[g(x)1\{X \in A_i\}]$ in a linear way. Variables μ_i and γ_i can be interpreted as the intensity of organ allocation, and the quality of organs allocated to the patients in class i, respectively. By using the derived utility function, problem (P_4) can be written in a more compact way as follows:

$$\max_{\mathcal{A}} \left(\sum_{i=1}^{n} \lambda_i \log \big(\frac{a\mu_i + b_i\gamma_i}{\lambda_i}\big) \right) \qquad (P_5)$$
$$\text{subject to} \quad 0 \leq \mu_i \leq \lambda_i \quad i = 1, 2, \ldots, n.$$

This optimization problem is very difficult to solve, since the search is over all the partitions in $\mathcal{A}$. In fact, partitioning the interval $[0, 1]$ into n subsets has infinite possibilities. One solution is to discretize the organ space into finitely disjoint subsets and solve the problem over the discrete organ space which yields a randomized allocation policy. However, the issue here is that the size of the latter is still huge and it involves an exponential number of decision variables growing with the number of subsets that the organ space is partitioned. Moreover, randomized policies are difficult to implement in practice and do not provide insight to this problem. Due to theses issues, and the dependency of the number of variables to the number of discretized subsets, we use the technique introduced by Bertsimas (1995) to transform the problem into a computationally tractable one, which also enables us to derive structural properties for the allocation problem. The technique is called the achievable region method and involves solving an optimization problem over $2n$ decision variables that does not depend on the number of the subsets explained above.

3.3 Analysis of the Optimal Policy

Due to the dependency of the utilities to the allocation partition $\mathcal{A}$ through the variables $\vec{\mu} = (\mu_1, \ldots, \mu_n)$ and $\vec{\gamma} = (\gamma_1, \ldots, \gamma_n)$, we express them by $\vec{\mu}(\mathcal{A})$ and $\vec{\gamma}(\mathcal{A})$. Since the space of the

decision (space of partitions $\mathcal{A}$) is complex, we use the achievable region method to transform the decision space into a more tractable one. For any allocation partition $\mathcal{A}$, the method finds vectors $\vec{\mu}(\mathcal{A})$ and $\vec{\gamma}(\mathcal{A})$ that can be achieved by that partition. In particular, the method characterizes the space of all performance measures $\vec{\mu}(\mathcal{A})$ and $\vec{\gamma}(\mathcal{A})$ that can be achieved by any feasible decision (allocation partition $\mathcal{A}$). Then it optimizes the objective over the new decision space to find the optimal value of the transformed performance measures, i.e., $\vec{\mu}^*(\mathcal{A})$ and $\vec{\gamma}^*(\mathcal{A})$. Finally, the method finds the partition $\mathcal{A}^*$ that achieves these optimal performance measures. Such a method is used in the multi-class scheduling literature as well, e.g., see Federgruen and Groenevelt (1988).

Let $\mathrm{AR}(\mathcal{A})$ denote the achievable region of the performance measures $\big(\vec{\mu}(\mathcal{A}), \vec{\gamma}(\mathcal{A})\big)$ corresponding to the allocation partition $\mathcal{A}$ defined by

$$\mathrm{AR}(\mathcal{A}) := \left\{ (\vec{\mu}, \vec{\gamma}) : \quad \sum_{i=1}^{n} \mu_i = \mu, \quad \gamma(S) \leq G(\mu(S)) \ \ \forall S \subseteq \{1, \ldots, n\} \right\}, \tag{3.3}$$

where for each $S \subseteq \{1, \ldots, n\}$, $\mu(S) = \sum_{i \in S} \mu_i$, $\gamma(S) = \sum_{i \in S} \gamma_i$, and $G(x) = \int_0^x g(t)dt$. In fact, for each subset of patient classes S, function $G(\cdot)$ provides an upper bound on the quality of share of organs allocated to the patients in that subset. Su and Zenios (2006) showed that (i) under an allocation partition $\mathcal{A}$, every achievable performance measure $\big(\vec{\mu}(\mathcal{A}), \vec{\gamma}(\mathcal{A})\big)$ must satisfy (3.3), and (ii) for any given $(\vec{\mu}, \vec{\gamma})$ satisfying (3.3) one can construct an allocation partition $\mathcal{A}_{(\vec{\mu}, \vec{\gamma})}$ corresponding to $(\vec{\mu}, \vec{\gamma})$ via an algorithm called the synthesis algorithm.

The result above helps transform the complex decision space of the partitions into the decision space over $(\vec{\mu}, \vec{\gamma}) \in \mathbb{R}_+^{2n}$ specified in (3.3). By using the newly introduced decision space (variables $(\vec{\mu}, \vec{\gamma})$), the proportional fairness objective function can be represented by

$$\sum_{i=1}^{n} \lambda_i \log(U_i) = \sum_{i=1}^{n} \lambda_i \log\big(\frac{a\mu_i + b_i\gamma_i}{\lambda_i}\big) = \sum_{i=1}^{n} \lambda_i \log\big(a\mu_i + b_i\gamma_i\big) - \lambda_i \log(\lambda_i).$$

We omit the constant term $\lambda_i \log(\lambda_i)$ which does not affect the optimal solution. Thus, the partitioning problem (P_5) can be reformulated in the new decision space as a nonlinear programming

problem as follows:

$$\max_{(\vec{\mu},\vec{\gamma})} \sum_{i=1}^{n} \Big(\lambda_i \log \big(a\mu_i + b_i\gamma_i \big) \Big) \tag{P_6}$$

subject to,

$$\gamma(S) \leq G\big(\mu(S)\big), \quad \forall S \subseteq \{1,\ldots,n\}, \tag{3.4}$$

$$0 \leq \mu_i \leq \lambda_i, \quad \forall i = 1,\ldots,n, \tag{3.5}$$

$$\sum_{i=1}^{n} \mu_i = \mu. \tag{3.6}$$

From now on, we focus on this problem which is a combinatorial optimization problem as it involves constraints (3.4) that form a polymatroid.

Definition 3.1. *An allocation policy $\mathcal{A}$ is called an assortative partition if*

$$A_1 = [0, \mu_1] \ , A_2 = [\mu_1, \mu_1 + \mu_2], \ldots, A_n = [\mu_1 + \ldots + \mu_{n-1}, \mu_1 + \ldots + \mu_n].$$

Note that the allocation domain i is of length μ_i, and since by assumption, patient groups are ordered such that $b_1 \geq b_2 \geq \ldots \geq b_n$, the policy being assortative is interpreted as follows: the organs with the highest quality are allocated to the patients with better post-transplant survival. The following lemma by Su and Zenios (2006) shows that the assortativeness property of an allocation policy is tied to the bindingness of certain constraints in (3.4) at optimality.

Lemma 3.1. *Any achievable performance measure $(\vec{\mu},\vec{\gamma})$ satisfying*

$$\sum_{k=1}^{i} \gamma_k = G(\sum_{k=1}^{i} \mu_k), \quad i = 1,\ldots,n,$$

corresponds to a partition which is assortative.

Let S_k for $k = 1,\ldots,n$ be a subset of size k of the patient indicies $\{1,\ldots,n\}$ and $\mathcal{S}_k$ be the set of such subsets, e.g., $\mathcal{S}_1 = \big\{\{1\},\{2\},\ldots,\{n\}\big\}$. The following proposition proves an interesting property about the activeness of constraints of problem (P_6) at optimality. Specifically, it shows that for every $k = 1,\ldots,n$, at most one of the constraints in (3.4) corresponding to the elements of $\mathcal{S}_k$ can be binding at the optimal solution.

Proposition 3.1. *At most one of the constraints of size k in* (3.4) *corresponding to the elements of $\mathcal{S}_k$ is binding at optimality for every $k = 1, \ldots, n$.*

Proof. We prove this proposition by using the proof by contradiction for constraints corresponding to $\mathcal{S}_1$, i.e., k=1. The proof for $k > 1$ is similar. We prove that among the following constraints, at most one of them can be binding:

$$\begin{aligned} \gamma_1 &\leq 1 - e^{-\mu_1}, \\ \vdots \quad &\quad \vdots \quad \quad \vdots \\ \gamma_n &\leq 1 - e^{-\mu_n}. \end{aligned}$$

Suppose this is not true and assume there exist some i and j such that $\gamma_i = 1 - e^{-\mu_i}$ and $\gamma_j = 1 - e^{-\mu_j}$ for $i \neq j$. This yields $\gamma_i + \gamma_j = 2 - e^{-\mu_i} - e^{-\mu_j}$. However, the constraint corresponding to $\{i, j\}$ (an element of $\mathcal{S}_2$) in (3.4) imposes that $\gamma_i + \gamma_j \leq 1 - e^{-(\mu_i + \mu_j)}$. Thus, we get:

$$2 - e^{-\mu_i} - e^{-\mu_j} \leq 1 - e^{-(\mu_i + \mu_j)} \tag{3.7}$$

$$\implies e^{-\mu_i} + e^{-\mu_j} - e^{-(\mu_i + \mu_j)} \geq 1 \tag{3.8}$$

Now, let the function $h(\cdot, \cdot)$ be defined by $h(x, y) = e^{-x} + e^{-y} - e^{-(x+y)}$. Note that for this function, we have $h(0, 0) = 1$ and

$$\begin{aligned} \frac{\partial h(x,y)}{\partial x} &= e^{-(x+y)} - e^{-x}, \\ \frac{\partial h(x,y)}{\partial y} &= e^{-(x+y)} - e^{-y}, \end{aligned}$$

both being negative for $x, y \geq 0$, meaning that $h(\cdot, \cdot)$ is a non-increasing function for $x, y \geq 0$. Therefore, we have $h(x, y) \leq 1$ for $x, y \geq 0$ and $h(x, y) < 1$ for $x, y > 0$. This argument proves that $e^{-\mu_i} + e^{-\mu_j} - e^{-(\mu_i + \mu_j)} - 1 \leq 0$ for $\mu_i, \mu_j \geq 0$ with equality holding for $\mu_i = \mu_j = 0$. Now, note that $\mu_i = \mu_j = 0$ cannot yield an optimal solution since it implies $\gamma_i = \gamma_j = 0$ and the objective goes to $-\infty$ in this case. Therefore, at optimality, we have $e^{-\mu_i} + e^{-\mu_j} - e^{-(\mu_i + \mu_j)} < 1$ which contradicts (3.8), and completes the proof for k=1. The proof for constraints corresponding to the elements of $\mathcal{S}_k$ for $k > 2$ follows by a similar logic. □

Next, we discuss two assumptions on the parameters of our problem under which optimal solution is an assortative partition policy. Assumption 3.1 is for strictly overloaded queuing systems where arrival rate of patients are significantly higher than that of donors.

Assumption 3.1. *The transplantation queuing system is strictly overloaded, i.e.,* $\lambda_i > \mu := 1$ *for all* $i = 1, \ldots, n$.

Then, we explore the setting where this assumption does not hold but still the optimal policy is assortative. In order to find the optimal solution of problem (P_6) in this case, we write the KKT condition for this nonlinear problem and show that under some looser conditions on λ_i, the problem still this property that constraints corresponding to the subsets $[j]$ for $j = 1, \ldots, n$ in (3.4) are binding at the optimal point. Note that due to the presence of constraints (3.4) in the model, which form a polymatroid, one may use combinatorial optimization techniques to find the optimal solution for problem (P_6). The theoretical results we get from KKT conditions coincide with the solution based on the combinatorial optimization techniques in Fujishige (2005). Before stating Theorem 3.1, which is the main results of this section, we consider the following assumption.

Assumption 3.2. *The nonlinear system of equations,*

$$\begin{cases} \frac{\lambda_i(a+b_i e^{-(\mu_1+\ldots+\mu_i)})}{a\mu_i+b_i e^{-(\mu_0+\ldots+\mu_{i-1})}(1-e^{-\mu_i})} = \frac{\lambda_{i+1}(a+b_{i+1} e^{-(\mu_1+\ldots+\mu_i)})}{a\mu_{i+1}+b_{i+1} e^{-(\mu_0+\ldots+\mu_i)}(1-e^{-\mu_{i+1}})}, \quad i = 1, \ldots, n-1, \\ \sum_{i=1}^{n} \mu_i = \mu = 1, \end{cases}$$

has a solution $\vec{\mu} = (\mu_1, \ldots, \mu_n)$ *such that* $0 < \mu_i < \lambda_i$ *for* $i = 1, \ldots, n$.

The following lemma shows that Assumption 3.2 is more general than Assumption 3.1 for $n = 1, 2, 3$.

Lemma 3.2. *If Assumption 3.1 holds, then the nonlinear system of equations in Assumption 3.2 has a solution.*

Proof. To prove the statement for $n = 1$, assume Assumption 3.1 holds, i.e., $\lambda_1 > 1$, then the system of non-linear equations reduces to a single equation $\mu_1 = \mu = 1$, which clearly has a solution $\mu_1 = 1$ in the interval $(0, \lambda_1)$, where $\lambda_1 > 1$ and the statement is trivial.

For $n = 2$, the system of non-linear equations is given by

$$\frac{\lambda_2(a + b_2 e^{-\mu_1})}{a\mu_2 + b_2 e^{-\mu_1}(1 - e^{-\mu_2})} = \frac{\lambda_1(a + b_1 e^{-\mu_1})}{a\mu_1 + b_1(1 - e^{-\mu_1})},$$
$$\mu_1 + \mu_2 = 1,$$

which can be reduced to a single equation by substituting $\mu_1 = x$ and $\mu_2 = 1 - x$ with $\max\{0, 1 - \lambda_2\} \leq x \leq \min\{1, \lambda_1\}$. Therefore, we need to find the roots of function $f(x)$ on the interval $(\max\{0, 1 - \lambda_2\}, \min\{1, \lambda_1\})$, where

$$f(x) = \lambda_2(a + b_2 e^{-x}) \left(ax + b_1(1 - e^{-x})\right) - \lambda_1(a + b_1 e^{-x}) \left(a(1 - x) + b_2 e^{-x}(1 - e^{-(1-x)})\right). \quad (3.9)$$

If Assumption 3.1 holds, i.e., $\lambda_1, \lambda_2 > 1$, the feasible interval for x is $[0, 1]$. Since $f(\cdot)$ is continuous and we have $f(0) = -\lambda_1(a+b_1)\left(a + b_2(1 - e^{-1})\right) < 0$ and $f(1) = \lambda_2(a+b_2e^{-1})\left(a + b_1(1 - e^{-1})\right) > 0$, by the intermediate value theorem it follows that the equation $f(x) = 0$ has a solution in the interval $(0, 1)$. This step shows that for $n = 2$, Assumption 3.1 implies Assumption 3.2 proving the statement.

Before proving the lemma for $n = 3$, we discuss the Borsuk's theorem for the existence of solutions of nonlinear equations (Frommer and Lang, 2005). In particular, for our problem the theorem provides sufficient conditions on the parameters a, b, and λ under which the nonlinear system of equations in Assumption 3.2 has a solution in the interior of $\{(\mu_1, \ldots, \mu_n) : 0 \leq \mu_i \leq \lambda_i \text{ for } i = 1, \ldots, n\}$. In fact, these conditions are a generalization of the intermediate value theorem for $n \geq 3$. These conditions can be numerically tested via interval analysis but it is difficult to derive closed form equations in a clean format on the parameters of the problem. Nonetheless, we tested these sufficient conditions for the problems that we knew the solution exists, but the tests were inconclusive.
To prove the statement for $n = 3$, first note that in the linear setting, the necessary an sufficient condition for existence and uniqueness of solution to a system of equations is that the Jacobian determinant be nonzero. In nonlinear setting if the Jacobian matrix has nonzero determinant, then one gets the same result locally, i.e., for small perturbations. For $n = 3$, the nonlinear system of

equations is given by

$$\frac{\lambda_2(a+b_2e^{-\mu_1})}{a\mu_2+b_2e^{-\mu_1}(1-e^{-\mu_2})}=\frac{\lambda_1(a+b_1e^{-\mu_1})}{a\mu_1+b_1(1-e^{-\mu_1})},$$
$$\frac{\lambda_3(a+b_3e^{-(\mu_1+\mu_2)})}{a\mu_3+b_3e^{-(\mu_1+\mu_2)}(1-e^{-\mu_3})}=\frac{\lambda_2(a+b_2e^{-(\mu_1+\mu_2)})}{a\mu_2+b_2e^{-\mu_1}(1-e^{-\mu_2})},$$
$$\mu_1+\mu_2+\mu_3=1,$$

which can be reduced to a system of two nonlinear equations by substituting $\mu_1 = x$, $\mu_2 = y$, and $\mu_3 = 1 - x - y$, where (x, y) is defined in a feasible two dimensional polygon $\mathcal{P} := \{(x, y) : 0 \leq x \leq \lambda_1, 0 \leq y \leq \lambda_2, 1 - \lambda_3 \leq x + y \leq 1\}$. In particular, we need to find the zeros of the function $f(x, y) = (f_1(x, y), f_2(x, y))$ in the interior of $\mathcal{P}$, where f_1 and f_2 are defined by

$$f_1(x,y)=\lambda_2(a+b_2e^{-x})\left(ax+b_1(1-e^{-x})\right)-\lambda_1(a+b_1e^{-x})\left(ay+b_2e^{-x}(1-e^{-y})\right),$$
$$f_2(x,y)=\lambda_3(a+b_3e^{-(x+y)})\left(ay+b_2(1-e^{-y})\right)-\lambda_2(a+b_2e^{-(x+y)})\left(a(1-x-y)+b_3e^{-(x+y)}(1-e^{-(1-x-y)})\right).$$

A sufficient condition for the continuous function f with continuous Jacobian to have a root in the interior of $\mathcal{P}$ is to ensure the system has a Jacobian with nonzero determinant locally at the extreme points of $\mathcal{P}$ (Ortega and Rheinboldt, 2000). This is true when the Jacobian determinant $det(J(x, y))$ is a concave function of the variables (x, y). To see the reason, assume there are two pints $(x_1, y_1), (x_2, y_2) \in \mathcal{P}$ such that $det(J(x_1, y_1)), det(J(x_2, y_2)) > 0$, then for $0 \leq \theta \leq 1$ we have

$$det\left(J(\theta(x_1,y_1)+(1-\theta)(x_2,y_2)\right)\geq\theta det(J(x_1,y_1))+(1-\theta)det(J(x_2,y_2))>0,$$

that is, the determinant function $det(J(x, y))$ is positive for any convex combination of the points (x_1, y_1) and (x_2, y_2), i.e., on the line segment between (x_1, y_1) and (x_2, y_2). Thus, in order to check the sign of the Jacobian determinant in $\mathcal{P}$, it suffices to check its sign at extreme points of the polygon $\mathcal{P}$, as every point in its interior is a convex combination of its extreme points.

Now, to prove the statement assume $\lambda_i > 1$ for $i = 1, 2, 3$. In this setting, the Jacobian determinant is a concave function and the polygon $\mathcal{P}$ has three extreme points, i.e., $(0, 0)$, $(1, 0)$, and $(0, 1)$. The Jacobian determinant of the non-linear system $f(x, y) = (0, 0)$ is positive at these points, thus positive on the entire $\mathcal{P}$.

□

The following example shows that there are sets of parameters for which Assumption 3.1 does not hold, but the system of nonlinear equations in Assumption 3.2 has a solution in the interior of $\{(\mu_1, \ldots, \mu_n) : 0 \leq \mu_i \leq \lambda_i\}$, supporting the fact that Assumption 3.2 includes more general set of parameters compared to Assumption 3.1.

Example 3.2. *Consider an example of an organ transplantation system with only 3 patient groups ordered in their post-transplant survival, i.e.,* $b_1 = 20, b_2 = 15, b_3 = 10$*, with the same pre-transplant survival, i.e.,* $a_1 = a_2 = a_3 = a = 2$*. Assume further that their arrival rates are* $\lambda_1 = 0.6, \lambda_2 = 0.7, \lambda_3 = 0.8$*. Then, for such an example, the nonlinear system of equations in Assumption 3.2 has a solution as follows:* $\mu_1 = 0.22, \mu_2 = 0.31, \mu_3 = 0.47$*, which clearly belongs to the interior of the polygon formed by constraints* (3.5)*. However, the condition in Assumption 3.1 does not hold for this problem. Therefore, the solution of optimization problem* (P_6) *for this set of parameters is an assortative partition policy.*

Next, in the following theorem we construct the condition under which the optimal solution of problem (P_6) is an assortative partition policy, i.e., Assumption 3.2.

Theorem 3.1. *Under Assumption 3.2, the optimal solution of problem* (P_6) *is an assortative partition policy.*

Proof. Let $F : \mathbb{R}^{2n}_{+} \to \mathbb{R}$ be a continuous real valued function on $(\vec{\mu}, \vec{\gamma})$ representing the objective function of problem (P_6) defined by,

$$F(\vec{\mu}, \vec{\gamma}) = \sum_{i=1}^{n} \Big(\lambda_i \log \big(a\mu_i + b_i \gamma_i \big) \Big).$$

Furthermore, for $S \subseteq \{1, \ldots, n\}$ let T_S be the Lagrange multiplier associated with the corresponding constraint in (3.4), L_i and H_i be the Lagrange multipliers associated to the i^{th} lower and upper constraints in (3.5), respectively, and Y be the multiplier associated with the single organ availability constraint (3.6). Let $\mathcal{L}$ be the Lagrangian function that adjoints the constraints to the objective function using the Lagrange multipliers, defined by:

$$\mathcal{L}(\vec{\mu}, \vec{\gamma}, \vec{T}, \vec{L}, \vec{H}, Y) = F(\vec{\mu}, \vec{\gamma}) + \sum_{S \subseteq \{1,\ldots,n\}} T_S \Big(G\big(\mu(S)\big) - \gamma(S) \Big) + \sum_{i=1}^{n} L_i \mu_i + \sum_{i=1}^{n} H_i(\lambda_i - \mu_i) + Y(\sum_{i=1}^{n} \mu_i - 1).$$

Now, KKT conditions for problem (P_6) can be stated through the following three conditions:

(I) **Primal Feasibility:** The variable vector $(\vec{\mu}, \vec{\gamma})$ must be feasible to the primal problem, that is,

$$\begin{aligned}
&\gamma(S) \le G\big(\mu(S)\big), \quad \forall S \subseteq \{1, \dots, n\}, \\
&0 \le \mu_i \le \lambda_i, \quad \forall i = 1, \dots, n, \\
&\sum_{i=1}^{n} \mu_i = \mu.
\end{aligned}$$

(II) **Dual Feasibility:** The dual variables $\vec{T} = \Big(T_S : S \subseteq \{1, \dots, n\}\Big)$, $\vec{L} = \Big(L_i : i \in \{1, \dots, n\}\Big)$, and $\vec{H} = \Big(H_i : i \in \{1, \dots, n\}\Big)$, must be nonnegative vectors.

(III) **Complementary Slackness:** The primal and dual variables must satisfy the following condition:

$$\begin{aligned}
&T_S\Big(G\big(\mu(S)\big) - \gamma(S)\Big) = 0, \quad \forall S \subseteq \{1, \dots, n\}, \\
&L_i \mu_i = 0, \quad \forall i = 1, \dots, n, \\
&H_i(\lambda_i - \mu_i) = 0, \quad \forall i = 1, \dots, n, \\
&Y(\sum_{i=1}^{n} \mu_i - \mu) = 0.
\end{aligned}$$

Furthermore, for each $i = 1, \dots, n$, partial derivative of the Lagrangian function $\mathcal{L}$ with respect to μ_i and γ_i at the optimal point $(\vec{\mu}, \vec{\gamma}, \vec{T}, \vec{L}, \vec{H}, Y)$ must be zero, that is, for each $i = 1, \dots, n$,

$$\frac{\partial \mathcal{L}}{\partial \mu_i}(\vec{\mu}, \vec{\gamma}, \vec{T}, \vec{L}, \vec{H}, Y) = \frac{a\lambda_i}{a\mu_i + b_i\gamma_i} + \sum_{\Big\{S \subseteq \{1,\dots,n\} : i \in S\Big\}} T_S \frac{\partial G(\mu(S))}{\partial \mu_i}(\vec{\mu}, \vec{\gamma}, \vec{T}, \vec{L}, \vec{H}, Y) + L_i - H_i + Y = 0, \quad (3.10)$$

$$\frac{\partial \mathcal{L}}{\partial \gamma_i}(\vec{\mu}, \vec{\gamma}, \vec{T}, \vec{L}, \vec{H}, Y) = \frac{b_i\lambda_i}{a\mu_i + b_i\gamma_i} - \sum_{\Big\{S \subseteq \{1,\dots,n\} : i \in S\Big\}} T_S \frac{\partial \gamma(S)}{\partial \gamma_i}(\vec{\mu}, \vec{\gamma}, \vec{T}, \vec{L}, \vec{H}, Y) = 0. \quad (3.11)$$

By Lemma 3.1, in order to have an assortative partition policy, constraints (3.6) must be non-binding at optimal solution, and among the constraints corresponding to the elements of the set $\mathcal{S}_k$ in (3.4), the constraint corresponding to the subset $[k]$ must be binding at the optimal solution for $k = 1, \dots, n$. We construct such a solution that satisfies the KKT optimality condition as follows: we let $\vec{L} = \vec{H} = 0$, $T_S = 0$ for each $S \subseteq \{1, \dots, n\}$ that $S \neq [k]$ for $k = 1, \dots, n$, and $G\big(\mu(S)\big) - \gamma(S) = 0$ for $S = [k]$ and each $k = 1, \dots, n$ with $\sum_{i=1}^{n} \mu_i = \mu$. This construction clearly satisfies the primal feasibility and complementary slackness. Furthermore, it is easy to see that such a solution satisfies

the dual feasibility. By using this solution and choosing $g(x) = e^{-x}$, as mentioned earlier, we have $G(x) = \int_0^x g(u)du = 1 - e^{-x}$, and the equations (3.10) and (3.11) can be rewritten as follows,

$$\frac{a\lambda_i}{a\mu_i + b_i\gamma_i} + \sum_{\left\{S=[k]:k=1,\ldots,n\right\}} T_S e^{-\mu(S)} + Y = 0, \tag{3.12}$$

$$\frac{b_i\lambda_i}{a\mu_i + b_i\gamma_i} - \sum_{\left\{S=[k]:k=1,\ldots,n\right\}} T_S = 0. \tag{3.13}$$

By equations (3.12) and (3.13) and eliminating Lagrange multipliers T_S and Y from the equations, we get the following system of nonlinear equations:

$$\frac{\lambda_i(a + b_i e^{-(\mu_1+\ldots+\mu_i)})}{a\mu_i + b_i e^{-(\mu_0+\ldots+\mu_{i-1})}(1 - e^{-\mu_i})} = \frac{\lambda_{i+1}(a + b_{i+1} e^{-(\mu_1+\ldots+\mu_i)})}{a\mu_{i+1} + b_{i+1} e^{-(\mu_0+\ldots+\mu_i)}(1 - e^{-\mu_{i+1}})} \quad i = 1, \ldots, n-1, \tag{3.14}$$

where $\mu_0 := 0$ by convention. Also, note that by equations (3.12) and (3.13), for each $S \subseteq \{1, \ldots, n\}$ the dual variables T_S are non-negative and satisfy the dual feasibility condition (II) as required for a KKT solution. Equations in (3.14) together with constraint (3.6), form a non-linear system of equations with n variables and n equations on the variables μ_i. By construction, any solution to this system of nonlinear equations that lies in the space $\{\vec{\mu} : 0 < \mu_i < \lambda_i, i = 1, \ldots, n\}$ is in fact the optimal solution of the problem (P_6), which is an assortative partition policy according to Lemma 3.1. Note that by Assumption 3.2 such a solution exists. Once $\vec{\mu}$ is characterized, we can easily construct the corresponding solution $\vec{\gamma}$, i.e., for each $i = 1, \ldots, n$, we have $\gamma_i = e^{-(\mu_0+\ldots+\mu_{i-1})}(1 - e^{-\mu_i})$. It remains to note that since the objective function $F(\cdot, \cdot)$ of the problem (P_6) is concave, and the constraints form a convex set, the KKT optimality solution is a unique solution. This completes the proof. □

3.4 Numerical Results

This section presents the numerical results of applying the methods discussed in Sections 3.2 and 3.3 of Chapter 3 to the U.S. heart transplantation waiting list. For the purpose of numerical study, we categorize patients based on their health status, age, blood-type, and VAD status into 128 classes. The input parameters of the optimization models (P_5) and (P_6) are estimated from

the UNOS/OPTN heart transplantation data sets. Specifically, λ_i, the arrival rate of patients in class i and μ, total arrival rate of donor hearts are estimated from the OPTN data sets for the 2006-2014 period. Pre-transplant quality of life coefficients, α_is, are estimated for every health class i by mapping from the coefficients for heart failure disease classes presented in Tengs and Wallace (2000). Note that without loss of generality, we set the post-transplant quality of life coefficient to be one, i.e., $\beta = 1$, and adjust the pre-transplant coefficients accordingly.

Table 3.1 summarizes the results of the simulation runs for the UA, MF, and PF policies: see Hasankhani and Khademi (2017), Hasankhani and Khademi (2019), and Su and Zenios (2006) for details. Furthermore, we include two policies by UNOS in our analysis, UNOS policy and recently proposed UNOS-7 Tiered heart allocation policy (see Chapter 2 for more discussion on the UNOS policies). We compare the proportional fair policy proposed in this study with these benchmark policies in terms of total utilities of the patient population, minimum expected utility (MEU), sum of logarithm of expected utilities (SLEUs), and the variance of waiting times. These benchmarks include a policy that minimizes the variance of the waiting time between patient classes (VWT policy), and an equity policy proposed by Su and Zenios (2006) (SZE policy).

In order to measure fairness in the simulation, we calculate the expected QALYs of patients in different classes under simulation from the time they join the waiting list until they die or receive an organ, i.e., the post-listing QALYs. The first three columns in Table 3.1 report the sum of the QALYs of patients, the minimum expected QALYs among patient groups, and sum of the logarithm of QALYs of the patients, respectively. The last column indicates the variance across patient classes of the expected waiting times, which is introduced to be a measure of fairness in the literature (Su and Zenios, 2006). All the measures reported are in terms of days except for the variance which is in terms of the square of a day. Note that since the patients change class due to health deterioration or age change, we consider the initial listing class of the patients in reporting the simulation results.

Results in Table 3.1 are in line with what we observed in Example 3.1, emphasizing on the fact that the PF policy has higher total utility outcome than that of MF and lower than that of UA policy. The price of fairness, i.e., utility loss with respect to UA, for MF and PF policies are around 6% and 2%, respectively. That is, the PF policy performs with a lower price in losing utility compared to

Table 3.1: Policy Comparison

Policies	**Total QALYs**($\times 10^8$)	**MEU**	**SLEUs**($\times 10^2$)	**Variance of Waiting Times**
UA	1.651	115	2642.32	8100
MF	1.560	133	2574.33	6888
PF	1.605	119	2929.26	4489
VWT	1.600	122	2625.04	2601
UNOS	1.524	117	2527.09	23409
UNOS 7-Tiered	1.528	116	2555.91	30625

MF. This is because MF policy allocates organs more to the patients who have the lowest expected utility, e.g., sicker patients, to maximize their utility. However, as a result of this allocation patients who expect to gain higher utilities will not receive enough donor organ to increase their utilities. On the other hand, since the goal of the proportional fairness is to have a non-positive aggregate proportional change compared to other allocations, its solution, i.e., PF policy, will produce policies performing better than MF policy in terms of aggregate utility while at the same time preserving a certain degree of fairness based on the Nash solution. Therefore, the PF policy has a significantly smaller price of fairness. Note that the price of fairness for VWT policy, which introduced in Chapter 2 as a policy focusing on fairness by equalizing the waiting time among patients, is around 3%. Furthermore, the PF policy outperforms UNOS and UNOS 7-Tiered policies by around 7% in terms of total utility. In addition, the minimum utility of the patients under PF policy is slightly higher than that of UA. In terms of minimum expected utility, the MF policy achieves the highest minimum utility among patients and all other policies perform almost similar in terms of this measure. In terms of the sum of logarithm of utility of patients, the PF policy outperforms all other policies. Policies that consider fairness in their prioritization, i.e., MF, PF, and VWT, achieve smaller variance for waiting time across different patients compared to the UA and UNOS policies. This is an interesting observation of the impact of incorporating fairness in transplant queuing system allocation rules.

In addition, we conduct an analysis on the percentage of hearts allocated to different patient classes under each policy and discuss the priority focus in each of them. This analysis helps us capture the utility allocation among different patient classes and compare them for different allocations.

In particular, we report the percentages of donor hearts allocated to each patient health, age, and VAD status class in the simulation. Figures 3.1-3.3 report the results of this analysis for the PF, UA, MF, and UNOS policies. We observe an interesting behavior from the PF policy. In fact, the results reported in Figure 3.1 show that in terms of health prioritization, the PF policy allocates only around 29% of the total hearts to patients in health class 1A, i.e., sickest patient class, less than the 49% of the UNOS policy but greater than the 18% of UA policy. The MF policy, on the other hand, is closer to UNOS policy with 41% allocation to the sickest patient group, and this is in line with its objective as it tries to maximize the lowest utility among patients, e.g., sickest patients. These results suggest that PF policy prioritize healthier and sicker patients in a same manner as it assigns almost the same percentage of hearts to patients in 1A and 2, the sickest and healthiest patient classes. Furthermore, compared to the UA policy, it imposes certain level of fairness with respect to sicker patients, as it shifts priority from healthier to sicker patients.

In terms of age prioritization also we observed an interesting behaviour from PF policy. Although it is not surprising to see that UA policy prioritizes younger patients more than that of UNOS and MF, we observe that PF policy even allocates slightly higher percentage of organs to younger patients compared to UA policy. Specifically, PF policy allocates 56% of total hearts to the younger patient groups, i.e., [18-35] and [34-50] compared to the 51% of the UA policy and 38% of the MF policy. The reason is that as we show in chapter 2, the improvement of the UA policy over UNOS policy in terms of total utility is mainly due to a shift in patients prioritization from sicker and older patients towards healthier and younger ones, with an emphasize on shift in health prioritization. Thus, relatively speaking, UA policy tries to allocate more organs to healthy patients than the young patients. That is, among two patients, the healthy-old one and the sick-young one, the policy allocates organ to healthy-old patient rather than to sick-young one. Nonetheless, our results in Figures 1.1 and 1.2 suggest that the improvement of the PF over UNOS policy is also because of a shift towards prioritizing healthier and younger patients in PF policy, but with more emphasize on the shift in age prioritization. These results are consistent with the findings in Ladin and Hanto (2011) for kidney, where they state that prioritizing younger patients is more equitable, not because they are likely to gain higher utilities, but because they have not experienced their "fair innings", i.e., they have not had an opportunity to live as long as older ones. Specifically, they write "Fair innings enhances equity by affording all patients the opportunity to achieve as much of a normal

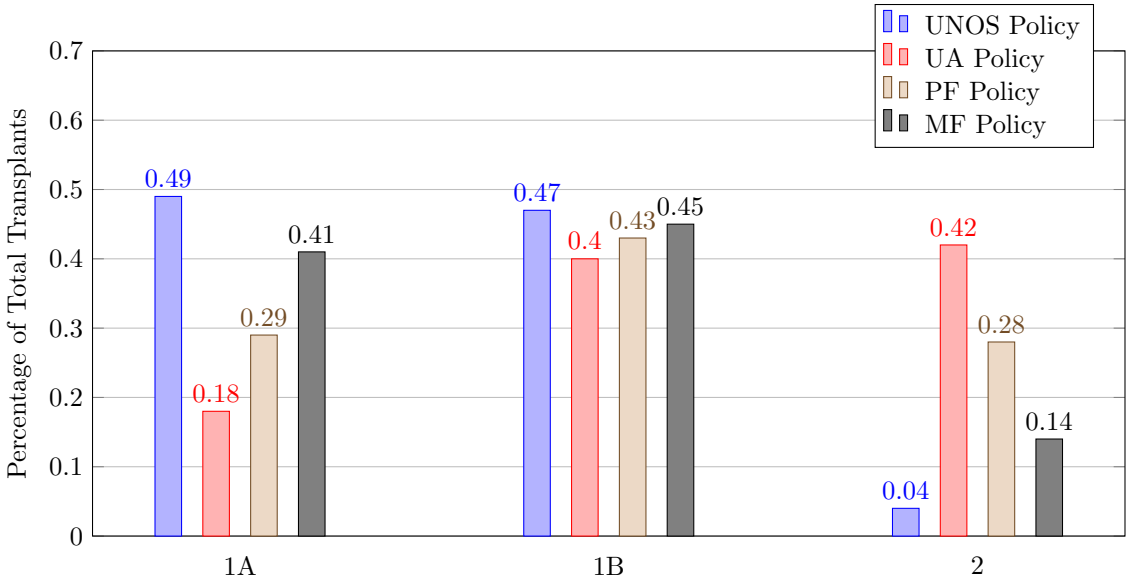

Figure 3.1: Percentage of Hearts Allocated to Each Health Group

lifespan as possible." Note that the impact of patients' age is considered in the quality of life coefficients used to estimate the QALYs of the patients in our analysis. On the other hand, MF policy prioritizes patients similar to the UNOS policy as its objective is to ensure the maximum amount of life-expectancy for the patients in the oldest age group, i.e., patients gaining the least utility level in terms of age categorization. Thus, it allocates more hearts to older patients compared to the PF and UA policies.

Finally, from the viewpoint of patient prioritization based on their VAD status, our results demonstrate a slight shift toward prioritizing patients without VAD in the two policies with the objective of fairness, PF and MF policy, compared to the UNOS policy. In addition, the PF policy performs similar to the UA policy in prioritizing patients according to their VAD status. All in all, our numerical results are in agreement with the theoretical results about the proportional fairness stating that it produces policies in the midway point between max-min fairness and utilitarian approach.

3.5 Conclusion

We study the problem of allocating donor organs to patients on the transplant waiting list under different fairness measures in the objective. Since the common measures for fairness have

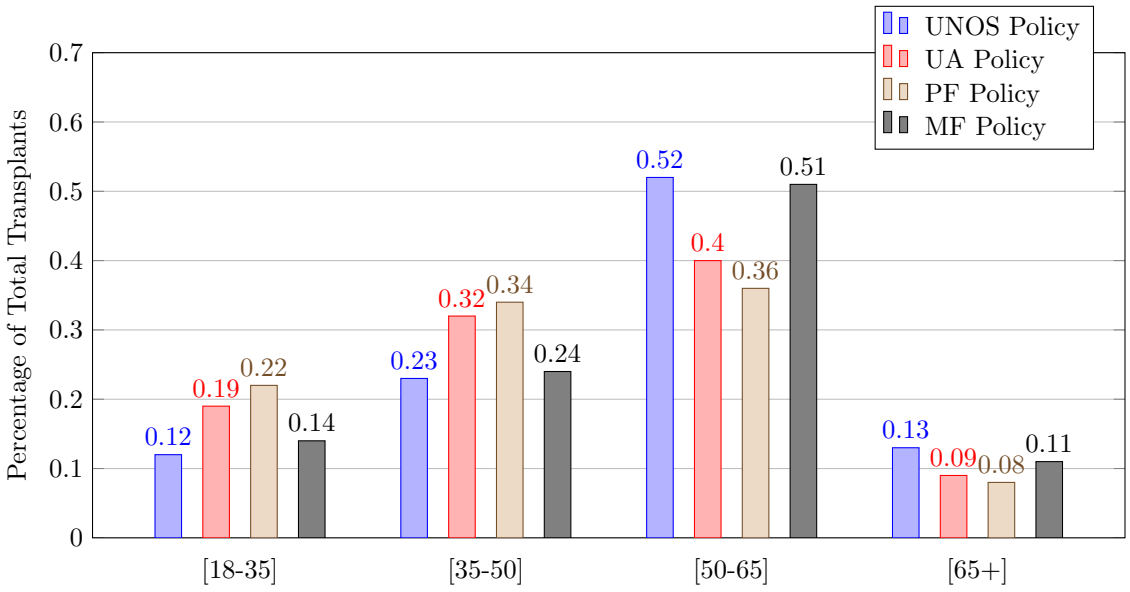

Figure 3.2: Percentage of Hearts Allocated to Each Age Group

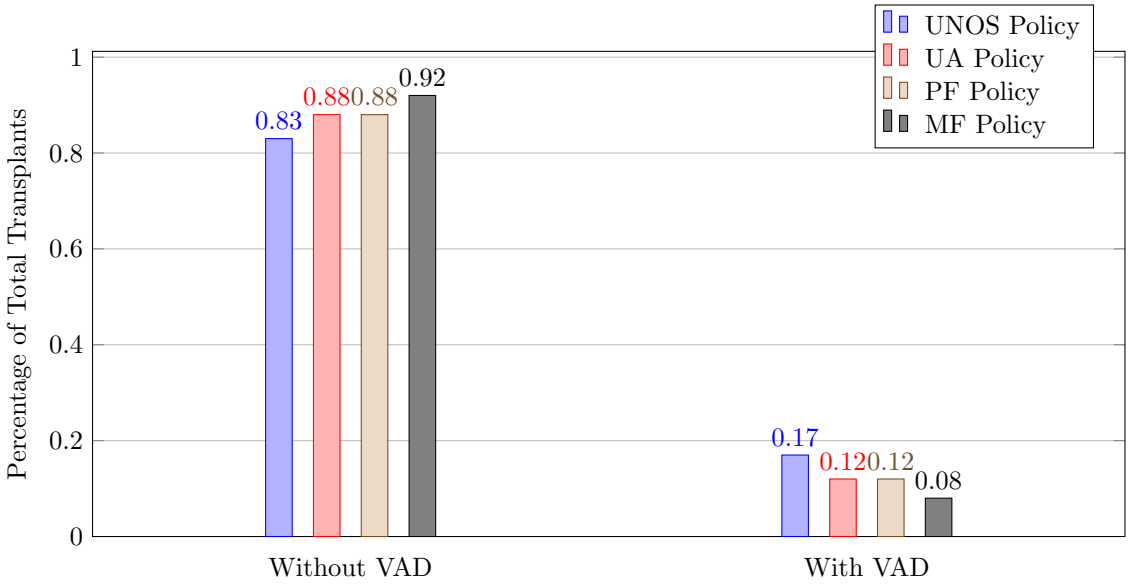

Figure 3.3: Percentage of Hearts Allocated to Each VAD Status Group

a high price and cause a significant performance loss, we propose incorporation of a new fairness measure in organ transplantation system. Specifically, we introduce an application of proportional fairness, which is a generalization of Nash standard, and analyze it both mathematically and numerically. In addition to proposing an application of proportional fairness measure, we study the performance of two existing policies that incorporate fairness, i.e., a policy based on max-min fairness measure, which maximizes the minimum expected utility among patients, as well as VWT policy, which is introduced in the literature of organ allocation as a policy that equalizes the waiting times among patients.

We formulate the organ transplantation problem with proportional fairness, being a measure of equity in its objective, as a queuing model and analyze its fluid approximation. Our analytical results show that under certain assumptions, the solution of the resulting optimization problem is an assortative partition policy, which is easy to implement in practice and provides analytical insights. In particular, under assortative partition allocation policies, good quality organs are assigned to healthier and younger patients who receive higher utilities. From a numerical viewpoint, we quantify the extent that incorporating proportional fairness measure in organ transplantation improves the price of fairness compared to existing fairness measures. While the efficiency loss is high under the max-min fairness, we show that the loss can be significantly reduced by incorporating proportional fairness in designing allocation policies. In addition, we numerically compare the performance of the policies studied in this work with that of the PF policy under different metrics, including total utility of the patients, minimum expected utility, sum of the logarithm of utilities, and variance of the waiting time of patients. Finally, we show via simulation that how these policies prioritize different patient classes in practice and how many percentages of organs are allocated to each patient health status, age, and VAD status classes. Results confirm that the model which has proportional fairness measure in its objective produces policies (the PF policy) that prioritize healthier patients more than UNOS and less than UA policies. Furthermore, interestingly, it puts slightly more priority on younger patients than UA policy. However, all in all, it yields a total utility, which is a measure of efficiency, less than that of UA and greater than that of MF. This observation is in line with the results in the existing literature of proportional fairness in bandwidth allocation in wireless networks which corroborate our findings.

Appendices

Appendix A Appendix of Chapter 1

A.1 Attributes

In order to create a reliable simulation model of the heart transplantation system and a flexible allocation policy module, several attributes and characteristics for patients and donated hearts were considered in this study. Tables 2 and 3 show these attributes for patients and hearts, respectively.

Table 2: Patient Characteristics

Attribute	Groups
Age group(4)	[18-35]; [35-50]; [50-65]; [65+]
Gender(2)	[Female]; [Male]
Blood type(4)	[O]; [A]; [B]; [AB]
Region(11)	[Region 1];. . .; [Region 11]
Ethnicity(7)	[White]; [African-American]; [Hispanic]; [Asian]; [American Indian/Alaska Native]; [Pacific Islander]; [Multiracial]
Disease(9)	[Dilated Myopathy (2 Groups)]; [Heart Re-transplant (Graft Failure)]; [Hypertrophic Cardiomyopathy]; [Restrictive Myopathy]; [Valvular Heart Disease]; [Congenital Heart Defect]; [Coronary Artery Disease]; [Other]
VAD status(2)	[1= If the patient has a VAD]; [0=Otherwise]
PTX status(2)	[1=If the patient has gone under transplantation before]; [0=Otherwise]
Health status(4)	[1A]; [1B] ; [2]; [Inactive (7)]
OPO(58)	[OPO 1];. . .; [OPO 58]

Table 3: Heart Characteristics

Attribute	Groups
Donor age group(4)	[18-35]; [35-50]; [50-65]; [65+]
Donor gender(2)	[Female]; [Male]
Donor blood type(4)	[O]; [A]; [B]; [AB]
Donor region(11)	[Region 1]; . . .; [Region 11]
Donor ethnicity(7)	[White]; [African-American]; [Hispanic]; [Asian]; [American Indian/Alaska Native]; [Pacific Islander]; [Multiracial]
Donor OPO(58)	[OPO 1];. . .; [OPO 58]

A.1.1 Disease Groups

UNOS considers more than 70 disease groups for patients with heart failure (United Network for Organ Sharing, 2015). Table 4 shows the number of patients in each disease group on the waiting list (Feb 2016). As can be seen from Table 4, some disease groups have small number of candidates, which make it impossible to create meaningful statistical distributions. In order to produce more accurate arrival distributions, we aggregated the UNOS heart disease categorization into 9 groups as listed in Table 5. We used the UNOS categorization of reasons for heart transplantation in aggregating disease groups (United Network for Organ Sharing, 2015) (Table 6).

Table 4: Waiting List Disease Group Categorization in Feb 2016 (Adults)

Disease Group	Registrations
All Diagnosis	3,886
Dilated Myopathy: Post-Partum	61
Dilated Myopathy: Viral	54
Heart Re-Tx/Gf: Acute Rejection	2
Heart Re-Tx/Gf: Chronic Rejection	10
Heart Re-Tx/Gf: Coronary Artery Disease	75
Heart Re-Tx/Gf: Hyperacute Rejection	2
Heart Re-Tx/Gf: Non-Specific	4
Heart Re-Tx/Gf: Other Specify	4
Heart Re-Tx/Gf: Primary Failure	6
Heart Re-Tx/Gf: Restrictive/Constrictive	3
Hypertrophic Cardiomyopathy	95
Arrhythmogenic Right Ventricular Dysplasia/Cardio	9
Restrictive Myopathy: Amyloidosis	20
Restrictive Myopathy: Idiopathic	25
Restrictive Myopathy: Other Specify	7
Restrictive Myopathy: Sarcoidosis	21
Restrictive Myopathy: Sec To Radiat/Chem	7
Valvular Heart Disease	40
Other, Specify	88
Not Reported	200
Congenital Heart Defect : Hypoplastic Left Heart	1
Congenital Heart Defect : Prior Surgery Unknown	7
Congenital Heart Defect : With Surgery	125
Congenital Heart Defect : Without Surgery	14
Coronary Artery Disease	117
Dilated Myopathy: Adriamycin	56
Dilated Myopathy: Alcoholic	7
Dilated Myopathy: Familial	112
Dilated Myopathy: Idiopathic	1,307
Dilated Myopathy: Ischemic	1,111
Dilated Myopathy: Myocarditis	22
Dilated Myopathy: Other Specify	274

Table 5: Disease Categorization in Model

Group	Diseases Included
Dilated Myopathy	1. Dilated Myopathy: Adriamycin
	2. Dilated Myopathy: Alcoholic
	3. Dilated Myopathy: Familial
	4. Dilated Myopathy: Idiopathic
	6. Dilated Myopathy: Myocarditis
	7. Dilated Myopathy: Other Specify
	8. Dilated Myopathy: Post-Partum
Dilated Myopathy : Viral	1. Dilated Myopathy : Viral
Restrictive Myopathy	1. Restrictive Myopathy: Amyloidosis
	2. Restrictive Myopathy: Idiopathic
	3. Restrictive Myopathy: Other Specify
	4. Restrictive Myopathy: Sarcoidosis
	5. Restrictive Myopathy: Sec To Radiat/Chem
Hypertrophic Cardiomiopathy	1. Hypertrophic Cardiomiopathy
Valvular Heart Disease	1. Valvular Heart Disease
Congenital Heart Defect	1. Congenital Heart Defect : Hypoplastic Left Heart
	2. Congenital Heart Defect : Prior Surgery Unknown
	3. Congenital Heart Defect : With Surgery
	4. Congenital Heart Defect : Without Surgery
Coronary Artery Disease	1. Coronary Artery Disease
	2. Dilated Myopathy: Ischemic
Heart Re-Tx/Gf	1. Heart Re-Tx/Gf: Acute Rejection
	2. Heart Re-Tx/Gf: Chronic Rejection
	3. Heart Re-Tx/Gf: Coronary Artery Disease
	4. Heart Re-Tx/Gf: Hyperacute Rejection
	5. Heart Re-Tx/Gf: Non-Specific
	6. Heart Re-Tx/Gf: Other Specify
	7. Heart Re-Tx/Gf: Primary Failure
	8. Heart Re-Tx/Gf: Restrictive/Constrictive
Other	1. Arrhythmogenic Right Ventricular Dysplasia/Cardio
	2. Not Reported
	3. Other/specify

Table 6: UNOS Table of Reasons for Heart Transplantation

Heart Diagnosis Categories	Heart Diagnoses
Cardiomyopathy	Dilated Myopathy: Idiopathic
	Dilated Myopathy: Myocarditis
	Dilated Myopathy: Other Specify
	Dilated Myopathy: Post-Partum
	Dilated Myopathy: Familial
	Dilated Myopathy: Adriamycin
	Dilated Myopathy: Viral
	Dilated Myopathy: Alcoholic
	Hypertrophic Cardiomyopathy
	Restrictive Myopathy: Idiopathic
	Restrictive Myopathy: Amyloidosis
	Restrictive Myopathy:Sarcoidosis
	Restrictive Myopathy: Endocardial Fibrosis
	Restrictive Myopathy: Other Specify
	Restrictive Myopathy: Sec To Radiat/Chem
Coronary Artery Disease	Coronary Artery Disease
	Dilated Myopathy: Ischemic
Congenital Heart Disease	Congenital Heart Disease
Valvular Heart Disease	Valvular Heart Disease
Retransplant/Graft Failure	Heart Re-Tx/GF: Coronary Artery Disease
	Heart Re-Tx/GF: Other Specify
	Heart Re-Tx/GF: Non-Specific
	Heart Re-Tx/GF: Acute Rejection
	Heart Re-Tx/GF: Hyperacute Rejection
	Heart Re-Tx/GF: Primary Failure
	Heart Re-Tx/GF: Chronic Rejection
	Heart Re-Tx/GF: Restrictive/Constrictive
Other	Cardiac Disease: Other Specify
	Heart: Other Specify
	Cancer

A.1.2 Health Status Assignment

This section closely follows UNOS/OPTN policy reports. Each heart transplant candidate is assigned a health status that reflects the candidate's medical urgency for transplant. Heart candidates (18+) at the time of registration may be assigned one of the following health statuses (Organ Procurement and Transplantation Network, 2015).

- Adult status 1A
- Adult status 1B
- Adult status 2
- Inactive status

Adult Heart Status 1A Requirements: To assign a candidate adult status 1A, the candidate's transplant program must submit a Heart Status 1A Justification Form to the OPTN Contractor. A candidate is not assigned adult status 1A until this form is submitted. If the candidate is at least 18 years old at the time of registration, then the candidate's transplant program may assign the candidate adult status 1A if either of the following conditions is met:
1. The candidate is admitted to the transplant hospital that registered the candidate on the waiting list, or an affiliated Veteran's Administration (VA) hospital, and the candidate also meets at least one of the requirements in Table 7.

Table 7: Adult Status 1A Requirements for Candidates Currently Admitted to the Transplant Hospital

If the candidate meets this condition:	**Then adult status 1A is valid for:**
Has one of the following mechanical circulatory support devices in place: • Total artificial heart (TAH) • Intra-aortic balloon pump • Extracorporeal membrane oxygenation (ECMO)	14 days, and must be recertified by an attending physician every 14 days from the date of the candidate's initial registration as adult status 1A to extend the adult status 1A registration.
Requires continuous mechanical ventilation.	14 days, and must be recertified by an attending physician every 14 days from the date of the candidate's initial registration as adult status 1A to extend the Status 1A registration.
Requires continuous infusion of a single high-dose intravenous inotrope or multiple intravenous inotropes, and requires continuous hemodynamic monitoring of left ventricular filling pressures. The OPTN Contractor will maintain a list of the OPTN-approved qualifying inotropes and doses.	7 days, and may be renewed for additional 7 day periods for each occurrence of an adult status 1A listing under this criterion for this candidate.

2. A candidate who is at least 18 years old at the time of registration, and may or may not be currently admitted to the transplant hospital, may be assigned adult status 1A if the candidate meets at least one of the requirements in Table 8.

Table 8: Adult Status 1A Requirements for Candidates Current Hospitalization Not Required

If the candidate meets this condition:	Then adult status 1A is valid for:
Has one of the following mechanical circulatory support devices in place:\begin{itemize}\item Left ventricular assist device (LVAD)\item Right ventricular assist device (RVAD) \item Left and right ventricular assist devices (BiVAD)\end{itemize}	30 days, and the candidate may be registered as adult status 1A for 30 days at any point after being implanted once an attending physician determines the candidate is medically stable. The 30 days do not have to be consecutive. However, if the candidate undergoes a procedure to receive another device, then the candidate qualifies for a new term of 30 days. Any 30 days granted by the new device would substitute and not supplement any time remaining from the previous adult status 1A classification.
Candidate has mechanical circulatory support and there is medical evidence of significant device-related complications including, but not limited to, thromboembolism, device infection, mechanical failure, or life-threatening ventricular arrhythmias. A candidates sensitization is not an acceptable device-related complication to qualify as adult status 1A. If a transplant program reports a complication that is not listed here, the registration will be retrospectively reviewed by the heart regional review board (RRB).	14 days, and must be recertified by an attending physician every 14 days from the date of the candidate's initial registration as adult status 1A to extend the adult status 1A registration.

If the attending physician does not update the qualifications for adult status 1A registration when required according to Tables 7 and 8, then the candidate's adult status 1A will expire and the candidate will be downgraded to adult status 1B.

Adult Heart Status 1B Requirements: To assign a candidate adult status 1B, the candidate's transplant program must submit a Heart Status 1B Justification Form to the OPTN Contractor. A candidate is not assigned adult status 1B until this form is submitted. The candidate's transplant program may assign the candidate as adult status 1B if the candidate is at least 18 years old at the time of registration and has at least one of the following devices or therapies in place:

- Left ventricular assist device (LVAD)
- Right ventricular assist device (RVAD)
- Left and right ventricular assist devices (BiVAD)
- Continuous infusion of intravenous inotropes

Candidates that continue to qualify for adult status 1B may retain this status for an unlimited period and this status does not require any recertification, unless the candidate's medical condition changes.

Adult Heart Status 2 Requirements: If the candidate is at least 18 years old at the time of registration and does not meet the criteria for adult status 1A or 1B but is suitable for transplant, then the candidate may be assigned adult status 2. The candidate may retain adult status 2 for an unlimited period and this status does not require recertification, unless the candidate's medical condition changes.

Status Updates: If a candidate's medical condition changes and the criteria used to justify that candidate's status is no longer accurate, then the candidate's transplant program must update the candidate's status and report the updated information to the OPTN Contractor within 24 hours of the change in medical condition. Hence, we decided to update the patients' health status daily in our simulation model.

A.1.3 Region

For the administration of organ allocation and appropriate geographic representation within the OPTN policy structure, the membership is divided into 11 geographic regions (Organ Procurement and Transplantation Network, 2015). Members belong to the Region in which they are located (Figure 4). Different states are categorized into 11 regions as follows:

- **Region 1:** Connecticut, Maine, Massachusetts, New Hampshire, Rhode Island, and Eastern Vermont.
- **Region 2:** Delaware, District of Columbia, Maryland, New Jersey, Pennsylvania, West Virginia, and the part of Northern Virginia in the Donation Service Area served by the Washington Regional Transplant Community (DCTC) OPO.
- **Region 3:** Alabama, Arkansas, Florida, Georgia, Louisiana, Mississippi, and Puerto Rico.
- **Region 4:** Oklahoma and Texas.
- **Region 5:** Arizona, California, Nevada, New Mexico, and Utah.

- **Region 6:** Alaska, Hawaii, Idaho, Montana, Oregon, and Washington.
- **Region 7:** Illinois, Minnesota, North Dakota, South Dakota, and Wisconsin.
- **Region 8:** Colorado, Iowa, Kansas, Missouri, Nebraska, and Wyoming.
- **Region 9:** New York and Western Vermont.
- **Region 10:** Indiana, Michigan, and Ohio.
- **Region 11:** Kentucky, North Carolina, South Carolina, Tennessee, and Virginia.

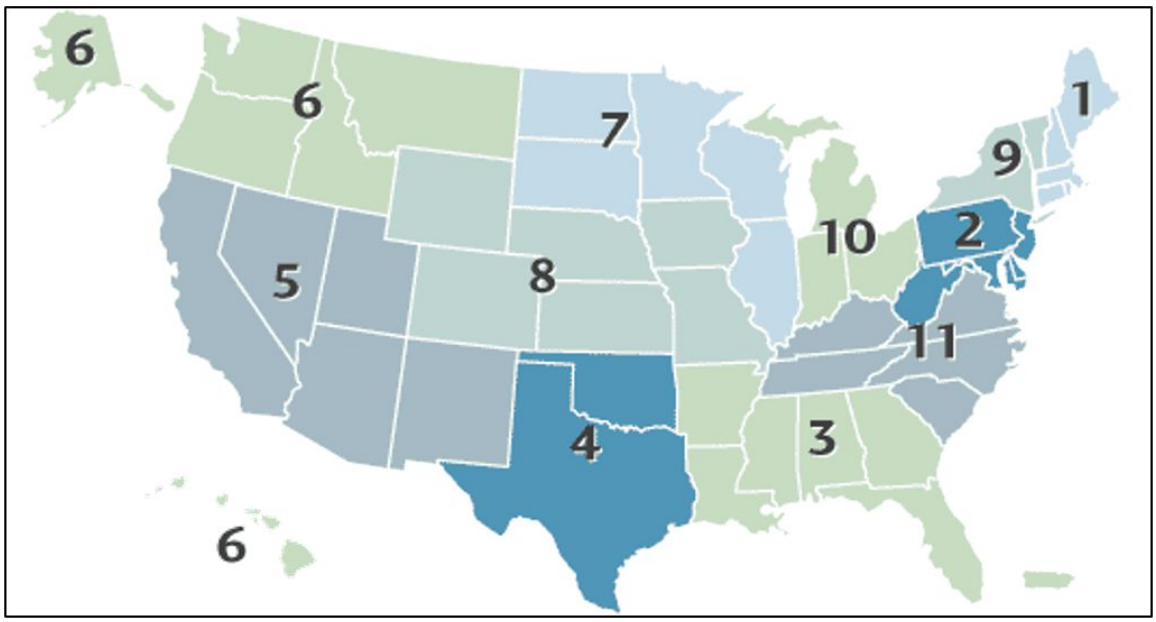

Figure 4: Map of UNOS Regional Categorization

OPO is an organization authorized by the Centers for Medicare and Medicaid Services, under Section 1138(b) of the Social Security Act, to procure organs for transplantation. Each region consists of several OPOs (Figure 5). There are 58 OPO centers in the U.S.; each includes one or more transplant centers (hospitals). Table 9 shows the number of OPOs and transplant centers in each region (United Network for Organ Sharing, 2015).

Figure 5: Map of OPO Locations

Table 9: Number of OPO and Transplant Centers in Each Region

Region	Number of OPO Centers	Number of Transplant Centers
1	2	14
2	5	35
3	10	30
4	4	30
5	8	33
6	3	9
7	4	22
8	5	19
9	4	14
10	6	20
11	7	24

Since the OPO-level arrival data were not available in UNOS datasets, in order to generate the OPO for an arrived patient/heart, we first generated her/its region, and then using Table 9, randomly assigned one of the OPOs of the generated region as her/its OPO.

A.2 Patient Arrival Analysis

In order to generate the attributes of an arrived patient, we used statistical methods to create a series of conditional relationships. Figure 6 demonstrates the three levels of these hierarchal relationships. We assessed the dependency of each of the attributes to time at the first level and to each other at the second and third levels in the patient arrival process. Since data for VAD were not available in UNOS datasets at the time of study, we assumed that it is dependent to time and included it in the first level of this hierarchy. We also excluded region and OPO from this statistical study, as yearly arrival rate generates the region arrival rates and region generates OPO. However, we reported the p-values of region dependency to time in the regression test for the first level. Another attribute that we did not consider in the first level of dependency was health status as health status arrival rates is more dependent to disease and age. Other patient attributes were included in the statistical tests.

First, for each group of patient attributes, we used regression to test its dependency to time (calendar year). For example, for blood type, we tested 4 null hypotheses, i.e., the dependency of blood type "O," "A," "B," and "AB" to time. In particular, for blood type "O," the two variables included in the regression are A_0 which stands for arrival of blood type "O" and T which shows time (in years). We tested whether the coefficient of time in equation $A_0 = aT + b$ equals zero or not. In fact, the null hypothesis is defined by:

$$\begin{cases} H_0 : \ a = 0, \\ H_1 : \ a \neq 0. \end{cases}$$

By choosing a significance level α, a p-value less than α rejects the null hypothesis, and shows that the variable depends on time. Similar statistical tests were used to test the dependency of blood type groups "A," "B," and "AB" to time. By repeating the same procedure for the other patient attributes, we created Table 10, which shows the p-values for each test (we used $\alpha = 0.1$ for the analysis reported in 10). Then, for each attribute, we defined the degree of dependency to time,

which is the percentage of groups of an attribute dependent on time. By comparing these degrees of dependency, we chose attributes gender, PTX status, and disease group to be dependent on time in our model. By doing so, we then created the first layer shown in Figure 6. Note that we used programming language R to perform our statistical tests throughout this thesis.

Table 10: Regression p-values for Testing the Time Dependency of Attributes

Attribute	**Groups**	**Regression p-value**	**Dependency to time?**	**Degree of dependency**
Gender	Female:	0.0004452	**Yes**	2 out of 2
	Male:	0.0004450	**Yes**	(100%)
Ethnicity	White:	0.0279300	**Yes**	4 out of 7
	African-American:	0.0001934	**Yes**	(57.14%)
	Hispanic:	0.0005916	**Yes**	
	Asian:	0.0055590	**Yes**	
	American Indian/Alaska Native:	0.2516000	**No**	
	Pacific Islander:	0.3977000	**No**	
	Multiracial:	0.6751000	**No**	
Blood type	O:	0.8458000	**No**	1 out of 4
	A:	0.3584000	**No**	(25%)
	B:	0.2806000	**No**	
	AB:	0.0718700	**Yes**	
Disease	Dilated Myopathy: Post-Partum	0.1939000	**No**	13 out of 32
	Dilated Myopathy: Viral	0.7376000	**No**	(40.62%)
	Heart Re-Tx/Gf: Acute Rejection	0.1313000	**No**	
	Heart Re-Tx/Gf: Chronic Rejection	0.1423000	**No**	
	Heart Re-Tx/Gf: Coronary Artery Disease	0.1100000	**No**	
	Heart Re-Tx/Gf: Hyperacute Rejection	0.1117000	**No**	
	Heart Re-Tx/Gf: Non-Specific	0.3074000	**No**	
	Heart Re-Tx/Gf: Other Specify	0.6850000	**No**	
	Heart Re-Tx/Gf: Primary Failure	0.8999000	**No**	
	Heart Re-Tx/Gf: Restrictive/Constrictive	0.0875900	**Yes**	
	Hypertrophic Cardiomyopathy	0.0005736	**Yes**	

Table 10 continued from previous page

	Arrhythmogenic Right Ventricular Dysplasia/Cardio	0.2825000	**No**	
	Restrictive Myopathy: Amyloidosis	0.9744000	**No**	
	Restrictive Myopathy: Idiopathic	0.0016430	**Yes**	
	Restrictive Myopathy: Other Specify	0.0001368	**Yes**	
	Restrictive Myopathy: Sarcoidosis	0.0001163	**Yes**	
	Restrictive Myopathy: Sec To Radiat/Chem	0.7919000	**No**	
	Valvular Heart Disease	0.1260000	**No**	
	Other, Specify	0.9980000	**No**	
	Not Reported	0.9143000	**No**	
	Congenital Heart Defect : Hypoplastic Left Heart	0.0783000	**Yes**	
	Congenital Heart Defect : Prior Surgery Unknown	0.0446000	**Yes**	
	Congenital Heart Defect : With Surgery	0.1449000	**No**	
	Congenital Heart Defect : Without Surgery	0.0175300	**Yes**	
	Coronary Artery Disease	0.2912000	**No**	
	Dilated Myopathy: Adriamycin	0.6545000	**No**	
	Dilated Myopathy: Alcoholic	0.0137200	**Yes**	
	Dilated Myopathy: Familial	0.3949000	**No**	
	Dilated Myopathy: Idiopathic	0.0000042	**Yes**	
	Dilated Myopathy: Ischemic	0.0818800	**Yes**	
	Dilated Myopathy: Myocarditis	0.0000056	**Yes**	
	Dilated Myopathy: Other Specify	0.0021600	**Yes**	
Age group	[18-35]:	0.1635000	**No**	1 out of 4
	[35-50]:	0.3096000	**No**	(25%)
	[50-65]:	0.0036680	**Yes**	
	[65+]:	0.1369000	**No**	
PTX status	1:	0.0012420	**Yes**	1 out of 2
	0:	0.1329000	**No**	(50%)

Table 10 continued from previous page

Region	Region 1:	0.1275000	**No**	3 out of 11
	Region 2:	0.1257000	**No**	(27.27%)
	Region 3:	0.1599000	**No**	
	Region 4:	0.0168600	**Yes**	
	Region 5:	0.9526000	**No**	
	Region 6:	0.1880000	**No**	
	Region 7:	0.9564000	**No**	
	Region 8:	0.2506000	**No**	
	Region 9:	0.0145800	**Yes**	
	Region 10:	0.0005045	**Yes**	
	Region 11:	0.2114000	**No**	

After creating the first level, the Chi-squared independency test was used to test the dependency of each attribute in the first level to the remaining attributes. Results (p-values) of the Chi-squared independency test of attributes gender, PTX status, and disease group are reported in Tables 11, 12, and 13, respectively. In the Chi-squared test the null hypothesis is to check the independency of the two tested variables. When the p-value reported by the test is smaller than a significance level, the null hypothesis is rejected and consequently the dependency of the variables is concluded.

Table 11: P-values for Chi-squared Independency Test for Gender

Independency test of gender and:	**P-value**
Blood type	0.0008254
Age	$< 2.2 \times 10^{-16}$
Ethnicity	$< 2.2 \times 10^{-16}$

Table 12: P-values for Chi-squared Independency Test for PTX Status

Independency test of PTX status and:	**P-value**
Blood type	$< 2.2 \times 10^{-16}$
Age	$< 2.2 \times 10^{-16}$
Ethnicity	$< 2.2 \times 10^{-16}$

Table 13: P-values for Chi-squared Independency Test for Disease

Independency test of disease and:	**P-value**
Blood type	0.6651
Age	$< 2.2 \times 10^{-16}$
Ethnicity	0.4259

Based on reported p-values of the tests, we developed the hierarchy such that each attribute in level one had only one dependent variable in level two. Since most of the p-values were smaller than the usual significance levels, we chose the attribute with the smallest p-value as the dependent variable for each of the attributes in level one (Table 14). Note that 2.2×10^{-16} is the smallest p-value that R programming language reports and this small number in fact shows a dependency between attributes.

Table 14: Second Level Dependency of Patient Attributes

Attribute	**Dependent Attributes**
Gender	Age, Ethnicity
PTX Status	Blood Type, Age, Ethnicity
Disease	Age

Age was the only dependent attribute to disease, and it was chosen as the second level variable depending on disease. The only remained choice for gender was ethnicity. For PTX status, though, we could choose blood type as its second level, we did not do so because blood type depends more on ethnicity than previous heart transplant (PTX status). The only remained variables are health status, and blood type. So far, we created three conditional branches, that is, gender/ethnicity branch, disease/age branch, and PTX status branch. Among these branches we chose health status as the third level variable for disease/age branch, because the health status arrival depends more on disease/age than to gender/ethnicity or PTX status. Also, blood type group arrival rates depend more on gender/ethnicity. Creating the conditional relationships for patient attributes helps to estimate patient attribute arrival distributions more accurately.

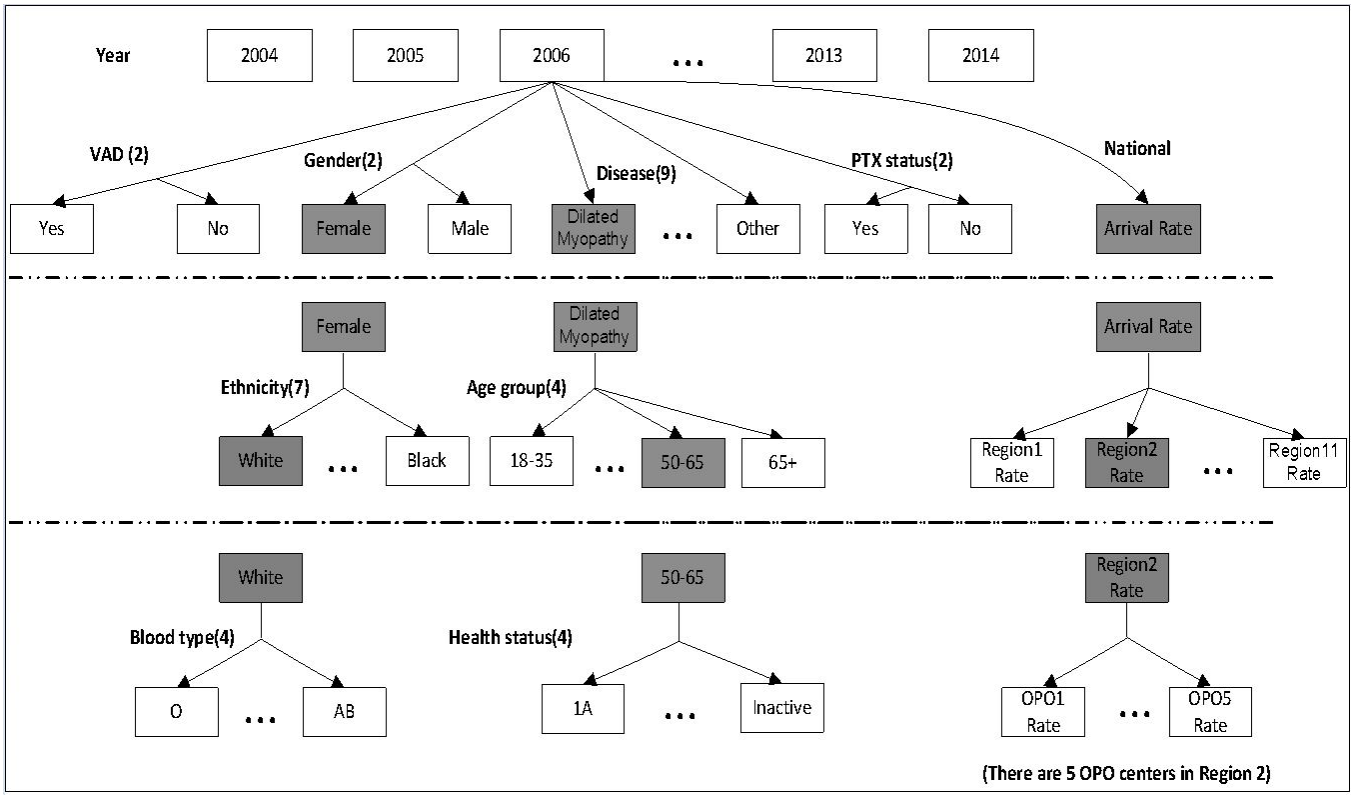

Figure 6: Pattern of Dependency in Patient Arrival Data

A.3 Heart Arrival Analysis

When a heart is procured to the system, the model assigns its various attributes according to a series of conditional relationships. We used the same statistical methods described in Appendix A.2 for patient arrivals to test the dependency of heart attributes to each other, as well as time (calendar year). We included all the attributes of a heart considered by UNOS in our analysis. Table 15 shows the p-values of time dependency test for each group of heart attributes, as well as their degree of dependency to time. Based on the results of Table 15, we created the first level of hierarchy, which involves age group, blood type, and ethnicity because these attributes have a larger degree of dependency to time compared to the other attributes. Tables 16, 17, and 18 show the p-values for Chi-squared independency test between each of the attributes in the first level with gender and region. However, since almost all the p-values were close to zero, we decided to consider the region to depend on blood type and gender to depend on age group in the second level. We generated the OPO of an arrived heart randomly based on its region. Figure A.4 shows these

conditional relationships.

Table 15: Regression p-values for Testing the Time Dependency of Attributes

Attribute	**Groups**	**Regression p-value**	**Dependency on time?**	**Degree of dependency**
Gender	Female:	0.1974000	No	**0 out of 2**
	Male:	0.1974000	No	(0%)
Ethnicity	White:	0.0006164	Yes	3 out of 7
	African-American:	0.0056930	Yes	(42.85%)
	Hispanic:	0.5378000	No	
	Asian:	0.0000042	Yes	
	American Indian/Alaska Native:	0.9271000	No	
	Pacific Islander:	0.2107000	No	
	Multiracial:	0.2567000	No	
Blood type	O:	0.1157000	No	2 out of 4
	A:	0.8177000	No	(50%)
	B:	0.0179900	Yes	
	AB:	0.0030470	Yes	
Age group	[18-35]:	0.1635000	No	1 out of 4
	[35-50]:	0.3096000	No	(25%)
	[50-65]:	0.0036680	Yes	
	[65+]:	0.1369000	No	
Region	Region 1:	0.0010610	Yes	3 out of 11
	Region 2:	0.5411000	No	(27.27%)
	Region 3:	0.0811700	Yes	
	Region 4:	0.3148000	No	
	Region 5:	0.5095000	No	
	Region 6:	0.7325000	No	
	Region 7:	0.1348000	No	
	Region 8:	0.1945000	No	
	Region 9:	0.0119400	Yes	
	Region 10:	0.6285000	No	
	Region 11:	0.5649000	No	

Table 16: P-values for Chi-squared Independency Test for Age Group

Independency test of age group and:	**P-value**
Region	$< 2.2 \times 10^{-16}$
Gender	$< 2.2 \times 10^{-16}$

Table 17: P-values for Chi-squared Independency Test for Blood Type

Independency test of blood type and:	**P-value**
Region	$< 2.2 \times 10^{-16}$
Gender	$< 6.7 \times 10^{-8}$

Table 18: P-values for Chi-squared Independency Test for Ethnicity

Independency test of ethnicity and:	**P-value**
Region	$< 2.2 \times 10^{-16}$
Gender	$< 2.2 \times 10^{-16}$

Table 19: Second Level Dependency of Heart Attributes

Attribute	**Dependent Attributes**
Age Group	Gender, Region
Blood Type	Region
Ethnicity	Gender, Region

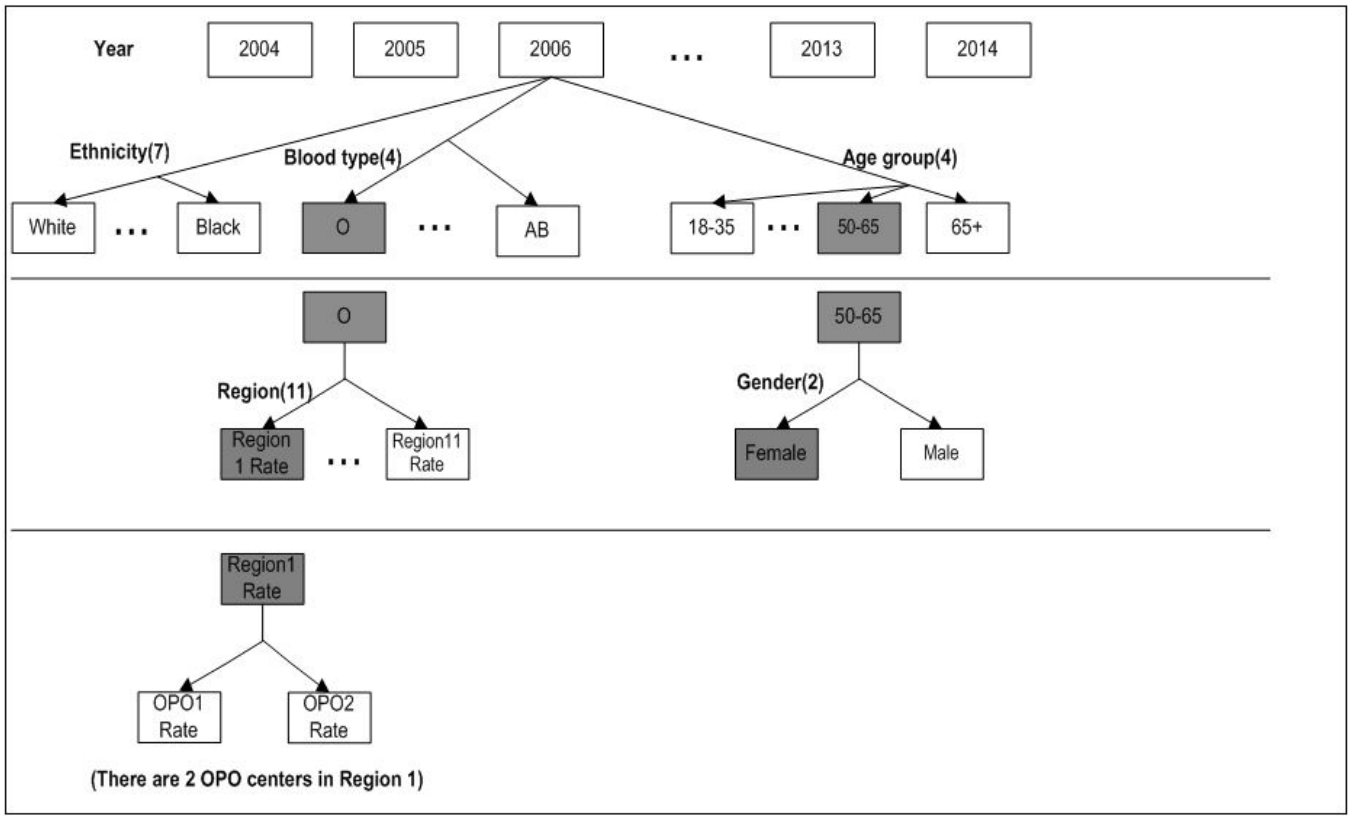

Figure 7: Pattern of Dependency in Heart Arrival Data

A.4 Patient Health Status Change Module

We validated the health status change module by comparing the portion of patients in each health status produced by our simulation model with the historical data reported in UNOS datasets (United Network for Organ Sharing, 2015). In particular, we used the Kolmogorov-Smirnov test to check whether the health status distributions produced by the model are statistically identical to the real health status distributions at the end of each calendar year during 2006-2014. P-values reported in Table 20 indicate that the Markov chain developed to describe the health status change of patients on the waiting list, accurately estimates the proportion of patients in each health status over time. The transition probability matrix of the Markov chain is given by:

$$P = \begin{array}{c} \\ 1A \\ 1B \\ 2 \\ \text{Inactive} \end{array} \begin{array}{c} \begin{array}{cccc} 1A & 1B & 2 & \text{Inactive} \end{array} \\ \begin{pmatrix} 0.97919 & 0.01864 & 0.00103 & 0.00114 \\ 0.00447 & 0.99267 & 0.00052 & 0.00234 \\ 0.00012 & 0.00071 & 0.99668 & 0.00249 \\ 0.00021 & 0.00012 & 0.00031 & 0.99936 \end{pmatrix} \end{array}$$

In order to estimate this matrix, we first estimated the monthly frequency of transition matrix using the SRTR annual data reports. Then, by using Chapman-Kolmogorov equations, we estimated the daily frequency of transition matrix by taking the 30^{th} root of the monthly transition frequencies.

Table 20: P-values for the Kolmogorov-Smirnov Test

Year	**2006**	**2007**	**2008**	**2009**	**2010**	**2011**	**2012**	**2013**	**2014**
P-value	0.7714	0.2286	1	0.7718	0.77	1	1	1	1

A.5 Delisting

In our simulation model, outflow of patients from waiting list occurs due to three reasons: transplant, death, and delisting. According to UNOS data, there are several reasons for delisting such as transplanted in another country, unable to contact candidate, medically unsuitable, refused transplant, transferred to another center, condition improved, too sick to transplant, transplanted at another Center, etc (United Network for Organ Sharing, 2015). Using UNOS delisting data, we calculated the number of delisted patients during each year from 2006 to the end of 2014. Table 21 shows the historical data for daily delisting rates (computed by dividing numbers delisted annually by 365) at each year. We model the delisting process as a nonstationary Poisson process. That is, at each day, using Table 21, we generate a Poisson random number with the mean of the daily delisting rate. The generated number determines the number of patients to be delisted at that day. We then picked the patients who are going to be delisted according to a distribution that depends on the health status. The rationale behind the choice of health status for the delisting process is that the delisting distribution significantly depends on health status, while weakly correlates with the other attributes according to the historical data reported by UNOS (United Network for Organ Sharing, 2015). For example, the daily delisting rate for year 2014 is equal to 2.42. Suppose that the Poisson random number generated using a mean of 2.42 is equal to 3 in the simulation. Therefore, we delist 3 patients from the waiting list. The health status removal distribution of patients in 2014 is given by (United Network for Organ Sharing, 2015):

- **Health status 1A:** 8.6 % of all delisted patients
- **Health status 1B:** 15 % of all delisted patients
- **Health status 2:** 14 % of all delisted patients
- **Health status 7 (Inactive):** 62.4 % of all delisted patients

Table 21: Number of Yearly and Daily Delisting for UNOS Waiting List During 2006-2014

Year	**2014**	**2013**	**2012**	**2011**	**2010**	**2009**	**2008**	**2007**	**2006**
Transplanted in another country	1	0	0	0	0	0	0	0	0
Unable to contact candidate	14	13	6	19	17	3	68	5	13
Medically unsuitable	0	0	0	0	0	0	0	0	0
Refused transplant	24	13	22	17	13	24	22	26	17
Transferred to another center	76	42	62	60	70	32	34	37	45
Other	218	191	154	214	122	120	165	97	129
Condition improved	203	149	151	171	173	202	255	315	196
Too sick to transplant	317	274	219	234	196	177	134	111	108
Transplanted at another center	30	25	17	16	9	10	11	7	8
Total removal	883	707	631	731	600	568	689	598	516
Daily removal rate	2.42	1.94	1.73	2	1.64	1.56	1.89	1.64	1.41

A.6 Pre-Transplant Death

Patients may die while waiting for a donor heart on the waiting list. We used the SRTR Cox proportional hazard model to generate the daily death probability for each patient on the waiting list (Scientific Registry of Transplant Recipients, 2015a). Although this model estimates the patient survival based on patient data from 07/01/2012 to 06/30/2013, we used it to generate death probabilities for the other years. The covariates for 1-year patient survival are reported in Table 22 (Scientific Registry of Transplant Recipients, 2015a). Covariates for VAD status, Region, and OPO were not available in the proportional hazard model. Hence, we assigned 0 for those covariates.

Table 22: Heart Waitlist Mortality Rates (07/01/2012-06/30/2013)

Characteristic	Level	Estimate	Standard Error	P-value
Age	17 and less	0.1383	0.2213	0.5321
	35-49	0.5141	0.1978	0.0093
	50-64	0.5834	0.1904	0.0022
	65+	0.7811	0.2059	0.0001
	18-34	0	(Ref.)	(Ref.)
Blood Type	A	-0.0188	0.0984	0.8486
	AB	-0.0324	0.2755	0.9064
	B	0.0438	0.1355	0.7465
	O	0	(Ref.)	(Ref.)
Diagnosis (Disease)	Cardiomyopathy	-0.1261	0.1091	0.2479
	Retransplant	0.7975	0.2066	0.0001
	Valvular Heart Disease	0.9104	0.2393	0.0001
	Congenital Heart Disease	0.6431	0.1977	0.0011
	Missing	0	(Ref.)	(Ref.)
	Other	0.139	0.3649	0.7032
Gender	Female	-0.1655	0.106	0.1185
	Male	0	(Ref.)	(Ref.)
Race (Ethnicity)	African-American/Black	-0.0048	0.113	0.9663
	Hispanic/Latino	0.0168	0.1582	0.9152
	Asian	0.061	0.2861	0.8313
	Other	-0.4669	0.5804	0.4212
	White	0	(Ref.)	(Ref.)
Health Status	1A	1.1268	0.202	<0.0001
	1B	0.3857	0.2012	0.0552
	Inactive	2.3946	0.1754	<0.0001
Waiting Time	>Median	-0.9484	0.0933	<0.0001

The mechanism of our pre-transplant survival module is such that it assigns a probability of death for each patient at the start of each day, generates a random number between 0 and 1, and determines if the patient is going to die during that day, that is,

- Suppose that for a patient, the covariate coefficient associated with his attributes are equal to $\beta_1, \beta_2, \ldots, \beta_{11}$ (we read these numbers from the estimate column reported in Table 22).
- Yearly probability of death (P_{yearly}) for the patient is equal to:

$$P_{\text{yearly}} = (\text{baseline hazard}).\exp\left(\sum_{i=1}^{11} \beta_i\right)$$

- We convert it to a daily probability of death P_{daily}, by

$$P_{\text{daily}} = 1 - \exp\left(-\frac{P_{\text{yearly}}}{365}\right)$$

- We generate a random number between 0 and 1 denoted by R:
  - If $P_{\text{daily}} \geq R$, the patient dies.
  - If $P_{\text{daily}} < R$, the patient will remain on the waiting list,

where exp(x) is the exponential function and baseline hazard is a function that assigns a baseline probability of death for a patient according to the patient's age. We used the U.S. population life tables during 2013 reported in the CDC database to estimate this baseline hazard function(Centers for Disease Control and Prevention, 2015) (Table 23).

Table 23: Abridged Life Table for the U.S. Total Population, 2013

Age of a Person (Years x to x+n)	Probability of Dying Between Ages x to x+n	Number Surviving to Age x	Number Dying Between Ages x to x+n	Person-Years Lived Between Ages x to x+n	Total Number of Person-Years Lived Above Age x	Life Expectancy at Age x
0-1	0.005958	100,000	596	99,475	7,882,785	78.8
1_5	0.001021	99,404	102	397,372	7,783,311	78.3
5_10	0.00059	99,303	59	496,355	7,385,939	74.4
10_15	0.000705	99,244	70	496,080	6,889,584	69.4
15-20	0.002227	99,174	221	495,400	6,393,505	64.5
20-25	0.004158	98,953	411	493,788	5,898,105	59.6
25-30	0.004869	98,542	480	491,535	5,404,318	54.8
30-35	0.005727	98,062	562	488,941	4,912,783	50.1
35-40	0.007072	97,500	690	485,855	4,423,842	45.4
40-45	0.009949	96,811	963	481,799	3,937,986	40.7
45-50	0.015604	95,848	1,496	475,781	3,456,188	36.1
50-55	0.024272	94,352	2,290	466,384	2,980,407	31.6
55-60	0.035563	92,062	3,274	452,547	2,514,024	27.3
60-65	0.05006	88,788	4,445	433,361	2,061,477	23.2
65-70	0.071576	84,343	6,037	407,404	1,628,116	19.3
70-75	0.109091	78,306	8,543	371,349	1,220,712	15.6
75-80	0.170567	69,764	11,899	320,641	849,363	12.2
80-85	0.271135	57,864	15,689	251,503	528,722	9.1
85-90	0.425836	42,175	17,960	166,078	277,219	6.6
90-95	0.614587	24,216	14,883	81,352	111,141	4.6
95-100	0.786379	9,333	7,339	25,247	29,789	3.2
100+	1	1,994	1,994	4,541	4,541	2.3

A.7 Post-Transplant Death

The mechanism of the post-transplant survival module is similar to the pre-transplant survival module. The only difference is that we used the post-transplant Cox proportional hazard model reported in the SRTR website (Scientific Registry of Transplant Recipients, 2015a) to generate the daily probability of death for patients after transplantation (Table 24). Some of the covariates pre-

sented in the Cox proportional hazard model were not available in our simulation and we did not consider them. However, some of these covariates such as bilirubin at transplant (mg/dL), dialysis at transplant, drugtreated HTN at listing, ischemic time (hrs), most recent CPRA/PRA, PA (Sys, mm Hg), and sudden death at listing have a possibility for missing data. Hence, we used the estimates for missing covariates in such attributes.

Table 24: 1-Year Patient Post-Transplant Survival

Characteristic	Level	Estimate	Standard Error	P-value
Bilirubin at Transplant (mg/dL)	mg/dL	0	0.014	<0.0001
	Missing	0	0.5145	0
Dialysis at Transplant	Yes	1	0.2255	0
	Unknown/Missing	0.6518	0.6263	0
	No	0	(Ref.)	(Ref.)
Donor Age	0-34	0.1602	0.1094	0
	35+	0	(Ref.)	(Ref.)
Donor Cause of Death	CVA/Stroke	0	0.1288	0
	Other	0	(Ref.)	(Ref.)
Drug-Treated HTN at Listing	Missing	0.2993	0.2348	0
	Yes	0	0	0
	No	0	(Ref.)	(Ref.)
Ischemic Time (hrs)	In Hours (hrs)	0	0	0
	Missing	1	0	0
Medical Condition	In ICU	0	0	0
	Hospitalized Not in ICU	0	0	0
	Not Hospitalized	0	(Ref.)	(Ref.)
Most Recent CPRA/PRA	Percent (%)	0	0	1
	Missing	0	0	0
PA (Sys, mm Hg)	Systolic (mm HG)	0	0	0
	Missing	1	0	0
Recipient Diagnosis	Cardiomyopathy	0.0761	0	0
	Congenital Heart Disease	0.522	0.2408	0.0302
	Other/Missing	0.4738	0.369	0.1991
	Coronary Artery Disease	0	(Ref.)	(Ref.)
Recipient Height (cm)	In Centimeters (cm)	0.0124	0.0054	0.021
Recipient Race/Ethnicity	Black	0.0408	0.1287	0.7513
	Hispanic/Latino	0.1307	0.1893	0.4899
	Asian	0.2627	0.2998	0.3808
	Multiracial/Other/Unknown/Missing	0.2733	0.5826	0.639
	White	0	(Ref.)	(Ref.)
Recipient Serum Creatinine (mg/dL)	>1.6	0.635	0.1094	<0.0001
	1.6 or Less	0	(Ref.)	(Ref.)
Recipient on Life Support (ECMO)	Yes	0.8371	0.3776	0.0266
	No	0	(Ref.)	(Ref.)
Recipient on VAD	Yes	0.4382	0.1115	0.0001
	No	0	(Ref.)	(Ref.)
Recipient on Ventilator	Yes	0.4903	0.3452	0.1556
	No	0	(Ref.)	(Ref.)
Sudden Death at Listing	Yes	0.073	0.1437	0.6115
	Unknown/Missing	0.4062	0.1637	0.0131
	No	0	(Ref.)	(Ref.)

The other possibility that can occur for patients in the post-transplant is the graft (heart) failure. Since in the arrival of patients, we considered such patients (patients whose PTX status is equal to 1), to avoid double-counting them, we did not include the graft failure event in the post-transplant phase.

A.8 Allocation Policies

A.8.1 Current UNOS Allocation Policy (Organ Procurement and Transplantation Network, 2015)

Waiting Time Accumulation: Waiting time for heart candidates begins when the candidate is first registered as an active heart candidate on the waiting list, and is calculated within each heart status. As a result, waiting time accrued at a higher status will be added to any time accumulated at a lower status, but waiting time accumulated at a lower status will not be added to any higher status. If a candidate's status is upgraded, waiting time accrued while registered at the lower status is not transferred to the higher status. Conversely, waiting time accrued while registered at a higher status is transferred to a lower status if the candidate is downgraded. Waiting time does not accrue while the candidate is inactive.

Heart Allocation Classifications and Rankings: Allocation of Hearts by Blood Type Within each heart status, hearts will be allocated to candidates according to the primary blood type matching requirements in Table 25.

Table 25: Primary Blood Type Matching Requirements

Hearts from donors with:	**Are allocated to the candidates with:**
Blood Type O	Blood type O or blood type B
Blood Type A	Blood type A or blood type AB
Blood Type B	Blood type B or blood type AB
Blood Type AB	Blood type AB

After hearts are allocated to primary blood type candidates, they are allocated to any secondary blood type compatible candidates, then to any eligible incompatible blood type candidates (Table 26).

Table 26: Secondary Blood Type Matching Requirements

Hearts from donors with:	**Are allocated to the candidates with:**
Blood Type O	Blood type A or blood type AB
Blood Type A	Not applicable
Blood Type B	Not applicable
Blood Type AB	Not applicable

Sorting Within Each Classification: Candidates are sorted within each classification by the total amount of waiting time that the candidate has accumulated at that status.

Allocation of Hearts from Donors at Least 18 years Old: Hearts from deceased donors at least 18 years old are allocated to candidates according to Table 28. Table 27 shows the zone definitions for the current UNOS policy.

Table 27: Zone Definition for the UNOS Policy

Zone	Includes transplant hospitals:
A	Within 500 nautical miles from the donor's hospital but outside of the donor's hospital DSA.
B	Within 1000 nautical miles from the donor's hospital but outside of the zone A and donor's hospital DSA.
C	Within 1500 nautical miles from the donor's hospital but outside of the zone B and donor's hospital DSA.
D	Within 2500 nautical miles from the donor's hospital but outside of the zone C and donor's hospital DSA.
E	More than 2500 nautical miles from the donor's hospital.

Table 28: Allocation of Hearts from Deceased Donors At Least 18 Years Old in the UNOS Policy

Classification	Candidates within:	And are:
1	OPO's DSA	Adult or pediatric status 1A and primary blood type match with the donor
2	OPO's DSA	Adult or pediatric status 1A and secondary blood type match with the donor
3	OPO's DSA	Adult or pediatric status 1B and primary blood type match with the donor
4	OPO's DSA	Adult or pediatric status 1B and secondary blood type match with the donor
5	Zone A	Adult or pediatric status 1A and primary blood type match with the donor
6	Zone A	Adult or pediatric status 1A and secondary blood type match with the donor
7	Zone A	Adult or pediatric status 1B and primary blood type match with the donor
8	Zone A	Adult or pediatric status 1B and secondary blood type match with the donor
9	OPO's DSA	Adult or pediatric status 2 and primary blood type match with the donor
10	OPO's DSA	Adult or pediatric status 2 and secondary blood type match with the donor
11	Zone B	Adult or pediatric status 1A and primary blood type match with the donor
12	Zone B	Adult or pediatric status 1A and secondary blood type match with the donor
13	Zone B	Adult or pediatric status 1B and primary blood type match with the donor
14	Zone B	Adult or pediatric status 1B and secondary blood type match with the donor
15	Zone A	Adult or pediatric status 2 and primary blood type match with the donor
16	Zone A	Adult or pediatric status 2 and secondary blood type match with the donor

Table 28 continued from previous page

Classification	Candidates within:	And are:
17	Zone B	Adult or pediatric status 2 and primary blood type match with the donor
18	Zone B	Adult or pediatric status 2 and secondary blood type match with the donor
19	Zone C	Adult or pediatric status 1A and primary blood type match with the donor
20	Zone C	Adult or pediatric status 1A and secondary blood type match with the donor
21	Zone C	Adult or pediatric status 1B and primary blood type match with the donor
22	Zone C	Adult or pediatric status 1B and secondary blood type match with the donor
23	Zone C	Adult or pediatric status 2 and primary blood type match with the donor
24	Zone C	Adult or pediatric status 2 and secondary blood type match with the donor
25	Zone D	Adult or pediatric status 1A and primary blood type match with the donor
26	Zone D	Adult or pediatric status 1A and secondary blood type match with the donor
27	Zone D	Adult or pediatric status 1B and primary blood type match with the donor
28	Zone D	Adult or pediatric status 1B and secondary blood type match with the donor
29	Zone D	Adult or pediatric status 2 and primary blood type match with the donor
30	Zone D	Adult or pediatric status 2 and secondary blood type match with the donor
31	Zone E	Adult or pediatric status 1A and primary blood type match with the donor
32	Zone E	Adult or pediatric status 1A and secondary blood type match with the donor
33	Zone E	Adult or pediatric status 1B and primary blood type match with the donor
34	Zone E	Adult or pediatric status 1B and secondary blood type match with the donor
35	Zone E	Adult or pediatric status 2 and primary blood type match with the donor
36	Zone E	Adult or pediatric status 2 and secondary blood type match with the donor

In order to determine the set of OPOs in each zone and for each OPO center, by using Figure 5, we calculated the distances between any pair of OPO centers (distances estimated by the Google Maps (Google, 2015)) and followed the definition of each zone.

A.8.2 Policy I

This section explains how we proposed the three-tiered zone allocation system. If a donor heart is matched with no one in its Designated Service Area (DSA), it is offered to Zone 1 (union of Zones A, B, and C of UNOS allocation rule). Similarly, if it is not matched with a patient in Zone 1, it is offered in hierarchy to patients in Zone 2 (Zone D of UNOS allocation rule) and Zone

3 (Zone E of UNOS allocation rule). Table 29 shows the zone definition for Policy I. Note that in each zone we considered the same health status, blood type match, and waiting time prioritization rules as UNOS. Table 30 shows the allocation procedure for Policy I in the model.

Table 29: Zone Definition for Policy I

Zone	**Includes transplant hospitals :**
1	Within 1500 nautical miles from the donor's hospital but outside of the donor's hospital DSA.
2	Within 2500 nautical miles from the donor's hospital but outside of the zone A and donor's hospital DSA.
3	More than 2500 nautical miles from the donor's hospital.

Table 30: Allocation of Hearts from Deceased Donors At Least 18 Years Old in Policy I

Classification	**Candidates within:**	**And are:**
1	OPO's DSA and Zone 1	Adult or pediatric status 1A and primary blood type match with the donor
2	OPO's DSA and Zone 1	Adult or pediatric status 1A and secondary blood type match with the donor
3	OPO's DSA and Zone 1	Adult or pediatric status 1B and primary blood type match with the donor
4	OPO's DSA and Zone 1	Adult or pediatric status 1B and secondary blood type match with the donor
5	Zone 2	Adult or pediatric status 1A and primary blood type match with the donor
6	Zone 2	Adult or pediatric status 1A and secondary blood type match with the donor
7	Zone 2	Adult or pediatric status 1B and primary blood type match with the donor
8	Zone 2	Adult or pediatric status 1B and secondary blood type match with the donor
9	OPO's DSA and Zone 1	Adult or pediatric status 2 and primary blood type match with the donor
10	OPO's DSA and Zone 1	Adult or pediatric status 2 and secondary blood type match with the donor
11	Zone 3	Adult or pediatric status 1A and primary blood type match with the donor
12	Zone 3	Adult or pediatric status 1A and secondary blood type match with the donor
13	Zone 3	Adult or pediatric status 1B and primary blood type match with the donor
14	Zone 3	Adult or pediatric status 1B and secondary blood type match with the donor
15	Zone 2	Adult or pediatric status 2 and primary blood type match with the donor
16	Zone 2	Adult or pediatric status 2 and secondary blood type match with the donor
17	Zone 3	Adult or pediatric status 2 and primary blood type match with the donor
18	Zone 3	Adult or pediatric status 2 and secondary blood type match with the donor

A.8.3 Policy II

To prioritize patients according to their health status, UNOS gives the first priority to health status 1A, the second priority to health status 1B, and finally the third priority to health status

2. The patients assigned with health status 7 (inactive) are not considered in the heart-patient matching algorithm. UNOS allocation rule gives priority to patients with a higher medical urgency status. However, it has caused a significant imbalance in the distribution of donated hearts. In particular, more than 67% of all transplants correspond to status 1A while status 1A patients are only 10% of those on the waiting list. Moreover, less than 30% of all transplants correspond to health status 1B while these patients compromise 40% of the waiting list. This disparity has caused some patients in status 1B relocate together with their families to other regions with shorter waiting time6. Also, prioritizing the sickest patients may not be optimal as they may experience a shorter post-transplant survival compared to status 1B patients. Thus, in Policy II we followed the UNOS allocation system except that status 1B was prioritized over 1A in each classification. Table 31 summarizes the allocation priority for this policy.

Table 31: Allocation of Hearts from Deceased Donors At Least 18 Years Old in Policy II

Classification	**Candidates within:**	**And are:**
1	OPO's DSA	Adult or pediatric status 1B and primary blood type match with the donor
2	OPO's DSA	Adult or pediatric status 1B and secondary blood type match with the donor
3	OPO's DSA	Adult or pediatric status 1A and primary blood type match with the donor
4	OPO's DSA	Adult or pediatric status 1A and secondary blood type match with the donor
5	Zone A	Adult or pediatric status 1B and primary blood type match with the donor
6	Zone A	Adult or pediatric status 1B and secondary blood type match with the donor
7	Zone A	Adult or pediatric status 1A and primary blood type match with the donor
8	Zone A	Adult or pediatric status 1A and secondary blood type match with the donor
9	OPO's DSA	Adult or pediatric status 2 and primary blood type match with the donor
10	OPO's DSA	Adult or pediatric status 2 and secondary blood type match with the donor
11	Zone B	Adult or pediatric status 1B and primary blood type match with the donor
12	Zone B	Adult or pediatric status 1B and secondary blood type match with the donor
13	Zone B	Adult or pediatric status 1A and primary blood type match with the donor
14	Zone B	Adult or pediatric status 1A and secondary blood type match with the donor
15	Zone A	Adult or pediatric status 2 and primary blood type match with the donor
16	Zone A	Adult or pediatric status 2 and secondary blood type match with the donor
17	Zone B	Adult or pediatric status 2 and primary blood type match with the donor
18	Zone B	Adult or pediatric status 2 and secondary blood type match with the donor
19	Zone C	Adult or pediatric status 1B and primary blood type match with the donor
20	Zone C	Adult or pediatric status 1B and secondary blood type match with the donor
21	Zone C	Adult or pediatric status 1A and primary blood type match with the donor
22	Zone C	Adult or pediatric status 1A and secondary blood type match with the donor

Table 31 continued from previous page

Classification	Candidates within:	And are:
23	Zone C	Adult or pediatric status 2 and primary blood type match with the donor
24	Zone C	Adult or pediatric status 2 and secondary blood type match with the donor
25	Zone D	Adult or pediatric status 1B and primary blood type match with the donor
26	Zone D	Adult or pediatric status 1B and secondary blood type match with the donor
27	Zone D	Adult or pediatric status 1A and primary blood type match with the donor
28	Zone D	Adult or pediatric status 1A and secondary blood type match with the donor
29	Zone D	Adult or pediatric status 2 and primary blood type match with the donor
30	Zone D	Adult or pediatric status 2 and secondary blood type match with the donor
31	Zone E	Adult or pediatric status 1B and primary blood type match with the donor
32	Zone E	Adult or pediatric status 1B and secondary blood type match with the donor
33	Zone E	Adult or pediatric status 1A and primary blood type match with the donor
34	Zone E	Adult or pediatric status 1A and secondary blood type match with the donor
35	Zone E	Adult or pediatric status 2 and primary blood type match with the donor
36	Zone E	Adult or pediatric status 2 and secondary blood type match with the donor

A.8.4 Policy III

Policy III considered the UNOS allocation rule except that in each zone waiting time is prioritized over health status, i.e., considering primary and secondary blood type match, patients are ranked first by longer waiting time. Section A.8.1 explains how the waiting time in each health status is accumulated.

A.9 Sensitivity Analysis

A.9.1 On Patient and Heart Arrival Rates

In this section, we conducted sensitivity analysis on the arrival of patients and hearts to assess the impacts of change in the number of arrivals on the outcomes such as total death (pre- and post-transplant deaths). We let the arrival rates of patients and hearts to increase and decrease by a certain percentage (e.g., 10 percent) and compare the total patient death (including pre- and post-transplant deaths) for the following seven cases: (1) baseline scenario, (2) daily arrival rates of patients increased by 10 percent compared to the baseline rates, (3) daily arrival rates of hearts increased by 10 percent compared to the baseline rates, (4) daily arrival rates of patients and hearts both increased by 10 percent compared to the baseline rates, (5) daily arrival rates of patients

decreased by 10 percent compared to the baseline rates, (6) daily arrival rates of hearts decreased by 10 percent compared to the baseline rates, (7) daily arrival rates of patients and hearts both decreased by 10 percent compared to the baseline rates. Figures 8, 9, and 10 summarize the result of the sensitivity analysis for the aforementioned cases.

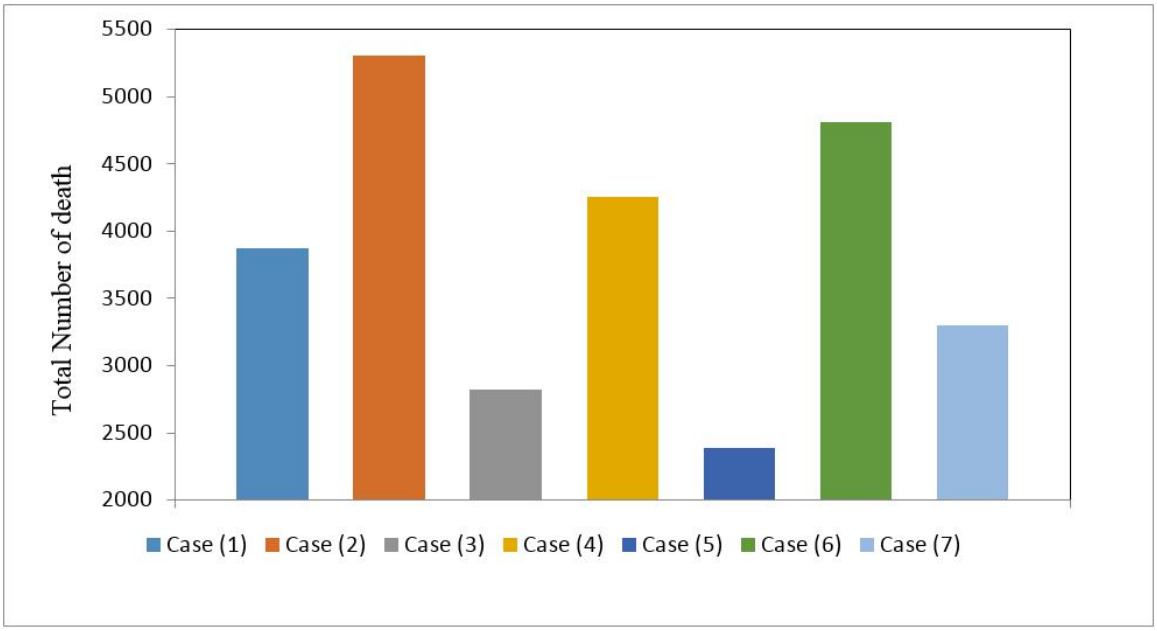

Figure 8: Total Number of Deaths for Different Patient and Heart Arrival Rates

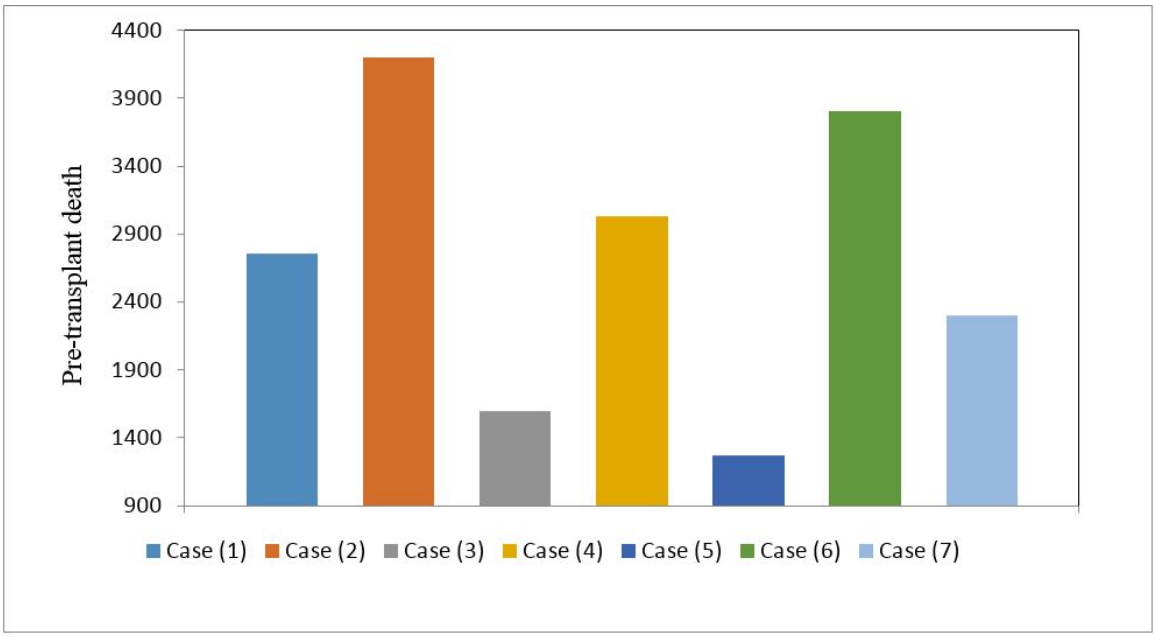

Figure 9: Pre-Transplant Deaths for Different Patient and Heart Arrival Rates

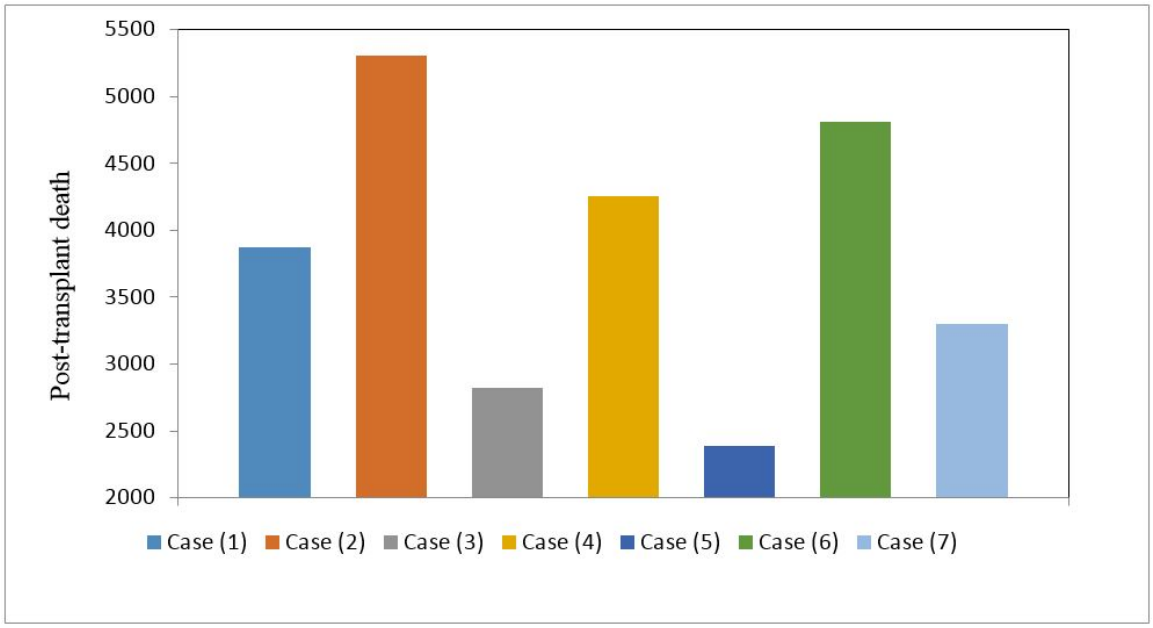

Figure 10: Post-Transplant Deaths for Different Patient and Heart Arrival Rates

A.9.2 On Allocation Priority Zones

As we have described in Chapter 1, allocation priority zones are defined based on the proximity of patients' hospital to the donor's hospital. Current UNOS allocation policy, considers 5 allocation priority zones, i.e., Zone A, Zone B, Zone C, Zone D, and Zoned E, in addition to DSA. Our proposed Policy I aggregates Zones A, B, and C in the current UNOS policy into one single priority zone. We conducted sensitivity analysis on different combinations of priority zones. Specifically, we considered a policy that combines Zones A and B into single priority zone (Policy IV). Similar to the other policies, we calculated the total number of deaths (including pre- and post-transplant deaths) for this policy (Figures 11, 12, and 13). We also conducted fairness analysis on policy IV. We measured the proportional fairness and max-min fairness for this policy using the same approach discussed in Section 1.2.4 of Chapter 1 (Figures 14 and 15). These measures are reported for the following three policies:

(1) Current UNOS allocation policy: After offering an available heart in its DSA, it shares the organ to patients in Zone A (within 500 miles of the OPO of the available heart), Zone B (within 500-1000 miles of the OPO of the available heart), Zone C (within 1000-1500 miles of the OPO of the available heart), Zone D (within 1500-2500 miles of the OPO of the available heart), and Zone E (more than 2500 miles distance from the OPO of the available heart), respectively.

(2) Policy I: This policy combines Zones A, B, and C in the UNOS policy. After offering an available heart in its DSA, this policy shares it to patients in Zone 1 (within 1500 miles of the OPO of the available heart), Zone 2 (within 1500-2500 miles of the OPO of the available heart), and Zone 3 (more than 2500 miles distance from the OPO of the available heart), respectively.

(3) Policy IV: This policy combines Zones A and B in the current UNOS policy. After offering an available heart in its DSA, this policy shares it to patients in Zone 1 (within 1000 miles of the OPO of the available heart), Zone 2 (within 1000-1500 miles of the OPO of the available heart), Zone 3 (within 1500-2500 miles of the OPO of the available heart), and Zone 4 (more than 2500 miles distance from the OPO of the available heart), respectively.

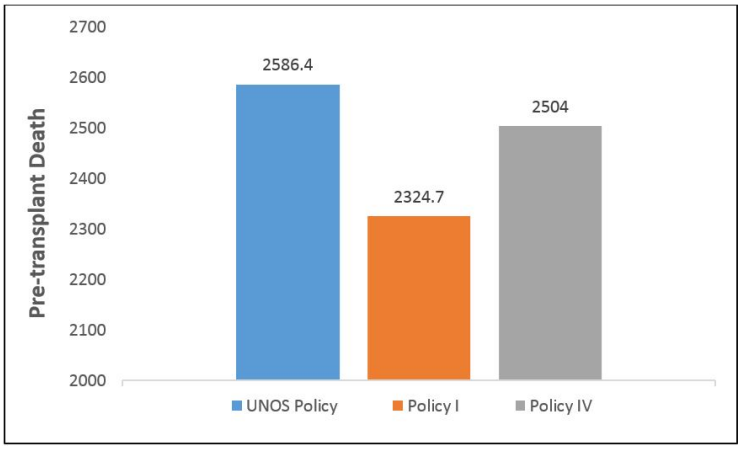

Figure 11: Pre-Transplant Deaths

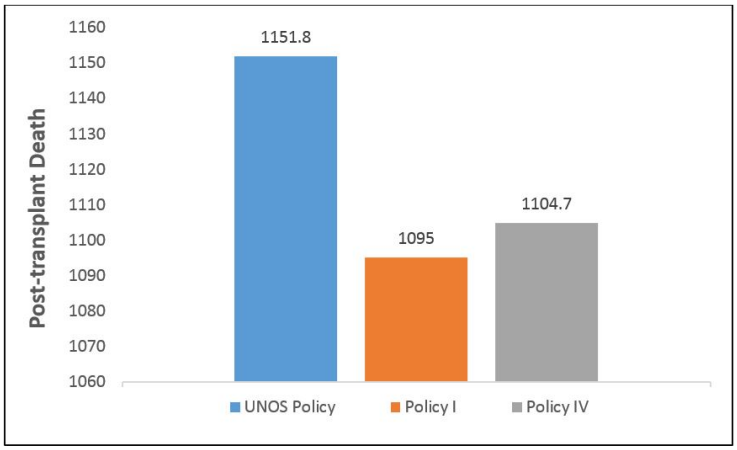

Figure 12: Post-Transplant Deaths

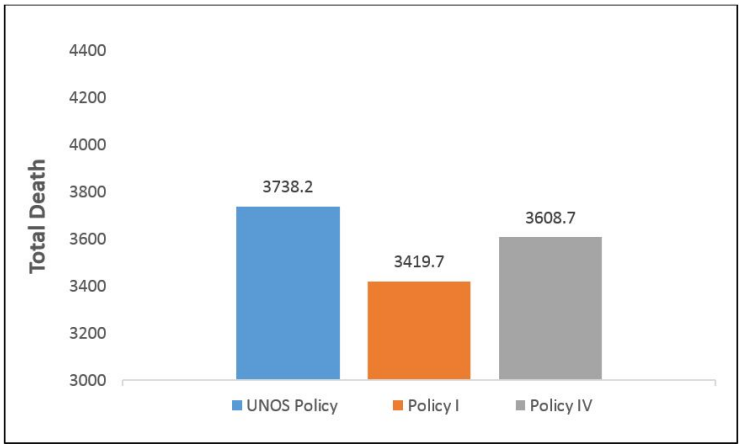

Figure 13: Total Deaths

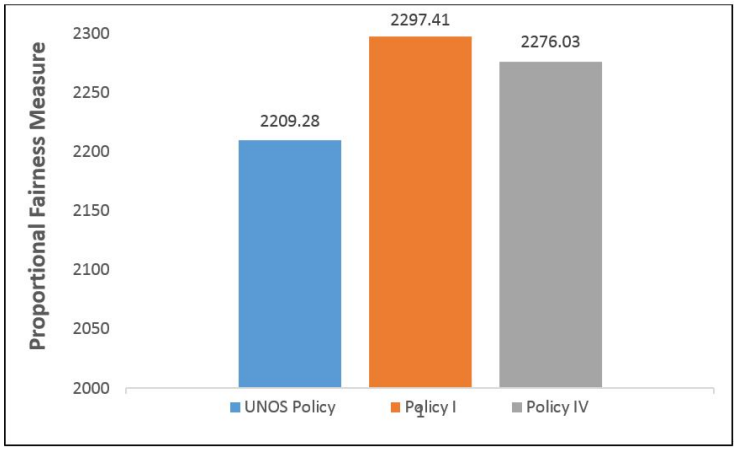

Figure 14: Proportional Fairness Measure

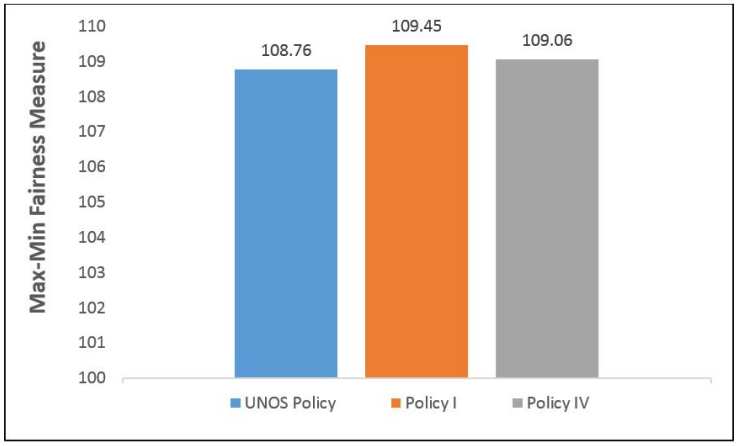

Figure 15: Max-Min Fairness Measure

Furthermore, we conducted a sensitivity analysis on the arrival rate of patients to check its effect on the order of the policies in terms of efficiency (number of total deaths). As can be seen from Figure 16, the order of policies remain unchanged as we increase the patient arrival rates. We increased arrival rates of patients by 10 percent in our planning horizon, and compared the total number of deaths for UNOS policy, three considered policies in Chapter 1 (Policies I, II, and III), and Policy IV. Our results show that order of the policies does not change by changing the input parameters in the described range.

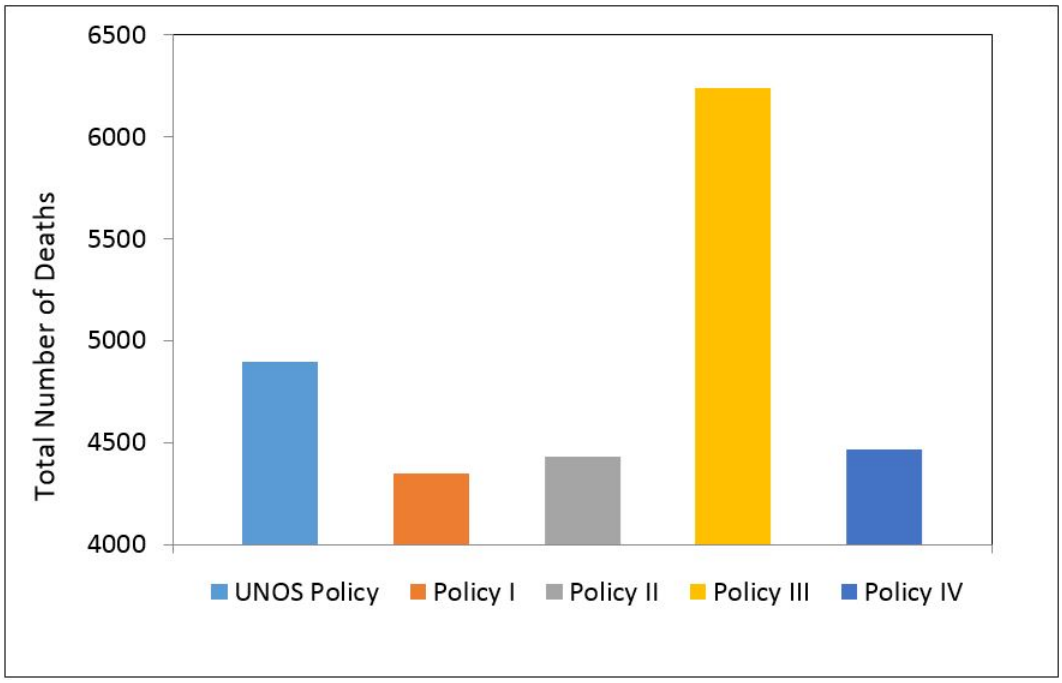

Figure 16: Total Number of Deaths for 10 Percent Increased Patient Arrival Rates for Different Policies

Appendix B Appendix of Chapter 2

Appendix B includes several details regarding the mathematical proofs of the theorems that appear throughout Chapter 2, model validation results, alternative objective functions, and further OPL analysis. In particular, Section B.1 provides notation tables and a mapping from mathematical model to application. Section B.2 provide proof for Theorem 2.1. Section B.3 studies the heart allocation problem in a Markovian setting and provides the mathematical analysis of the optimal solution of problem (P_U) introduced therein. Section B.4 provides an overview of the simulation model used to test the performance of allocation policies in this study, as well as the results of statistical tests performed for validation purposes of the assumptions made in Section B.3 under which an upper bound for the Markovian network is justified. Section B.5 provides details about the benchmark policies studied in Section 2.6.1 and derives the optimal policies for alternative objective functions introduced in Section 2.5 of Chapter 2. Section B.6 studies the reformulated fluid model which incorporates the proximity considerations in heart allocation system. Section B.7 describes details of the fairness constraints imposed in Section 2.6.4. Finally, Section B.8 provides detailed insights on the mechanism of the OPL policy in the absence and presence of fairness constraints.

B.1 Lists of Notations and Abbreviations

This section provides lists of notations and abbreviations used throughout the text. In particular, Tables 32, 33, 34, and 35 describe the notations used in mathematical formulations in Sections 2.3, 2.4, B.3, and B.5, respectively. Furthermore, Table 36 provides a list of abbreviations used in Chapter 2 and its appendix.

Table 32: Notations Used in Stochastic Formulation in Section 2.3

Notation	Description
i	Patient type index
h	Heart type index
I	Number of patient classes
H	Number of heart types
$\mathcal{I}$	Set of patient type indicies
$\mathcal{H}$	Set of heart type indicies
p	List of patients (defined on $\mathcal{P}$)
p_n	n^{th} patient's information on list p
i_n	Class that patient n in list p belongs to
τ_n	Arrival time of patient n in list p
z_n	Binary variable indicating whether patient n has declined the current offer
b_i^h	Total cumulative offers of heart type h to patient type i
κ	Decision epoch indicator
s_κ	State of MDP at epoch κ
a_κ	Action of MDP at epoch κ
$e(\kappa)$	Event type (defined on $\mathcal{E}$)
$b(\kappa)$	Heart offer history (defined on $\mathcal{B}$)
$t(\kappa)$	Current time (defined on $\mathbb{R}^+$)
$\mathcal{K}$	Final decision epoch
$H(s)$	A set indicating available heart at state s
$P(s)$	Set of eligible patients (for transplant) at state s
$a_n^h(s)$	A binary variable indicating if the available heart type h is offered to patient n on list
$\mathcal{A}(s)$	Action space at state s
$\mathcal{S}$	State space
$F(s_\kappa, a_\kappa, \omega(s_\kappa, a_\kappa))$	State evolution mapping governing transition probabilities
$h(s_\kappa, a_\kappa, s_{\kappa+1})$	Immediate reward of transition from s_κ to $s_{\kappa+1}$ when action a_κ is taken
$r(s_\kappa)$	Final reward
$X_i(t)$	Number of patients in class i at time t
Π	Set of all admissible policies
π	Allocation policy
$J_\pi(s)$	Value function of MDP with initial state s under policy π
$V(s)$	Optimal value function of MDP with initial state s
k	Index of fairness constraints
K	Total number of fairness constraints
$\mathcal{F}_k$	Set of patient class indices under consideration in fairness constraint k
$\mathcal{G}_k$	Set of heart type indices under consideration in fairness constraint k
a_k	Lower bound imposed in fairness constraint k
A	A K by IH matrix of fairness constraints coefficients
N	Maximum number of patients that we keep track of in the system
$\mathcal{N}$	Maximum number of times a donor heart can be offered before its wasted

Table 33: Notations Used in Fluid Approximation (P_1) in Section 2.4

Notation	Description
λ_i	Arrival rate of patients in class i
μ^h	Arrival rate of heart type h
$x_i(t)$	Number of patients in class i at time t
ρ_{ij}	Rate at which patients of class i become patient of class j
ρ	Class change matrix with elements ρ_{ij}
d_i	Pre-transplant death rate of patients in class i
d	Pre-transplant diagonal death rate matrix with elements d_i
q_i^h	Heart type h offer acceptance for patients in class i
q^h	Diagonal offer Acceptance probability matrix with q_i^h as its diagonal elements
$u_i^h(t)$	Rate of allocating heart type h to patients in class i at time t
INF	Set of infeasible pair of patients/hearts for transplantation
$\Omega(t)$	Set of feasible controls at time t
$\mathcal{T}$	End of the planning horizon
β_i	QALYs for patients in class i waiting on the waiting list
α_i^h	QALYs for patients of class i receiving a heart type h
η_i	Future QALYs for patients of class i who are on the transplant waiting list at time $\mathcal{T}$
$V_F(x_0)$	Optimal value function of the fluid approximation (P_1) with initial state x_0
$k_i(t)$	Shadow price associated to evolution of i^{th} constraint at time t in (5)
$y_i^h(t)$	Shadow price associated to evolution of ih^{th} auxiliary state variable at time t
$w_i(t)$	Shadow price associated to i^{th} non-negativity constraint in (6)
γ_k	Shadow price associated to the k^{th} fairness constraint

Table 34: Notations Used in Stochastic Formulation in Section B.3

Notation	Description
$X_i(t)$	Number of patients on the waiting list of class i at time t
$Y_i(t)$	Number of patients in class i in the post-transplant phase at time t
$\{T_n : n \geq 0\}$	Sequence of jump times of Markov queuing network in Section B.3
$a_i^h(t)$	Probability of assigning a heart type h to a patient in class i
A	Action space of queuing network in Section B.3
Q	Generator matrix of the queuing network in Section B.3
$q((x,y),a,(x',y'))$	Transition rate from state (x,y) to (x',y') when action a is taken
d_i'	Post-transplant death rate for patients in class i
$A(x,y)$	Set of all admissible actions in state (x,y)
$b((x,y),a)$	Expected drift of the Markovian queuing network in Section B.3
γ_i	QALYS for the patients in class i in the post-transplant phase
δ_i	Future QALYs for patients of class i who are on the post-transplant phase at time $\mathcal{T}$
$r(x(t),y(t))$	Reward rate function
$g(x(\mathcal{T}),y(\mathcal{T}))$	Final reward function
$J_\pi(x,y)$	Value function of queuing network in Section B.3 with initial state (x,y) under policy π
$V(x,y)$	Optimal value function of the queuing network in Section B.3 with initial state (x,y)
$V_{\hat{F}}(x_0,y_0)$	Optimal value function of the fluid approximation (P_U) with initial state (x_0,y_0)
$V_{\hat{F}}^{(m)}(x_0,y_0)$	Optimal value function of the descritized fluid model (P_U) with initial state (x_0,y_0)

Table 35: Notations Used in Alternative Objective Function Formulation in Section B.5

Notation	Description
$\hat{k}_i(t)$	Shadow prices associated to the i^{th} state evolution constraint in optimal control problem (P_2)
$\hat{y}_i^h(t)$	Shadow price associated to evolution of ih^{th} auxiliary state variable at time t in problem (P_2)
$\tilde{k}_i(t)$	Shadow prices associated to the i^{th} state evolution constraint in optimal control problem (P_3)
$\tilde{y}_i^h(t)$	Shadow price associated to evolution of ih^{th} auxiliary state variable at time t in problem (P_3)
a_i^h	Allocation rate of heart type h to patients in class i
a_i	Total allocation rate of hearts to patients in class i
W_i	Expected waiting time of patients in class i
$\lambda = \sum_{i=1}^{I} \lambda_i$	Total arrival rates of patients
$\mu = \sum_{h=1}^{H} \mu^h$	Total arrival rates of hearts

Table 36: Abbreviations Used Throughout the Text

Abbreviation	Description
UNOS	United Network for Organ Sharing
SRTR	Scientific Registry of Transplant Recipient
HF	Heart Failure
DSA	Designated Service Area
OPO	Organ Procurement Organization
VAD	Ventricular Assist Device
OPTN	Organ Procurement and Transplantation Network
UB	Upper Bound
LB	Lower Bound
OPL	Optimal Priority List Policy (Optimal solution of problem (P_1))
SZE	Su and Zenios Efficiency Policy
SZQ	Su and Zenios Equity Policy
BRS	Broadening Regional Sharing Policy
MPD	Minimization of Pre-Transplant Death Policy
MTW	Minimization of Total Wastage of Hearts Policy
MWT	Mean Waiting Time Policy
VWT	Variance of Waiting Time Policy
STD	Standard Deviation

B.2 Theorem 2.1

Theorem 2.1. *A feasible triple of state and control variables (x, z, u) is an optimal solution for (P_1) if and only if there exist shadow prices $k(t)$ and $y(t)$ with one sided limits everywhere, a non-decreasing I-dimensional vector function $w(t)$, and a non-negative K- dimensional adjoint vector γ*

such that

$$\dot{k}(t) \leq (k(t) - w(t))(d + \hat{\rho} - \rho^T) - \beta, \quad \forall\ t \in [0, \mathcal{T}],\ k(\mathcal{T}) = \eta, \tag{15}$$

$$\textit{if } x_i(t) > 0\ ,\ \dot{k}_i(t) = [(k(t) - w(t))(d + \hat{\rho} - \rho^T)]_i - \beta_i, \tag{16}$$

$$\dot{y}(t) = 0, \quad \forall\ t \in [0, \mathcal{T}],\ y(\mathcal{T}) = \gamma A, \tag{17}$$

$$\gamma \cdot (Az(\mathcal{T})) = 0, \gamma \geq 0 \tag{18}$$

$$u^h(t) \in \underset{v}{argmax}\Big\{\Big(\big(\alpha^h - k(t)\big)q^h + y^h(t)\Big)v : v \in \mathbb{R}_+^{|I|},\ e \cdot v \leq \mu^h(t),\ v_i^h = 0;\ (i,h) \in\ INF\Big\}\ \ \forall h \in \mathcal{H}. \tag{19}$$

Proof. Formulation (P_1) is an optimal control problem with state variable $x(t)$ and control variable $u(t)$, which involves integral constraints. First, we transform integral constraints (7) by introducing a new state variable $z(t) = \big(z_i^h(t)\big)_{i\in\mathcal{I}, h\in\mathcal{H}}$, and by setting $z_i^h(t) = \int_0^t u_i^h(\tau)d\tau$ with $z_i^h(0) = 0$ as follows:

$$\sum_{i\in\mathcal{F}_k}\sum_{h\in\mathcal{G}_k} z_i^h(\mathcal{T}) \geq a_k \sum_{i\in\mathcal{I}}\sum_{h\in\mathcal{G}_k} z_i^h(\mathcal{T}), \quad \forall k = 1, \ldots, K,$$

yielding the equivalent constraints of the following form,

$$(1 - a_k)\sum_{i\in\mathcal{F}_k}\sum_{h\in\mathcal{G}_k} z_i^h(\mathcal{T}) - a_k \sum_{i\in\mathcal{I}\setminus\mathcal{F}_k}\sum_{h\in\mathcal{G}_k} z_i^h(\mathcal{T}) \geq 0, \quad \forall k = 1, \ldots, K, \tag{20}$$

with the additional constraints

$$\dot{z}_i^h(t) = u_i^h(t), \quad \forall i \in \mathcal{I}, h \in \mathcal{H}, t \in [0, \mathcal{T}], \tag{21}$$

$$z_i^h(0) = 0, \quad \forall i \in \mathcal{I}, h \in \mathcal{H}, \tag{22}$$

which is due to the fact that $z_i^h(t)$ is non-decreasing and therefore of bounded variation and (21) holds for almost all $t \in [0, \mathcal{T}]$. We assume that (21) serves as a true reformulation, and analyze this surrogate reformulation.

Constraints in (20) are a set of linear final time constraints on the state variable $z(t)$, which can be written as $Az(\mathcal{T}) \geq 0$ where A is a K by $I \times H$ matrix whose element on k^{th} row and ih^{th} column,

$a_{k,ih}$, for each $h \in \mathcal{G}_k$ is defined by,

$$a_{k,ih} = \begin{cases} 1 - a_k, & \text{if } i \in \mathcal{F}_k, \\ -a_k, & \text{if } i \in \mathcal{I} \setminus \mathcal{F}_k. \end{cases}$$

Also, the constraints in (21) are evolution, and the constraints in (22) are the initial value constraints of the state variable $z(t)$. Then, the optimal control problem (P_1) with integral constraints can be written equivalently as the following linear optimal control problem with finial time constraints:

$$\begin{cases} V_F(x_0) = \max \quad \int_0^{\mathcal{T}} \big(\sum_{h=1}^{H} \alpha^h q^h u^h(t) + \beta x(t) \big) dt + \eta x(\mathcal{T}) \\ \text{subject to ,} \\ \qquad \dot{x}(t) \;=\; \lambda(t) - \sum_{h=1}^{H} q^h u^h(t) - (d + \hat{\rho} - \rho^T) x(t), \quad \forall t \in [0, \mathcal{T}] \\ \qquad \dot{z}(t) = u(t), \quad \forall t \in [0, \mathcal{T}] \\ \qquad u(t) \in \Omega(t) := \{ u(t) : \; e.u^h(t) \le \mu^h(t); \; u^h(t) \ge 0, \; \forall h; \\ \qquad\qquad\qquad\qquad u_i^h(t) = 0, \; \forall (i,h) \in \text{ INF} \}, \\ \qquad x(t) \ge 0, \quad \forall t \in [0, \mathcal{T}] \\ \qquad x(0) = x_0 \\ \qquad z(0) = 0, \\ \qquad Az(\mathcal{T}) \ge 0. \end{cases}$$

Let the functions $F(\cdot,\cdot,\cdot)$, $f_1(\cdot,\cdot,\cdot)$, and $f_2(\cdot,\cdot,\cdot)$ denote the total QALYs and system state evolution at time t, respectively, that is,

$$\begin{aligned} F(x(t), u(t), t) &= \sum_{h=1}^{H} \alpha^h q^h u^h(t) + \beta x(t), \\ f_1(x(t), u(t), t) &= \lambda(t) - \sum_{h=1}^{H} q^h u^h(t) - (d + \hat{\rho} - \rho^T) x(t), \\ f_2(x(t), u(t), t) &= u(t). \end{aligned}$$

Also, let the function S denote the final reward at time $\mathcal{T}$, i.e., $S(x(\mathcal{T}), \mathcal{T}) = \eta x(\mathcal{T})$. Define the functions g and a as follows:

$$g(x(t), t) = x(t),$$
$$a(z(\mathcal{T}), \mathcal{T}) = Az(\mathcal{T}),$$

where A is a K by IH matrix of fairness constraints (assume we consider K fairness constraints). Functions $F(\cdot,\cdot,\cdot)$, $f_1(\cdot,\cdot,\cdot)$, $f_2(\cdot,\cdot,\cdot)$, and $g(\cdot,\cdot)$ are continuously differentiable with respect to all their arguments. In fact, they are linear. Hence, the differentiability requirements are satisfied. We first prove that non-negativity of state constraint is of order one, in the sense that $g(x(t), t) \geq 0$ does not explicitly depend on u, but its first derivative with respect to t depends on u. The order of a state constraint is defined as the number of times that we differentiate $g(\cdot,\cdot)$ with respect to t until control variable u appears (Hartl et al., 1995). Define $g^0(\cdot,\cdot,\cdot)$ and $g^1(\cdot,\cdot,\cdot)$ as the following:

$$g^0(x(t), u(t), t) = g = g(x(t), u(t), t),$$

$$g^1(x(t), u(t), t) = \dot{g} = g_x(x(t), t) f(x(t), u(t), t) + g_t(x(t), t),$$

where the subscripts denote partial derivatives. We have $g_x(x(t), t) = e$ and $g_t(x(t), t) = 0$. Therefore, $g^1(x(t), u(t), t) = e.f_1(x(t), u(t), t)$, and since f_1 explicitly depends on u, consequently, g^1 also depends on u, showing that the state constraint $g(x(t), t) \geq 0$ is of order one.

Hence, by applying Theorem 2 (Necessary conditions) in Seierstad and Sydsaeter (1986, chap. 5), and Theorem 7.1 in Hartl et al. (1995) we can characterize the optimal policy as follows:

Let $(x^*(t), z^*(t), u^*(t))$ be a feasible solution solving problem (P_1) with $g(x,t)$ a C^2-function of (x,t). Then, there exist a scalar k_0, vector functions $k(t) = (k_1(t), \ldots, k_I(t))$ and $y(t) = (y_1^1(t), \ldots, y_I^1(t), \ldots, y_1^H(t), \ldots, y_I^H(t))$ with one sided limits everywhere, a non-decreasing vector function $w(t) = (w_1(t), ..., w_I(t))$, and a non-negative adjoint vector γ, such that,

(I). $k_0 = 0 \quad \text{or} \quad k_0 = 1.$

(II). $(k_0, k(t), y(t), w(\mathcal{T}) - w(0), \gamma) \neq 0 \quad \text{for all } t \in [0, \mathcal{T}].$

(III). $u^*(t)$ maximizes $H(x^*(t), z^*(t), u, k(t), y(t), t)$ for $u \in \Omega(t)$ and for all $t \in (0, \mathcal{T})$,

where

$$H(x^*(t), z^*(t), u, k(t), y(t), t) = \sum_{h=1}^{H} [k_0\alpha^h - k(t)].q^h u^h + k(t).\lambda(t)$$
$$+[k_0\beta - k(t)(d + \hat{\rho} - \rho^T)].x^*(t) + y(t)u(t).$$

(IV). $w_i(t)$ is constant on any interval where $x_i^*(t) > 0$, and $w_i(t)$ is continuous at all $t \in (0, T)$ where $x_i^*(t) = 0$ and $\dot{x}_i^*(t)$ is discontinuous.

(V). (a) If we define $k^*(t) = k(t) + w(t)$, then $k^*(t)$ is continuous, and has a continuous derivative, $\dot{k}^*(t)$, at all points of continuity of $u^*(t)$ and $w(t)$, and we have:

$$\dot{k}^*(t) = -\frac{\partial \bar{L}^*}{\partial x} \ (\frac{\partial \bar{L}}{\partial x} \text{ evaluated at } (x^*(t), u^*(t), k^*(t), w(t), t)),$$

where $\bar{L} = H - w(t).(g_x(x,t).f(x,u,t) + g_t(x,t))$. Therefore, we have

$$\dot{k}^*(t) = -k_0\beta + [k(t) - w(t)](d + \hat{\rho} - \rho^T). \tag{23}$$

(b) $y(t)$ is continuous, and has a continuous derivative, $\dot{y}(t)$, at all points of continuity of $u^*(t)$ and we have:

$$\dot{y}(t) = -\frac{\partial \bar{L}^*}{\partial z} \ (\frac{\partial \bar{L}}{\partial z} \text{ evaluated at } (z^*(t), u^*(t), y^*(t), t)),$$

Therefore, we have

$$\dot{y}(t) = 0, \tag{24}$$

meaning that $y(t)$ is constant for $t \in [0, \mathcal{T}]$, i.e., $y(t) = c$.

(VI). The following transversality conditions hold at the final time $\mathcal{T}$:

(a) $k(\mathcal{T}) = k_0\big(\frac{\partial S}{\partial x(\mathcal{T})}\big) = k_0\eta$.

(b) $y(\mathcal{T}) = k_0\big(\frac{\partial S}{\partial z(\mathcal{T})}\big) + \gamma\big(\frac{\partial a}{\partial z(\mathcal{T})}\big) = \gamma A$ where γ is the K-dimensional adjoint variable vector associated to the fairness constraints $a(z^*(\mathcal{T}), \mathcal{T}) = Az(\mathcal{T}) \geq 0$.

(c) $\gamma a(z^*(\mathcal{T}), \mathcal{T}) = 0$, $\gamma \geq 0$.

Without loss of generality, we normalize $w(t)$ by setting $w(\mathcal{T}) = 0$. This follows from Note 3.a in Seierstad and Sydsaeter (1986, chap. 5). Now, by condition (III), $u^*(t)$ maximizes

$$\begin{cases} \sum_{h=1}^{H}[k_0\alpha^h q^h - k(t)q^h + y^h(t)].u^h + k(t).\lambda(t) + [k_0\beta - k(t)(d + \hat{\rho} - \rho^T)].x^*(t), \\ \text{subject to } u \in \Omega(t), \end{cases} \tag{P_H}$$

where $y^h(t) = (y_1^h(t), \ldots, y_I^h(t))$. Since the maximization is with respect to the control variable u, by ignoring those terms in objective function of (P_H) that are independent of u, we can write (P_H) equivalently as the following: $u^*(t)$ maximizes

$$\begin{cases} \sum_{h=1}^{H}[k_0\alpha^h q^h - k(t)q^h + y^h(t)].u^h, \\ \text{subject to, } u \in \Omega(t). \end{cases} \tag{$\bar{P}_H$}$$

Optimality condition (I)-(VI) is called normal when $k_0 = 1$ and abnormal when $k_0 = 0$. Fontes and Frankowska (2015) showed that under certain constraint qualifications on state constraints, optimality condition requires $k_0 = 1$. First, by considering the following lemma we show that necessary conditions for (P_1) cannot be satisfied with $k_0 = 0$. Note that the problem-specific argument in Akan et al. (2012) to prove this step is not applicable to our setting where fairness constraints are involved.

Lemma B.1. *(Fontes and Frankowska, 2015). Let $(x^*(t), z^*(t), u^*(t))$ be the optimal solution of (P_1). Under certain regularity conditions, if the following constraint qualification holds, then the necessary conditions (I)-(VI) will be satisfied with $k_0 = 1$.*

CQn *(Constraint Qualification for Normality) Assume that for every $\tau > 0$ such that $x^*(\tau) = 0$, function $g(x,t)$ is continuously differentiable on a neighborhood of $x^*(\tau)$, and there exist $\epsilon > 0$ and $\delta > 0$ satisfying*

$$\inf_{u \in \Omega(t)} - \nabla g(x^*(\tau), \tau).f_1(x^*(\tau), u, t) < -\delta$$

for a.e. $t \in \{r \in [\tau - \epsilon, \tau] \cap [0, \mathcal{T}] : \max_{\xi \in \partial^*(-g(x^*(r),r)}[\xi.f_1(x^*(r), u^*(r), r)] \geq 0\}$,
where for a function $h(\cdot)$, $\partial^* h(x)$ is the reachable Jacobian at x, and is defined as:

$$\partial^* h(x) = \limsup_{y \to x}\{h'(y)\},$$

where $h'(y)$ denotes the Jacobian of $h(\cdot)$ at y.

Now, we apply Lemma B.1 to the optimal control problem (P_1) to show that the necessary optimality condition is satisfied with $k_0 = 1$. First, note that the function $g(\cdot,\cdot)$ in the state constraint $g(x,t) \geq 0$ is continuously differentiable everywhere and we have $\nabla g(x^*(\tau),\tau) = e$, where e is the row vector of ones. Also, due to differentiability of $g(\cdot,\cdot)$ and consequently $-g(\cdot,\cdot)$, the reachable Jacobian set of $-g(\cdot,\cdot)$ at any point $(x(t),t)$ is a singleton consists of its Jacobian at $(x(t),t)$, i.e., $\partial^*(-g(x^*(t),t) = \{\nabla - g(x^*(t),t)\} = \{-e\}$.

Now, suppose that for some $\tau \in (0,\mathcal{T}]$ we have $x^*(\tau) = 0$ and suppose there exist $\epsilon > 0$ such that $t \in \{r \in [\tau-\epsilon,\tau] \cap [0,\mathcal{T}] : [-e.f_1(x^*(r),u^*(r),r)] \geq 0\}$, meaning that t belongs to an interval right before the time τ where the sum of components of the state evolution constraint is non-positive. Then, for such a t we have $f_1(x^*(\tau),u(t),t) = \lambda(t) - \sum_{h=1}^{H} q^h u^h(t)$. Since $(u^h(t) = 0, \forall h \in \mathcal{H})$ is a feasible control that belongs to $\Omega(t)$, we plug it into f and we have $f_1(x^*(\tau),0,t) = \lambda(t)$. Therefore,

$$\inf_{u\in\Omega(t)} - \nabla g(x^*(\tau),\tau).f_1(x^*(\tau),u,t) \leq -e.f_1(x^*(\tau),0,t) \leq -e.\lambda(t) = -\sum_{i\in\mathcal{I}} \lambda_i(t).$$

By setting $\delta = \sum_{i\in\mathcal{I}} \lambda_i(t) - \delta_1$ for some small $\delta_1 > 0$, we conclude that for all $t \in \{r \in [\tau-\epsilon,\tau]\cap[0,\mathcal{T}] : [-e.f_1(x^*(r),u^*(r),r)] \geq 0\}$, we have:

$$\inf_{u\in\Omega(t)} - \nabla g(x^*(\tau),\tau).f_1(x^*(\tau),u,t) \leq -e.f_1(x^*(\tau),0,t) \leq -e.\lambda(t) = -\sum_{i\in\mathcal{I}} \lambda_i(t) < -\delta.$$

Therefore, the constraint qualification for normality holds for the optimal control problem (P_1) and the optimality conditions (I)-(VI) are satisfied with $k_0 = 1$. Note that Akan et al. (2012) used a proof of contradiction approach to show normality of the optimal control without constraints, which is a special case of our setting. However, that approach is not applicable in our problem.

Hence, if we plug $k_0 = 1$ in the objective function of $(\bar{P}_H)$, we have: $u^*(t)$ solves

$$\begin{cases} \max \sum_{h=1}^{H} [\alpha^h q^h - k(t) q^h + y^h(t)].u^h(t), \\ \text{subject to,} \\ e.u^h(t) \leq \mu^h(t), \forall h \in \mathcal{H}, \\ u_i^h(t) = 0, \forall (i,h) \in \text{INF}, \\ u^h(t) \geq 0, \forall h \in \mathcal{H}, . \end{cases} \qquad (\tilde{P}_H)$$

Note that problem $(\tilde{P}_H)$ is a separable linear program with respect to its decision variables $u^h(t)$, i.e., solving $(\tilde{P}_H)$ is equivalent to solving H linear programs for $h = 1, \ldots, H$ separately as follows:

$$\begin{cases} \max[\alpha^h q^h - k(t) q^h + y^h(t)].u^h(t), \\ \text{subject to,} \\ e.u^h(t) \leq \mu^h(t), \\ u_i^h(t) = 0, \forall (i,h) \in \text{INF}, \\ u^h(t) \geq 0. \end{cases}$$

This shows that the optimal solution is a priority index policy with respect to coefficient $\alpha^h q^h - k(t) q^h + y^h(t)$ proving (19).

In order to prove (15) and (16), we claim that $[\dot{k}(t) + \beta - (k(t) - w(t))(d + \hat{\rho} - \rho^T)].x^*(t) = 0$. To see this, suppose that $x_i(t) \neq 0$ or equivalently $x_i(t) > 0$ for some $i \in \mathcal{I}$ and $h \in \mathcal{H}$. Then, by condition (IV) we conclude that $w_i(t)$ is constant, which implies that $\dot{w}_i(t) = 0$. Now, by condition (V), we have: $\dot{k}_i^*(t) = \dot{k}_i(t) = -\beta_i + [(k(t) - w(t))(d + \hat{\rho} - \rho^T)]_i$, and this implies $\dot{k}_i(t) + \beta_i - [(k(t) - w(t))(d + \hat{\rho} - \rho^T)]_i = 0$. Conversely, suppose that $\dot{k}_i(t) + \beta_i - [(k(t) - w(t)(d + \hat{\rho} - \rho^T))]_i \neq 0$ or equivalently $\dot{k}_i(t) < -\beta_i + [(k(t) - w(t))(d + \hat{\rho} - \rho^T)]_i = \dot{k}_i^*(t)$. Hence, by condition (V) we see that $\dot{w}_i(t) > 0$ and this implies $x_i(t) = 0$ (since otherwise, if $x_i(t) > 0$, by condition (IV), $w_i(t)$ has to be constant, which contradicts the fact that $\dot{w}_i(t) > 0$). Therefore, we conclude the following results

$$\dot{k}(t) \leq (k(t) - w(t))(d + \hat{\rho} - \rho^T) - \beta, \quad \text{for } t \in [0, \mathcal{T}], \; k(\mathcal{T}) = \eta,$$
$$\text{if } x_i(t) > 0 \; , \; \dot{k}_i(t) = [(k(t) - w(t))(d + \hat{\rho} - \rho^T)]_i - \beta_i.$$

Furthermore, (17) follows from optimality conditions (V-b) and (VI-b). Finally, (18) is immediate by condition (VI-c).

(ii) Conversely, suppose that a feasible control $\bar{u} \in \Omega(t)$ and its associated state trajectory $(\bar{x}, \bar{z})$ satisfy the necessary conditions (I)-(VI). Since $f_1(x, u, t)$ and $f_2(x, u, t)$ are linear on (x, z, u), $g(x, t)$ is linear on x, and Hamiltonian $H(x, z, u, k, y, t)$ is concave on (x, z, u), by Theorem 1 in Seierstad and Sydsaeter (1986, chap. 5) (Sufficient conditions) we conclude that $(\bar{x}, \bar{z}, \bar{u})$ is the optimal solution of (P_1), which completes the proof of Theorem 2.1. □

B.3 An Upper Bound in a Markovian Setting

It is shown in several studies that the fluid approximation provides a lower bound (in minimization case) to the optimal solution of the corresponding stochastic system. For example, Gurvich et al. (2014) studied a matching queue, in which items of different classes arrive to the system and wait on multiple queues to be matched with items of other classes. They approximated the matching system by a fluid model and used it to generate lower bounds on the objective function of the original system and characterize the asymptotic optimal solutions for both balanced and imbalanced matching networks. Jiménez and Koole (2004) studied a time-varying queuing model for a call center and showed that a fluid approximation generates a lower bound on the performance of the system in several overloaded situations. Altman et al. (2001) showed that for a certain class of queuing systems the fluid approximation provides a lower bound on the workload of the queuing system. Bäuerle (2000, 2002) considered the class of control problems for networks with linear dynamics. They showed that the fluid approximation of the network provides a lower bound on the objective function of the stochastic problem. They also studied how to construct asymptotically optimal decision rules. We generate upper bounds on the performance of the original system based on work presented in Bäuerle (2000, 2002). However, the methods developed do not directly apply as the expected drift of the Markov process in our formulation is a function of both state and action variables. Therefore, we adopted the methodology to address such technicalities.

In order to assess the quality of solutions produced by the fluid approximation, we provide an upper bound in a Markovian setting and the absence of fairness constraints. Bäuerle (2000, 2002) provided an upper bound on the optimal value function for a class of stochastic networks. Specifically,

Bäuerle (2002) developed an upper bound for a class of Markovian stochastic networks in finite and infinite horizon, where the expected drift of the process is linear on control and the reward rate is linear on state variables. Also, Bäuerle (2000) studied an infinite-horizon Markovian stochastic network where the drift of the process is linear on control and the cost rate is lower-semicontinuous in state and convex in control and derived an upper bound. The Markovian stochastic network of the heart transplantation queue considered in this study differs from the ones considered in Bäuerle (2000, 2002) as the expected drift in our network is a function of both state and action. However, we adopt and apply the methods discussed in Bäuerle (2002) to derive the upper bound. Nonetheless, the application of Markovian queuing networks to measure suboptimality of allocation rules in transplantation queuing networks is novel.

This section formulates the heart transplantation system studied in Section 2.3 as a Markovian stochastic queuing network. To that end, we assume that the interarrival times of all stochastic processes involved are independent, stationary, and exponentially distributed. In fact, the statistical tests on the UNOS heart transplantation data confirms the validity of these assumptions; see EC.4.2. for validation results. However, the probability of death on the waiting list depends on many other factors in the Cox proportional hazard model and our analysis shows that the dependency to waiting-time is "weak," i.e., the probability of death for a patient waiting 9 months (average waiting time in heart transplantation queue is 7 months) is only increased by 2%, on average, compared to no waiting if everything else is fixed. Furthermore, recall from the stochastic formulation in Section 3 that we keep track of a total of N patients. This assumption is not restrictive as one may assume a large N.

For $i \in \mathcal{I}$, define $X_i(t)$ as the number of type i patients on the transplant waiting list, $Y_i(t)$ as the number of type i patients on the post-transplant phase at time t, and let the state process of the system be $\{(X(t), Y(t)) : t \geq 0\}$ where $X(t) = (X_1(t), \ldots, X_I(t))$ and $Y(t) = (Y_1(t), \ldots, Y_I(t))$. Hence, there are $2I$ number of queues including patients on both pre- and post-transplant lists and the state space of the model is $S = \{(x, y) \in \mathbb{N}_0^{2I} : (x, y) \cdot e \leq N\}$ where $\mathbb{N}_0$ denotes the set of non-negative integers, and e is a $2I$ dimensional vector of ones. The state process $\{(X(t), Y(t)) : t \geq 0\}$ is a continuous time Markov process and note that in this formulation we keep track of patients in the post-transplant phase such that the reward rates become a linear function of the state. The

controller can take action continuously over time, and without loss of generality one may restrict the control (action) of the system to discrete sequence of points in time where the state process of the system has a jump. Therefore, let the sequence $\{T_n : n \geq 0\}$ with $T_0 := 0$ be the sequence of jump times of the Markov process $\{(X(t), Y(t)) : t \geq 0\}$, which corresponds to the decision epochs of the model. Let the control variable $a_i^h(t)$ be the probability of assigning an available heart type h to a patient in class i, and $a(t) = (a_i^h(t) : i \in \mathcal{I}, h \in \mathcal{H})$. The action space can be written as $A := \{(a_i^h : i \in \mathcal{I}, h \in \mathcal{H}) : \sum_i \sum_h a_i^h = 1, 0 \leq a_i^h \leq 1 \ \forall i \in \mathcal{I}, h \in \mathcal{H};\ a_i^h(t) = 0,\ \forall (i,h) \in \text{ INF}\}$, which is a compact and convex set. Let $Q = (q((x,y), a, (x',y')))$ be the generator of the stochastic process $\{(X(t), Y(t)) : t \geq 0\}$, where $q((x,y), a, (x',y'))$ is the transition rate from state (x,y) to state (x',y') given that $(x,y) \cdot e \neq N$ when action a is taken, given by

$$q((x,y), a, (x',y')) = \begin{cases} \lambda_i & x' = x + e_i, y' = y, \\ \rho_{ij} x_i & x' = x - e_i + e_j, y' = y, \\ d_i x_i & x' = x - e_i, y' = y, \\ \sum_h \mu^h a_i^h (1 - (1 - p_i^h)^{\mathcal{N}}) & x' = x - e_i, y' = y + e_i, \\ d_i' y_i & x' = x, y' = y - e_i, \end{cases}$$

where d_i' denotes the death rate for patients in class i after transplantation, d' is a diagonal matrix representing post-transplant death rates with d_i' on its diagonal, e_i is the I-dimensional unit vector whose i^{th} element is 1, and e is a $2I$ dimensional vector of ones. In the case where $(x,y) \cdot e = N$, the transition rate from state (x,y) to (x',y') is similar to the case where $(x,y) \cdot e \neq N$, except $q((x,y), a, (x + e_i, y)) = 0$. Note that the other transition rates are equal to zero and that $q(\cdot)$ is uniformly bounded as both state variable (x,y) and action a are bounded.

Define $A(x,y) := \{a \in A : x_i = 0 \implies \sum_h a_i^h = 0\}$ as the set of all admissible actions in state (x,y) and note that $A(x,y) \neq \emptyset$ for all $(x,y) \in S$, meaning that there is at least one admissible action in every state. For all $(x,y), (x',y') \in S$ and $a \in A(x,y)$ let $b : S \times A \to \mathbb{R}^{2I}$ with $b((x,y), a) = \sum_{(x',y') \in S} ((x',y') - (x,y)) q((x,y), a, (x',y'))$ be the expected drift of the network, which can be written as

$$b((x,y),a) = \begin{cases} \Big(\lambda - \sum_{h=1}^{H} q^h \mu^h a^h - (d + \hat{\rho} - \rho^T)x, \sum_{h=1}^{H} q^h \mu^h a^h - d'y\Big) & (x,y)\cdot e < N, \\ \Big(- \sum_{h=1}^{H} q^h \mu^h a^h - (d + \hat{\rho} - \rho^T)x, \sum_{h=1}^{H} q^h \mu^h a^h - d'y\Big) & (x,y)\cdot e = N. \end{cases}$$

The reward rate function $r : S \to \mathbb{R}_+$ with $r(x(t), y(t)) = \beta x(t) + \gamma y(t)$ is linear on state variable which accounts for the pre- and post-transplant QALYs, where $\gamma = (\gamma_1, \ldots, \gamma_I)$ is the QALYs coefficient vector for the patients in the post-transplant phase. Similarly, the final reward function $g : S \to \mathbb{R}_+$ at the end of the planning horizon $\mathcal{T}$ is given by $g(x(\mathcal{T}), y(\mathcal{T})) = \eta x(\mathcal{T}) + \delta y(\mathcal{T})$ where $\delta = (\delta_1, \ldots, \delta_I)$ is the future QALYs coefficient vector for the patients who are still alive in the post-transplant phase at the end of the planning horizon. For an initial state $(x, y) \in S$ and a fixed decision rule π, let the expected total QALYs be

$$J_\pi(x,y) = \mathbb{E}^\pi \Big\{ \int_0^{\mathcal{T}} r(x(\tau), y(\tau)) d\tau + g(x(\mathcal{T}), y(\mathcal{T})) | (x(0), y(0)) = (x,y) \Big\}.$$

The decision maker solves for

$$V(x,y) = \sup_{\pi \in \Pi} \Big\{ J_\pi(x,y) \Big\},$$

where Π is the set of all admissible policies.

A fluid approximation to the stochastic network is given by

$$\begin{cases} V_{\hat{F}}(x_0, y_0) = \max \int_0^{\mathcal{T}} r(x(t), y(t)) dt + g(x(\mathcal{T}), y(\mathcal{T})) \\ \text{subject to} \\ (\dot{x}(t), \dot{y}(t)) = b((x(t), y(t)), a(t)), \\ (x(0), y(0)) = (x_0, y_0), \\ x(t) \geq 0, y(t) \geq 0, \\ N - e_{2I} \cdot (x,y) \geq 0, \\ a(t) \in A, \end{cases} \qquad (P_U)$$

The following theorem, shows that the value function of problem (P_U) provides an upper bound to the optimal value function of the stochastic Markovian network, $V(x, y)$.

Theorem B.1. *For all initial states* $(x, y) \in S$, $V(x, y) \leq V_{\hat{F}}(x, y)$.

In order to solve the optimal control problem (P_U), the planning horizon is discretized. Let $V_{\hat{F}}^{(m)}(x, y)$ be the optimal value function of the discretized version of the optimal control problem (P_U) where m denotes the number of discretization steps. Because the optimal control problem is linear, its discretized version is an LP which can be solved efficiently. Also, since problem (P_U) satisfies conditions in a corollary for Theorem 3 in Budak et al. (1969), as the number of discretization steps increases, the optimal value of the discretized version of the optimal control problem converges to $V_{\hat{F}}$, i.e., $V_{\hat{F}}^{(m)}(x, y) \to V_{\hat{F}}(x, y)$ as $m \to \infty$, for all x.

Remark B.1. *Although in the original system in Section 2.3 some probability distributions are not memoryless based on statistical tests on real data, we "heuristically" use the bound presented in this section, i.e.,* $V_{\hat{F}}^{(m)}(\cdot)$*, to assess the quality of feasible allocation policies. Furthermore, we show in Section B.3.2 that the optimal solution of problem* (P_U) *is also a priority index policy depending on shadow prices associated to* x *and* y *evolution constraints. In Section B.3.2, we test the quality of solutions produced by such priority rules.*

B.3.1 Proof of Theorem B.1

Theorem B.1. *For all initial states* $(x, y) \in S$, $V(x, y) \leq V_{\hat{F}}(x, y)$.

Proof. Proof. Suppose that $\pi \in \Pi$ is an arbitrary decision rule for the Markovian stochastic queuing network. As stated in the main text of Chapter 2, the state process $\{(X(t), Y(t)) : t \geq 0\}$ is a Markov process whose generator is $Q = (q((x, y), \pi(x, y), (x', y')))$. Using the Dynkin's formula for this Markov process, we obtain

$$M(t) = (X(t), Y(t)) - (x, y) - \int_0^t b((X(s), Y(s)), \pi(X(s), Y(s)))ds, \tag{25}$$

where $M(t)$ is a martingale with the initial condition $M(0) = 0$ and $b(\cdot, \cdot)$ is the expected drift of the network (Athreya and Kurtz, 1973, Display 5). Note that in transforming the Markov process via Dynkin's formula we used the fact that the expected drift is uniformly bounded (condition (1) in Athreya and Kurtz (1973)) and its derivative exists (condition (2) in Athreya and Kurtz (1973)).

These conditions hold because the expected drift is a linear function of state and action, where both of them are bounded (defined on bounded state and action sets). First, note that:

(a) For our stochastic queuing network, the expected drift

$$b((x,y),a) = \begin{cases} \Big(\lambda - \sum_{h=1}^{H} q^h \mu^h a^h - (d + \hat{\rho} - \rho^T)x, \sum_{h=1}^{H} q^h \mu^h a^h - d'y\Big) & (x,y)\cdot e < N, \\ \Big(- \sum_{h=1}^{H} q^h \mu^h a^h - (d + \hat{\rho} - \rho^T)x, \sum_{h=1}^{H} q^h \mu^h a^h - d'y\Big) & (x,y)\cdot e = N, \end{cases}$$

is bounded as both state and action variables belong to bounded spaces, which yields the following:

$$\mathbb{E}^{\pi}\Big\{ \int_0^t b\Big(\big(X(s),Y(s)\big), \pi\big(X(s),Y(s)\big)\Big) ds\Big\} = \int_0^t \mathbb{E}^{\pi}\Big\{ b\Big(\big(X(s),Y(s)\big), \pi\big(X(s),Y(s)\big)\Big)\Big\} ds.$$

(b) The expected drift is linear on its arguments. Therefore, we have:

$$\mathbb{E}^{\pi}\Big\{ b\Big(\big(X(s),Y(s)\big), \pi\big(X(s),Y(s)\big)\Big)\Big\} = b\Big(\mathbb{E}^{\pi}\big\{\big(X(s),Y(s)\big)\big\}, \mathbb{E}^{\pi}\big\{\pi\big(X(s),Y(s)\big)\big\}\Big).$$

Then, we take the expectation of (25) considering (a) and (b) and noting by the optional sampling theorem that the expectation of the martingale $M(t)$ is equal to zero (the expectation of $M(0)$), which yields:

$$\begin{aligned} 0 = {} & \mathbb{E}^{\pi}\big\{\big(X(t),Y(t)\big)\big\} - (x,y) \\ & - \int_0^t \Big(\lambda(s) - \sum_{h=1}^{H} q^h \mu^h \mathbb{E}^{\pi}\big\{\pi^h\big(X(s),Y(s)\big)\big\} - (d + \hat{\rho} - \rho^T)\mathbb{E}^{\pi}\{X(s)\}, \\ & \sum_{h=1}^{H} q^h \mu^h \mathbb{E}^{\pi}\big\{\pi^h\big(X(s),Y(s)\big)\big\} - d'\mathbb{E}^{\pi}\{Y(s)\}\Big) ds, \end{aligned}$$

which yields the following for the case where $(X(t), Y(t)) \cdot e < N$,

$$\begin{aligned}
&\mathbb{E}^{\pi}\Big\{\big(X(t), Y(t)\big)\Big\} = (x, y) \\
&+ \int_0^t \Big(\lambda(s) - \sum_{h=1}^{H} q^h \mu^h \mathbb{E}^{\pi}\big\{\pi^h\big(X(s), Y(s)\big)\big\} - (d + \hat{\rho} - \rho^T)\mathbb{E}^{\pi}\{X(s)\}, \\
&\sum_{h=1}^{H} q^h \mu^h \mathbb{E}^{\pi}\big\{\pi^h\big(X(s), Y(s)\big)\big\} - d'\mathbb{E}^{\pi}\{Y(s)\}\Big) ds, \qquad (26)
\end{aligned}$$

and, for the case where $(X(t), Y(t)) \cdot e = N$, we have

$$\begin{aligned}
&\mathbb{E}^{\pi}\Big\{\big(X(t), Y(t)\big)\Big\} = (x, y) \\
&+ \int_0^t \Big(-\sum_{h=1}^{H} q^h \mu^h \mathbb{E}^{\pi}\big\{\pi^h\big(X(s), Y(s)\big)\big\} - (d + \hat{\rho} - \rho^T)\mathbb{E}^{\pi}\{X(s)\}, \\
&\sum_{h=1}^{H} q^h \mu^h \mathbb{E}^{\pi}\big\{\pi^h\big(X(s), Y(s)\big)\big\} - d'\mathbb{E}^{\pi}\{Y(s)\}\Big) ds \qquad (27)
\end{aligned}$$

Define $\big(\hat{x}(t), \hat{y}(t)\big) := \mathbb{E}^{\pi}\big\{\big(X(t), Y(t)\big)\big\}$, and $\hat{a}(t) := \mathbb{E}^{\pi}\big\{\pi\big(X(t), Y(t)\big)\big\}$. We have $\big(X(t), Y(t)\big) \geq 0$, $(X(t), Y(t)) \cdot e \leq N$, and $\pi\big(X(t), Y(t)\big) \in A$, almost surely. Hence, we have $\big(\hat{x}(t), \hat{y}(t)\big) \geq 0$ and $\big(\hat{x}(t), \hat{y}(t)\big) \cdot e \leq N$, and $\hat{a}(t) \in A$ as the action space A is convex. So, by rewriting (26) and (27) we get

$$\big(\hat{x}(t), \hat{y}(t)\big) = (x, y) + \int_0^t b\big((\hat{x}(s), \hat{y}(s)), \hat{a}(s)\big) ds.$$

This can be written by plugging the expected drift function as follows

$$\begin{cases}
(x, y) + \int_0^t \Big(\lambda(s) - \sum_{h=1}^{H} q^h \mu^h \hat{a}^h(s) - (d + \hat{\rho} - \rho^T)\hat{x}(s), \sum_{h=1}^{H} q^h \mu^h \hat{a}^h(s) - d'\hat{y}(s)\Big) ds, & (\hat{x}, \hat{y}) \cdot e < N, \\
(x, y) + \int_0^t \Big(-\sum_{h=1}^{H} q^h \mu^h \hat{a}^h(s) - (d + \hat{\rho} - \rho^T)\hat{x}(s), \sum_{h=1}^{H} q^h \mu^h \hat{a}^h(s) - d'\hat{y}(s)\Big) ds, & (\hat{x}, \hat{y}) \cdot e = N.
\end{cases}$$

This is equivalent to $(\hat{x}_0, \hat{y}_0) = (x, y)$ with

$$\big(\dot{\hat{x}}(t), \dot{\hat{y}}(t)\big) = b\big((\hat{x}(t), \hat{y}(t)), \hat{a}(t)\big)$$
$$= \begin{cases} (\lambda(t) - \sum_{h=1}^{H} q^h \mu^h \hat{a}^h(t) - (d + \hat{\rho} - \rho^T)\hat{x}(t), \sum_{h=1}^{H} q^h \mu^h \hat{a}^h(t) - d'\hat{y}(t)), & (\hat{x}, \hat{y}) \cdot e < N, \\ (-\sum_{h=1}^{H} q^h \mu^h \hat{a}^h(t) - (d + \hat{\rho} - \rho^T)\hat{x}(t), \sum_{h=1}^{H} q^h \mu^h \hat{a}^h(t) - d'\hat{y}(t)), & (\hat{x}, \hat{y}) \cdot e = N. \end{cases}$$

Therefore, the pair $\Big((\hat{x}(t), \hat{y}(t)), \hat{a}(t)\Big)$ is feasible for the fluid model (P_U) for every decision rule π. Note that the expected total QALYs for the stochastic queuing network for an arbitrary policy π is given by

$$\begin{aligned} J_\pi(x, y) =& \mathbb{E}^\pi\Big\{ \int_0^{\mathcal{T}} \Big[\beta X(t) + \gamma Y(t)\Big] dt + \eta X(\mathcal{T}) + \delta Y(\mathcal{T}) \Big| \big(X(0), Y(0)\big) = (x, y) \Big\} \\ =& \int_0^{\mathcal{T}} \Big[\beta \mathbb{E}^\pi\big\{X(t) \mid \big(X(0), Y(0)\big) = (x, y)\big\} + \gamma \mathbb{E}^\pi\big\{Y(t) \mid \big(X(0), Y(0)\big) = (x, y)\big\}\Big] dt \\ &+ \eta \mathbb{E}^\pi\{X(\mathcal{T}) | \big(X(0), Y(0)\big) = (x, y)\} + \delta \mathbb{E}^\pi\{Y(\mathcal{T}) | \big(X(0), Y(0)\big) = (x, y)\} \\ =& \int_0^{\mathcal{T}} \Big[\beta \hat{x}(t) + \gamma \hat{y}(t)\Big] dt + \eta \hat{x}(\mathcal{T}) + \delta \hat{y}(\mathcal{T}) \\ =& \int_0^{\mathcal{T}} r(\hat{x}(t), \hat{y}(t)) dt + g(\hat{x}(\mathcal{T}), \hat{y}(\mathcal{T})). \end{aligned}$$

This implies that for every decision rule $\pi \in \Pi$, and initial state $(x, y) \in S$, because the triple of state-action $\big((\hat{x}, \hat{y}), \hat{a}\big)$ is feasible for the fluid problem (P_U), we have

$$J_\pi(x, y) = \int_0^{\mathcal{T}} r(\hat{x}(t), \hat{y}(t)) dt + g(\hat{x}(\mathcal{T}), \hat{y}(\mathcal{T})) \ \leq V_{\hat{F}}(x, y),$$

meaning that the value function of the stochastic queuing network for every decision rule $\pi \in \Pi$, $J_\pi(x, y)$, is bounded above by the optimal value function of the fluid model (P_U), $V_{\hat{F}}(x, y)$. Taking supremum over all feasible decision rules yields

$$\sup_\pi J_\pi(x, y) \leq V_{\hat{F}}(x, y) \implies V(x, y) \leq V_{\hat{F}}(x, y),$$

which shows that the optimal value function of the fluid model (P_U) provides an upper bound to

the optimal value function of the stochastic queuing network. □

B.3.2 Policy Derivation for Problem (P_U)

Fluid approximation (P_U) of the Markovian stochastic queuing network of the heart transplantation allocation problem introduced in Section B.3 is a linear optimal control problem with state variable (x, y) and action a as shown below:

$$\begin{cases} V_{\hat{F}}(x_0, y_0) = \max \int_0^{\mathcal{T}} r(x(t), y(t))dt + g(x(\mathcal{T}), y(\mathcal{T})) \\ \text{subject to} \\ (\dot{x}(t), \dot{y}(t)) = b((x(t), y(t)), a(t)), \\ (x(0), y(0)) = (x_0, y_0), \\ x(t) \geq 0, y(t) \geq 0, \\ N - e_{2I} \cdot (x, y) \geq 0, \\ a(t) \in A, \end{cases} \tag{P_U}$$

where $r(x(t), y(t)) = \beta x(t) + \gamma y(t)$ is the cost rate function, $g(x(\mathcal{T}), y(\mathcal{T})) = \eta x(\mathcal{T}) + \delta y(\mathcal{T})$ is the final cost function, $b((x(t), y(t)), a(t))$ is the expected drift, and e_{2I} is a $2I$-dimensional vector of ones. The necessary and sufficient optimality conditions for the linear optimal control problem provides the following LP for each heart type h at each time t, whose solution provide the optimal control

$$\begin{cases} \max \Big(k^2(t) - k^1(t)\Big) q^h u^h(t), \\ \text{subject to,} \\ e.u^h(t) \leq \mu^h(t), \\ u_i^h(t) = 0, \forall (i, h) \in \text{ INF}, \\ u^h(t) \geq 0, \end{cases} \tag{28}$$

where $k^1(t)$ and $k^2(t)$ are the shadow prices associated to $\dot{x}(t)$ and $\dot{y}(t)$ constraints, respectively. Similar arguments as in proof of Theorem 2.1 provides the following condition that can be used to

Table 37: Each Objective Function Component for OPLS Policy

	Objective Function (Life-Days $\times 10^6$)			
Policy	**Pre-TX**	**Post-TX**	**Final**	**Total**
OPLS	7.43	160.21	0.024	167.66

Table 38: Mean and Standard Deviation of Waiting Time for OPLS Policy

	Waiting Time (Days)	
Policy	**Mean**	**STD**
OPLS	96	72

calculate these shadow prices

$$\dot{k^1}(t) = -\beta + (d + \hat{\rho} - \rho^T)(k^1(t) - w_1(t)) + \bar{w}_3(t), \tag{29}$$

$$\dot{k^2}(t) = -\gamma + d'(k^2(t) - w_2(t)) + \bar{w}_3(t), \tag{30}$$

with final condition $k^1(\mathcal{T}) = \eta$ and $k^2(\mathcal{T}) = \delta$. In addition, vectors $w_1(t)$ and $w_2(t)$ and scalar $w_3(t)$ are the shadow prices associated to constraints $x(t) \geq 0$, $y(t) \geq 0$, and $N - e_{2I} \cdot (x, y) \geq 0$, respectively. Note that $\bar{w}_3(t)$ is a I-dimensional vector whose elements are all $w_3(t)$.
As can be seen from the derived LP in (28), given the shadow price vectors $k^1(t)$ and $k^2(t)$, the optimal solution of problem (P_U) at each time t is a priority index policy with priority coefficient $\big((k_i^2(t) - k_i^1(t)\big)q_i^h$, which prioritizes patients with higher coefficients. This provides a patient priority list that can be used to simulate the optimal solution of the optimal control problem (P_U). We denote this policy by OPLS. Tables 37 and 38 report the results of simulating the OPLS policy in terms of life years and mean and standard deviation of waiting time. Results in the tables indicate that the OPLS policy performs very similarly to the OPL policy in terms of these measures.

In addition, this section presents the results of solving the discretized fluid problem (P_U), which yields an upper bound on the value function of the stochastic formulation in Section 2.3 in the absence of fairness constraints, and the results of simulating the OPL policy that yields a lower bound. In particular, Table 39 assesses the upper and lower bounds on the total LYs of the patient population for each region in the U.S., and reports the optimality gap calculated by $\frac{\mathrm{UB}(r) - \mathrm{LB}(r)}{\mathrm{UB}(r)} \times 100\%$, where

Table 39: Optimality Gap in a Markovian Setting

Region	**R1**	**R2**	**R3**	**R4**	**R5**	**R6**	**R7**	**R8**	**R9**	**R10**	**R11**	**Total**
Optimality Gap (%)	7.7	7.0	3.2	2.8	4.5	1.4	4.3	6.5	2.2	2.8	3.9	4.3

UB(r) and LB(r) stand for the upper and lower bound in region r, respectively. The optimality gap ranges from 1.4% to 7.7% across regions and it is 4.3% in the country, which suggests that the proposed OPL policy is near optimal.

B.4 Simulation and Assumption Validation

This section provides details about the simulation model, the allocation policies studied and simulated in Chapter 2, as well as the results of statistical tests performed for validation purposes.

A simulation model of the stochastic heart transplantation system on a daily basis, calibrated and validated by data from UNOS/SRTR, is used for numerical studies (Hasankhani and Khademi, 2017). This simulation model is different from the TSAM provided by SRTR. In particular, TSAM makes the following assumptions: (1) arrivals of patients and donors are input to the model with a data file, (2) the initial waiting list is input to the model with a data file, (3) an entire history of waiting list health status changes must be input to the model for each patient. The simulation model relaxes those assumptions by creating models for arrivals of patients and hearts, as well as models for change of health status in the waiting list. It consists of six main modules: (1) patient arrival module, (2) heart arrival module, (3) patient health status change module, (4) pre-transplant survival module, (5) allocation module, and (6) post-transplant survival module. Figure 17 in Section B.4 illustrates the flow of the simulation model. In addition, Table 40 in Section B.4 provides a mapping of heart transplantation system elements from practical aspects to the simulation and mathematical models.

The patient arrival module generates patient arrivals to the waiting list and assigns various clinical and demographic attributes according to conditional distributions. The patient arrival is modeled as a non-stationary Poisson process with the arrival rate depending on year. Similar to the patient arrival module, heart arrival module generates a newly donated heart and assigns its attributes that will be used in the allocation process. In the simulation model, the daily health status progression of patients on the waiting list is modeled as a Markov chain and data from UNOS/SRTR is used

to estimate its transition probability matrix using maximum likelihood estimator. By using a Cox survival model, at each day of the simulation, the pre-transplant survival module generates the probability of death for patients on the waiting list. The post-transplant survival module uses another Cox model to generate death probabilities for patients on the post-transplant phase. Note that the simulation model considers all the characteristics of patients and donated hearts reported in UNOS/SRTR data sets such as ethnicity, gender, number of transplants before listing, and disease. The allocation module is responsible for matching the available hearts with patients. In particular, once a heart is procured, this module seeks to match the available heart with a patient on the waiting list by using certain priority rules, which is called the allocation policy. The UNOS allocation policy is used as a baseline policy for the simulation model for validation purposes.

The simulation model is validated by using the UNOS allocation policy in the allocation module and comparing the outputs for several measures such as yearly patient arrivals, yearly heart arrivals, waiting list size at the end of each year, yearly transplants performed, yearly deaths on the waiting list, and 1- and 5-year post-transplant survivals with those reported by UNOS/SRTR. Also, the Markov chain model used in health status change module is validated by comparing the percentage of patients in each health status in our simulation model with the historical data reported by UNOS. The statistical tests for comparing the outcomes of the simulation model and real data and associated p-values confirm the validity of the simulation model. For details regarding model creation, calibration, and validation see Hasankhani and Khademi (2017). The simulation model is used to compare the performance of the several allocation policies under different measures, which are discussed in Sections 2.6 and B.5. The modules of the simulation model are validated and the results are reported in Hasankhani and Khademi (2017). We provide the results of the validation of the assumptions made throughout the Chapter 2. The health status change module is validated and the results are reported in Table 48. The pre-transplant survival module is responsible for generating patient deaths while waiting on transplantation waiting list, which makes use of a Cox proportional hazard model. Furthermore, patients delisting due to reasons other than death is also considered in the simulation model. The heart allocation module, is a set of user defined rules which finds a patient match for an available donor heart. Finally, patients receiving a donor heart move to the post-transplant phase, and the post-transplant survival module is responsible for generating survival of transplanted patients. Another Cox model is used in the post-transplant survival module to

determine survival times of different types of patients after transplantation. Figure 17 represents the overview of the simulation model, as well as the interaction between different modules. Furthermore, Table 40 illustrates a mapping from the practical aspects of the heart transplantation to simulation and mathematical models. UNOS policy was used as a baseline policy in the simulation model to validate different modules of the simulation model, as well as the whole model. The validation results of all modules and the corresponding statistical tests with their p-values are reported in Hasankhani and Khademi (2017) and we do not duplicate them in this work and refer the interested reader to that study. However, we report the results of the statistical tests for the components that are necessary for the assumptions made in Section B.3 where we present an upper bound in a Markovian setting.

In order to simulate the OPL policy, we create a patient priority list for each donor heart type in each day of simulation according to the descending order of coefficient $\big(\alpha_i^h - k_i(t)\big)q_i^h + y_i^h(t)$ in the presence, and $\big(\alpha_i^h - k_i(t)\big)q_i^h$ in the absence of the fairness constraints. Upon arrival of a donor heart, the simulation model preserves the same geographical (regional sharing) and blood type matching rules but instead of prioritizing patients by their health status, prioritizes based on the priority list corresponding to the available heart type and simulation day. Furthermore, similar to UNOS policy, first-come first-served waiting time priority rule is used within each class of eligible patients. The benchmark policies and the ones derived by considering alternative objectives, explained in Section B.5, are also simulated in a similar fashion.

B.4.1 UNOS Policies

UNOS Policy (2006-2018): UNOS policy prioritizes patients according to their health status (1A>1B>2) while it considers certain blood type matching, and regional sharing rules. Tables 41 and 42 indicate the primary and secondary blood type matching rules, respectively. Also, Table 43 provides the definition of the priority Zones in the UNOS allocation. Furthermore, patients within a same priority class are prioritized based on their waiting time. This policy offers an available heart to patients on the waiting list according to Table 44, which summarizes the UNOS allocation policy for the hearts from adult deceased donors (at least 18 years old). Note that in the simulation model, due to the limited cold ischemia time of heart (4-6 hours), we assume that a donor heart is offered to at most $\mathcal{N} = 4$ patients and is wasted if no match is found. Next, we describe the new 7-tiered

Table 40: Practical Aspects of Allocation in Simulation and Mathematical Modeling

Practical Aspect	**Simulation Model**	**Mathematical Modeling**
Patient Arrival	Patient Arrival Module: Poisson arrivals	$\lambda_i(t)$: Patient type i arrival rate
Heart Arrival	Heart Arrival Module: Poisson Arrivals	$\mu^h(t)$: Heart type h arrival rate
Patients Death	Pre-transplant Survival Module: A Cox proportional hazard model	d_i: Patient type i pre-transplant death rate
Patients Delisting	Patients Delisting Module: Delisting based on fitted historical distributions	Delisting rate is included in the patients' death rate.
Patients Class Change	Patients Class Change Module: A Markov chain based on historical frequency of class changes	ρ_{ij}: Rate at which patients of class i move to j. $\hat{\rho_{ii}} = \sum_j \rho_{ij}$
Heart Acceptance (Wastage)	Allocation Module: Due to limited cold ischemic time for heart, a donor heart is offered to at most four patients and if no match found the heart will be wasted.	q^h: Heart type h acceptance probability. A diagonal matrix. q_i^h : Diagonal element i, denoting heart type h acceptance probability for patient class i
Proximity Constraints	Allocation Module: UNOS proximity zones (DSA, Zones A-E)	Not explicitly modeled.
Blood Type Compatibility	Allocation Module: UNOS primary and secondary ABO matching.	INF: Set of infeasible pairs of patients and hearts. Including primary and secondary ABO matching. $u_i^h(t) = 0, \forall (i,h) \in \text{INF}$
Avoiding Transplant of Inactive Patients	Allocation Module: Does not consider inactive patients in the allocation procedure.	INF: Set of infeasible pairs of patients and hearts. Including inactive patients transplant avoid. $u_i^h(t) = 0, \forall (i,h) \in \text{INF}$

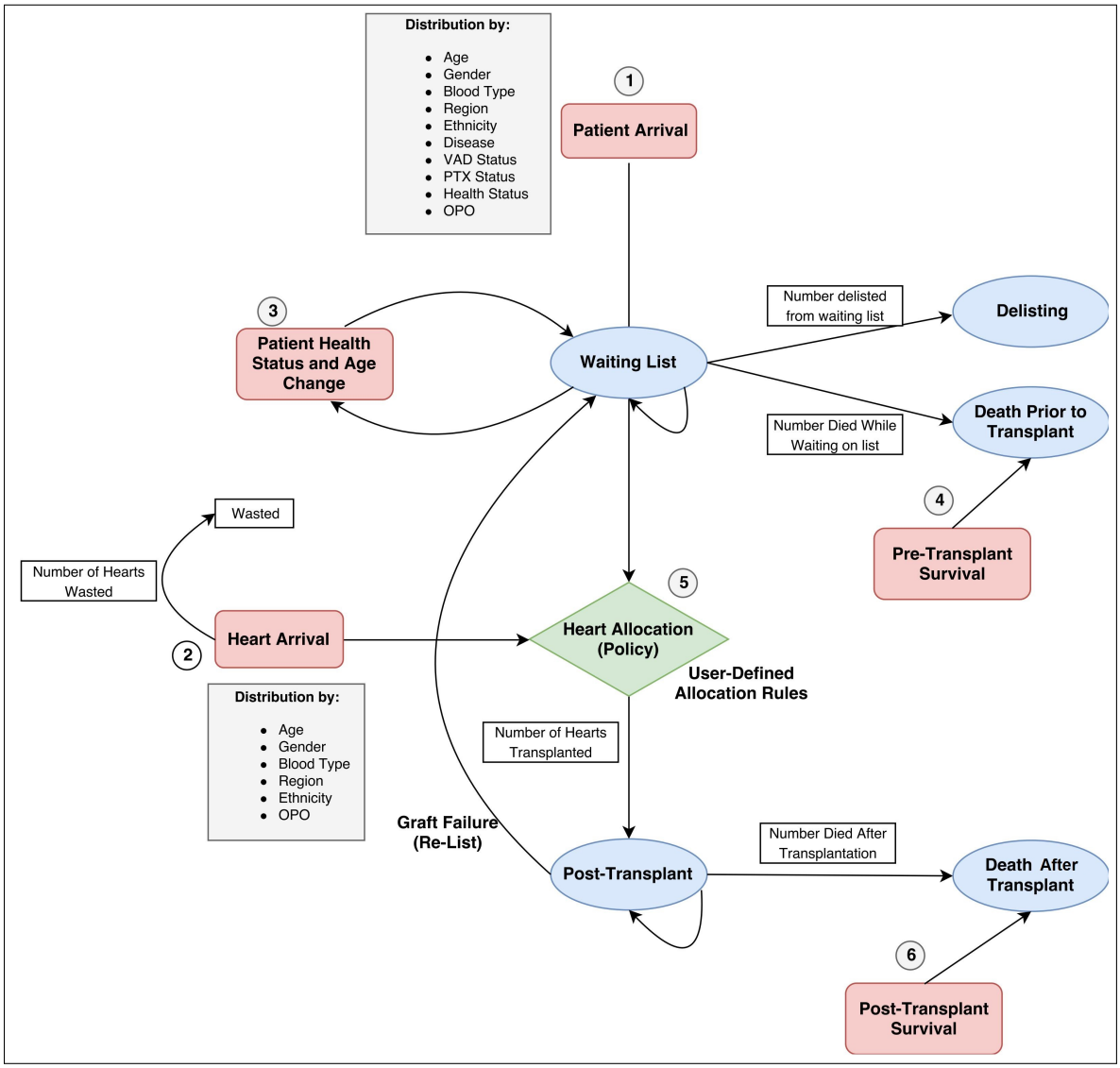

Figure 17: Heart Allocation Simulation Model

policy and its implementation.

Table 41: Primary Blood Type Matching Requirements

Hearts from donors with:	**Are allocated to the candidates with:**
Blood Type O	Blood type O or blood type B
Blood Type A	Blood type A or blood type AB
Blood Type B	Blood type B or blood type AB
Blood Type AB	Blood type AB

Table 42: Secondary Blood Type Matching Requirements

Hearts from donors with:	**Are allocated to the candidates with:**
Blood Type O	Blood type A or blood type AB
Blood Type A	Not applicable
Blood Type B	Not applicable
Blood Type AB	Not applicable

Table 43: Priority Zone Definition

Zone	**Includes transplant hospitals:**
A	Within 500 nautical miles from the donor hospital but outside of the donor's hospital DSA.
B	Within 1000 nautical miles from the donor hospital but outside of the zone A and donor's hospital DSA.
C	Within 1500 nautical miles from the donor hospital but outside of the zone B and donor's hospital DSA.
D	Within 2500 nautical miles from the donor hospital but outside of the zone C and donor's hospital DSA.
E	More than 2500 nautical miles from the donor hospital.

UNOS 7-Tiered Policy: The newly proposed 7-tiered policy, which is in effect since January 2018, categorizes patients into seven health status groups, and broadens the regional sharing of the hearts. The new definition of each health status provided by UNOS is used in the simulation model to categorize the patients on the waiting list. Note that since the simulation model is keeping track of all patient characteristics that UNOS data reports, this categorization is straightforward. Table 45 summarizes a mapping from previous 3-tiered to newly proposed 7-tiered health status classification by UNOS to provide a big picture of the new classification. The UNOS 7-tiered policy considered as

Table 44: Allocation of Hearts from Adult Deceased Donors in the UNOS Policy

Classification	Candidates that are within the:	And are:
1	OPO's DSA	Adult or pediatric status 1A and primary blood type match with the donor
2	OPO's DSA	Adult or pediatric status 1A and secondary blood type match with the donor
3	OPO's DSA	Adult or pediatric status 1B and primary blood type match with the donor
4	OPO's DSA	Adult or pediatric status 1B and secondary blood type match with the donor
5	Zone A	Adult or pediatric status 1A and primary blood type match with the donor
6	Zone A	Adult or pediatric status 1A and secondary blood type match with the donor
7	Zone A	Adult or pediatric status 1B and primary blood type match with the donor
8	Zone A	Adult or pediatric status 1B and secondary blood type match with the donor
9	OPO's DSA	Adult or pediatric status 2 and primary blood type match with the donor
10	OPO's DSA	Adult or pediatric status 2 and secondary blood type match with the donor
11	Zone B	Adult or pediatric status 1A and primary blood type match with the donor
12	Zone B	Adult or pediatric status 1A and secondary blood type match with the donor
13	Zone B	Adult or pediatric status 1B and primary blood type match with the donor
14	Zone B	Adult or pediatric status 1B and secondary blood type match with the donor
15	Zone A	Adult or pediatric status 2 and primary blood type match with the donor
16	Zone A	Adult or pediatric status 2 and secondary blood type match with the donor
17	Zone B	Adult or pediatric status 2 and primary blood type match with the donor
18	Zone B	Adult or pediatric status 2 and secondary blood type match with the donor
19	Zone C	Adult or pediatric status 1A and primary blood type match with the donor
20	Zone C	Adult or pediatric status 1A and secondary blood type match with the donor
21	Zone C	Adult or pediatric status 1B and primary blood type match with the donor
22	Zone C	Adult or pediatric status 1B and secondary blood type match with the donor
23	Zone C	Adult or pediatric status 2 and primary blood type match with the donor
24	Zone C	Adult or pediatric status 2 and secondary blood type match with the donor
25	Zone D	Adult or pediatric status 1A and primary blood type match with the donor
26	Zone D	Adult or pediatric status 1A and secondary blood type match with the donor
27	Zone D	Adult or pediatric status 1B and primary blood type match with the donor
28	Zone D	Adult or pediatric status 1B and secondary blood type match with the donor
29	Zone D	Adult or pediatric status 2 and primary blood type match with the donor
30	Zone D	Adult or pediatric status 2 and secondary blood type match with the donor
31	Zone E	Adult or pediatric status 1A and primary blood type match with the donor
32	Zone E	Adult or pediatric status 1A and secondary blood type match with the donor
33	Zone E	Adult or pediatric status 1B and primary blood type match with the donor
34	Zone E	Adult or pediatric status 1B and secondary blood type match with the donor
35	Zone E	Adult or pediatric status 2 and primary blood type match with the donor
36	Zone E	Adult or pediatric status 2 and secondary blood type match with the donor

Table 45: Mapping from 3-tiered to 7-tiered Health Status Classification

Three-tiered status	Seven-tiered status
1A	1
	2
	3
1B	4
2	5
	6
Inactive	7

a benchmark policy in this study is similar in implementation to the UNOS policy, which makes use of similar blood type matching rules and Zone definitions as in Tables 41, 42, and 43. Furthermore, patients within a same priority class are prioritized according to their waiting time in the"first-in first-served" fashion. However, a donor heart under the 7-tiered policy is offered to a wider area around the DSA of the available heart's OPO compared to the UNOS policy as shown in Table 46, which provides the details of the proposed 7-tiered allocation policy, which is implemented in simulation.

B.4.2 Validation of Assumptions in Section B.3

Assumptions considered to obtain the upper bound in Section B.3 state that the interarrival and interdeparture times in the heart transplantation waiting system are exponentially distributed and stationary. Note that Hasankhani and Khademi (2017) report the results for non-stationary Poisson processes and we refer the reader to that study for the validation results. Such assumptions help us treat the problem in Section B.3 as a Markovian queuing network, and are validated by conducting statistical tests on patient and heart arrivals, as well as death and delisting rates. Furthermore, patient class change due to health improvement/deterioration is modeled by a Markov chain which is also validated by using the real data. In particular, the chi-squared goodness of fit test with a significant level of $\alpha = 0.05$ is used to test the validity of the null hypotheses (whether the patient/heart arrivals and patient death/delisting follow Poisson distributions). Table 47 reports the p-values associated to these statistical tests, where a p-value larger than the considered significance level ($\alpha = 0.05$) suggests that the null hypotheses cannot be rejected. In addition, the Markov chain that is developed to model the health status change of patients on the waiting list is validated by comparing the proportion of patients in each health status produced by the simulation model with the historical data reported by UNOS/SRTR. In particular, we used the Kolmogorov-Smirnov test

Table 46: Allocation of Hearts from Adult Deceased Donors in the UNOS 7-Tiered Policy

Classification	Candidates that are within the:	And are:
1	OPO's DSA+Zone A	Adult Status 1 or pediatric status 1A and primary blood type match with the donor
2	OPO's DSA+Zone A	Adult Status 1 or pediatric status 1A and secondary blood type match with the donor
3	Zone B	Adult Status 1 or pediatric status 1A and primary blood type match with the donor
4	Zone B	Adult Status 1 or pediatric status 1A and secondary blood type match with the donor
5	OPO's DSA+Zone A	Adult Status 2 and primary blood type match with the donor
6	OPO's DSA+Zone A	Adult Status 2 and secondary blood type match with the donor
7	Zone B	Adult Status 2 and primary blood type match with the donor
8	Zone B	Adult Status 2 and secondary blood type match with the donor
9	OPO's DSA	Adult Status 3 or pediatric status 1B and primary blood type match with the donor
10	OPO's DSA	Adult Status 3 or pediatric status 1B and secondary blood type match with the donor
11	OPO's DSA	Adult Status 4 and primary blood type match with the donor
12	OPO's DSA	Adult Status 4 and secondary blood type match with the donor
13	Zone A	Adult Status 3 or pediatric status 1B and primary blood type match with the donor
14	Zone A	Adult Status 3 or pediatric status 1B and secondary blood type match with the donor
15	OPO's DSA	Adult Status 5 and primary blood type match with the donor
16	OPO's DSA	Adult Status 5 and secondary blood type match with the donor
17	Zone B	Adult Status 3 or pediatric status 1B and primary blood type match with the donor
18	Zone B	Adult Status 3 or pediatric status 1B and secondary blood type match with the donor
19	OPO's DSA	Adult Status 6 or pediatric status 2 and primary blood type match with the donor
20	OPO's DSA	Adult Status 6 or pediatric status 2 and secondary blood type match with the donor
21	Zone C	Adult Status 1 or pediatric status 1A and primary blood type match with the donor
22	Zone C	Adult Status 1 or pediatric status 1A and secondary blood type match with the donor
23	Zone C	Adult Status 2 and primary blood type match with the donor
24	Zone C	Adult Status 2 and secondary blood type match with the donor
25	Zone C	Adult Status 3 or pediatric status 1B and primary blood type match with the donor
26	Zone C	Adult Status 3 or pediatric status 1B and secondary blood type match with the donor
27	Zone A	Adult Status 4 and primary blood type match with the donor
28	Zone A	Adult Status 4 and secondary blood type match with the donor
29	Zone A	Adult Status 5 and primary blood type match with the donor
30	Zone A	Adult Status 5 and secondary blood type match with the donor
31	Zone A	Adult Status 6 or pediatric status 2 and primary blood type match with the donor
32	Zone A	Adult Status 6 or pediatric status 2 and secondary blood type match with the donor
33	Zone D	Adult Status 1 or pediatric status 1A and primary blood type match with the donor
34	Zone D	Adult Status 1 or pediatric status 1A and secondary blood type match with the donor
35	Zone D	Adult Status 2 and primary blood type match with the donor
36	Zone D	Adult Status 2 and secondary blood type match with the donor
37	Zone D	Adult Status 3 or pediatric status 1B and primary blood type match with the donor
38	Zone D	Adult Status 3 or pediatric status 1B and secondary blood type match with the donor
39	Zone B	Adult Status 4 and primary blood type match with the donor
40	Zone B	Adult Status 4 and secondary blood type match with the donor
41	Zone B	Adult Status 5 and primary blood type match with the donor
42	Zone B	Adult Status 5 and secondary blood type match with the donor
43	Zone B	Adult Status 6 or pediatric status 2 and primary blood type match with the donor
44	Zone B	Adult Status 6 or pediatric status 2 and secondary blood type match with the donor
45	Zone E	Adult Status 1 or pediatric status 1A and primary blood type match with the donor
46	Zone E	Adult Status 1 or pediatric status 1A and secondary blood type match with the donor
47	Zone E	Adult Status 2 and primary blood type match with the donor
48	Zone E	Adult Status 2 and secondary blood type match with the donor
49	Zone E	Adult Status 3 or pediatric status 1B and primary blood type match with the donor
50	Zone E	Adult Status 3 or pediatric status 1B and secondary blood type match with the donor
51	Zone C	Adult Status 4 and primary blood type match with the donor
52	Zone C	Adult Status 4 and secondary blood type match with the donor
53	Zone C	Adult Status 5 and primary blood type match with the donor
54	Zone C	Adult Status 5 and secondary blood type match with the donor
55	Zone C	Adult Status 6 or pediatric status 2 and primary blood type match with the donor
56	Zone C	Adult Status 6 or pediatric status 2 and secondary blood type match with the donor
57	Zone D	Adult Status 4 and primary blood type match with the donor
58	Zone D	Adult Status 4 and secondary blood type match with the donor
59	Zone D	Adult Status 5 and primary blood type match with the donor
60	Zone D	Adult Status 5 and secondary blood type match with the donor
61	Zone D	Adult Status 6 or pediatric status 2 and primary blood type match with the donor
62	Zone D	Adult Status 6 or pediatric status 2 and secondary blood type match with the donor
63	Zone E	Adult Status 4 and primary blood type match with the donor
64	Zone E	Adult Status 4 and secondary blood type match with the donor
65	Zone E	Adult Status 5 and primary blood type match with the donor
66	Zone E	Adult Status 5 and secondary blood type match with the donor
67	Zone E	Adult Status 6 or pediatric status 2 and primary blood type match with the donor
68	Zone E	Adult Status 6 or pediatric status 2 and secondary blood type match with the donor

Table 47: P-values for the Chi-Squared Goodness of Fit Test

Process	**P-Value**
Patient Arrival	0.058
Heart Arrival	0.051
Patient Death and Delisting	0.051

Table 48: P-values for the Kolmogorov-Smirnov Test

Year	**2006**	**2007**	**2008**	**2009**	**2010**	**2011**	**2012**	**2013**	**2014**
P-value	0.7714	0.2286	1	0.7718	0.7700	1	1	1	1

to check whether the health status distributions produced by the model are statistically identical to the real health status distributions at the end of each calendar year during the period 2006-2014. P-values for such statistical tests are reported in Table 48, which suggest that at a $\alpha = 0.05$ significance level the Markovian assumptions cannot be rejected.

B.5 Benchmark Policies and Alternative Objective Funnctions

This section provides details of the benchmark policies introduced in Section 2.6.1, and analyzes the policy derivation for heart allocation problem with alternative objective functions studied in Section 2.5 of Chapter 2.

B.5.1 Benchmark Policies

UNOS Policy (2006-2018). The UNOS allocation policy prioritizes patients on the waiting list in three different levels, i.e., geographical (proximity to the donor hospital), health status, and waiting time level. In particular, once a heart becomes available in an OPO, the policy first categorizes patients on the waiting list based on their distance from the heart procurement OPO into six zones, each including all transplant centers within some distance of the donor hospital. The policy first offers the procured heart to the patients in the DSA of the same OPO as the heart is (Zone DSA); if no one is matched, the heart will be offered in hierarchy to patients in Zones A, B, C, D, and E. At each zone it prioritizes patients by their health status (1A > 1B > 2) and then primary and secondary blood type match with the donor heart. Within each class, patients are ranked by their waiting time (see B.4.1 for more details).

UNOS 7-Tiered Policy. UNOS has revised the previous 3-tiered health status policy and proposed a new policy which categorizes patients into seven groups based on their health status and considers a broader regional sharing of donor hearts. Specifically, there is a correspondence between the health statuses of the 3-tiered and 7-tiered grouping systems, i.e., roughly speaking, status 1A is divided into three new statuses 1-3; status 1B is new status 4, status 2 is divided into two new statuses 5-6; and inactive status is new status 7. The mechanism of the 7-tiered policy is similar to that of UNOS policy, i.e., there is still three levels of prioritization, geographical, health status, and waiting time. Prioritization based on health status and the regional sharing of donor hearts are changed accordingly but the blood type matching eligibility is preserved under this policy. Eligible patients in the same class are prioritized according to their waiting time (see B.4.1).

Su and Zenios Efficiency (SZE) Policy. Su and Zenios (2006) studied the problem of efficient allocation of donor kidneys, and developed a mathematical programming model to find the optimal kidney allocation in the case of full and hidden information. The problem setup is similar to ours, where there are classes of patients and donor kidneys arriving to the system, and the patients may depart due to transplant or death. However, they do not consider patients' class change, i.e., health improvement/deterioration. Utility for a patient is defined by a combination of pre- and post-transplant quality-adjusted life expectancy and the objective is to maximize the utilitarian efficiency, i.e., the sum of utilities of all patient classes, subject to organ availability and truth-telling constraints. The focus is on post-transplant heterogeneity as the pre-transplant death rates are assumed to be constant across all patient classes. They showed that the optimal policy is an assortative partition policy, whose solution provides a priority list of patients, which depend on the type of available organ. We adopt and apply their method to the heart transplantation case study and simulate it in the case of full patient information. Parameters and data required in this model are estimated from the UNOS/SRTR real data.

Su and Zenios Equity (SZQ) Policy. Su and Zenios (2006) also studied an objective of equity among patient classes by maximizing the minimum utility over patient classes. They showed that the optimal solution of the equity problem is also an assortative partition policy, which provides a patient priority for allocation. We adopt their techniques into heart transplantation and simulate the SZQ policy in the case of full patient information, similar to the SZE policy.

Broadened Regional Sharing (BRS) Policy. The geographic disparity is an important problem in organ allocation and sharing organs can address it; see Ata et al. (2016) and references therein. Hasankhani and Khademi (2017) proposed a policy similar to UNOS that broadens the regional sharing of the donor hearts. Specifically, when a donor heart becomes available, it is first offered to the patients in the DSA of the available heart, and if no one is matched, it is offered to the patients in Zone 1 (union of Zones A, B, and C of UNOS allocation rule), Zone 2 (Zone D in UNOS allocation rule), and Zone 3 (Zone E in UNOS allocation policy) in hierarchy. Note that in each prioritization zone, the same health status, blood type match, and waiting time prioritization rules are considered as UNOS. The rationale for combining the UNOS priority Zones A, B, and C is that the 4- to 6-hour cold ischemic time for heart is equivalent to 1500 airline miles similar to the definition of Zone 1.

UNOS Health Reversed (UNOS-HR) Policy. As mentioned earlier in this section, in terms of health status of the patients, UNOS allocation policy prioritizes sicker patients over healthier ones, i.e., prioritization order in terms of health status of patients is as follows: 1A>1B>2. We consider a simple benchmark policy which is similar to the UNOS policy in terms of geographic and waiting time priorities but reverses the health priority order in which donor hearts are allocated to the patients. In particular, this policy prioritizes healthier patients in the following order: 2>1B>1A.

Heart Allocation Scoring System (HAS) Policy. Designing a heart allocation system is a top priority in heart transplantation and UNOS Heart Subcommittee plans to design such a scoring system similar to kidney and lung. There are two main challenges for such a design: (1) identifying appropriate score components, and (2) estimating the coefficients of each score component in the formula. There is not any available scoring system for heart and, thus, no scoring components are available. Therefore, we design many score components, estimate their coefficients (which is discussed later), and measure the resulting score-based allocation policy via our validated simulation model. Then, we choose the scoring system with the highest performance as the heart allocation scoring system. Note that considering a combination of some common sense score components and optimally estimating their coefficients does not necessarily produce good policies as many of candidates that were tested produced significantly poor policies. Therefore, introducing such a combination of score components is novel and a contribution by itself. In order to address the

second challenge, we use the approximate dynamic programming approach proposed by Bertsimas et al. (2013) to estimate the coefficients of a given set of score components based on real data from heart transplantation. Recall that score components are functions of certain patient/heart characteristics with specific weights corresponding to each patient/heart pair. For a pair of patient i and heart h, we finalize four pre-selected score components including: $f_1(i,h)$ =$\big($1-DPI(h)$\big)\times$ POST(i), $f_2(i,h)$ =DPI(h)$\times$WT(i), $f_3(i,h)$ = |AGE(i)-AGE(h)|, and $f_4(i,h)$ =PRE(i), where DPI(h) denotes the donor profile index of the donor heart taking values in interval $[0,1]$ (higher quality hearts have lower DPI), POST(i) denotes the expected post-transplant survival of a patient type i averaged over heart types, WT(i) denotes the waiting time of a patient type i, Age(i) and Age(h) denote the age of patient type i and age of donor h, and PRE(i) denotes the expected pre-transplant survival of a patient type i. Then, for a pair (i,h) of patient and heart type, the heart allocation score (HAS) function can be written as

$$\begin{aligned}\text{HAS}(i,h) =& w_0 + w_1 \cdot \big(1 - \text{DPI}(h)\big) \cdot \text{POST}(i) + w_2 \cdot \text{DPI}(h) \cdot \text{WT}(i) + \\ & w_3 \cdot |\text{AGE}(i) - \text{AGE}(h)| + w_4 \cdot \text{PRE}(i),\end{aligned}$$

with w_j for $j = 1,2,3,4$ being the weight associated to the j^{th} score component f_j.

After selecting the score components, the score weights are calculated by fitting a regression model on the heart transplantation historical data such that the efficiency of the allocation policy is maximized in the absence and presence of fairness constraints. For the HAS policy, optimal values of score components are estimated as follows: $w_1 = 1.466, w_2 = 1.079, w_3 = 0.006, w_4 = 0.007$ with a regression intercept of $w_0 = 806$. These optimal values are used to simulate the policies. Once the weights are estimated, for a given pair of patient-heart, the HAS is calculated and the patients will be offered with donor hearts based on their score. We calculate the HAS for patient-heart pairs in two cases and simulate the allocation policies in each case, i.e., absence of fairness constraints (HAS policy) and presence of 50+ age fairness constraints (HAS-F policy). This method is flexible to incorporate other fairness constraints. Results of simulating HAS is reported in Table 2 in Chapter 2. Here, we report the results of simulating the HAS-F policy. For the HAS-F policy, the estimated values of the weights are as follow: $w_1 = 1.69, w_2 = 0.031, w_3 = 0.01, w_4 = 0.005$ with a regression intercept of $w_0 = 750$.

Table 49: Each Objective Function Component for HAS-F Policy

	Objective Function (Life-Days $\times 10^6$)			
Policy	**Pre-TX**	**Post-TX**	**Final**	**Total**
HAS-F	7.11	161.13	0.024	168.26

Table 50: Mean and Standard Deviation of Waiting Time for HAS-F Policy

	Waiting Time (Days)	
Policy	**Mean**	**STD**
HAS-F	109	92

B.5.2 Alternative Objective Functions

Section 2.5 analyzes the heart transplantation system with alternative objective functions including (1) minimizing pre-transplant mortality, (2) minimizing total wastage of donor organs, (3) minimizing the mean of waiting times for patient classes, and (4) minimizing the variance of waiting times across patient classes and develops optimal allocation policies under these objectives. This section provides details of deriving optimal policies for (1) and (2). Analysis of (3) is presented here and (4) is analyzed in Zenios (1999).

Minimization of Pre-Transplant Death: We reformulate the optimal control problem (P_1) by replacing its objective function with a function indicating the total mortality on the waiting list during the planning horizon where fairness constraints are present. Note that the analysis in this section is different from that presented in Akan et al. (2012) because we consider fairness constraints in the set of constraints. Therefore, the objective function can be written as

$$\min \int_0^{\mathcal{T}} e.d\ x(t)dt,$$

where d is the pre-transplant death rate matrix. Then, an optimal control problem of the following form has to be solved in order to find the optimal allocation rule:

$$\begin{cases} \min \int_0^{\mathcal{T}} e.d\ x(t)dt \\ \text{subject to } (2.4) - (2.7). \end{cases} \tag{P_2}$$

Problem (P_2) is an optimal control problem with integral constraints on the control variables, which can be transformed to a linear optimal control problem with boundary state constraints. An analogous arguments as in the proof of Theorem 2.1 and writing necessary and sufficient optimality conditions for the linear optimal control problem yields the following LP for each heart type h, whose solution provides the optimal control of the problem (the optimal allocation rule when a heart of type h is available) at time t

$$\begin{cases} \min \left(\hat{k}(t)q^h - \hat{y}^h(t)\right)u^h(t) \\ \text{subject to} \\ e.u^h(t) \leq \mu^h(t), \\ u_i^h(t) = 0, \forall (i,h) \in \text{ INF}, \\ u^h(t) \geq 0, \end{cases}$$

where $\hat{k}(t)$ is the shadow price associated to the state evolution constraints in (2.5), and can be calculated by solving the following linear system of ODEs (in an overloaded system),

$$\dot{\hat{k}}(t) = d + \hat{k}(t)(d + \hat{\rho} - \rho^T),$$

with final condition $\hat{k}(\mathcal{T}) = 0$. Furthermore, $\hat{y}^h(t)$ is the shadow price vector associated to the evolution of auxiliary state variables (introduced to transform the integral constraints into linear ones). The necessary and sufficient optimality condition suggests that $\hat{y}_i^h(t)$ is constant in $[0, \mathcal{T}]$ and this constant value is the ih^{th} element of the vector γA, and γ_k is the shadow price associated to the k^{th} fairness constraint (fairness constraints after transforming integral constraints to linear ones), i.e., $\hat{y}_i^h(t) = \left(\gamma A\right)_{ih} = \sum_{k=1}^K \gamma_k a_{k,ih}$.

As can be seen from the derived LP, given the shadow price vector $\hat{k}(t), \hat{y}^h(t)$, the optimal solution

of problem (P_2) at each time t is a priority index policy with priority coefficient $q_i^h \hat{k}_i(t) - \hat{y}_i^h(t)$, which prioritizes patients with lower coefficients. This provides a patient priority list that can be used to simulate the policy that minimizes pre-transplant mortality. In particular, once we have the priority list, the policy can be simulated in the same fashion as the OPL policy.

Minimization of Heart Wastage: Another objective function considered in this section is to minimize total wastage of donor organs which is equivalent to maximizing total number of transplants during the planning horizon where the fairness constraints are incorporated. The objective function can be written as

$$\max \sum_{h=1}^{H} \int_0^{\mathcal{T}} e \cdot q^h u^h(t) dt,$$

and the optimal control problem associated to this objective is as follows

$$\begin{cases} \max \sum_{h=1}^{H} \int_0^{\mathcal{T}} e \cdot q^h u^h(t) dt \\ \text{subject to } (2.4) - (2.7). \end{cases} \tag{P_3}$$

Note that formulation (P_3) is different from that presented in Akan et al. (2012) for the minimization of heart wastage due to the presence of fairness constraints, thus a distinct analysis. Similar to the proof of Theorem 2.1, transforming the optimal control problem (P_3) with integral constraints (2.7) to a linear problem with boundary state constraints, and following the necessary and sufficient optimality conditions provide the following LP whose solution can be used to find the optimal policy, which is also a priority index type. Hence, when a heart type h is available at time t, the LP

$$\begin{cases} \max \Big(\big(e - \tilde{k}(t)\big) \cdot q^h + \tilde{y}^h(t) \Big) u^h \\ \text{subject to} \\ e.u^h(t) \leq \mu^h(t), \\ u_i^h(t) = 0, \forall (i,h) \in \text{ INF}, \\ u^h(t) \geq 0, \end{cases}$$

is solved and the optimal solution of the problem (P_3) is found, where $\tilde{k}(t)$ is the shadow price vector associated to the state evolution constraints in (2.5), and can be calculated by solving the following linear system of ODEs (in an overloaded system),

$$\dot{\tilde{k}}(t) = \tilde{k}(t)(d + \hat{\rho} - \rho^T),$$

with final condition $\tilde{k}(\mathcal{T}) = 0$, whose solution implies $\tilde{k}(t) = 0$ for $t \in [0, \mathcal{T}]$. In addition, $\tilde{y}^h(t)$ is the shadow price vector associated to the evolution of auxiliary state variables introduced to apply the integral fairness constraints transformation. Similarly, by letting γ be the shadow price vector associated to the transformed fairness constraints, we have $\tilde{y}_i^h(t) = \big(\gamma A\big)_{ih} = \sum_{k=1}^{K} \gamma_k a_{k,ih}$.
Hence, the optimal solution of problem (P_3) at each time t is a priority index policy with priority coefficient $q_i^h + \tilde{y}_i^h(t)$, which prioritizes patients with higher coefficients. In fact, when a heart type h is available, this policy prioritizes patients with higher acceptance probability of the donor heart while it considers the impact of the fairness constraints in prioritizing patients. The priority list is used to simulate the policy that minimizes total wastage of donor hearts, in a similar fashion as the OPL policy is simulated.

Minimization of Mean and STD of Waiting Times: In the rest of this section, we provide details of the MWT and VWT policies. As described in the main text of Chapter 2, in Zenios (1999) the expected waiting time for patient class i is derived to be $W_i = \frac{1}{d_i}\big(1 - \frac{\sum_h \mu^h a_i^h}{\lambda_i}\big)$, where d_i is the pre-transplant death rate for patient class i, λ_i is the arrival rate of patient class i, and a_i^h is the percentage of heart type h allocated to patient class i. By using this expression and letting $a_i = \sum_{h=1}^{H} \mu^h a_i^h$ denote the total allocation rates to a patient in class i, we formulate the following problem that minimizes the average expected waiting time among patient groups in long run

$$\begin{cases} \min_{a_i} & \Big[\frac{1}{I}\sum_{i=1}^{I} \frac{1}{d_i}\big(1 - \frac{a_i}{\lambda_i}\big)\Big] \\ & \text{subject to} \\ & \sum_{i=1}^{I} a_i = \mu, \\ & a_i \geq 0, \forall i = 1, \ldots, I. \end{cases}$$

The problem is a Knapsack problem whose solution is a priority index policy with respect to the coefficient $-\frac{1}{d_i\lambda_i}$ that prioritizes the patients with lower coefficient. Specifically, when a heart is available for transplantation, the policy offers the available heart to the patient classes with lower $-\frac{1}{d_i\lambda_i}$ or equivalently lower $d_i\lambda_i$, which is denoted by MWT.

UNOS considers disparities in the expected time to transplant for different patient groups as a measure of equity in organ allocation: reducing the variability in expected waiting times improves the equity (Organ Procurement and Transplantation Network, 2016b). In fact, during the last decades, UNOS revisited allocation policies to improve equity. For example, after the implementation of the kidney allocation system the variability in the expected time to transplant among patients has been significantly reduced (Organ Procurement and Transplantation Network, 2016b). Reducing the variability in the expected waiting time of different customer types is also proposed in the queuing literature as a measure of equity. For example, Avi-Itzhak and Levy (2004) used an axiomatic approach for a G/D/1 queuing system and showed that the variance of the waiting time can be used as a yardstick for comparing the equity of proposed designs and extended it to more general queuing systems. As mentioned earlier, Zenios (1999) studied the organ transplantation waiting list as a queuing model with reneging, and analyzed the system analytically to find allocation policies considering equity by equalizing the expected waiting time of patient classes. In particular, by letting $\lambda = \sum_{i=1}^{I} \lambda_i$, $\mu = \sum_{h=1}^{H} \mu^h$, $\rho = \frac{\lambda}{\mu}$, and $\bar{d} = \sum_{i=1}^{I} \frac{\lambda_i d_i}{\lambda}$ and assuming that (1) the demand exceeds the supply (i.e., $\lambda > \mu$), (2) the organ arrival rate is much larger than the individual patient death rates (i.e., $\mu >> d_i, i = 1, \ldots, I$), and (3) $\max_i d_i < \frac{\rho\bar{d}}{\rho-1}$, a policy that equalizes the expected waiting time over patient classes (VWT Policy) randomizes patient groups proportional to $\frac{\lambda_i}{\rho}\left(\frac{(1-\rho)d_i+\rho\bar{d}}{\bar{d}}\right)$. Note that assumptions (1), (2), and (3) made in Zenios (1999) hold for heart transplantation set of parameters.

B.6 Fluid Model with Geographical Considerations

The fluid model (P_1) does not consider the location of patients and donor hearts as one of the factors defining patient and heart types. Therefore, the OPL policy is found for each transplantation region separately. However, regional sharing of donor hearts may improve efficiency and fairness by providing more transplant opportunities. In this section, we reformulate the fluid model (P_1) to incorporate locations of patients and hearts into our formulation. The problem setup, vari-

ables, and parameters are the same as the fluid model (P_1) in Section 2.4, except that in order to apply geographical considerations in allocation rules we add OPO as one of the factors defining patient/heart types to represent their location. Thus, the model variables are modified as follows. Let $x_{io}(t)$ be the number of patients in class i listed on the waiting list of OPO o, and $u_{io}^{ho'}(t)$ be the allocation rate of heart type h procured in OPO o' to the patients in class i listed on the waiting list of OPO o. Note that there are 59 OPOs in the U.S. and we let $\mathcal{O} = \{1, \ldots, 59\}$ denote the set of all OPOs. All the parameters $\alpha, \beta, \eta, \lambda, q, d, \hat{\rho}, \rho^T$, and μ are modified accordingly to depend on OPOs. Objective function which is the total QALYs of the patient population and the state evolution constraints, state variable non-negativity constraints, and fairness constraints are also modified to include the patient/heart OPOs. The proximity constraints are included in the set of admissible actions $\Omega(t)$ in the following way: Based on the limited cold ischemic time for heart (4 hours), the air distance corresponding to this time period, and the distances between the 59 OPOs in the U.S. heart transplantation system, we choose 500 miles threshold as allowable distance for regional sharing of donor hearts, i.e., a heart procured in an specific OPO can be shared among patients of the OPOs that are included in a circle with radius 500 miles around the procured OPO. Therefore, the following set of constraints are added to the set of admissible actions $\Omega(t)$:

$$\sum_{i \in \mathcal{I}} \sum_{h \in \mathcal{H}} u_{io}^{ho'} = 0, \text{ for } o \notin \text{CIR}(o'), o' \in \mathcal{O},$$

where for each $o' \in \mathcal{O}$, $\text{CIR}(o')$ is the set of all OPOs within the 500 miles (air distance) from the OPO o' and are found by using the UNOS regional data and Google maps. Then, the reformulated fluid model can be written as follows:

$$V_F(x_0) = \max \int_0^{\mathcal{T}} \big(\sum_{h\in\mathcal{H}} \sum_{o'\in\mathcal{O}} \alpha^{ho'} q^{ho'} u^{ho'}(t) + \sum_{o\in\mathcal{O}} \beta_o x_o(t) \big) dt + \sum_{o\in\mathcal{O}} \eta_o x_o(\mathcal{T}) \qquad (P_o)$$

subject to

$$\dot{x}_o(t) \;=\; \lambda_o(t) - \sum_{h\in\mathcal{H}} \sum_{o'\in\mathcal{O}} q^{ho'} u^{ho'}(t) - (d_o + \hat{\rho}_o - \rho_o^T) x_o(t), \quad x_o(0) = x_o^0, \quad o \in \mathcal{O}$$

$$x_o(t) \geq 0,\ t \geq 0, \quad o \in \mathcal{O}$$

$$\int_0^{\mathcal{T}} \Big(\sum_{i\in\mathcal{F}_k} \sum_{h\in\mathcal{G}_k} \sum_{o'\in\mathcal{O}} u_{io}^{ho'}(t) \Big) dt \geq a_k \int_0^{\mathcal{T}} \Big(\sum_{i\in\mathcal{I}} \sum_{h\in\mathcal{G}_k} \sum_{o'\in\mathcal{O}} u_{io}^{ho'}(t) \Big) dt, \quad k = 1, \ldots, K, \text{ and } o \in \mathcal{O},$$

$$u(t) \in \Omega(t) := \Big\{ u(t) :\ e.u^{ho'}(t) \leq \mu^{ho'}(t);\ u^{ho'}(t) \geq 0,\ \forall h, o' \in \mathcal{O};$$

$$\sum_{o\in\mathcal{O}} \sum_{o'\in\mathcal{O}} u_{io}^{ho'} = 0,\ \forall (i,h) \in \text{ INF};$$

$$\sum_{i\in\mathcal{I}} \sum_{h\in\mathcal{H}} u_{io}^{ho'} = 0,\ \forall o \notin \text{CIR}(o'), o' \in \mathcal{O} \Big\}.$$

where $x_o(t) = \big(x_{1,o}(t), \ldots, x_{I,o}(t)\big)$ is the state variable vector for patients in OPO o, $x_o^0 = \big(x_{1,o}^0, \ldots, x_{I,o}^0\big)$ is the initial population vector in OPO o, and $\lambda_o(t) = \big(\lambda_{1,o}(t), \ldots, \lambda_{I,o}(t)\big)$ is the arrival rate vector of patients in OPO o. Furthermore, $u^{ho'}(t) = \big(u_{io}^{ho'}(t) : i \in \mathcal{I}, o \in \mathcal{O}\big)$ is the allocation rate vector of a heart available in OPO o' with type h and $\mu^{ho'}(t)$ is the heart type h arrival rate in OPO o'.

Note that in the reformulated model, we model the fairness considerations in such a way that they hold for patients in every OPO, e.g., during the planning horizon $[0, \mathcal{T}]$: at least a_k percent of total donor hearts of specific type belonging to set $\mathcal{G}_k$ must be allocated to the patients belonging to the set $\mathcal{F}_k$ in each OPO $o \in \mathcal{O}$. Similar arguments as in proof of Theorem 2.1 characterizes the structure of the optimal solution of problem (P_o) and shows that the solution is a priority index policy with respect to coefficients depending on the shadow prices of the fairness constraints. We call this policy OPL-RS and simulate this policy along with other benchmarks via the validated simulation model. The results are reported in Table 2.2 of Chapter 2 where the simulation performance of different allocation policies are reported.

Also, note that for computational purposes we assume pre-transplant death rate (d) and life quality coefficients (β) and (η) be the same across all OPOs. Furthermore, we used the same acceptance probability matrix (q^h) and class change matrices ($\hat{\rho}$ and ρ) for different OPOs. The reason is that

these quantities are independent of the proximity considerations. However, for the post-transplant life expectancy coefficients ($\alpha^{h,o'}$), we adjusted the life expectancies as when a donor heart in an OPO allocated to a patient in another OPO with higher distance, its quality is affected and most likely is going to be deteriorated compared to the case where it is allocated to a patient in the same OPO (this reduction in life expectancy is reflected in the organ failure Cox model presented for heart in the SRTR risk adjustment models): see Colvin et al. (2017). Nonetheless, the formulation (P_o) is flexible enough to incorporate any dependency of parameters to OPO location upon availability of data.

B.7 Fairness Analysis of OPL

Section 2.6.4 in Chapter 2 studies the OPL policy in the presence of several age, health, and combination of age-health constraints. Table 51 below shows the details of the constraints that imposed in each grouping, where for each one, K denotes the number of fairness constraints imposed, and for each $k = 1, \cdots, K$, $\mathcal{G}_k$ denotes the set of heart types under consideration in constraint k (i.e., $\mathcal{H}$ is the set of all heart types), $\mathcal{F}_k$ the set of patient classes under consideration in fairness constraint k (e.g., $\{I \in \mathcal{I} : \text{HS}(i) = 1A\}$ is the set of patient classes whose health status is 1A and $\{I \in \mathcal{I} : \text{age}(i) \geq 35\}$ is the set of patient classes older than 35 years), and a_k the lower bound associated to constraint k. Recall that Theorem 2.1 provides the optimal solution of problem (P_1) in the presence of each set of constraints, which is a priority index policy. We analyze OPL in the presence of fairness constraints via simulation and compare their improvement over UNOS with the OPL policy in the absence of fairness constraints. Numerical results are reported in Section 2.6.4.

Age Fairness Constraints. This set of constraints consists of one or more constraints ensuring the percentage of total hearts allocated to patients in a specific range of age group during the planning horizon is at least that under the UNOS policy. Such constraints can be seen as fairness constraints assuring that the OPL policy is as fair as the UNOS policy in allocating donated hearts in terms of age. We consider five age groupings including (i) [35+], (ii) [50+], (iii) [65+], (iv) [50-65] and [65+], and (v) [35-50] and [50-65] and [65+]. For example, for [50+], UNOS allocates 65% of the total donated hearts to the patients older than 50 years (Figure 18b). Hence, a constraint of

Table 51: Details for Fairness Constraints

Fairness constraints	**Heart Types Involved ($\mathcal{G}_k$)**	**Patient Classes Involved ($\mathcal{F}_k$)**	**Lower Bound (a_k)**	**Number of Constraints (K)**
Age [35+]	All heart types ($\mathcal{H}$)	$\{I \in \mathcal{I} : \text{age}(i) \geq 35\}$	0.88	K=1
Age [50+]	All heart types ($\mathcal{H}$)	$\{I \in \mathcal{I} : \text{age}(i) \geq 50\}$	0.65	K=1
Age [65+]	All heart types ($\mathcal{H}$)	$\{I \in \mathcal{I} : \text{age}(i) \geq 65\}$	0.13	K= 1
Health [1A]	All heart types ($\mathcal{H}$)	$\{I \in \mathcal{I} : \text{HS}(i) = 1A\}$	0.49	K=1
Health [1B]	All heart types ($\mathcal{H}$)	$\{I \in \mathcal{I} : \text{HS}(i) = 1B\}$	0.47	K= 1
Health [2]	All heart types ($\mathcal{H}$)	$\{I \in \mathcal{I} : \text{HS}(i) = 2\}$	0.04	K= 1
Age [50-65]	All heart types ($\mathcal{H}$)	$\{I \in \mathcal{I} : 50 \leq \text{age}(i) \leq 65\}$	0.52	K=2
Age [65+]	All heart types ($\mathcal{H}$)	$\{I \in \mathcal{I} : \text{age}(i) \geq 65\}$	0.13	
Age [35-50]	All heart types ($\mathcal{H}$)	$\{I \in \mathcal{I} : 35 \leq \text{age}(i) \leq 50\}$	0.23	K=3
Age [50-65]	All heart types ($\mathcal{H}$)	$\{I \in \mathcal{I} : 50 \leq \text{age}(i) \leq 65\}$	0.52	
Age [65+]	All heart types ($\mathcal{H}$)	$\{I \in \mathcal{I} : \text{age}(i) \geq 65\}$	0.13	
Health [1A]	All heart types ($\mathcal{H}$)	$\{I \in \mathcal{I} : \text{HS}(i) = 1A\}$	0.49	K=2
Health [1B]	All heart types ($\mathcal{H}$)	$\{I \in \mathcal{I} : \text{HS}(i) = 1B\}$	0.47	
Health [1A]	All heart types ($\mathcal{H}$)	$\{I \in \mathcal{I} : \text{HS}(i) = 1A\}$	0.49	K=2
Age [65+]	All heart types ($\mathcal{H}$)	$\{I \in \mathcal{I} : \text{age}(i) \geq 65\}$	0.13	
Health [1A]	All heart types ($\mathcal{H}$)	$\{I \in \mathcal{I} : \text{HS}(i) = 1A\}$	0.49	K=3
Health [1B]	All heart types ($\mathcal{H}$)	$\{I \in \mathcal{I} : \text{HS}(i) = 1B\}$	0.47	
Age [65+]	All heart types ($\mathcal{H}$)	$\{I \in \mathcal{I} : \text{age}(i) \geq 65\}$	0.13	

type

$$\int_0^{\mathcal{T}} \Big(\sum_{\{i:\text{age}(i)\geq 50\}} \sum_h u_i^h(t) \Big) dt \geq 0.65 \int_0^{\mathcal{T}} \Big(\sum_i \sum_h u_i^h(t) \Big) dt$$

is considered as a fairness constraint in problem (P_1), where $\{i : \text{age}(i) \geq 50\}$ denotes the set of patient indices whose age are greater than 50 years, ensuring an allocation of at least 65% of donor hearts to such patients. Similar constraints are added and analyzed for each group separately.

Health Fairness Constraints. Fairness constraints on health are also imposed in the optimal control problem (P_1), ensuring that the OPL policy allocates at least the same percentage of hearts as the UNOS policy does to patients with certain health statuses. In particular, we consider four health status groupings, i.e., (i) [1A], (ii) [1B], (iii) [2], and (iv) [1A] and [1B]. We analyze the optimal solution of problem (P_1) under each group of fairness constraints separately. For example, by Figure 18b, UNOS allocates 49% of total hearts to 1A patients, thus the following health fairness constraint

$$\int_0^{\mathcal{T}} \Big(\sum_{\{i:\text{Health}(i)=1A\}} \sum_h u_i^h(t) \Big) dt \geq 0.49 \int_0^{\mathcal{T}} \Big(\sum_i \sum_h u_i^h(t) \Big) dt$$

is imposed, where $\{i : \text{health}(i) = 1A\}$ denotes the set of patient indices with health status 1A. Similar constraints are considered for other health groupings.

Age-Health Fairness Constraints. We also analyze two combinations of age-health fairness groups, i.e., (i) [65+] and [1A], and (ii) [50-65] and [65+] and [1A]. For example, the latter involves three fairness constraints in the optimal control problem (P_1), i.e., two constraints on age and one on health. By Figure 18b, UNOS allocates 52% of total hearts to patients in age group [50-65], 13% to patients in [65+] age group, and 49% to patients with health status 1A. Hence, the imposed

fairness constraints are as follows:

$$\int_0^{\mathcal{T}} \Big(\sum_{\{i:50\leq \text{age}(i)\leq 65\}} \sum_h u_i^h(t) \Big) dt \geq 0.52 \int_0^{\mathcal{T}} \Big(\sum_i \sum_h u_i^h(t) \Big) dt$$
$$\int_0^{\mathcal{T}} \Big(\sum_{\{i:\text{age}(i)\geq 65\}} \sum_h u_i^h(t) \Big) dt \geq 0.13 \int_0^{\mathcal{T}} \Big(\sum_i \sum_h u_i^h(t) \Big) dt$$
$$\int_0^{\mathcal{T}} \Big(\sum_{\{i:\text{Health}(i)=1A\}} \sum_h u_i^h(t) \Big) dt \geq 0.49 \int_0^{\mathcal{T}} \Big(\sum_i \sum_h u_i^h(t) \Big) dt,$$

B.8 Further Analysis of OPL Policy

This section provides the priority coefficients of the OPL policy (in the absence and presence of different fairness constraints) in color coded tables for the allocation of each heart type h, which helps us understand how the policy performs in terms of prioritization based on age and health status of patients.

In the Absence of Fairness Constraints. Table 2.3 in Section 2.6.3 illustrates the OPL policy priority coefficients which are averaged over heart type, time, and patients characteristics except for age and health status. This section provides similar tables for each of sixteen heart types for OPL policy (heart type 16 is excluded due to insufficiency of data). In particular, the numbers in Tables 53-67 are for the case where fairness constraints are absent and numbers are average of quantities $\big(\alpha_i^h - k_i(t)\big)q_i^h$ over time, and over the other characteristics of patients (except for age and health status). Table 52 shows the mapping between heart types considered in this study and the age and blood type of the donor heart. Note that for infeasible pairs of patients and hearts in allocation we put NA as coefficient in the tables.

In the Presence of Fairness Constraints. In order to understand the patient prioritization in the presence of fairness constraints, we conduct an analysis similar to that in Section 2.6.3 of Chapter 2 and present color-coded tables for the OPL policy patient prioritization coefficients in the presence of each age, health, and combination of age-health fairness constraints. In particular, Tables 68-78 provide the average over time, heart type, and other patient characteristics of the priority coefficient of OPL policy in the presence of several fairness constraints. Comparing the priority coefficients in Table 2.3 with those in Tables 68-78 reveals that: (1) the [35+] fairness grouping containing a single constraint on the patients older than 35 years shifts the allocation priority from the youngest

Table 52: Mapping between Heart Types and Age and Blood type of Donor Hearts

Heart Type	**Age Group**	**Blood Type**
1	[18-35]	O
2	[18-35]	A
3	[18-35]	B
4	[18-35]	AB
5	[35-50]	O
6	[35-50]	A
7	[35-50]	B
8	[35-50]	AB
9	[50-65]	O
10	[50-65]	A
11	[50-65]	B
12	[50-65]	AB
13	[65+]	O
14	[65+]	A
15	[65+]	B
16	[65+]	AB

Table 53: Color-Coded Graph for OPL Policy without Fairness Constraints (Heart type 1)

Health GroupAge Group	[18-35]	[35-50]	[50-65]	[65+]
1A	9451.75	6830.38	3858.69	2452.14
1B	10330.62	7316.52	4137.73	2060.95
2	9987.37	5842.15	5514.90	6403.52

Table 54: Color-Coded Graph for OPL Policy without Fairness Constraints (Heart type 2)

Health GroupAge Group	[18-35]	[35-50]	[50-65]	[65+]
1A	9159.13	6528.95	3713.90	2141.06
1B	9910.72	7352.75	4151.35	2851.39
2	9809.52	8770.95	4414.51	2409.12

Table 55: Color-Coded Graph for OPL Policy without Fairness Constraints (Heart type 3)

Health GroupAge Group	[18-35]	[35-50]	[50-65]	[65+]
1A	9942.47	6562.14	3473.14	1909.45
1B	9828.78	6776.78	4193.68	2065.05
2	10103.98	8866.96	3325.18	1720.39

Table 56: Color-Coded Graph for OPL Policy without Fairness Constraints (Heart type 4)

Health GroupAge Group	[18-35]	[35-50]	[50-65]	[65+]
1A	8669.89	6201.93	4486.51	1577.37
1B	9223.56	6924.85	4255.33	3020.79
2	9633.63	6948.99	4111.03	2292.62

Table 57: Color-Coded Graph for OPL Policy without Fairness Constraints (Heart type 5)

Health GroupAge Group	[18-35]	[35-50]	[50-65]	[65+]
1A	9449.36	6811.87	2988.58	863.33
1B	8750.33	6700.207	3577.13	1374.24
2	10469.72	8157.46	5040.80	5411.05

Table 58: Color-Coded Graph for OPL Policy without Fairness Constraints (Heart type 6)

Health GroupAge Group	[18-35]	[35-50]	[50-65]	[65+]
1A	9400.38	6145.19	3470.40	1197.09
1B	10126.54	7087.75	3391.25	1704.89
2	10285.47	6432.37	5896.87	2205.885

Table 59: Color-Coded Graph for OPL Policy without Fairness Constraints (Heart type 7)

Health GroupAge Group	[18-35]	[35-50]	[50-65]	[65+]
1A	8325.94	6162.03	3310.36	1353.77
1B	9883.22	6340.02	3442.12	977.46
2	11074.06	5850.47	3456.26	1324.29

Table 60: Color-Coded Graph for OPL Policy without Fairness Constraints (Heart type 8)

Health GroupAge Group	[18-35]	[35-50]	[50-65]	[65+]
1A	6850.35	6640.65	2536.18	1087.57
1B	9693.64	6958.98	3657.99	2879.19
2	9920.64	5986.23	2937.81	3469.26

Table 61: Color-Coded Graph for OPL Policy without Fairness Constraints (Heart type 9)

Health GroupAge Group	[18-35]	[35-50]	[50-65]	[65+]
1A	9120.64	5880.84	2900.51	1735.72
1B	10213.11	6040.29	4225.98	1882.94
2	10633.56	7468.03	2472.72	2149.85

Table 62: Color-Coded Graph for OPL Policy without Fairness Constraints (Heart type 10)

Health GroupAge Group	[18-35]	[35-50]	[50-65]	[65+]
1A	9111.76	6318.25	2834.75	585.62
1B	9814.92	7602.79	4059.18	2003.57
2	11400.31	5122.83	2670.71	2354.74

Table 63: Color-Coded Graph for OPL Policy without Fairness Constraints (Heart type 11)

Health GroupAge Group	[18-35]	[35-50]	[50-65]	[65+]
1A	9354.25	5967.19	3006.06	733.24
1B	8681.42	5745.42	3530.73	1408.26
2	10433.26	5484.21	2767.69	2683.11

Table 64: Color-Coded Graph for OPL Policy without Fairness Constraints (Heart type 12)

Health GroupAge Group	[18-35]	[35-50]	[50-65]	[65+]
1A	13036.77	4317.99	2148.74	NA
1B	10786.75	5671.73	3680.07	2042.61
2	9709.12	8953.25	2129.88	1890.90

Table 65: Color-Coded Graph for OPL Policy without Fairness Constraints (Heart type 13)

Health GroupAge Group	[18-35]	[35-50]	[50-65]	[65+]
1A	9788.129	6092.61	3153.92	2387.92
1B	NA	7484.04	6548.36	1437.16
2	NA	1790.06	5520.97	NA

Table 66: Color-Coded Graph for OPL Policy without Fairness Constraints (Heart type 14)

Health GroupAge Group	[18-35]	[35-50]	[50-65]	[65+]
1A	NA	NA	4013.75	NA
1B	8313.78	6157.08	5237.22	NA
2	NA	NA	5369.02	12604.04

Table 67: Color-Coded Graph for OPL Policy without Fairness Constraints (Heart type 15)

Health GroupAge Group	[18-35]	[35-50]	[50-65]	[65+]
1A	NA	NA	NA	NA
1B	10001.36	NA	4900.78	1084.407
2	NA	NA	NA	NA

patient group (age group [18-35]) to the ones older than 35 years, (2) the [50+] fairness grouping containing a single constraint on the patients older than 50 years shifts the allocation priority from the younger patient groups (age groups [18-35] and [35-50]) to the ones older than 50 years, (3) the [65+] fairness grouping containing a single constraint on the patients older than 65 years shifts the allocation priority from the patients younger than 65 years to the ones in age group [65+] (note that although the priority order in the color-coded tables does not change in this case, the priority coefficients for patients older than 65 years increases while it decreases for the younger ones), (4) the [50-65] and [65+] fairness grouping containing two constraints one on the patients in age group [50-65] and one on the patients older than 65 years, shifts the allocation priority towards these patients (as can be seen from Tables 69 and 71, the priority order in this grouping is similar to that in [50+] but the former has higher priority coefficients for patients older than 65 years because it considers two separate constraints on patients in age groups [50-65] and [65+] while the [50+] grouping combines the two older age groups which emphasizes on prioritizing [50-65] patients more than the [65+] ones since they have a better post-transplant outcomes), (5) the [35-50] and [50-65] and [65+] fairness grouping containing three constraints one on the patients in age group [35-50], one on the patients in age group [50-65], and one on the patients older than 65 years, shifts the allocation priority towards these patients compared to the absence of fairness constraints, i.e., Table 2.3. As can be seen from Tables 68 and 72, the priority order in this grouping is similar to that in [35+].

Table 68: Color-Coded Graph for OPL Policy with Age Fairness Constraints ([35+])

Health GroupAge Group	[18-35]	[35-50]	[50-65]	[65+]
1A	4311.10	6877.52	3966.54	1836.84
1B	4635.35	7413.94	4887.55	2602.07
2	5240.97	7278.59	4661.74	3970.79

Table 69: Color-Coded Graph for OPL Policy with Age Fairness Constraints ([50+])

Health GroupAge Group	[18-35]	[35-50]	[50-65]	[65+]
1A	6876.80	3707.52	4614.56	2484.87
1B	7201.05	4243.94	5535.57	3250.09
2	7806.67	4108.59	5309.76	4618.82

Table 70: Color-Coded Graph for OPL Policy with Age Fairness Constraints ([65+])

Health GroupAge Group	[18-35]	[35-50]	[50-65]	[65+]
1A	9139.80	5970.51	3059.53	2612.32
1B	9464.05	6506.93	3980.54	3377.55
2	10069.66	6371.58	3754.73	4746.27

Furthermore, comparing the coefficients in Tables 71 and 72 illustrates an increase in coefficients for age groups [35-50] and a decrease in coefficients for age group [65+] in this grouping, (6) the [1A] fairness grouping containing a single constraint on the patients with health status 1A, increases the priority coefficient for 1A patients and consequently decreases the coefficients for 1B and 2 patients shifting the priority from healthier patients (with health status 1B and mostly 2) towards sicker patients (1A patients) compared to the case where no fairness constraint is present in the model, (7) the [1B] fairness grouping containing a single constraint on the patients with health status 1B, increases the priority coefficient for 1B patients and decreases the coefficients for 1A and 2 patients shifting the priority from healthier and sicker patients, with health status 2 and 1A respectively, towards patients with medium health status (1B patients) compared to the case where fairness constraints are not present in the model, (8) the [2] fairness grouping containing a single constraint on the patients with health status 2, does not change the priority coefficient of patients since in the optimal control problem (P_1), such a constraint is redundant and its corresponding shadow price is zero, which suggests that the fairness grouping [2] has no impact on the optimal allocation policy (the reason is that the OPL policy in the absence of fairness constraints is fairer than UNOS in allocating hearts to healthier patients with health status 2), (9) the [1A] and [1B] fairness grouping containing two constraints, one on the patients with health status 1A and one on the 1B patients, increases the priority coefficients for these patients compared to the case where fairness constraints

Table 71: Color-Coded Graph for OPL Policy with Age Fairness Constraints ([50-65] and [65+])

Health GroupAge Group	[18-35]	[35-50]	[50-65]	[65+]
1A	6949.29	3780.00	4454.08	2931.64
1B	7273.54	4316.43	5375.09	3696.86
2	7879.16	4181.07	5149.28	5065.59

Table 72: Color-Coded Graph for OPL Policy with Age Fairness Constraints ([35-50] and [50-65] and [65+])

Health GroupAge Group	[18-35]	[35-50]	[50-65]	[65+]
1A	4098.32	7071.02	4711.46	-1288.7
1B	4422.57	7607.45	5632.47	-523.57
2	5028.19	7472.09	5406.66	845.16

Table 73: Color-Coded Graph for OPL Policy with Health Fairness Constraints ([1A])

Health GroupAge Group	[18-35]	[35-50]	[50-65]	[65+]
1A	10698.5	7529.2	4618.2	2488.6
1B	8395.3	5438.2	2911.8	626.3
2	9000.9	5302.9	2686.0	1995.1

Table 74: Color-Coded Graph for OPL Policy with Health Fairness Constraints ([1B])

Health GroupAge Group	[18-35]	[35-50]	[50-65]	[65+]
1A	9091.61	5922.32	3011.34	881.64
1B	9983.76	7026.65	4500.25	2214.77
2	10021.47	6323.39	3706.54	3015.59

Table 75: Color-Coded Graph for OPL Policy with Health Fairness Constraints ([2])

Health GroupAge Group	[18-35]	[35-50]	[50-65]	[65+]
1A	9358.52	6189.24	3278.25	1148.56
1B	9682.77	6725.66	4199.26	1913.78
2	10288.39	6590.31	3973.45	3282.51

Table 76: Color-Coded Graph for OPL Policy with Health Fairness Constraints ([1A] and [1B])

Health GroupAge Group	[18-35]	[35-50]	[50-65]	[65+]
1A	11772.47	8603.18	5692.20	3562.50
1B	8039.91	5082.80	2556.41	270.93
2	21.13	-3676.9	-6293.8	-6984.7

Table 77: Color-Coded Graph for OPL Policy with Age-Health Combination of Fairness Constraints ([65+] and [1A])

Health GroupAge Group	[18-35]	[35-50]	[50-65]	[65+]
1A	10140.07	6970.78	4059.80	4813.58
1B	8196.87	5239.75	2713.36	3311.35
2	8802.49	5104.40	2487.55	4680.08

Table 78: Color-Coded Graph for OPL Policy with Age-Health Combination of Fairness Constraints ([50-65] and [65+] and [1A])

Health GroupAge Group	[18-35]	[35-50]	[50-65]	[65+]
1A	7881.10	4711.81	5368.04	4253.28
1B	6297.10	3339.99	4380.81	3110.26
2	6902.72	3204.64	4155.00	4478.99

are absent (note that the priority coefficients for health status 2 patients significantly reduces in this grouping as the optimal policy puts its priority on 1A and 1B patients together), (10) the [65+] and [1A] fairness grouping containing one age constraint on the patients older than 65 years and one health constraint on the 1A patients, increases the priority coefficients for these patients compared to the case where fairness constraints are absent (comparing the coefficients reveals that in Table 77 priority coefficients are higher for 1A patients (and all the age groups in 1A row) and those older than 65 years while coefficients for 1B and 2 patients in the column of [65+] age group decreases compared to 70 since the [1A] fairness constraint has more impact on the optimal solution of the problem (P_1) than the [65+] constraint), (11) the [50-65] and [65+] and [1A] fairness grouping containing two age constraints and one health constraint, increases the priority coefficients for these patients compared to the case where fairness constraints are absent (comparing the coefficients reveals that in Table 78 priority coefficients are higher for patients in age group [50-65] compared to 70). Furthermore, by Table 2.8 the OPL policy in the presence of this threshold performs similar to the UNOS policy as these constraints restrict percentage allocation of hearts to age groups [50-65], [65+] and health group [1A] to be at least as low as UNOS (recall that we showed earlier that the improvement of OPL over UNOS is due to prioritizing healthier and younger patients in OPL policy and by imposing such constraints improvement vanishes, which results in a policy similar to UNOS).

Furthermore, as discussed in Section 2.6.3, the OPL policy is further analyzed via the simulation model to provide insights about its prioritization criteria in practice. In fact, we compare the percentage of hearts allocated to different patient classes in simulating OPL and UNOS and the results are summarized in Figure 18. Our results show that the OPL policy is significantly different

than UNOS policy in prioritizing patients on the waiting list. In particular, the results indicate that the OPL policy allocates more donor hearts to healthier patients (with health status 2) and less to the sickest patients (with health status 1A) compared to the UNOS policy. While the UNOS policy tends to allocate 49% of the total available hearts to patients with health status 1A, the proposed OPL policy prefers to assign only 18% to this health group and allocates 45% of the donated hearts to patients with health status 2, compared to 4% for the UNOS policy. Also, the percentage of hearts assigned to younger age groups (age groups [18-35] and [35,50]) is greater for the OPL policy than the UNOS allocation. In fact, the UNOS policy assigns 65% of donor hearts to patients older than 50 years old, where the OPL policy assigns 51% to such patients. However, as shown in Figure 18c, the percentage of transplants performed on the patients with different VAD statuses is not significantly different for the two policies. This observation holds true because the post-transplant survival for patients with VAD is similar to those without VAD (Colvin-Adams et al., 2015). Also, the proportion of donor hearts transplanted in each of the allocation zones (i.e., DSA, Zone A, B, C, D, and E) are reported for the two policies in Figure 18d. In the simulation of the UNOS policy around 77% of all transplants are performed in the DSA of the donor heart and 23% in the proximity Zones A-E, whereas, the OPL policy assigns 96% of the hearts in the DSA of the available hearts and only 4% of the transplants are done in Zones A-E. These numbers indicate that finding a match for an available heart within closer distances of the procured OPO is easier in the OPL policy than that of UNOS practice. Note that the OPL policy does not directly take proximity zones into account but changing patient prioritization can indirectly change the proportion of organs assigned to each zone. In this case, because the OPL policy prioritizes healthier patients and the proportion of healthier patients is higher on the waiting list (Stevenson, 2015), there is more opportunity to assign patients in the DSA of the donor heart. Note that in B.6 the regional aspect of allocation is taken into account and the OPL policy is analyzed in the presence of certain geographical considerations in the fluid model.

Finally, as mentioned earlier in Chapter 2, we conduct similar analysis on OPL-F policy (the OPL policy with fairness constraints over age group [65+] and health group 1A) as we did on OPL in Section 2.6.3. Specifically, Tables 79 and 80 report the difference between the performance of OPL-F and UNOS policies in terms of LYs gain and number of death increments broken down to patient's health and age groups. Results indicate that OPL-F policy performs similar to the UNOS policy

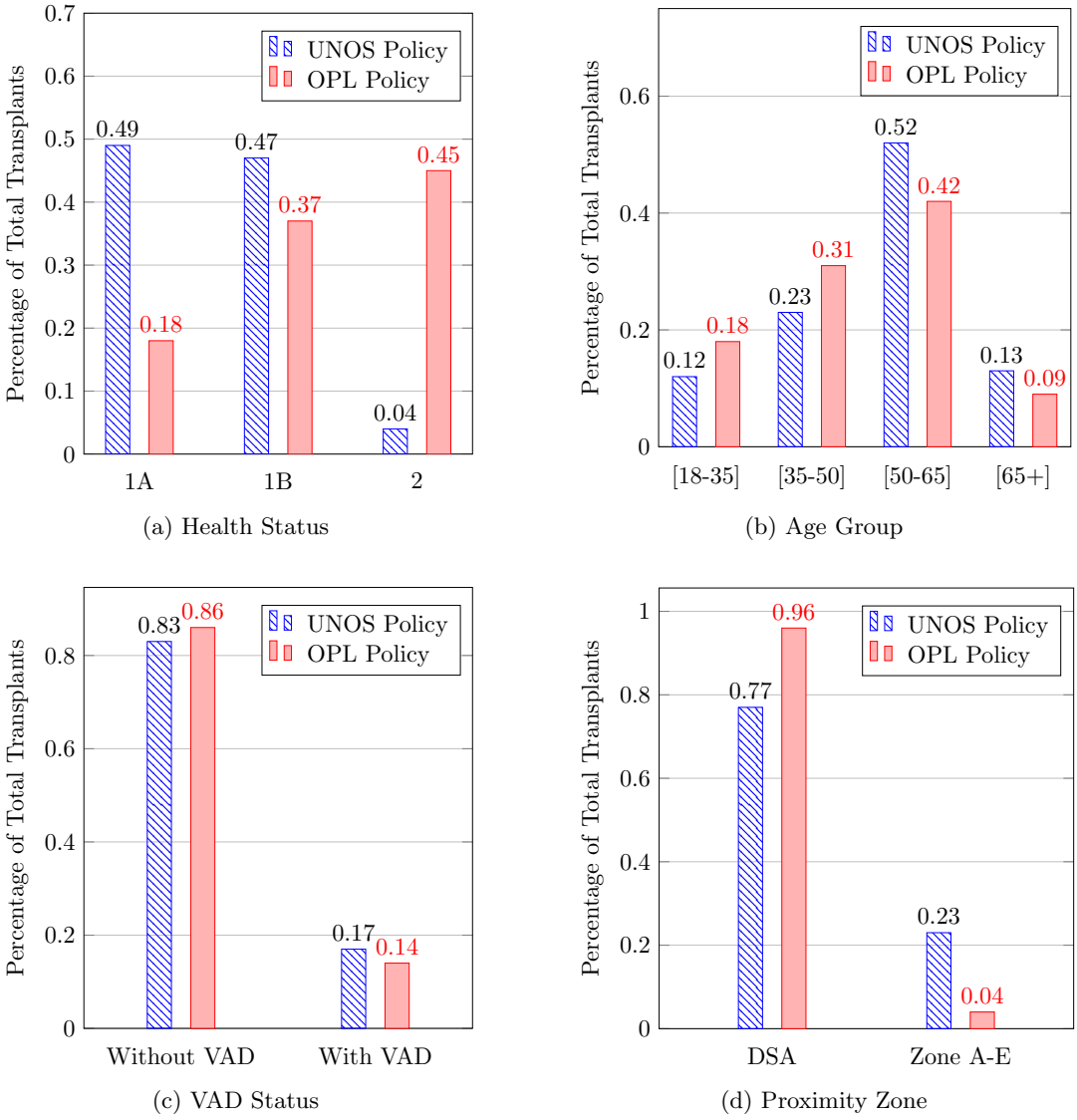

Figure 18: Health, Age, VAD, and Zone Priorities for UNOS and OPL

Table 79: LYs/Death Trade-off for Patient Health Groups (OPL-F minus UNOS

Health Group	1A	1B	2	Inactive	Total
Death	7	34	-38	52	55
Total Life-Days ($\times 10^7$)	-0.043	0.013	0.044	-0.0009	0.141

Table 80: LYs/Death Trade-off for Patient Age Groups (OPL-F minus UNOS)

Age Group	[18-35]	[35-50]	[50-65]	[65+]	Total
Death	-5	-17	79	-2	55
Total Life-Days ($\times 10^7$)	0.009	0.133	-0.005	0.003	0.141

in terms of both pre-transplant deaths and total LYs. In addition, similar analysis is conducted for comparing OPL with the newly proposed UNOS 7-tiered policy and the results are reported in Tables 81 and 82. Note that since UNOS 7-tiered policy considers new 7-tiered health classes, we simulate the 7-tiered policy but in order to have a meaningful comparison between OPL and UNOS 7-tiered, in breaking down the reported LYs and death differences into each patient health group, we report them for a three-tiered system. Results of comparing UNOS 7-Tiered with OPL is very similar to that of UNOS as the 7-tiered policy produces 625 more pre-transplant deaths but gains 1.49×10^7 more total life days compared to OPL. This analysis together with the analysis presented in Section 2.6.3 provide decision makers with a tool to quantify the cost that policy makers have to trade off in order to gain an increase in total LYs by switching to a policy based on the utilitarian approach.

Table 81: LYs/Death Trade-off for Patient Health Groups (OPL minus UNOS-7-tiered)

Health Group	1A	1B	2	Inactive	Total
Death	221	30	-116	490	625
Total Life-Days ($\times 10^7$)	-4.82	1.63	4.7	-0.015	1.49

Table 82: LYs/Death Trade-off for Patient Age Groups (OPL minus UNOS-7-tiered)

Age Group	[18-35]	[35-50]	[50-65]	[65+]	Total
Death	-52	-286	510	453	625
Total Life-Days ($\times 10^7$)	1.08	0.62	-0.13	-0.075	1.49

Bibliography

Jae-Hyeon Ahn and John C Hornberger. Involving patients in the cadaveric kidney transplant allocation process: A decision-theoretic perspective. *Management Science*, 42(5):629–641, 1996.

Mustafa Akan, Oguzhan Alagoz, Baris Ata, Fatih Safa Erenay, and Adnan Said. A broader view of designing the liver allocation system. *Operations Research*, 60(4):757–770, 2012.

Oguzhan Alagoz, Lisa M Maillart, Andrew J Schaefer, and Mark S Roberts. The optimal timing of living-donor liver transplantation. *Management Science*, 50(10):1420–1430, 2004.

Oguzhan Alagoz, Lisa M Maillart, Andrew J Schaefer, and Mark S Roberts. Determining the acceptance of cadaveric livers using an implicit model of the waiting list. *Operations Research*, 55 (1):24–36, 2007.

Eitan Altman. *Constrained Markov decision processes*, volume 7. CRC Press, 1999.

Eitan Altman, Tania Jiménez, and Ger Koole. On the comparison of queueing systems with their fluid limits. *Probability in the Engineering and Informational Sciences*, 15(02):165–178, 2001.

Itai Ashlagi, Duncan S Gilchrist, Alvin E Roth, and Michael A Rees. Nonsimultaneous chains and dominos in kidney-paired donation—revisited. *American Journal of Transplantation*, 11(5): 984–994, 2011.

Barış Ata, Anton Skaro, and Sridhar Tayur. OrganJet: Overcoming geographical disparities in access to deceased donor kidneys in the United States. *Management Science*, 63(9):2776–2794, 2016.

Baris Ata, Yichuan Ding, and Stefanos Zenios. An achievable-region-based approach for kidney allocation policy design with endogenous patient choice. *Manufacturing & Service Operations Management*, 2020.

Krishna B Athreya and Thomas G Kurtz. A generalization of Dynkin's identity and some applications. *The Annals of Probability*, pages 570–579, 1973.

Benjamin Avi-Itzhak and Hanoch Levy. On measuring fairness in queues. *Advances in Applied Probability*, 36(3):919–936, 2004.

Achal Bassamboo and Ramandeep S Randhawa. On the accuracy of fluid models for capacity sizing in queueing systems with impatient customers. *Operations Research*, 58(5):1398–1413, 2010.

Nicole Bäuerle. Asymptotic optimality of tracking policies in stochastic networks. *Annals of Applied Probability*, pages 1065–1083, 2000.

Nicole Bäuerle. Optimal control of queueing networks: an approach via fluid models. *Advances in Applied Probability*, 34(02):313–328, 2002.

Nicole Bäuerle and Ulrich Rieder. Optimal control of single-server fluid networks. *Queueing Systems*, 35(1):185–200, 2000.

Dimitri P Bertsekas, Robert G Gallager, and Pierre Humblet. *Data networks*, volume 2. Prentice-Hall International New Jersey, 1992.

Dimitris Bertsimas. The achievable region method in the optimal control of queueing systems; formulations, bounds and policies. *Queueing systems*, 21(3-4):337–389, 1995.

Dimitris Bertsimas, Vivek F Farias, and Nikolaos Trichakis. The price of fairness. *Operations research*, 59(1):17–31, 2011.

Dimitris Bertsimas, Vivek F Farias, and Nikolaos Trichakis. Fairness, efficiency, and flexibility in organ allocation for kidney transplantation. *Operations Research*, 61(1):73–87, 2013.

Thomas Bonald, Laurent Massoulié, Alexandre Proutiere, and Jorma Virtamo. A queueing analysis of max-min fairness, proportional fairness and balanced fairness. *Queueing systems*, 53(1-2):65–84, 2006.

BMo Budak, EM Berkovich, and EN Solov'eva. Difference approximations in optimal control problems. *SIAM Journal on Control*, 7(1):18–31, 1969.

Anh L Bui, Tamara B Horwich, and Gregg C Fonarow. Epidemiology and risk profile of heart failure. *Nature Reviews Cardiology*, 8(1):30–41, 2011.

Centers for Disease Control and Prevention. Life tables. https://www.cdc.gov/nchs/products/life$_t$*ables.htm*, 2015.

James F Childress. Fairness in the allocation and delivery of health care: the case of organ transplantation. In *A time to be born and a time to die. The ethics of choice*, page 205. de Gruyterd Hawthorne, NY, 1991.

M Colvin, JM Smith, MA Skeans, LB Edwards, K Uccellini, JJ Snyder, AK Israni, and BL Kasiske. OPTN/SRTR 2015 Annual Data Report: heart. *American Journal of Transplantation*, 17(S1): 286–356, 2017.

M Colvin-Adams, M Valapour, M Hertz, B Heubner, K Paulson, V Dhungel, MA Skeans, L Edwards, V Ghimire, C Waller, et al. Lung and heart allocation in the United States. *American Journal of Transplantation*, 12(12):3213–3234, 2012.

M Colvin-Adams, JM Smithy, BM Heubner, MA Skeans, LB Edwards, C Waller, MA Schnitzler, JJ Snyder, AK Israni, and Bert L Kasiske. Optn/srtr 2012 annual data report: heart. *American Journal of Transplantation*, 14(S1):113–138, 2014.

M Colvin-Adams, JM Smith, BM Heubner, MA Skeans, LB Edwards, CD Waller, ER Callahan, JJ Snyder, AK Israni, and BL Kasiske. OPTN/SRTR 2013 annual data report: heart. *American Journal of Transplantation*, 15(S2):1–28, 2015.

Israel David and Uri Yechiali. A time-dependent stopping problem with application to live organ transplants. *Operations Research*, 33(3):491–504, 1985.

Ryan R Davies, Maryjane Farr, Scott Silvestry, Liz Robbins Callahan, Leah Edwards, Dan M Meyer, Kimberly Uccellini, Kevin M Chan, and Joseph Rogers. The new United States heart allocation policy: progress through collaborative revision, 2017.

Connie L Davis and Francis L Delmonico. Living-donor kidney transplantation: a review of the current practices for the live donor. *Journal of the American Society of Nephrology*, 16(7):2098–2110, 2005.

Awi Federgruen and H Groenevelt. M/g/c queueing systems with multiple customer classes: Characterization and control of achievable performance under nonpreemptive priority rules. *Management Science*, 34(9):1121–1138, 1988.

Fernando ACC Fontes and Hélène Frankowska. Normality and nondegeneracy for optimal control problems with state constraints. *Journal of Optimization Theory and Applications*, 166(1):115–136, 2015.

Andreas Frommer and Bruno Lang. Existence tests for solutions of nonlinear equations using borsuk's theorem. *SIAM journal on numerical analysis*, 43(3):1348–1361, 2005.

Satoru Fujishige. *Submodular functions and optimization*. Elsevier, 2005.

Robert G Gallager. *Stochastic processes: theory for applications*. Cambridge University Press, 2013.

Google. Google maps. http://maps.google.com/, 2015.

Itai Gurvich, Amy Ward, et al. On the dynamic control of matching queues. *Stochastic Systems*, 4(2): 479–523, 2014.

J Michael Harrison and Assaf Zeevi. A method for staffing large call centers based on stochastic fluid models. *Manufacturing & Service Operations Management*, 7(1):20–36, 2005.

Richard F Hartl, Suresh P Sethi, and Raymond G Vickson. A survey of the maximum principles for optimal control problems with state constraints. *SIAM Review*, 37(2):181–218, 1995.

Farhad Hasankhani and Amin Khademi. Efficient and fair heart allocation policies for transplantation. *MDM Policy & Practice*, 2(1):2381468317709475, 2017.

Farhad Hasankhani and Amin Khademi. Is it time to include post-transplant survival in heart transplantation allocation rules? *Available at SSRN 3416214*, 2019.

Tania Jiménez and Ger Koole. Scaling and comparison of fluid limits of queues applied to call centers with time-varying parameters. *OR Spectrum*, 26(3):413–422, 2004.

Ehud Kalai and Meir Smorodinsky. Other solutions to nash's bargaining problem. *Econometrica: Journal of the Econometric Society*, pages 513–518, 1975.

Mahsa Kiani, Burak Eksioglu, Tugce Isik, Alexandria Thomas, and John Gilpin. Evaluating appointment postponement in scheduling patients at a diagnostic clinic. *arXiv preprint arXiv:1905.11201*, 2019.

Mahsa Kiani, Tugce Isik, and Burak Eksioglu. Dynamic tuberculosis screening for healthcare employees. *arXiv preprint arXiv:2007.05568*, 2020.

JA Kobashigawa, M Johnson, J Rogers, JD Vega, M Colvin-Adams, L Edwards, D Meyer, M Luu, N Reinsmoen, AI Dipchand, et al. Report from a forum on US heart allocation policy. *American Journal of Transplantation*, 15(1):55–63, 2015.

Nan Kong, Andrew J Schaefer, Brady Hunsaker, and Mark S Roberts. Maximizing the efficiency of the US liver allocation system through region design. *Management Science*, 56(12):2111–2122, 2010.

Keren Ladin and Douglas W Hanto. Rational rationing or discrimination: balancing equity and efficiency considerations in kidney allocation. *American Journal of Transplantation*, 11(11):2317–2321, 2011.

Chris P Lee, Glenn M Chertow, and Stefanos A Zenios. Optimal initiation and management of dialysis therapy. *Operations Research*, 56(6):1428–1449, 2008.

Li Li, Martin Pal, and Yang Richard Yang. Proportional fairness in multi-rate wireless lans. In *IEEE INFOCOM 2008-The 27th Conference on Computer Communications*, pages 1004–1012. IEEE, 2008.

Donna Mancini and Katherine Lietz. Selection of cardiac transplantation candidates in 2010. *Circulation*, 122(2):173–183, 2010.

Sabato Manfredi. Congestion control for differentiated healthcare service delivery in emerging heterogeneous wireless body area networks. *IEEE Wireless Communications*, 21(2):81–90, 2014.

DM Meyer, Joseph G Rogers, LB Edwards, ER Callahan, SA Webber, MR Johnson, JD Vega, MJ Zucker, and JC Cleveland. The future direction of the adult heart allocation system in the United States. *American Journal of Transplantation*, 15(1):44–54, 2015.

Sean Meyn. Stability and optimization of queueing networks and their fluid models. *Lectures in Applied Mathematics-American Mathematical Society*, 33:175–200, 1997.

John F Nash. The bargaining problem. *Econometrica: Journal of the econometric society*, pages 155–162, 1950.

Organ Procurement and Transplantation Network. Policies. https://optn.transplant.hrsa.gov/governance/policies, 2015.

Organ Procurement and Transplantation Network. Adult heart allocation changes 2016. https://optn.transplant.hrsa.gov/governance/public-comment/adult-heart-allocation-changes-2016, 2016a.

Organ Procurement and Transplantation Network. Organ transplantation: Report on equity in access. https://optn.transplant.hrsa.gov/media/2159/equity_in_access_report_201705.pdf, 2016b.

Organ Procurement and Transplantation Network. Organ data source. https://optn.transplant.hrsa.gov/data/organ-datasource/heart, 2017.

James M Ortega and Werner C Rheinboldt. *Iterative solution of nonlinear equations in several variables*. SIAM, 2000.

Ohad Perry and Ward Whitt. A fluid approximation for service systems responding to unexpected overloads. *Operations Research*, 59(5):1159–1170, 2011.

Govind C Persad, Alan Wertheimer, and Ezekiel J Emanuel. Standing by our principles: meaningful guidance, moral foundations, and multi-principle methodology in medical scarcity. *The American Journal of Bioethics*, 10(4):46–48, 2010.

Warren B Powell. *Approximate Dynamic Programming: Solving the curses of dimensionality*, volume 703. John Wiley & Sons, 2007.

Martin L Puterman. *Markov decision processes: discrete stochastic dynamic programming*. John Wiley & Sons, 2014.

John Rawls. *A theory of justice*. Harvard university press, 2009.

Dale G Renlund, David O Taylor, Abdallah G Kfoury, and Robert S Shaddy. New UNOS rules: historical background and implications for transplantation management. *The Journal of Heart and Lung Transplantation*, 18(11):1065–1070, 1999.

RFI. Kidney allocation concepts: request for information. *OPTN/UNOS Kidney Transplantation Committee*, 2008.

Sheldon M Ross. *Introduction to probability models*. Academic press, 2014.

Burhaneddin Sandıkçı, Lisa M Maillart, Andrew J Schaefer, Oguzhan Alagoz, and Mark S Roberts. Estimating the patient's price of privacy in liver transplantation. *Operations Research*, 56(6):1393–1410, 2008.

Sergei V Savin, Morris A Cohen, Noah Gans, and Ziv Katalan. Capacity management in rental businesses with two customer bases. *Operations Research*, 53(4):617–631, 2005.

Scientific Registry of Transplant Recipients. Risk adjustment models. http://www.srtr.org/reports-tools/riskadjustment- models-transplant-programs, 2015a.

Scientific Registry of Transplant Recipients. Thoracic simulated allocation model. https://www.srtr.org/media/1201/tsam.pdf, 2015b.

Atle Seierstad and Knut Sydsaeter. *Optimal control theory with economic applications*. Elsevier North-Holland, Inc., 1986.

Amartya Sen, Master Amartya Sen, Sen Amartya, James Eric Foster, James E Foster, et al. *On economic inequality*. Oxford University Press, 1997.

Steven M Shechter, Cindy L Bryce, Oguzhan Alagoz, Jennifer E Kreke, James E Stahl, Andrew J Schaefer, Derek C Angus, and Mark S Roberts. A clinically based discrete-event simulation of end-stage liver disease and the organ allocation process. *Medical Decision Making*, 25(2):199–209, 2005.

Tajinder P Singh, Christopher S Almond, David O Taylor, and Dionne A Graham. Decline in heart transplant wait-list mortality in the United States following broader regional sharing of donor hearts. *Circulation: Heart Failure*, pages CIRCHEARTFAILURE–111, 2012.

Jacqueline M Smits, Undine Samuel, and Guenther Laufer. Bridging the gap in heart transplantation. *Current Opinion in Organ Transplantation*, 22(3):221–224, 2017.

Lynne Warner Stevenson. Crisis awaiting heart transplantation: sinking the lifeboat. *JAMA Internal Medicine*, 175(8):1406–1409, 2015.

Lynne Warner Stevenson, Robert L Kormos, James B Young, James K Kirklin, and Sharon A Hunt. Major advantages and critical challenge for the proposed United States heart allocation system. *The Journal of Heart and Lung Transplantation*, 35(5):547–549, 2016.

Xuanming Su and Stefanos Zenios. Patient choice in kidney allocation: the role of the queueing discipline. *Manufacturing & Service Operations Management*, 6(4):280–301, 2004.

Xuanming Su and Stefanos A Zenios. Patient choice in kidney allocation: a sequential stochastic assignment model. *Operations Research*, 53(3):443–455, 2005.

Xuanming Su and Stefanos A Zenios. Recipient choice can address the efficiency-equity trade-off in kidney transplantation: a mechanism design model. *Management Science*, 52(11):1647–1660, 2006.

Michael D Swenson. Scarcity in the intensive care unit: Principles of justice for rationing icu beds. *The American journal of medicine*, 92(5):551–555, 1992.

Tammy O Tengs and Amy Wallace. One thousand health-related quality-of-life estimates. *Medical care*, pages 583–637, 2000.

The White House Office of Science and Technology Policy. A call to action to help reduce the waiting list for organ transplants. https://obamawhitehouse.archives.gov/blog/2016/09/01/call-action-help-reduce-waiting-list-organ-transplants, 2016.

United Network for Organ Sharing. Unos/optn data source. https://optn.transplant.hrsa.gov/converge/latestData/advancedData.asp, 2015.

United Network for Organ Sharing. United network for organ sharing webpage. https://www.UNOS.org., 2019.

Wilbert B van den Hout, Jacqueline MA Smits, Mario C Deng, Manfred Hummel, Friedrich Schoendube, Hans H Scheld, Guido G Persijn, Gunther Laufer, et al. The heart-allocation simulation model: a tool for comparison of transplantation allocation policies. *Transplantation*, 76(10):1492–1497, 2003.

H Peyton Young. *Equity: in theory and practice*. Princeton University Press, 1995.

Nooshin Yousefi, Farhad Hasankhani, and Mahsa Kiani. Appointment scheduling model in healthcare using clustering algorithms. *arXiv preprint arXiv:1905.03083*, 2019.

Stefanos A Zenios. Modeling the transplant waiting list: A queueing model with reneging. *Queueing systems*, 31(3-4):239–251, 1999.

Stefanos A Zenios. Optimal control of a paired-kidney exchange program. *Management Science*, 48 (3):328–342, 2002.